ES 1–124 ISSN 0003–2654

ROYAL SOCIETY
OF
CHEMISTRY

The Analyst

A monthly international journal dealing with all branches of the theory and practice of analytical chemistry, including instrumentation and sensors, and physical, biochemical, clinical, pharmaceutical, biological, environmental, automatic and computer-based methods

Vol.115 No.1 January 1990

The Analyst

The Analytical Journal of The Royal Society of Chemistry

Editorial Office: The Royal Society of Chemistry, Thomas Graham House, Science Park, Milton Road, Cambridge CB4 4WF. Telephone 0223 420066. Telex No. 818293 ROYAL. Fax 0223 423623.

Advertisements: Advertisement Department, The Royal Society of Chemistry, Burlington House, Piccadilly, London, W1V 0BN. Telephone 01-437 8656. Telex No. 268001. Fax 01-437 8883.

The Analyst (ISSN 0003–2654) is published monthly by The Royal Society of Chemistry, Thomas Graham House, Science Park, Milton Road, Cambridge CB4 4WF, UK. All orders accompanied with payment should be sent directly to The Royal Society of Chemistry, The Distribution Centre, Blackhorse Road, Letchworth, Herts. SG6 1HN, England. 1990 Annual subscription rate UK £220.00, EEC £233.00, Rest of World £253.00, USA $493.00. Purchased with *Analytical Abstracts* UK £476.00, EEC £520.00, Rest of World £547.00, USA $995.00. Purchased with *Analytical Abstracts* plus *Analytical Proceedings* UK £561.00, EEC £611.00, Rest of World £645.00, USA $1187.00. Purchased with *Analytical Proceedings* UK £279.00, EEC £296.50, Rest of World £321.00, USA $626.00. Air freight and mailing in the USA by Publications Expediting Inc., 200 Meacham Avenue, Elmont, NY 11003.
USA Postmaster: Send address changes to: *The Analyst*, Publications Expediting Inc., 200 Meacham Avenue, Elmont, NY 11003. Second class postage paid at Jamaica, NY 11431. All other despatches outside the UK by Bulk Airmail within Europe, Accelerated Surface Post outside Europe. PRINTED IN THE UK.

Information for Authors

Full details of how to submit material for publication in *The Analyst* are given in the Instructions to Authors in the January issue. Separate copies are available on request.

The Analyst publishes papers on all aspects of the theory and practice of analytical chemistry, fundamental and applied, inorganic and organic, including chemical, physical, biochemical, clinical, pharmaceutical, biological, environmental, automatic and computer-based methods. Papers on new approaches to existing methods, new techniques and instrumentation, detectors and sensors, and new areas of application with due attention to overcoming limitations and to underlying principles are all equally welcome. There is no page charge.

The following types of papers will be considered:

Full papers, describing original work.

Short papers: the criteria regarding originality are the same as for full papers, but short papers generally report less extensive investigations or are of limited breadth of subject matter.

Communications, which must be on an urgent matter and be of obvious scientific importance. Rapidity of publication is enhanced if diagrams are omitted, but tables and formulae can be included. Communications receive priority and are usually published within 5–8 weeks of receipt. They are intended for brief descriptions of work that has progressed to a stage at which it is likely to be valuable to workers faced with similar problems. A fuller paper may be offered subsequently, if justified by later work.

Reviews, which must be a critical evaluation of the existing state of knowledge on a particular facet of analytical chemistry.

Every paper (except Communications) will be submitted to at least two referees, by whose advice the Editorial Board of *The Analyst* will be guided as to its acceptance or rejection. Papers that are accepted must not be published elsewhere except by permission. Submission of a manuscript will be regarded as an undertaking that the same material is not being considered for publication by another journal.

Regional Advisory Editors. For the benefit of potential contributors outside the United Kingdom, a Panel of Regional Advisory Editors exists. Requests for help or advice on any matter related to the preparation of papers and their submission for publication in *The Analyst* can be sent to the nearest member of the Panel. Currently serving Regional Advisory Editors are listed in each issue of *The Analyst.*

Manuscripts (three copies typed in double spacing) should be addressed to:
The Editor, *The Analyst,*
Royal Society of Chemistry,
Thomas Graham House,
Science Park,
Milton Road,
CAMBRIDGE CB4 4WF, UK

Particular attention should be paid to the use of standard methods of literature citation, including the journal abbreviations defined in Chemical Abstracts Service Source Index. Wherever possible, the nomenclature employed should follow IUPAC recommendations, and units and symbols should be those associated with SI.

All queries relating to the presentation and submission of papers, and any correspondence regarding accepted papers and proofs, should be directed to the Editor, *The Analyst* (address as above). Members of the Analytical Editorial Board (who may be contacted directly or via the Editorial Office) would welcome comments, suggestions and advice on general policy matters concerning *The Analyst.*

Fifty reprints of each published contribution are supplied free of charge, and further copies can be purchased.

Identification of Medicinal Additives in Animal Feedingstuffs by High-performance Liquid Chromatography

Maria K. Cody, Georgina B. Clark, Brian O. B. Conway and Neil T. Crosby
Department of Trade and Industry, Laboratory of the Government Chemist, Queen's Road, Teddington, Middlesex TW11 0LY, UK

A method is described for the detection of 25 drugs used as prophylactics or as growth promoters in commercial animal feedingstuffs. The sample was extracted with aqueous acetonitrile, the co-extractives were removed with a silica cartridge and the eluate was examined by high-performance liquid chromatography, using two columns and five mobile phases. Thirteen animal feedingstuffs containing different combinations of drugs were prepared and used to test the method.

Keywords: *Medicinal additive; animal feedingstuff; high-performance liquid chromatography; identification*

Medicated animal feedingstuffs play a crucial role in intensive livestock production systems throughout the world. In 1984 it was estimated[1] that approximately one third of all UK feedingstuffs contain medicinal compounds licensed for inclusion without a veterinary prescription, mainly in the poultry and pig industries. Such medicated products can perform two functions; firstly, they act as prophylactics in the prevention of disease, and secondly, as growth promoters when added at sub-therapeutic levels to improve the efficiency of feed conversion. In the European Community, the use of these substances in feedingstuffs is controlled by Council Directive 70/254/EEC,[2] which has been amended many times over the last few years. The latest consolidated version of the annexes to this directive was published as Commission Directive 85/429/EEC.[3] This contains a list of 21 coccidiostats and other medicinal substances that are permitted for use under certain conditions. Most of these products are available on the UK market.[4]

Acceptable methods of analysis are needed for the control and measurement of these drugs in animal feedingstuffs. There are adequate methods of analysis for the determination of a number of single compounds and statutory methods for the determination of ten such additives are listed in reference 5. However, although the presence of medicinal additives in feedingstuffs must be declared, it is necessary to check their presence and that of any other compounds before proceeding to a full quantitative analysis. There are very few methods for the determination of a range of prophylactic drugs.

A multi-drug identification scheme was proposed by Hammond and Weston[6] in 1969 and this was tested and approved by the Analytical Methods Committee[7] in 1978. This scheme is based on extraction with acetonitrile - chloroform, fractionation through an alumina column and detection using thin layer chromatography (TLC). However, problems have been encountered using the scheme, probably as a result of variations in the characteristics of the alumina used to separate the drugs into fractions. Since that time other drugs have become available and, further, the technique of high-performance liquid chromatography (HPLC) has found increasing use for the detection and determination of medicinal compounds owing to its increased specificity and sensitivity over methods based on TLC or non-specific colorimetric reactions. Hence, the development of a systematic scheme for the identification and, possible, quantification of commonly used medicinal additives in animal feedingstuffs based on HPLC was undertaken.

The system now proposed is capable of identifying up to 25 medicinal additives present in animal feedingstuffs. This scheme involves an extraction with aqueous acetonitrile, a simple silica cartridge clean-up and identification using HPLC. Full details of the method are given in Appendix I. The development of the system is discussed and the results of a detailed trial are presented. Particular problems encountered during the trial are examined.

Experimental

Method Development

The development of the scheme can be divided into the following three main areas of work: (1) extraction of the drugs from feeding stuffs; (2) purification of the sample extract; and (3) detection and separation of the components of the purified extract.

(1) *Extraction*

Initially acetone, acetonitrile, chloroform, dichloromethane (DCM), dimethylformamide (DMF) and methanol - water (50 + 50 v/v) were compared. Each drug (10 mg) was placed in a 250-ml flask and the appropriate solvent was added to the mark. The flask was then placed in an ultrasonic bath for 5 min. The resulting solution was passed through a 0.5-μm filter. Acetone, chloroform and DCM solutions were carefully evaporated to dryness at a temperature below 40 °C. The residue was then re-dissolved in methanol - water (50 + 50) and the solution subjected to HPLC. Other solutions were examined using HPLC without evaporation. The concentration of each solution was determined from the peak area with reference to a calibration graph constructed by subjecting various dilutions of a stock solution of each drug in methanol to HPLC. The results are shown in Table 1.

Although the results are presented quantitatively, it should be remembered that no attempt was made to control the temperature or to ensure that equilibrium had been attained. The values are intended only as a semi-quantitative guide to the relative solubility of each drug in the solvents tested and, hence, an approximate estimate of the ability of each solvent to extract the drugs from animal feedingstuffs.

All six solvents appeared to solubilise between 15 and 20 of the drugs to at least 80% under the idealised test conditions. However, of the solvents used acetone and chloroform appeared to be the least powerful extractants and hence were not studied further. The use of DMF which, although it is a powerful extraction solvent, has a relatively high boiling-point and hence is difficult to remove by evaporation, might give rise to the loss of drugs. Solutions in DMF were also less

Table 1. Extraction of drugs at a concentration of 40 mg l^{-1} using various solvents

Drug	Recovery, %					
	Acetone (b.p., 50 °C)	Acetonitrile (b.p., 82 °C)	Chloroform (b.p., 62 °C)	DCM (b.p., 42 °C)	DMF (b.p., 153 °C)	Methanol - H_2O (50 + 50)
Olaquindox	51	55	65	47	59	106
Amprolium	5	55	0	0	100	100
Ronidazole	101	101	101	111	102	99
Clopidol	4	62	3	1	92	92
Diaveridine	86	96	90	91	98	94
Sulphadimidine	99	98	98	103	98	94
Carbadox	76	101	100	63	100	97
Dimetridazole	98	99	99	100	98	99
Ipronidazole	89	98	91	92	95	99
Nitrofurazone	97	104	75	84	97	97
Furazolidone	56	99	76	96	60	*
Dinitolmide	105	100	105	101	55	102
Acinitrazole	101	56	97	89	98	66
Arprinocid	100	100	101	101	98	103
Ethopabate	100	97	100	100	97	98
Halofuginone	12	70	0	0	88	97
Pyrimethamine	92	103	101	99	88	100
Sulphaquinoxaline	49	100	24	54	102	100
Nifursol	78	92	76	79	81	92
Sulphanitran	84	109	69	81	111	66
Nitrovin	26	26	0	0	86	111
Methyl benzoquate	10	*	93	44	98	0
Robenidine	102	107	79	111	89	114
Buquinolate	67	38	97	81	73	9
Decoquinate	44	22	101	102	96	0

* Not tested.

readily separable by HPLC. Dichloromethane and acetonitrile gave similar results but the latter was the better solvent for amprolium, clopidol, carbadox, halofuginone and sulphaquinoxaline and, therefore, was the preferred solvent. Hexane was also tested but without success. No significant amount of any of the drugs was found to dissolve in hexane under the chosen conditions. Therefore, it might be possible to use hexane in a pre-extraction step to remove lipid material from high-fat feeds, which might otherwise interfere in the subsequent identification by HPLC.

Later work in these laboratories on the determination of sulphadimidine[8] suggested that for some feeds, especially aged feeds, the presence of a small volume of water in the extracting solvent was required to penetrate into the matrix and improve the extraction efficiency. A limited study of the effect of including 5% of water in a mixture with acetonitrile was undertaken (Table 2).

From the results shown in Table 2 it can be seen that the presence of this small amount of water is desirable, especially for the drugs normally added to feedingstuffs at low levels (ethopabate, halofuginone and pyrimethamine). This assumes that the presence of water does not increase the difficulties at the chromatography stage by the co-extraction of too many feed constituents. Therefore, acetonitrile with water (95 + 5, v/v) was chosen as the extraction solvent for the proposed scheme.

Table 2. Effect of 5% water on the extraction of drugs from feeds

Drug	Recovery, %	
	MeCN	MeCN +5% water
Amprolium	43	89
Sulphaquinoxaline	51	72
Halofuginone	≈10	40
Ethopabate	≈10	93
Pyrimethamine	Difficult to detect	35

(2) *Extract purification*

Co-extracted feed constituents need to be removed to prevent them interfering at the determination stage. Traditional "clean-up" methods have included preparative thin layer chromatography (PTLC), partition between two solvents or adsorption chromatography with alumina- or silica-packed glass columns. Although these are adequate as purification techniques, they are often cumbersome to use and/or involve a lot of preparation. For this reason the use of disposable silica-based cartridges was examined. Cartridges packed with two types of polar materials (silica and cyano-bonded), a non-polar material (C_{18}) and a cation-exchange resin were studied. The silica cartridge appeared to be the most generally applicable "clean-up" system using blank feeds, although it was not as efficient as cation exchange. However, the cationic "clean-up" cartridge was only selective for ten of the drugs, the others being washed off with the impurities. Therefore, a silica cartridge appeared to be the best compromise and was used in subsequent work.

(3) *Detection (HPLC)*

A number of commercially available columns were examined for their ability to separate the drugs listed in Appendix II. These were as follows: (a) cyano-bonded column, 5 μm, (LiChroCART cartridge, Merck); (b) Rosil, 5 μm, RP-18, (cartridge system, Alltech); (c) LiChrosorb, RP-8, 7 μm (cartridge system, Merck); (d) Versapak, RP-18, 10 μm, (cartridge system, Alltech); (e) Spherisorb, 5 μm, ODS (column, Phase Sep); (f) LiChrosorb, 5 μm, RP-18 (column, Merck); (g) LiChrosorb, RP-8, 5-μm cartridge sensitised for basic compounds (Merck); and (h) LiChrosorb, RP-8, 5 μm (cartridge system, Merck). The column dimensions were 250 × 4.6 mm i.d. in all instances.

These columns were each tested using four mobile phases (MPs) of composition acetonitrile (x) - acetate buffer (150 ml) - water [1000 − (x + 150)], where x = 100, 225, 350 and 800 ml (*i.e.*, for MP225, x = 225 ml). Of these columns, column (b) gave satisfactory results for 23 of the 25 drugs in the scheme. Cartridge system (c) gave excellent peak shapes for the individual drugs but failed to resolve a significant

number in a mixture of drugs, without resorting to the use of a large number of mobile phases. Cartridge column (g) separated 18 of the 25 drugs including amprolium. Therefore, the Rosil, RP-18, 5-μm cartridge system column (b) gave the best over-all performance but did not give a good peak with amprolium under the conditions in the scheme. Amprolium is an important medicinal additive; it is found in the commercially available pre-mixes Pancoxin (with ethopabate and sulphaquinoxaline) and Amprolmix (with ethopabate). Hence amprolium could not be excluded from the scheme and for this reason it was thought necessary to use two columns, the Rosil, RP-18, 5-μm cartridge system column (b) and the LiChrosorb, RP-8, 5-μm cartridge column sensitised for basic compounds (g), which is satisfactory for amprolium.

Acetonitrile with an acetate buffer solution at pH 3.5, proved to be the optimum eluent system for most of the drugs; however, some exceptions to this will be discussed later. The use of methanol as the organic modifier was also investigated but it did not prove as effective as acetonitrile. Hence the mobile phases used for most of the drugs are based on varying proportions of acetonitrile in an aqueous, buffered solution. Further details are given in Appendix I. Another area of the development work involved the 4-hydroxyquinolines (methyl benzoquate, buquinolate and decoquinate). Poor peak shapes were observed for these drugs using the acetonitrile - acetate buffer mobile phase and a variety of columns. Methanol had been used as the organic modifier in previous work[9] and from close examination of the structures of these drugs it appeared that, to obtain good chromatographic traces, the mobile phase should be buffered at pH 8 to minimise ionisation. The effect of changing the mobile phase can be seen in Fig. 1.

A brief study was undertaken to determine whether wavelength selection could be used to aid identification of drug peaks where resolution is incomplete. Although wavelength selection can be a useful tool to aid confirmation of peaks in HPLC, its use was limited here; only arprinocid, amprolium, clopidol and pyrimethamine could be completely eliminated at wavelengths above 330 nm. For this reason it was decided that a single wavelength of 254 nm should be used for detection of the drugs, with the advantage that a single wavelength filter-type UV detector can then be used. It is considered to be better to attempt complete chromatographic separation than to attempt discrimination primarily by wavelength selection.

Validation of the Method

Thirteen animal feeds were "spiked" with combinations of up to 25 drugs as in Appendix II. The composition of the feeds was unknown to the analyst undertaking the trial. Twelve of these unknown feeds were examined by one operator and the other by a person with no previous experience of the method.

The "spiked" feeds were left for at least 3 weeks before they were analysed to permit any possible interactions between the drugs and feed constituents. Each feed was then extracted with aqueous acetonitrile, a portion of the filtered solution was evaporated to dryness and the residue was taken up in DCM. This solution was passed through a silica Sep-Pak cartridge, the Sep-Pak was dried and the drugs were eluted from the column using acetonitrile - acetate buffer (50 + 50). The eluate was examined on an HPLC system using a Rosil, RP-18, 5-μm column (b) and a LiChrosorb, RP-8, 5-μm, cartridge column sensitised for basic compounds (g). (The full experimental details are given in Appendix I.)

Results and Discussion

The results of the trial are given in Table 3. On the whole the results were encouraging; all the drugs in the "spiked" animal feeds were identified correctly and no peaks were wrongly assigned in the blank feeds. Where no figures for the recoveries are given, only a qualitative identification was attempted. For an example of the type of chromatographic traces obtained see Fig. 2. Most peaks were Gaussian in shape with minimum tailing and were well separated from other drugs.

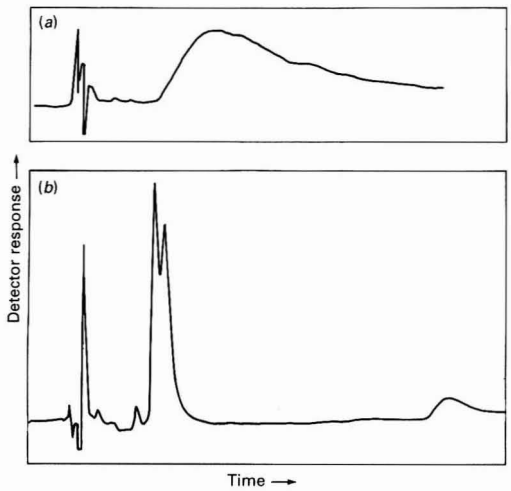

Fig. 1. Chromatograms of a mixture of methyl benzoquate, buquinolate and decoquinate, performed on the same day using the same system. (*a*) Mixture on the system using acetonitrile and acetate buffer as the mobile phase; and (*b*) as in (*a*) but using methanol and phosphate buffer as the mobile phase

The problems which did occur were associated with carbadox, halofuginone and nitrovin. Only a very small peak was obtained for carbadox and the recovery was very low (approximately 15%). Halofuginone was difficult to detect on MP225 using column (g), if ipronidazole was present. Therefore it was necessary to use MP350 and column (b) for this drug. However, the combination of this mobile phase and column gave a poor peak shape, which made identification difficult. The extraction of nitrovin gave erratic recoveries and in some instances it was necessary to use a concentrated extract for identification.

Only limited work was performed to assess the recoveries of the drugs, but the results were encouraging. At least 15 of the drugs had recoveries exceeding 70%. This suggests that the scheme could form the basis of a quantitative method for at least some of these medicinal additives. Initially it was thought that the scheme might prove cumbersome and time consuming. However, only 1–2 d were needed for an experienced operator to analyse a sample containing all 25 drugs. The use of a two-column system makes the screening procedure faster and the identification of drugs can be confirmed by the second column if necessary.

The tetracycline group of antibiotics (tetracycline, chlortetracycline and oxytetracycline hydrochloride), which might be used in conjunction with the drugs included in the scheme, was examined to test whether they interfere chromatographically with the remaining medicaments in the scheme. In all instances the tetracyclines eluted before any of the peaks of interest.

It is recommended that the columns should be tested using known samples of drugs before the scheme is employed as this should eliminate any problems due to batch to batch variations in the columns and varying chromatographic conditions. Nevertheless, some indication of the retention times of the drugs are given (Table 3). These serve only as a guide and should not be used for peak identification purposes.

Table 3. Results of a trial of the proposed scheme

Drug	No. of feed	Recovery, %	Approximate retention time*/min
1. Olaquindox	7	85	4(B)
	6	—	
2. Amprolium	2	—	6(B)
	6	—	
	9	55	
3. Clopidol	1	105	10(B)
	12	—	
	6	—	
	10	90	
	11	71	
4. Ronidazole	6	—	7(B)
	7	72	
	10	75	
5. Dimetridazole	5	64,74	8(A)
	6	—	14(B)
	7	54	
	12	—	
6. Nitrofurazone	13	85	5(A)
			14(B)
7. Carbadox	6	—	16(B)
	7	—	
8. Sulphadimidine	7	90,70	7(A)
	6	—	
9. Diaveridine	13	≈95	18(B)
10. Furazolidone	5	>100	10(A)
	6	—	19(B)
	7	87,94	
	10	93	
	13	—	
	12	—	
11. Dinitolmide	2	91	13(A)
	6	—	
	11	88	
12. Acinitrazole	6	—	14(A)
	9	88	
	10	75	
13. Ipronidazole	6	—	23(A)
	7	—	
	9	70	
	11	68	
	12	—	
14. Ethopabate	1	80	16(F)
	2	70	
	6	—	
	9	—	
15. Sulphaquinoxaline	1	73	30(A)
	2	73	
	6	—	
	9	82	
16. Arprinocid	5	≈46	40(A)
	6	—	25(F)
	12	—	
17. Halofuginone	1	—	11(F)
	2	—	18(G)
	5	—	
	6	—	
18. Nifursol	6	—	10(E)
	9	48	
	11	80	
19. Sulphanitran	2	81,84	15(E)
	6	—	
20. Pyrimethamine	1	—	14(F)
	2	51	
	6	—	
21. Nitrovin	6	—	18(E)
	7	>100,26?	
	10	≈40	
	11	85	
	12	—	
22. Methyl benzoquate	6	—	4(C)
	11	>100	10(D)
	12	—	
23. Buquinolate	5	102	4(C)
	6	—	8(D)
24. Robenidine	5	24	5(C)
	6	—	12(D)
	9	56	
	11	77	
25. Decoquinate	5	53	9(C)
	6	—	34(D)

* The letters in parentheses refer to the chromatographic system on which these drugs are examined (see Table 4).

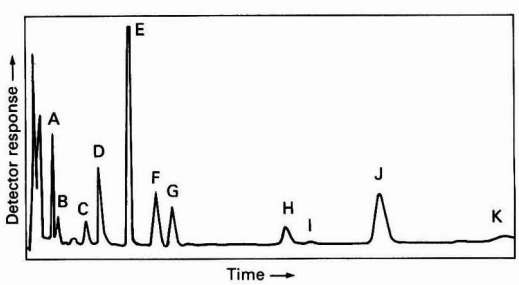

Fig. 2. Chromatogram of sample number 6 on MP225 using the Rosil RP-18, 5-μm column. A, Clopidol; B, ronidazole; C, sulphadimidine; D, dimetridazole; E, furazolidone; F, dinitolmide; G, acinitrazole; H, ipronidazole; I, ethopabate; J, sulphaquinoxaline; and K, arprinocid

Although the feeds were "spiked" at around the recommended commercial level for each drug, the systems were not operating at their maximum sensitivity and there was scope for detecting much lower amounts for some. Similarly, the peaks could be enhanced for some drugs by adjusting the wavelength. The wavelength of 254 nm was selected because it gave a peak for all the drug standards examined.

Conclusion

The proposed drug identification scheme was designed to be able to identify any or all of the named medicinal additives if present in animal feeds. Validation using an extensive trial showed that the scheme was capable of doing this; one feed was correctly found to contain all 23 of the medicaments present.

The proposed scheme might appear complex, however, the differing structures and physiochemical properties of these compounds rendered the use of a simple isocratic system impossible. Equally, a single column was not available to resolve all the drugs without using a large number of mobile phases. For example, using MP225 a good peak shape is obtained for halofuginone. However, when ipronidazole is present it is recommended that MP350 and column (b) are used for halofuginone, but under these conditions a poorly shaped peak is obtained for this drug.

Another problem involved finding the optimum extraction solvent for all the drugs. For example, the recovery of the drug carbadox was low and distorted peaks were obtained in the chromatogram (although carbadox was identified correctly in the trial of the scheme). This was due to a solubility problem; an alternative extraction solvent and perhaps normal phase chromatography would be more desirable for carbadox than the conditions chosen here. Nitrovin was the other problem

drug with only low recoveries being obtained. However, a good HPLC method for nitrovin has been reported previously.[10] Apart from these additives (halofuginone, carbadox and nitrovin) all the drugs can be identified quickly and easily.

The proposed scheme has been designed on the premise that all the drugs listed could be found together, or in any combinations, within an animal feed irrespective of commercial practice. For example, just because amprolium is generally used in poultry feeds it could still be looked for in pig feeds because any drug might be present as a result of cross-contamination problems at the point of manufacture.

The major advantage of this scheme is the potential to identify any one of 25 drugs in 1–2 d, whereas previously it would be necessary to perform up to 25 separate methods before ascertaining which medicinal additives were present in the feed. The scheme only needs to be performed in its entirety if the presence of all 25 drugs is suspected. If a feed was received and it was suspected that clopidol, dimetridazole and methyl benzoquate were present, only the chromatographic conditions recommended for these drugs would need to be employed. This analysis would take a maximum of 1 d for all of the drugs compared with a minimum of 3 d if an individual method was performed for each.

High-performance liquid chromatography is not regarded as an unequivocal identification technique. However, it is a non-destructive method; therefore, if further confirmation of peak identities is required the separated drugs can be examined using a wide range of complementary analytical methods including mass spectrometry.

Further developments could include rendering the method quantitative for specific compounds, increasing its sensitivity for the identification of residues of drugs in animal tissues and the option of using a single column with gradient elution.

APPENDIX I

Scope

This method can be used to identify up to 25 medicinal additives occurring either singly, or in any combination together, in animal feedingstuffs. The limit of detection is <3 mg kg^{-1}.

Principle

Medicinal compounds are extracted using aqueous acetonitrile and then co-extractives are removed using a silica cartridge. The eluate is examined by HPLC using a combination of up to two stationary phases and five mobile phases, depending on the particular compounds present and the degree of confirmation required.

Reagents

1. *Acetonitrile, HPLC grade.*
2. *Methanol, HPLC grade.*
3. *Acetonitrile - water*, 95 + 5 v/v.
4. *Methanesulphonic acid*, 2% v/v.
5. *Ammonia solution, sp. gr.* 0.88.
6. *Dimethylformamide, AnalaR.*
7. *Acetonitrile - acetate buffer*, 50 + 50.
8. *Dichloromethane, AnalaR.*
9. *Glacial acetic acid, AnalaR.*
10. *Ammonium acetate, AnalaR.*
11. *Stock standard solutions.* Prepared in a variety of solvents (2–7) and different concentrations according to the solubilities of the drugs. For further details see Table 4.
12. *Working standards.* Prepared by appropriate dilution of the stock solution using acetonitrile - acetate buffer.

Table 4. Identification of medicinal additives by HPLC

Compound	Level commonly found in feeds/ mg kg^{-1}	Standard solutions: Solvent	Stock/ mg ml^{-1}	Working standard/ μg ml^{-1}	Chromatographic system	Extraction solution
Acinitrazole	350	MeOH	0.5	30	A	1
Amprolium	60–125	MeOH	1.0	6	B	3
Arprinocid	60	MeOH	1.0	3–10	A, F	1, 2
Buquinolate	100	MSA*	1.0	3–10	D, C	1
Carbadox	50	MeOH - $CHCl_3$	0.1	5	B	3
Clopidol	100–125	MeOH - H_2O - NH_3	0.5	10–20	B	3
Decoquinate	20–40	MSA	1.0	3–6	D, C	1
Diaveridine	60	MeOH	0.1	6	B	3
Dimetridazole	125–200	MeOH	1.0	5–30	A, B	1
Dinitolmide	62.5–125	MeOH	0.1	10	A	1
Ethopabate	4–8	MeOH	1.0	0.5	A, F	1, 2
Furazolidone	100–400	MeOH	0.1	5–30	A, B	1, 3
Halofuginone	3	MeOH	0.1	0.3	F, G	2
Ipronidazole	40–80	MeOH	0.1	5–10	A	1
Methyl benzoquate	8	MSA	1.0	1.0	D, C	1
Nifursol	50–75	MeOH - H_2O	0.1	3–7	E	1
Nitrofurazone	50–100	MeOH	0.1	5–10	A, B	1
Nitrovin	10–25	DMF	0.1	2.5	E	2
Olaquindox	25–100	MeOH	0.05	2.5–10	B	3
Pyrimethamine	5–10	MeOH	0.5	0.5–0.75	F	2
Robenidine	33–66	MeOH	1.0	3.3	D, C	1
Ronidazole	120	MeOH	1.0	3–12	B	3
Sulphadimidine	100–165	MeOH	1.0	10	A	1
Sulphanitran	300	MeOH	0.1	10	E	1
Sulphaquinoxaline	100–200	MeOH - H_2O - NH_3 50 + 50 + 1	0.5	10	A	1

* MSA = methanesulphonic acid.

Mobile Phases

1. *Buffers*

(A) Ammonium acetate (19.27 g) was added to acetic acid (30 ml) and the resulting mixture was made up to 1 l with de-mineralised water.

(B) An equimolar solution of disodium hydrogen phosphate and sodium dihydrogen phosphate was prepared and adjusted to pH 8 using sodium hydroxide (1 M).

2. *Mobile Phases*

Acetate buffer [150 ml, prepared as in (A) above] was added to x ml of acetonitrile and $(850 - x)$ ml of de-mineralised water (where x = 100, 225, 325 or 350). The mixture was then filtered using 0.45-μm membrane filter-paper.

Phosphate buffer [200 ml, prepared as in (B) above] was added to 800 ml of methanol. The mixture was then filtered using 0.45-μm membrane filter-paper.

Apparatus

Mechanical shaker.

Rotary evaporator.

Glass-fibre (rapid filtering grade) microfibre filters, GF/A grade.

Ultrasonic bath.

Silica Sep-Paks (Waters Associates).

Glass syringe (10 ml) *fitted with a luer lock.*

High-performance liquid chromatography system. Pump, UV detector and valve injector fitted with a 20-μl loop.

Columns. A Rosil, RP-18, 5-μm (cartridge system, All-tech), and a LiChrosorb RP-8, 5-μm column sensitised for basic compounds (Merck).

Procedure

(1) Add 100 ml of acetonitrile - water to a 250-ml conical flask containing 10 g of the ground sample. Shake for 60 min and filter. Transfer an aliquot of the filtrate (10 ml) into a flask suitable for rotary evaporation and evaporate to dryness at 40 °C under vacuum. Dissolve the residue in 10 ml of DCM and place the flask in an ultrasonic bath for a few minutes. Condition a silica cartridge by passing 2 ml of DCM in a steady, dropwise flow. Discard this eluate then add the extract, rinse the flask with a few millilitres of DCM and add the washings to the cartridge. Dry the cartridge using a stream of nitrogen for at least 30 min. Then add approximately 10 ml of acetonitrile - acetate buffer (50 + 50) and collect the eluate (solution 1) in a 10-ml calibrated flask. Filter this solution using a 0.2-μm membrane filter unit if necessary.

(2) For the identification of medicinal additives present only at low levels (<15 mg kg^{-1}) it is necessary to prepare a more concentrated solution as follows. Take 50 ml of the initial extract, evaporate to dryness and dissolve the residue in 10 ml of DCM. Pass through the cartridge as before, dry and elute (again in 10 ml). This eluate (solution 2) represents a 5-fold concentration of solution 1.

(3) Solution 1 might prove incompatible with MP100, producing poorly shaped peaks. Dilute solution 2 by adding 2 ml to a 10-ml calibrated flask. Make up to the mark with water. The resulting solution is solution 3.

Chromatography

All systems operate at a flow-rate of 1.5 ml min^{-1} and a detection wavelength of 254 nm is used throughout.

Set up systems A and B initially (Table 5) using the appropriate columns and MP225 and MP100, respectively, concurrently if possible to save operator time. Allow the systems to stabilise for 30 min. Test each system using standard solutions of the drug indicated (Table 5) to establish the stop time for the chromatogram. The stop time determines the end of the useful run of the chromatogram. Standard solutions of the other drugs indicated, prepared as in Table 4, should also be injected at intervals to determine retention times and to establish that satisfactory resolution is being achieved.

Identification

(1) Examine 20 μl of solution 1 using system A and record the retention times of any peaks on the chromatogram up to the stop time. Check for the presence of acinitrazole, arprinocid, dimetridazole, dinitolmide, ethopabate, furazolidone, ipronidazole, nitrofurazone, sulphadimidine and sulphaquinoxaline by comparing the retention time of any unknown peak obtained from solution 1 with values established by injections of known standard solutions on the same day or by additions of known solutions to the extract,

Table 5. High-performance liquid chromatographic systems for the identification of medicinal additives in animal feeds

System	Column	Mobile phase	Extract solution*	"Stop" standard	Approximate stop time/min	Compounds identified in approximate order of elution
A	Rosil RP-18	225	1	Arprinocid	45	Nitrofurazone, sulphadimidine, dimetridazole, furazolidone, dinitolmide, acinitrazole, ipronidazole, ethopabate, sulphaquinoxaline, arprinocid (Fig. 3)
B	LiChrosorb RP-8(B)	100	3	Furazolidone	25	Olaquindox, amprolium, ronidazole, clopidol, dimetridazole, nitrofurazone, carbadox, diaveridine, furazolidone (Fig. 4)
C	LiChrosorb RP-8(B)	800	1 or 2	Decoquinate	15	Buquinolate, methyl benzoquate, robenidine, decoquinate
D	Rosil RP-18	800	1	Decoquinate	35	Buquinolate, methyl benzoquate, robenidine, decoquinate
E	LiChrosorb RP-8(B)	325	1 + 2	Nitrovin	25	Nifursol, sulphanitran, nitrovin
F	LiChrosorb RP-8(B)	225	2	Arprinocid	30	Halofuginone, pyrimethamine, ethopabate, arprinocid
G	Rosil RP-18	350	3	Halofuginone	20	Halofuginone

* Solution 1 = eluate; solution 2 = solution 1 concentrated 5-fold; and solution 3 = solution 2 diluted 5-fold with water.

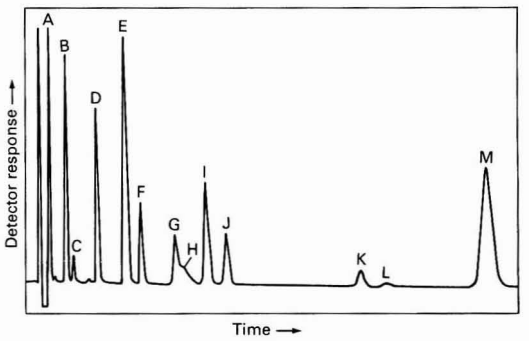

Fig. 3. Mixture of drug standards on MP225 using the Rosil RP-18 5-μm column (system A). A, Olaquindox; B, clopidol; C, ronidazole; D, nitrofurazone; E, sulphadimidine; F, dimetridazole; G, furazolidone; H, diaveridine; I, dinitolmide; J, acinitrazole; K, ipronidazole; L, ethopabate; M, sulphaqinoxaline; and N, arprinocid (off-scale)

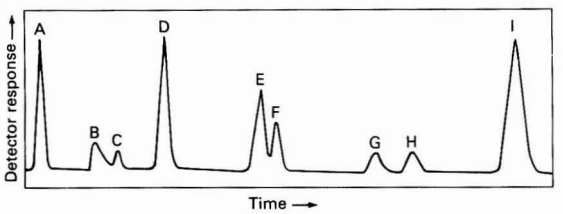

Fig. 4. Mixture of drug standards on MP100 using the LiChrosorb RP-8 5-μm cartridge sensitised for basic compounds (system B). A, Olaquindox; B, amprolium; C, ronidazole; D, clopidol; E, dimetridazole; F, nitrofurazone; G, diaveridine; H, furazolidone; and I, sulphadimidine

whereupon an enhancement of the peak height should be observed. When all peaks have been tentatively identified, change to MP800 and leave for 30 min to equilibrate.

(2) Examine 20 μl of solution 3 using System B as in (1) above and check for the presence of amprolium, carbadox, clopidol, diaveridine, olaquindox and ronidazole. Confirm the identity of any peak obtained also using the procedure described in (1) above. Change to MP325 and leave for 30 min to equilibrate. It might also be useful to use this mobile phase to confirm the identification of furazolidone, nitrofurazone and dimetridazole.

(3) Examine 20 μl of solutions 1 and 2 sequentially using system E. Check for the presence of nifursol and sulphanitran in solution 1 and for nitrovin in solution 2. Confirm as described in (1) above.

(4) Examine 20 μl of solution 1 using system D. Check for the presence of buquinolate, decoquinate, methyl benzoquate and robenidine. Confirm the identity as before and by using system C.

(5) If necessary, use system C to confirm the presence of buquinolate, decoquinate, robenidine and methyl benzoquate.

(6) Examine 20 μl of solution 2 using system F. Check for the presence of arprinocid, ethopabate, halofuginone and pyrimethamine. Confirm as before.

(7) If ipronidazole is thought to be present, the halofuginone might not be detectable on MP225 using the Lichrosorb, RP-8, 5-μm cartridge sensitised for basic compounds. Therefore, if ipronidazole is present, halofuginone should be looked for using system G (see Table 4).

APPENDIX II

Thirteen animal feeds were "spiked" with up to 25 drugs as shown below. The drugs were weighed accurately into a weighing boat, transferred into a container with wheatflour (total mass of drugs and wheatflour, 1 g), the weighing boat was re-weighed and the amount of drug in the pre-mix was calculated from the difference in these masses. The pre-mix was then mixed well using a "Turbula" mixer (Bachofen). A portion of the pre-mix (0.1 g) was added to one of several commercial feedingstuffs (9.9 g), which had first been ground to pass through a 0.5-mm sieve. The feedingstuff and pre-mix were mixed further to allow even dispersal of the drug. The feed was left for at least 3 weeks to allow any possible interactions between the drugs and other constituents of the feed to take place.

Drug	Drug level in the feed/mg kg^{-1}
Feed No. 1: poultry feed—	
Ethopabate	5
Halofuginone	3
Pyrimethamine	5
Clopidol	200
Sulphaquinoxaline	250
Robenidine	60
Feed No. 2: poultry feed—	
Ethopabate	5
Halofuginone	3
Pyrimethamine	5
Amprolium	100
Sulphaquinoxaline	125
Dinitolmide	100
Sulphanitran	50
Feed No. 3: poultry feed—	
Blank feed, containing no medicinal additives	—
Feed No. 4: poultry feed—	
Blank feed, containing no medicinal additives	—
Feed No. 5: poultry feed—	
Halofuginone	5
Arprinocid	10
Robenidine	30
Dimetridazole	500
Decoquinate	50
Furazolidone	100
Buquinolate	100
Feed No. 6: poultry feed—	
Olaquindox; sulphadimidine; sulphaquinoxaline; amprolium; furazolidone; arprinocid; clopidol; dinitolmide; halofuginone; ronidazole; acinitrazole; nifursol; dimetridazole; ipronidazole; sulphanitran; carbadox; ethopabate; pyrimethamine; nitrovin; decoquinate; robenidine; methyl benzoquate; and buquinolate	—
Feed No. 7: pig feed—	
Carbadox	18
Nitrovin	10
Ipronidazole	100
Olaquindox	100
Ronidazole	100
Dimetridazole	200
Sulphadimidine	150
Furazolidone	200
Feed No. 8: poultry feed—	
Blank feed, containing no medicinal additives	—
Feed No. 9: turkey feed—	
Ethopabate	30
Robenidine	5
Amprolium	60
Sulphaquinoxaline	100
Acinitrazole	300
Ipronidazole	100
Nifursol	50

Drug	Drug level in the feed/mg kg^{-1}
Feed No. 10: cattle feed—	
Furazolidone	50
Nitrovin	25
Ronidazole	50
Acinitrazole	100
Clopidol	25
Feed No. 11: turkey feed—	
Nitrovin	10
Methyl benzoquate	10
Dinitolmide	60
Nifursol	100
Robenidine	50
Ipronidazole	50
Clopidol	50
Feed No. 12: Poultry Feed—	
Nitrovin	10
Methyl benzoquate	10
Furazolidone	400
Ipronidazole	100
Clopidol	125
Arprinocid	60
Dimetridazole	50
Feed No. 13: Poultry Feed—	
Furazolidone	72
Nitrofurazone	71
Diaveridine	50

The authors thank the Ministry of Agriculture, Fisheries and Food for funding this work.

References

1. Anon, *Feed Compounder*, 1984, **4** (8), 8.
2. "Official Journal of the European Communities," Special Edition, Volume 18, HM Stationery Office, London, 1973, p. 4.
3. "Official Journal of the European Communities," **L 245** of 12.9.85, p. 1.
4. "Handbook of Medicinal Feed Additives, 1988–9," Seventh Edition, HGM Publications, Bakewell, 1988.
5. "Statutory Instrument 1985," No. 273, The Medicines (Animal Feeding Stuffs) (Enforcement) Regulations, HM Stationery Office, London, 1985.
6. Hammond, P. W., and Weston, R. E., *Analyst*, 1969, **94**, 921.
7. Analytical Methods Committee, *Analyst*, 1978, **103**, 513.
8. Conway, B., *Analyst*, 1988, **113**, 1397.
9. Merson, G. H. J., Hill, L. A., and Johnson, S. F., *Analyst*, 1985, **110**, 761.
10. Chen, J., Wang, F., and Yang, S., *Fenxi Huaxue*, 1985, **13**, 935 (in Chinese); *Anal. Abstr.*, 1986, **48**, 7G15.

Paper 9/00678H
Received February 13th, 1989
Accepted August 29th, 1989

High-performance Liquid Chromatographic Determination of Cinnamaldehyde

Masatoki Katayama, Yoshio Mukai and Hirokazu Taniguchi
Meiji College of Pharmacy, 1-35-23 Nozawa, Setagaya-ku, Tokyo 154, Japan

A sensitive method for the determination of cinnamaldehyde is described, using high-performance liquid chromatography with spectrofluorimetric detection. Cinnamaldehyde was first reacted with 4,5-dimethyl-*o*-phenylenediamine in an acidic medium and the resulting fluorescent benzimidazole derivative was analysed on a reversed-phase column with 0.02 M acetate buffer (pH 4.0) - methanol (1 + 1) containing 5 mmol l^{-1} dodecyltrimethylammonium bromide as the mobile phase. Cinnamaldehyde was determined in aqueous solution in the range 0.001–30 μg ml^{-1}.

Keywords: *Cinnamaldehyde; high-performance liquid chromatography; 4,5-dimethyl-o-phenylenediamine; 5,6-dimethyl-2-styrylbenzimidazole; 5,6-dimethyl-2-phenylbenzimidazole*

Cinnamaldehyde is the main component of the essential oil in cinnamon bark. Cinnamon bark is frequently used as a stomachic, an antipyretic and an antiallergic drug and as a tonic in traditional Chinese medicines. The determination of cinnamaldehyde provides important information on the efficiency of the preparation of traditional Chinese medicines.

Cinnamaldehyde has been determined by thin-layer chromatography (TLC),[1,2] gas chromatography (GC)[3,4] and high-performance liquid chromatography (HPLC).[5–7] These methods have been applied to the determination of cinnamaldehyde in cinnamon bark and traditional Chinese medicines in the range 10–200 μg ml^{-1}.

A sensitive method for the determination of cinnamaldehyde would be useful for the evaluation of commercial preparations of cinnamon bark and traditional Chinese medicines. We have previously reported the HPLC analysis of aromatic aldehydes by means of spectrofluorimetric detection following derivatisation with 4,5-dimethyl-*o*-phenylenediamine (DMPD).[8] Using this method, vanillin could be determined at levels as low as 0.05 ng ml^{-1}. In this paper, the determination of cinnamaldehyde by HPLC following derivatisation with DMPD was studied.

Two fluorescent compounds, 5,6-dimethyl-2-phenylbenzimidazole and 5,6-dimethyl-2-styrylbenzimidazole, were isolated from the reaction of cinnamaldehyde with DMPD, and a reaction mechanism is proposed.

Experimental

The ^1H nuclear magnetic resonance (NMR) spectra were recorded on a JEOL GX-400 Fourier transform NMR instrument. Chemical shifts are reported in p.p.m. (δ) relative to Me_4Si. The infrared (IR) spectra were measured with a JASCO DS-701G spectrophotometer. Mass spectra (MS) were recorded on a JEOL JMS-D300 spectrometer. Elemental analysis was carried out with a Perkin-Elmer 240B elemental analyser.

Reagents

All reagents were of analytical-reagent grade (Japan Industrial Standards). Cinnamaldehyde was purified by distillation under a stream of N_2. A standard cinnamaldehyde solution was prepared by dissolving 10 mg of cinnamaldehyde in 20 ml of ethanol and diluting to 100 ml with water. The DMPD solution (0.04%) was prepared by dissolving 40 mg of DMPD (Tokyo Kasei, Japan) in 30 ml of 0.5 mol l^{-1} sulphuric acid and diluting to 100 ml with water. This reagent was stable for 1 week if kept in the dark.

Authentic Samples for the Identification of the Fluorescent Product

Authentic samples of two benzimidazoles for the identification of the fluorescent product from the cinnamaldehyde - DMPD reaction were synthesised in the following manner.

5,6-*Dimethyl-2-phenylbenzimidazole*

4,5-Dimethyl-*o*-phenylenediamine (4 g) dissolved in 40 ml of MeOH and $Cu(O_2CCH_3)_2$ (12 g) dissolved in 120 ml of water were mixed, and benzaldehyde (4 g) was added. The mixture was refluxed for 12 h. After cooling, the precipitate was collected, washed with 20 ml of MeOH and dissolved in a further 300 ml of MeOH. The solution was refluxed while passing a stream of H_2S for 30 min. The reaction mixture was filtered and the filtrate was evaporated to dryness. The residue was recrystallised from EtOH - water (1 + 1) to give white needles; yield 2.48 g, m.p. 253 °C. Analysis: calculated for $C_{15}H_{14}N_2$ C, 81.05; H, 6.35; N, 12.60%; found C, 81.07; H, 6.25; N, 12.48%. IR $\nu_{max.}$ (cm^{-1}) (KBr): 3310, 1460. ^1H NMR [$(CD_3)_2SO$]: δ 2.37 (6H, s, CH_3), 7.39 (2H, s, Ar–H), 7.50–7.58, 8.12–8.22 (5H, Ar–H). MS: *m/z* 222 (M^+).

5,6-*Dimethyl-2-styrylbenzimidazole*

4,5-Dimethyl-*o*-phenylenediamine (5 g) dissolved in 50 ml of EtOH and $Cu(O_2CCH_3)_2$ (12 g) dissolved in 120 ml of water were mixed, and cinnamaldehyde (5 g) was added. The mixture was refluxed for 12 h. After cooling, the precipitate was collected, washed with 20 ml of MeOH and dissolved in 200 ml of MeOH - water (1 + 1). The solution was refluxed while passing a stream of H_2S for 30 min. The reaction mixture was filtered and the filtrate was evaporated to dryness. The residue was subjected to column chromatography on silica gel [Wako-gel C-200; eluent, hexane - EtO_2CCH_3 (4 + 1)] and the fluorescent fraction was collected. The solvent was removed and the residue was recrystallised from benzene to give white needles; yield 0.9 g, m.p. 244 °C. Analysis: calculated for $C_{17}H_{16}N_2$ C, 82.23; H, 6.49; N, 11.28%; found C, 82.02; H, 6.41; N, 11.30%. IR $\nu_{max.}$ (cm^{-1}) (KBr): 1690 (C=C). ^1H NMR ($CDCl_3$): δ 2.31 (6H, s, CH_3), 7.20 (1H, s, C=CH), 7.31 (2H, s, Ar–H), 7.57 (1H, s, C=CH), 7.57–7.65 (5H, Ar–H). MS: *m/z* 242 (M^+).

Pre-column Derivatisation for the Determination of Cinnamaldehyde

To 1.0 ml of DMPD solution was added 1.0 ml of sample solution containing 0.001–30 μg ml^{-1} of cinnamaldehyde in a light-proof screw-capped test-tube. The mixture was heated

for 50 min on a boiling water-bath, cooled to room temperature and then 0.5 ml of 0.5 mol l^{-1} sodium hydroxide solution was added. A 20-μl aliquot of the mixture was injected on to the HPLC column.

HPLC Apparatus and Conditions

These were as follows: pump, Shimadzu LC-4A liquid chromatograph; guard column, Zorbax ODS (50 × 4.6 mm i.d., 7 μm, DuPont); analytical column, Zorbax ODS (250 × 4.6 mm i.d., 7 μm, DuPont); sample volume, 20 μl; column temperature, 30 °C; detector, Shimadzu RF-530 fluorescence spectromonitor ($\lambda_{ex.}$ = 330 nm, $\lambda_{em.}$ = 400 nm); mobile phase, 0.02 M acetate buffer (pH 4.0) - MeOH (1 + 1) containing 5 mmol l^{-1} dodecyltrimethylammonium bromide; and flow-rate, 1.0 ml min^{-1}.

Results and Discussion

Pre-column Derivatisation

Pre-column derivatisation was carried out by reacting cinnamaldehyde with a solution of DMPD in dilute sulphuric acid followed by addition of sodium hydroxide solution. The concentration of sulphuric acid affected the HPLC trace. In order to obtain an acceptable reaction time and the optimum peak height, a sulphuric acid concentration in the range 0.01–0.03 mol l^{-1} was required for the preparation of the DMPD solution. Therefore, the DMPD solution was prepared using 0.015 mol l^{-1} sulphuric acid. The optimum peak height was obtained when the concentration of the DMPD solution was higher than 0.02% m/v. Therefore, a 0.04% m/v DMPD solution was used. The reaction time and temperature for the pre-column derivatisation of cinnamaldehyde using DMPD were examined. As a result, the optimum peak height was obtained after heating for 40 min on a boiling water-bath. Therefore, a reaction time of 50 min was adopted. The shape of the peak was influenced by the amount of sodium hydroxide. When 0.1–1.0 mol l^{-1} sodium hydroxide was used, the peak was sharp. Therefore, a 0.5 mol l^{-1} sodium hydroxide solution was used.

HPLC Conditions

The HPLC conditions for the determination of cinnamaldehyde were the same as those employed previously for vanillin.[8]

Determination of Cinnamaldehyde

Fig. 1 shows a chromatogram of the DMPD derivatives of cinnamaldehyde; two peaks were observed. The calibration graph was constructed from peak 2 and was linear from 0.001 to 30 μg ml^{-1} of cinnamaldehyde in aqueous solution, and the relative standard deviation for 0.05 μg ml^{-1} of cinnamaldehyde was 4.31% (n = 6). The sensitivity of the proposed method was better than that given by GC[3,4] and other HPLC[5–7] methods.

The origin of peaks 1 and 2 will be discussed below.

Fluorescent Product From the Cinnamaldehyde - DMPD Reaction

As mentioned above, the chromatogram shown in Fig. 1 exhibits two peaks. As regards the origin of the two peaks, peak 2 was thought to be derived from cinnamaldehyde and peak 1 from a by-product of cinnamaldehyde. In order to confirm the identities of peaks 1 and 2, cinnamaldehyde was dissolved in dilute sulphuric acid (0.015 mol l^{-1}) and the solution was heated for 50 min on a boiling water-bath. The acidic solution was then examined by HPLC[9,10] using

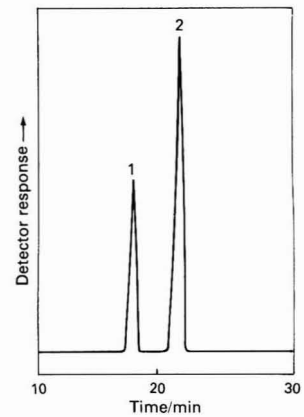

Fig. 1. Chromatogram of the DMPD derivatives of cinnamaldehyde. Cinnamaldehyde taken, 5.0 μg ml^{-1}. 1, 5,6-Dimethyl-2-phenylbenzimidazole; and 2, 5,6-dimethyl-2-styrylbenzimidazole

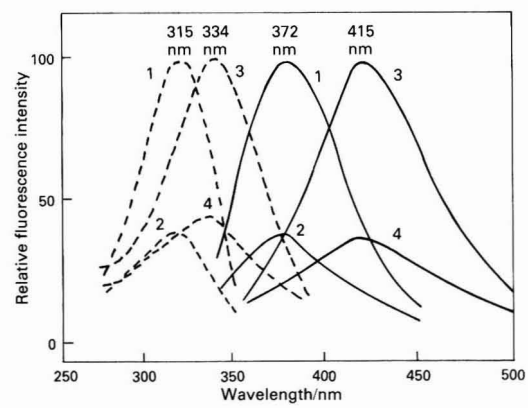

Fig. 2. Excitation (broken line) and emission (solid line) spectra of the DMPD derivatives in eluate. 1, 5,6-Dimethyl-2-phenylbenzimidazole; 2, fluorescent product from benzaldehyde; 3, 5,6-dimethyl-2-styrylbenzimidazole; and 4, fluorescent product from cinnamaldehyde

cyclohexane-1,3-dione, which is a known fluorescent pre-column derivatisation reagent for all aliphatic and some aromatic aldehydes. Benzaldehyde, acetaldehyde and cinnamaldehyde were found to be present in the heated acidic solution of cinnamaldehyde. It was postulated that the acetaldehyde and benzaldehyde originated from cinnamaldehyde and that subsequently two fluorescent benzimidazole derivatives were formed by the condensation of benzaldehyde and cinnamaldehyde, respectively, with DMPD. Acetaldehyde has been shown not to give a fluorescent product with DMPD.[11] It has also been reported that the fluorescent products from the reaction of aromatic aldehydes with DMPD are 5,6-dimethyl-2-phenylbenzimidazole derivatives.[11] Therefore, the authentic samples of 5,6-dimethyl-2-phenylbenzimidazole and 5,6-dimethyl-2-styrylbenzimidazole synthesised in this work were used in an attempt to identify the fluorescent products by HPLC. It was found that the retention time of peak 1 was identical with that of authentic 5,6-dimethyl-2-phenylbenzimidazole and that of peak 2 with 5,6-dimethyl-2-styrylbenzimidazole. Moreover, the eluent fractions containing peaks 1 and 2 were also isolated. The excitation, emission and absorption spectra of the fractions corresponding to peaks 1 and 2 were identical with those of 5,6-dimethyl-2-phenylbenzimidazole and 5,6-dimethyl-2-styrylbenzimidazole, respectively (Figs. 2 and 3). From these results, it was

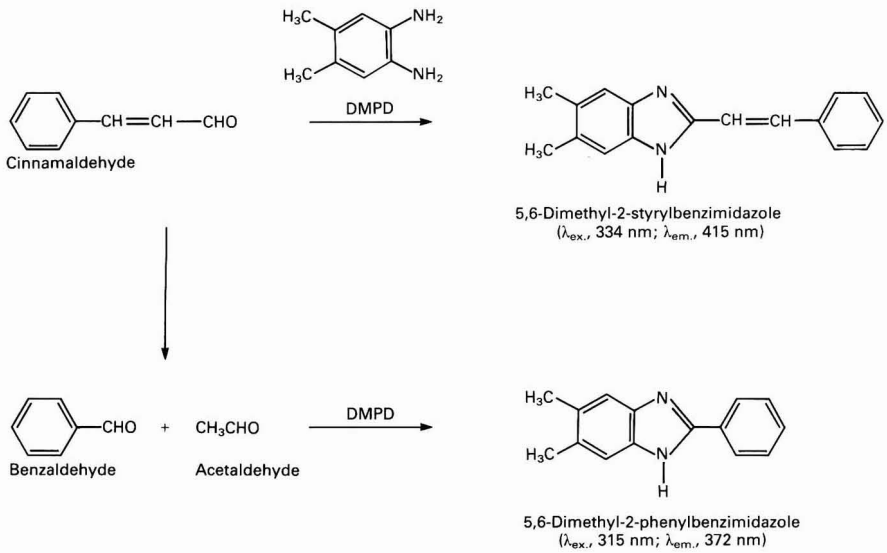

Scheme 1

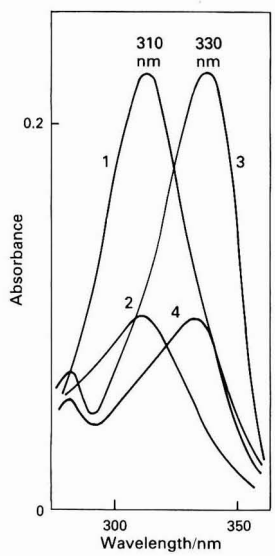

Fig. 3. Absorption spectra of the DMPD derivatives in eluate. 1, 5,6-Dimethyl-2-phenylbenzimidazole; 2, reaction product from benzaldehyde; 3, 5,6-dimethyl-2-styrylbenzimidazole; and 4, reaction product from cinnamaldehyde

concluded that the formation of benzaldehyde was due to some of the cinnamaldehyde reacting with DMPD to form 5,6-dimethyl-2-phenylbenzimidazole, while the remainder reacted with DMPD to form 5,6-dimethyl-2-styrylbenzimidazole (Scheme 1).

In conclusion, DMPD can be used as a fluorescent pre-column derivatisation reagent for the determination of cinnamaldehyde in the range 0.001–30 μg ml^{-1}. The proposed DMPD method is more sensitive than either the GC[3,4] or other HPLC[5–7] methods.

References

1. Dhont, J. H., and Dijkman, G. J. C., *Analyst*, 1967, **92**, 431.
2. Barber, E. D., and Sawicki, E., *Anal. Chem.*, 1968, **40**, 984.
3. Datta, P. R., and Susi, H., *Anal. Chem.*, 1962, **34**, 1028.
4. Chen, W., *Yaoxue Tongbao*, 1987, **22**, 612.
5. Yoshizaki, F., Terasawa, N., and Hisamichi, S., *Jpn. J. Orient. Med.*, 1984, **35**, 23.
6. Komae, H., and Hayashi, N., *J. Chromatogr.*, 1975, **114**, 258.
7. Salagoity-Auguste, M. H., Tricard, C., and Sudraud, P., *J. Chromatogr.*, 1987, **392**, 379.
8. Katayama, M., Mukai, Y., and Taniguchi, H., *Anal. Sci.*, 1987, **3**, 565.
9. Stahovec, W. L., and Mopper, K., *J. Chromatogr.*, 1984, **298**, 399.
10. Suzuki, Y., *Bunseki Kagaku*, 1985, **34**, 314.
11. Katayama, M., Mukai, Y., and Taniguchi, H., *Anal. Sci.*, 1987, **3**, 369.

Paper 9/02243K
Received May 30th, 1989
Accepted August 14th, 1989

Determination of Alkylketene Dimer Sizing Agent Products in Paper by Capillary Gas Chromatography

Peter J. Dart
Albright and Wilson, Avonmouth Works, Bristol BS11 0YT, UK
David V. McCalley
Department of Science, Bristol Polytechnic, Frenchay, Bristol BS16 1QY, UK

A capillary gas chromatographic procedure has been developed for the analysis of alkylketene dimers (AKDs), which are used as sizing agents in paper manufacture. The method is based on the hydrolytic extraction and quantification of long-chain ketones, the identities of which were confirmed by combined gas chromatography - mass spectrometry. The procedure gives good precision (relative standard deviation *ca.* 1%) and acceptable recoveries of AKD products from both surface and internally sized papers (104 and 88%, respectively). It can also be used to determine the fate of AKDs in continuously operated paper-making equipment.

Keywords: *Alkylketene dimer; paper; sizing agent; gas chromatography; long-chain ketone*

"Sizing" is a process carried out to produce paper or board that has an enhanced resistance to penetration by liquids such as water and printing inks. Rosin, which consists of a mixture of resin acids such as abietic acid, is often used as a sizing agent. However, the process can lead to a variety of problems; for instance, the use of chalk to control the pH (typically at 4.0–5.5) leads to evolution of carbon dioxide and foaming.[1] In addition to this problem, a variety of other reasons have led many producers to move to neutral or alkaline systems.[2]

Alkylketene dimers (AKDs) (**I**) are neutral sizing agents that are now widely used.

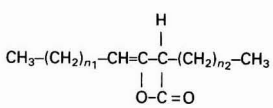

(I)

A fatty acid fraction consisting mainly of palmitic and stearic acids normally acts as the starting material for the preparation of AKDs. This results in values of 13 or 15 for n_1 and n_2 in the structural formula. It has been proposed that AKDs act via a chemical reaction between the lactone ring and cellulose surface hydroxyl groups to form a β-ketoester,[3,4] as shown below.

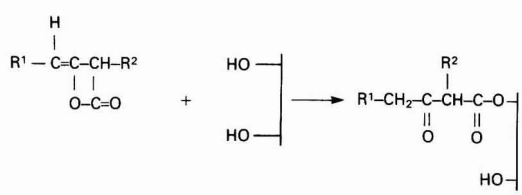

Infrared (IR) and nuclear magnetic resonance spectrometry, calorimetric and solvent extraction studies have been presented to support the above mechanism.[5,6] However, similar investigations have found little or no evidence for the reaction,[2,7] indicating the need for further studies.

Little detailed work has been reported on the quantitative analysis of AKDs in paper and wastewaters. Hydrolysis of AKDs (reacted or unreacted) gives the corresponding ketones according to the following reaction scheme[4]:

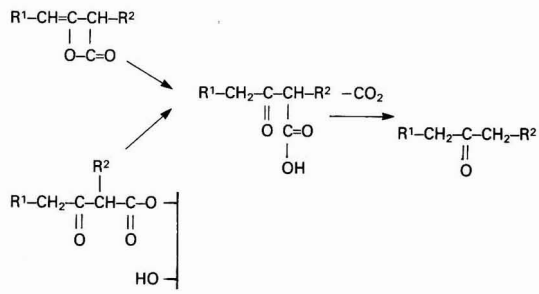

The determination of the ketones by high-performance liquid chromatography (HPLC) with a refractive index detector has been reported,[4,8] and their determination by IR spectrometry has also been investigated.[1]

Although simple tests for water absorption of paper are performed readily, knowledge of the AKD content is still important for the understanding of the process. To minimise production costs the determination of the distribution of AKDs in paper-making machinery can indicate ways in which the sizing agent is lost. Further, the amounts of AKDs retained in paper, together with "cure promoter" chemicals, can influence the storage time required for the paper to achieve sufficient "hardness" for use. In this work, we have investigated further the quantitative analysis of AKDs and report a simple alternative method using capillary gas chromatography (GC) to monitor AKDs via the determination of their hydrolysis products. This method is potentially more sensitive than HPLC with refractive index detection and offers the possibility of confirmation of peak identity by combined gas chromatography - mass spectrometry (GC - MS) which is performed more readily at present than HPLC - MS.

Experimental

Reagents

Analytical-reagent grade sodium carbonate and acetone were obtained from BDH (Poole, Dorset, UK) and HPLC-grade hexane from FSA (Loughborough, Leicestershire, UK). Silanised glass-wool was obtained from Phase Separations (Queensferry, Clwyd, UK).

The AKD suspension was a commercial product, Keydime C (Albright and Wilson, Avonmouth, Bristol, UK). Solid AKDs were obtained from the same source. The AKDs were synthesised from a mixture consisting of stearic and palmitic acids using a proprietary procedure in which the corresponding acid chlorides are reacted in the presence of a suitable catalyst.

Apparatus

A Model 8500 gas chromatograph (Perkin-Elmer, Beaconsfield, Buckinghamshire, UK) equipped with a flame ionisation detector (FID) was used in all experiments. The column used was made of fused silica (12 m × 0.22 mm i.d.) and was coated with a 0.25-μm bonded methyl silicone phase (BP-1, SGE, Melbourne, Australia). The carrier gas was helium at a flow-rate of 1.0 ml min^{-1}. The column was temperature programmed from 150 to 300 °C at 10 °C min^{-1} with a final hold time of 10 min. Samples (1.0 μl) were injected by split injection using the hot-needle technique and a split ratio of 1:10. The injector and detector were maintained at 350 °C. Peak areas and peak heights were obtained from the in-line data station.

A Model 5995C GC-MS instrument (Hewlett-Packard, Wokingham, Surrey, UK) was used for combined GC-MS using identical GC conditions (see above) and the following MS conditions: open split interface, transfer line 320 °C, ion source 240 °C and quadrupole separator 240 °C.

Procedure for Analysis of AKDs

Cut 2.5 g of the paper into small pieces and transfer into a 250-ml flask. Add 25 ml of 0.1 M sodium carbonate solution, reflux for 2 h and then transfer the paper into a Soxhlet cup. Boil down the sodium carbonate solution until almost dry (2–3 ml) and, using the same flask as a receiver, extract the paper with acetone for 4 h. Evaporate to dryness and extract the ketones with three 5-ml aliquots of boiling hexane, transferring into a 25-ml calibrated flask. Add 5 ml of a 250 mg l^{-1} solution of octacosane in hexane as internal standard and dilute to volume with hexane.

Reflux the backwater obtained from normal paper production with sodium carbonate solution and filter through a 0.45-μm membrane filter to remove the fines. Extract the fines from the same process by refluxing with acetone for 4 h and, after removal of the acetone, extract the ketones with hexane as before. Acidify the filtered backwater with dilute HCl and extract with hexane.

Hydrolyse the solid AKDs by a similar procedure; wash the product free of sodium carbonate and purify by recrystallisation from toluene - ethanol (2 + 1).

Calculation of Results

The calibration graph was constructed by weighing known amounts of the AKDs and plotting this value against the GC peak area or peak height of the ketones produced after hydrolysis. For a given batch of AKDs, the amount of each ketone produced was found to be in a constant ratio. Hence the amount of AKDs in a sample sized using this batch could be obtained by comparing the response of samples and standards for one specified ketone. However, a better value should be obtained from an average of several or all of the individual results. Alternatively, the comparison can be based on the combined peak response of the major ketones for samples and standards. The advantage of the latter approach is that the method can still be used for the calculation of AKDs in unknown paper samples, in situations where a standard of the exact AKD mixture (whose composition depends on the stearic acid - palmitic acid content of the starting material) used to size the paper is not available. In the HPLC method,[4] the ketones are not resolved, eluting as a composite peak; hence the procedure is similar. For the proposed GC procedure, the use of this method assumes a similar FID response to each ketone; this assumption was verified in the present study by comparison of results for the same sample using AKD standards from different batches, synthesised from fatty acid mixtures of variable stearic acid - palmitic acid content.

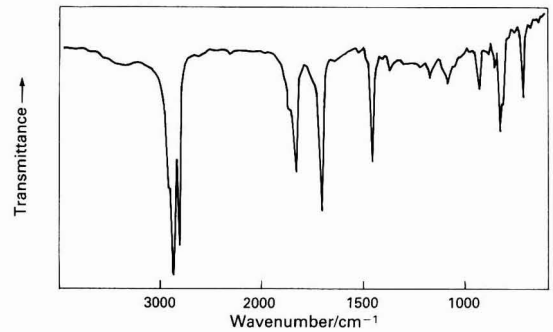

Fig. 1. Infrared spectrum (KBr disc) of AKDs synthesised from a stearic acid - palmitic acid mixture

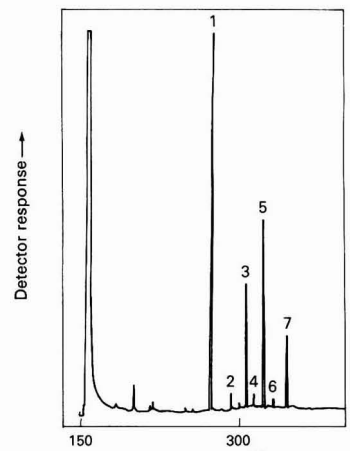

Fig. 2. Chromatogram of the hydrolysis products of AKDs on a 12-m methyl silicone phase capillary column. 1, Octacosane (internal standard); 2, pentadecyl tridecyl ketone; 3, dipentadecyl ketone; 4, hexadecyl pentadecyl ketone; 5, heptadecyl pentadecyl ketone; 6, heptadecyl hexadecyl ketone; and 7, diheptadecyl ketone. Column temperature programmed from 150 to 300 °C at 10 °C min^{-1} with a final hold time of 10 min. Injector/detector temperature, 350 °C. Injection volume, 1 μl; split ratio, 1:10

Results and Discussion

The AKD mixture gave a characteristic IR spectrum (Fig. 1) with major absorption peaks at 1850 and 1720 cm^{-1}. These peaks are due to C=O and C=C absorptions, respectively, and are at high wavenumbers due to the presence of the lactone ring. The peaks were completely absent from the spectrum of the hydrolysis product, which gave a typical C=O stretching peak at 1705 cm^{-1}.

Initial attempts were made to analyse AKD standards directly by GC. However, multiple peaks were obtained which were attributed to thermal decomposition of the material. Hence, subsequent investigation was confined to the GC analysis of the ketones obtained by hydrolysis of the AKDs. Split injection using the "cold-needle" technique showed

Table 1. Some significant ions in the mass spectra of the major ketones produced by hydrolysis of AKDs

Compound	m/z	Possible identity
$C_{15}H_{31}COC_{15}H_{31}$ ..	450	$M^{\cdot+}$
	254	$[C_{15}H_{31}C(OH)=CH_2]^{\cdot+}$
	239	$C_{15}H_{31}C\equiv O^+$
	85, 71, 57, 43	Alkyl-chain fragments
$C_{15}H_{31}COC_{17}H_{35}$ ..	478	$M^{\cdot+}$
	282	$[C_{17}H_{35}C(OH)=CH_2]^{\cdot+}$
	267	$C_{17}H_{35}C\equiv O^+$
	254	$[C_{15}H_{31}C(OH)=CH_2]^{\cdot+}$
	239	$C_{15}H_{31}C\equiv O^+$
	85, 71, 57, 43	Alkyl-chain fragments
$C_{17}H_{35}COC_{17}H_{35}$ ..	506	$M^{\cdot+}$
	282	$[C_{17}H_{35}C(OH)=CH_2]^{\cdot+}$
	267	$C_{17}H_{35}C\equiv O^+$
	85, 17, 57, 43	Alkyl-chain fragments

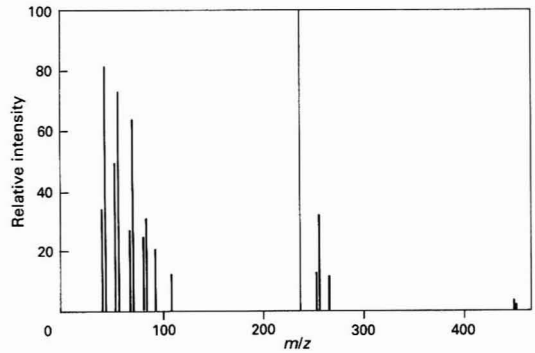

Fig. 3. Mass spectrum of dipentadecyl ketone

considerable discrimination of C_{32}–C_{38} pure alkane standards which were used to test the injector[9]; these alkanes had retention times (15.2–21.7 min) and relative molecular masses similar to those of the ketones under investigation. However, use of the "hot-needle" method combined with a high injection port temperature reduced the discrimination to negligible levels. Fig. 2 shows the separation of the hydrolysis products of an AKD mixture obtained by GC analysis on a short fused-silica capillary column coated with a thin film of methyl silicone phase; three major peaks were obtained. The mixture was analysed by GC - MS in order to confirm peak identity. The major peaks 3 (t_R = 15.7 min), 5 (t_R = 17.4 min) and 7 (t_R = 19.7 min) were identified as dipentadecyl ketone, heptadecyl pentadecyl ketone and diheptadecyl ketone, respectively, based on the following interpretations. In each instance the compounds gave small but distinct molecular ions (relative intensity 2–5%) at the expected *m/z* values. Very intense ions (base peak or near base peak) occurred due to alpha-cleavage and formation of the acylium ion $RC\equiv O^+$. The unsymmetrical ketone (heptadecyl pentadecyl ketone) gave, as expected, the acylium ions $RC\equiv O^+$ and $R'C\equiv O^+$ which were equally intense. Further strong peaks were attributed to beta-cleavage to give the ion $[RC(OH)=CH_2]^{\cdot+}$ via a MaClafferty rearrangement.

As before, the unsymmetrical ketone yielded two ions of this type. Table 1 gives some of the significant ions in the mass spectrum of each compound; the mass spectrum of dipentadecyl ketone is shown as a representative example in Fig. 3. The area of the three major peaks constituted over 90% of the total area of all the peaks detected by GC. The minor peaks 2, 4 and 6 gave spectra of similar appearance and were tentatively identified as pentadecyl tridecyl ketone, hexadecyl pentadecyl ketone and heptadecyl hexadecyl ketone, respectively. These minor diketones were assumed to be the hydrolysis products of small amounts of AKDs formed from fatty acids other than stearic and palmitic acids in the starting material. The identity and amount of all the ketones were as expected considering the composition of the feedstock; no other significant peaks that might indicate side reactions were detected. Direct insertion probe MS at high temperature also failed to reveal any further products other than those shown by GC - MS.

Calibration graphs were constructed of the peak response for individual and total ketones (see under Experimental) obtained by injection of the solution in the final 25-ml calibrated flask against the amount of AKDs taken in milligrams. Based on total ketones the response was linear (correlation coefficient = 0.999) at least over the working range studied (0.67–2.68 mg of AKDs). The response for the individual ketones dipentadecyl ketone, heptadecyl pentadecyl ketone and diheptadecyl ketone was also linear with correlation coefficients of 0.999 in each instance. One of the standards was injected five times on to the column in order to calculate the precision of the measurements; a glass liner packed with glass-wool was utilised throughout the procedure, yielding a relative standard deviation (RSD) for total ketone response of less than 1%. The packed-liner method was found to give superior performance to use of an empty liner.

In the method used to calculate the amount of AKDs, the amounts of ketone hydrolysis products from samples are compared with those from standards treated in the same way. This procedure should compensate for possible incomplete hydrolysis of the AKDs. However, the availability of the purified hydrolysis product (see under Experimental) and consideration of the equation for the reaction allowed a yield of 88% to be calculated, which appeared to be a constant value. This high value is consistent with the spectroscopic and chromatographic data reported above. Initial investigations of the recovery of the procedure were performed by adding the sizing agent to pre-formed paper. In this "surface-sizing" process, a solution of the AKDs in hexane was placed on a sheet, the solvent dried and the AKD content calculated as above. The sheets contained 0.01% Percol 110L, an anionic polyacrylamide retention aid which conceivably might have interfered with the analytical method. However, although a few extra peaks were obtained when analysing paper samples, these appeared in the early part of the chromatogram. Surface sizing gave very high recoveries, close to 100%, with excellent precision as shown in Table 2. However, although surface sizing of paper imparts some resistance to liquids, penetration of the sizing agent is limited and no intimate mixing with the fibres takes place. A minimum reaction time occurs giving the smallest chance for the formation of β-ketoesters. To give a better measurement of the recovery of the procedure, experiments were performed in which the AKDs were mixed intimately with paper pulp prior to formation into a crude sheet and drying in a flat-bottomed evaporating basin; analysis

Table 2. Recovery of AKDs from paper samples. Results are the means of quintuplicate recovery experiments

	Mean recovery, %	Standard deviation, %	RSD, %
Surface sized	104	1.04	1.00
Internally sized (closed system)	88	0.81	0.93

Table 3. Distribution of AKDs in small-scale paper-making equipment. Results are the means of triplicate determinations

AKDs added (2.22 mg)	AKDs found/ mg	Distribution, %
Sheet	1.32	59.6
Fines	0.45	20.3
Backwater	0.26	11.7
	Total:	91.6%

of the AKDs was then performed in the normal way. This procedure constitutes a closed system with no physical losses in which the paper is "internally sized" and provides a better approximation to the conditions under which paper is normally made. Table 2 shows that a reduced recovery of the AKDs was obtained (88%), although excellent precision is again indicated. It is possible that this reduced recovery is caused by reaction of the AKDs with cellulose hydroxyl groups and retention in the paper despite treatment with sodium carbonate and extraction with acetone. However, further studies are necessary to confirm this hypothesis.

Investigation of other reagents for the hydrolysis reaction (*e.g.*, methanolic KOH) did not give increased recovery. Addition of an ester cleaving agent might improve the recovery, although it has been suggested that alkali is sufficient to break the linkage.[2]

In normal paper manufacture, a continuous process is operated in which the AKDs are added, some are retained on paper formed on wire sheets whereas some are lost on paper fines and in the backwater associated with the process. The distribution of added AKDs in the various components of the process was studied by sampling from a small-scale paper-making machine. Table 3 shows the distribution of AKDs in the system, in which a few sheets were made. The results indicate that approximately 92% of the AKDs added to the system were recovered. Significant amounts of AKDs are lost from the system in fines and in the backwater, emphasising the need for recirculation. The cost factor is significant in large-scale systems which are capable of producing over 100 tons of paper per day. The distribution of AKDs varies according to the particular operating conditions of the process equipment; we have already used the method successfully to investigate this distribution in full size paper-making equipment during production trials.

References

1. Browning, B. L., "Analysis of Paper," Second Edition, Marcel Dekker, New York, 1977.
2. Rohringer, P., Bernheim, M., and Werthemann, D. P., *Tappi*, 1955, **68**, 83.
3. Davis, J. W., Roberson, W. H., and Weisgerber, C. A., *Tappi*, 1956, **69**, 21.
4. Kamutzki, W., and Krause, T., *Papier (Darmstadt)*, 1982, **36**, 311.
5. Odberg, L., Lindstrom, T., Liedberg, B., and Gustavsson, J., *Tappi*, 1987, **70**, 135.
6. Nahm, S. H., *J. Wood Chem. Technol.*, 1986, **6**, 89.
7. Roberts, J. C., and Garner, D. N., *Cellul. Chem. Technol.*, 1984, **18**, 275.
8. Kamutzki, W., *Thesis*, Technical University of Darmstadt, 1983.
9. Grob, K., Jr., and Neukom, H. P., *J. High Resolut. Chromatogr. Chromatogr. Commun.*, 1979, **2**, 15.

Paper 9/02477H
Received June 13th, 1989
Accepted July 14th, 1989

Determination of Trace Amounts of Cadmium, Lead, Copper and Zinc in Natural Waters by Inductively Coupled Plasma Atomic Emission Spectrometry With Thermospray Nebulisation, After Enrichment on Chelex-100

Koen Vermeiren, Carlo Vandecasteele* and Richard Dams
Laboratory for Analytical Chemistry, Institute for Nuclear Sciences, Rijksuniversiteit Gent, Proeftuinstraat 86, 9000 Gent, Belgium

Enrichment on Chelex-100, followed by evaporation when necessary, was used for the pre-concentration of Cd, Pb, Cu and Zn from natural waters. The measurements were carried out with inductively coupled plasma atomic emission spectrometry using a thermospray nebulisation system to reach the required sensitivity. The detection limits corresponding to three times the standard deviation of the blank (in 1% v/v HNO_3) after a 30-fold enrichment are 0.02 μg l^{-1} for Cd, 0.33 μg l^{-1} for Pb and 0.03 μg l^{-1} for Cu and Zn. Matrix effects, which are fairly serious with thermospray nebulisation, were taken into account by using the standard additions method. Results obtained for several river water samples were compared with those found by analysis of the non-enriched sample with inductively coupled plasma mass spectrometry or graphite furnace atomic absorption spectrometry. In all instances the agreement was satisfactory.

Keywords: *Water analysis; pre-concentration; thermospray nebulisation; matrix effect; inductively coupled plasma atomic emission spectrometry*

Sensitive and accurate analysis methods are required to monitor the pollution by heavy metals of surface waters that serve as raw materials for the production of drinking water. In this work Cd, Pb, Cu and Zn were determined in some water samples from the Belgian rivers Samber and Maas by inductively coupled plasma atomic emission spectrometry (ICP-AES). One mineral and one tap water sample were also analysed. The elements Cd, Pb, Cu, and Zn were selected, because they are considered to be major water pollutants and their average concentration in river water is comparable to or below the detection limit of ICP-AES using pneumatic nebulisation.[1] For Cd, and to a lesser extent Pb, this is still the case even after a 10-fold pre-concentration by evaporation.[1] A thermospray nebulisation system (TNS), developed in this laboratory,[2,3] was applied to improve the detection limits. Matrix effects associated with the TNS are more important than with pneumatic nebulisation and were studied as a function of the matrix concentration. Because the concentrations of the trace elements considered (with the exception of Zn) are, however, in the samples studied, comparable to the detection limits attainable even with the TNS,[3] an enrichment was still required.

Boniforti *et al.*[4] compared ion exchange with Chelex-100, complexation with ammonium pyrrolidinedithiocarbamate (APDC) followed by extraction in isobutyl methyl ketone and coprecipitation with the hydroxides of Fe and Mg for the enrichment of Cr, Mn, Fe, Co, Ni, Cu and Zn from sea water. They concluded that ion exchange was the method of choice because lower blanks, better recoveries (except for Cr) and higher pre-concentration factors could be obtained.

Because the affinities of Chelex-100[5] for Cd, Pb, Cu and Zn are high and those for matrix elements such as Na, Ca and Mg are low, removal of the matrix can be achieved simultaneously with the fixation of the trace elements. For the above reasons, ion exchange with Chelex-100 was chosen. The pre-concentration was optimised so that it could handle all kinds of natural waters, from mineral water to sea water. A 30-fold simultaneous pre-concentration of Cd, Pb, Cu and Zn was aimed at during this optimisation. The approach is similar to that of Berman *et al.*[6] who also used pre-concentration by ion exchange with Chelex-100 for the determination of five trace elements (Fe, Mn, Cu, Zn and Ni) in sea water by ICP-AES. However, they used ultrasonic nebulisation to introduce the metal concentrates into the plasma.

To evaluate the accuracy of the results obtained for the river water samples, each element was also determined with at least one independent technique. Inductively coupled plasma mass spectrometry (ICP-MS) and graphite furnace atomic absorption spectrometry (GFAAS) were used, as they are very sensitive, hence permitting direct analysis of the non-enriched river water samples.

Experimental

Reagents

Chelex-100 (sodium form, 200–400 mesh) was obtained from Bio-Rad Laboratories (Richmond, California, USA). Sub-boiling HNO_3 was prepared in the laboratory. Suprapur NH_4OH and CH_3COOH (Merck, Darmstadt, FRG) were used for preparation of the buffer and a Milli-Q (Millipore, Bedford, MA, USA) system was used for the preparation of 18 MΩ water. The ion-exchange columns were manufactured from polypropylene tips (Finntip 62, 5 ml) purchased from Labsystems (Helsinki, Finland).

Analytical-reagent grade $NaNO_3$ (Carlo Erba, Milan, Italy) and $Ca(NO_3)_2$ (UCB, Brussels, Belgium) were used for the study of the matrix effects.

Element standards (Fluka, Buchs, Switzerland, 1.00 g l^{-1}) were used as stock solutions for the preparation of the standard solutions. For the dilution 1% v/v HNO_3 was used.

Instrumentation and Measurement Conditions

The ICP-AES instrumentation includes a computer-controlled monochromator (Jobin-Yvon 1000 VHR), a Plasma-Therm HFP-2500 D r.f. generator and a laboratory-built TNS consisting of an electrically heated stainless-steel capillary (30 × 0.018 cm) mounted in a heated spray chamber (HSC).[3] Samples are injected using a flow injection system as described in reference 3. The operating conditions are summarised in Table 1.

For some measurements a Meinhard TR-50-C3 pneumatic nebuliser in combination with an impaction-based spray chamber was used (PNS).

* To whom correspondence should be addressed.

Table 1. Operating conditions of the TN-HSC

Sample flow-rate	1.3 ml min^{-1}
Power applied to the capillary	45 W
Carrier gas flow-rate	0.9 l min^{-1}
Power applied to the heating tape	70 W
Cooling water temperature	10–20 °C

Table 2. Measurement conditions for the ICP-MS determination of Cd, Pb and Zn

Mass range	62–212 u
Number of sweeps per measurement	120
Number of channels	4096
Integration time per channel (per sweep)	250 μs
Number of measurements per sample	3

Table 3. Measurement conditions for the determination of Cu with GFAAS

Sample volume	50 μl
Lamp current	7 mA
Drying time (120 °C/250 °C)	20 s/20 s
Ashing time (700 °C)	20 s
Atomisation time (2300 °C)	5 s
Cleaning time (2700 °C)	3 s
Number of measurements per sample	3

The most sensitive emission line (*i.e.*, 220.353 nm for Pb II, 228.802 nm for Cd I, 324.754 nm for Cu I and 213.856 nm for Zn I) could be used in each instance as it was free from spectral interference. For the measurement of the elements Cd, Pb, Cu and Zn, spectral windows were measured around the profile maximum.[7] Each window consisted of 50 channels centred around the analysis line. The separation between channels was 0.027 nm. An integration time of 125 ms per channel was used. Each sample was measured four times with the measurements being performed at the compromise observation height of 13 mm. The physical slit height and slit width were 5 mm and 30 μm, respectively.

For the ICP-MS measurements a VG PlasmaQuad was used, equipped with a PNS. The measurement conditions are summarised in Table 2. Cadmium and Pb were measured with this technique using their most abundant isotopes (^{114}Cd and ^{208}Pb, respectively) and Zn was also measured with ICP-MS using the ^{66}Zn isotope. The ^{64}Zn isotope could not be used for measurement because it suffered interference from $^{32}S^{16}O_2^+$. This ion is produced from sulphate in the samples. The mean sulphate content in the Maas is about 40 mg l^{-1}.[8]

Copper was determined with GFAAS, because its determination with ICP-MS suffers from interferences. The ^{63}Cu isotope suffers interference from $^{40}Ar^{23}Na$ and ^{65}Cu from $^{32}S^{33}S$ and from $^{33}S^{16}O^{16}O$. A Perkin-Elmer 3030 atomic absorption spectrometer equipped with a deuterium background correction system, an HGA 400 programmer and an AS-40 autosampler was therefore used. Table 3 summarises the measuring parameters.

Results and Discussion

Pre-concentration on Chelex-100

Because the spectrometer used for the ICP-AES determinations is a slow scanning monochromator equipped with a small computer system (Digital PDP 11/04), a sample volume of 5 ml per element is necessary with the TNS to produce a steady-state signal sufficiently long to carry out the measurements (see also Table 1). This means that to obtain a 30-fold enrichment, the necessary starting volume is 750 ml.

Influence of the amount of resin

To evaluate the optimum amount of resin for each sample type, 750 ml of sample (buffered at pH 5.0; see below), to which known amounts of Cd, Pb, Cu and Zn were added, was passed through a certain amount of Chelex-100. The eluate was collected into eight fractions, which were analysed with ICP-AES (using the PNS). This procedure allows a possible breakthrough to be detected and provides an approximate recovery value. The smallest amount of resin yielding an almost quantitative retention of the elements was considered to be optimum.

Initial experiments carried out with 750 ml of mineral and tap water showed that 1 g of Chelex-100 is sufficient for the enrichment of Cd, Pb, Cu and Zn. Using this amount of resin for the enrichment of Cd, Cu and Zn from sea water (which was used as the water sample most heavily loaded with salt matrix) resulted, however, in recoveries of only 13% for Cd, 69% for Cu and 62% for Zn. No tests were carried out for lead, as the detection limit for this element is insufficient. The lower values for Cu and Zn are the result of their competition with the matrix ions (Na, Ca and Mg) present in the sample. The low recovery for cadmium is also due to the formation of chloride complexes. Calculations on the basis of the equilibrium constants[9] show that the ratio Cd^{2+}/Cd_{tot} is only 0.004 in sea water (c_{Cl^-} = 0.585 M or 20.74 g l^{-1}) but 0.876 in a typical drinking water sample (c_{Cl^-} = 0.0014 M or 50 mg l^{-1}). Using 3 g of Chelex-100 instead of 1 g, for a test sample containing 250 μg of each of Cd, Pb, Cu and Zn, these elements could not be detected in the solution passed through the column.

Influence of pH

The influence of pH was only partly examined. Almost quantitative recoveries were obtained in the pH range 4.7–5.2, in agreement with the findings of other workers[10,11] and the recommendations of the manufacturer.[5] For river water, we found that the recovery of Cd diminished slowly with pH (82% at pH 5.5, 77% at pH 6.0), whereas that for Pb decreased more rapidly (only 15% at pH 6.0).

Before enrichment, the 750 ml sample was adjusted to pH 5.0 ± 0.5 with HNO_3 - NH_4OH. Afterwards, a 7.5-ml aliquot of CH_3COOH - NH_4OH buffer (0.5 M, pH 5.00) was added, which adjusted the pH further to 5.00 ± 0.05. Before the separation, the resin was purified with nitric acid leaching and equilibrated with 20 ml of 0.005 M CH_3COOH - NH_4OH buffer solution.

Flow-rate

A peristaltic pump was used (Gilson, Minipuls 2) to obtain a flow-rate of 2.5 ml min^{-1}. For a 750-ml sample, the total enrichment time is approximately 6 h. For most samples the enrichment was, therefore, carried out overnight. With some river water samples an expansion of the resin was observed, resulting in a lower flow-rate.

Elution of the bound trace elements

For Cd and Pb fixed on 1 g of Chelex-100 it was found that 10 ml of 1% HNO_3 was sufficient to remove these ions completely. When 3 g of Chelex-100 are used, the necessary elution volume is naturally greater. Fig. 1 shows the elution histograms of 250 μg of Cd, Zn and Cu bound to 3 g of Chelex-100 with 1% HNO_3. As can be seen, the elution of Cd and Zn is very fast. For Pb (not shown in Fig. 1) a volume of 30 ml was sufficient. However, to elute the strongly bound Cu completely, 65 ml of 1% HNO_3 are required.

To obtain sufficient enrichment for each element, an elution volume of 65 ml of 1% HNO_3 was used in each instance. The acidic eluate was evaporated to near dryness in a covered and pre-cleaned PTFE beaker and the residue was redissolved in 25 ml of 1% HNO_3. If only Cd, Zn, and Pb (not Cu) are of interest then this evaporation step is not required as these elements can be eluted with 30 ml of eluate.

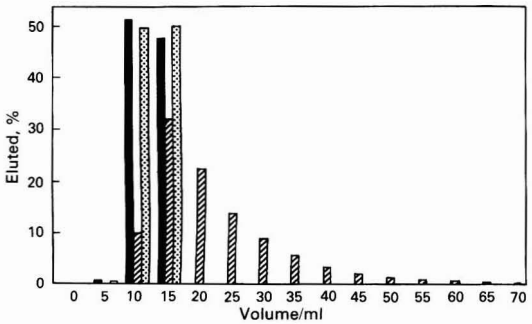

Fig. 1. Elution histograms of 250 μg of Cd (■), Cu (▨) and Zn (▤) bound to 3.0 g of Chelex-100 with 1% HNO_3

Table 4. Element blanks (ng) associated with the proposed enrichment procedure

Element	Blank 1–3, ICP-AES	Blank 4, ICP-MS
Cd	<8	<1
Pb	<100	17 ± 1
Cu	<15	<5
Zn	12 ± 3	<18

Blank

Low element blanks are of course a prerequisite for the analysis of natural water samples. During initial experiments high blank values were found for Pb (>400 ng) and to a lesser extent also for Cu (>75 ng) and Zn (>150 ng). First, it was necessary to purify the commercial Chelex-100 resin. This was realised by rinsing the column with 50 ml of 10% HNO_3, 10 ml of 1% HNO_3 and 10 ml of 18 MΩ water, respectively. Further, the earlier used CH_3COOH - CH_3COONa buffer was replaced by the purer CH_3COOH - NH_4OH buffer. Finally, the use of polypropylene tips instead of coloured Eppendorf tips or Suprasil quartz columns resulted in a substantial reduction of the blank.

Table 4 summarises the residual blank values after the above precautions had been taken. Three blanks were determined by ICP-AES (using the TNS, no correction for matrix effects was applied) and a fourth with ICP-MS. The blanks were treated exactly the same as the analysed samples. They incorporate the impurities of all reagents used in addition to the contaminations resulting from contact with all materials used. The blank measured by ICP-MS proves that the actual blank values for Cd and Pb are much lower than can be determined by ICP-AES.

After filtration, the samples were acidified to pH 1.0 with sub-boiling HNO_3. Before enrichment, they were adjusted to pH 5.0 with Suprapur NH_4OH. The blanks from these reagents, measured by the evaporation of 25 ml followed by its uptake in 25 ml of 1% HNO_3, were negligible.

Detection limits

For Cd, Pb, Cu and Zn the attainable detection limits [3s (s = standard deviation), 1% HNO_3] after a 30-fold pre-concentration are 0.02, 0.33, 0.03 and 0.03 μg l^{-1}, respectively. For real water samples, slightly worse detection limits are obtained.

Matrix Effects

The reason for the occurrence of matrix effects (defined as the relative sensitivity in the presence of a matrix to that in the absence of a matrix) when using the TNS was discussed in detail in a previous paper.[3] With respect to the analysis of natural waters, it was necessary to study the matrix effect quantitatively. The matrices studied were $NaNO_3$ and $Ca(NO_3)_2$, and the analytes Cd, Cu and Zn. The matrices were chosen because Na and Ca are the major constituents in many natural water samples. Their nitrate salts were used because the elution takes place with 1% HNO_3. The matrix concentrations were varied between 30 and 3000 mg l^{-1} whereas the analyte concentration was kept at 1 mg l^{-1}.

Table 5. Matrix effect for Cd, Cu and Zn as a function of the concentration of $NaNO_3$. Analyte concentration, 1 mg l^{-1}

Matrix concentration/ mg l^{-1}	Matrix effect		
	Cd	Cu	Zn
30	0.92	0.99	1.02
100	0.83	0.95	0.98
300	0.77	0.90	0.91
1000	0.74	0.82	0.80
3000	0.68	0.68	0.63

Table 6. Matrix effect for Cd, Cu and Zn as a function of the $Ca(NO_3)_2$ concentration. Analyte concentration, 1 mg l^{-1}

Matrix concentration/ mg l^{-1}	Matrix effect		
	Cd	Cu	Zn
30	0.96	0.93	0.94
100	0.87	0.92	0.88
300	0.84	0.86	0.83
1000	0.74	0.82	0.74
3000	0.68	0.77	0.70

Table 7. Data concerning the matrix ions on enrichment of 750 ml of seawater on 3.0 g of Chelex-100

Element	A*/ mg l^{-1}	B†/ mg	C‡		D§/ mg l^{-1}
			mg	%	
Ca	452	339	7.06	2.2	304
Mg	1056	792	10.0	1.3	402
Na	11150	8363	20.1	0.2	803

* A = concentration in seawater.
† B = amount applied on resin.
‡ C = amount bound on resin.
§ D = residual matrix concentration in the final 25-ml 1% HNO_3 fraction.

Tables 5 and 6 give the relative sensitivities for Cd, Cu and Zn, respectively, in the presence of both matrices. The measurement precision was better than 1% relative standard deviation (four measurements). As can be seen, significant sensitivity reductions occur for matrix concentrations of about 100 mg l^{-1}. The over-all mean sensitivity at the highest matrix concentration is about 30% smaller than that in the absence of a matrix. For a matrix effect of 0.70, the residual gain in sensitivity of the TNS *versus* a classical PNS is still a factor of 17.[3] The exact reasons for the inter-element differences have not yet been elucidated, but might be due to the "aerosol ionic redistribution" process.[12]

Residual Matrix Concentrations After Enrichment

The residual matrix concentration after enrichment should be lower than 100 mg l^{-1} before matrix effects can be neglected with the TNS. Kingston *et al.*,[13] who determined trace elements in sea water with AAS following enrichment on Chelex-100, described a method to selectively remove matrix ions (as Ca, Mg and Na) before the trace elements were stripped from the column. By using a CH_3COOH - NH_4OH buffer all matrix ions are replaced by NH_4^+, which can be volatilised as NH_4NO_3 during the ashing step of the AAS determination, finally resulting in decreased background

absorption. With the TNS system, however, the interference problems can obviously not be omitted in this way. Further, the method suffers from a number of disadvantages.

Table 7 summarises important data for a sea water sample concerning the binding and subsequent removal of Na, Ca and Mg on Chelex-100. Although Ca, Mg and Na are removed for 97.8, 98.7 and 99.8%, respectively, the total matrix concentration remaining in the final solution amounts to 1.5 g l^{-1}, resulting in a signal depression of approximately 30% (see Tables 5 and 6). Hence correction is necessary.

First, internal standardisation was performed with Y (50 μg l^{-1}) as internal standard. This method would have the advantage that only one sample fraction of 750 ml needs to be enriched. As a volume of 5 ml is required for every element quantification, a final volume of 25 ml is indeed sufficient for the measurement of all analytes (Cd, Pb, Cu and Zn) and the internal standard (Y). Simple aqueous standards (also containing Y at 50 μg l^{-1}) could be used for calibration. It appears, however, from Tables 5 and 6 that an important undercompensation occurs for Cd at the lower concentrations of $NaNO_3$. Overcompensation occurs for Cu at the highest concentrations of $Ca(NO_3)_2$. Internal standardisation, albeit simple and fast to implement, hence does not allow accurate correction in each instance. Therefore the standard additions method was the preferred method to correct for these interferences.

Standard Additions Procedure

From considerations of sample consumption, already discussed above, it is clear that in order to carry out the standard additions while maintaining the pre-concentration factor of 30, two sample fractions must be enriched. First, a 750-ml fraction (denoted as M) is enriched on a column. The second sample fraction (MS) is pre-concentrated after the addition of a known amount of all the elements to be determined. In order to also know the recovery for each individual sample, a third sample fraction (MS′) was enriched. After elution of the trace elements from this column, an equal amount of the trace elements is added, as for the second column. The amount of standard added was 2.50 μg. This addition was performed by adding 250 μl (Transferpette, Brand, Wertheim, FRG) of a 10 mg l^{-1} multi-element standard of Cd, Pb, Cu and Zn. If repeated analysis on a certain sample type always provides quantitative recoveries, one can of course omit the last column experiment. In practice, the different sample fractions were enriched simultaneously using a multi-channel peristaltic pump. If desired, the enrichment could be operated overnight using a timer system.

The uncertainty on the analytical result, obtained by a single determination using the standard additions procedure, is largely determined by measurement imprecisions (on M, and to a lesser extent on MS). The uncertainty on the standard added can be neglected compared with those on the measured intensities. A basic equation of the error propagation theory[14] was used to calculate the standard deviation on the final concentration value as given in Tables 9–12.

Analysis of River Water

Sampling

Six river water samples were taken from the Belgian rivers Samber and Maas, known to be considerably polluted with heavy metals. Fig. 2 shows their geographic location and the sampling positions. Table 8 gives the concentrations of Na, Ca and Mg at each sampling location, as measured by ICP-AES using a pneumatic nebuliser. In all instances it was possible to sample in the middle of the river, either from the top of a bridge or from a sluice. The samples were taken with a pre-cleaned polyethylene bottle (2 l), from which the mouth had been removed, attached at the end of a two-piece aluminium bar (total length, approximately 6 m). For sampling from a bridge, the plastic container was lowered and raised by means of a double length of nylon cord (maximum sampling depth, approximately 10 m).

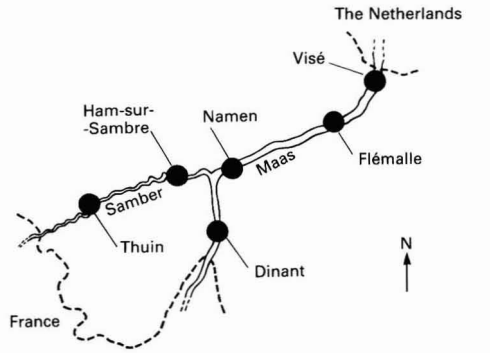

Fig. 2. Geographic location of the Maas and Samber rivers (● indicates the sampling positions)

Table 8. Concentrations of Na, Ca and Mg in the river water samples

River	Na/ mg l^{-1}	Ca/ mg l^{-1}	Mg/ mg l^{-1}
Samber—			
Thuin	16	109	10
Ham-sur-Sambre	106	241	15
Maas—			
Dinant	6	79	5
Namen	18	96	6
Flémalle	18	100	7
Visé	18	93	7

On each site about 8 l of water were sampled and transferred into a 10-l pre-cleaned PVC container. Within 24 h, two fractions (2 l + 0.25 l) of the homogenised sample were filtered on a Whatmann (cellulose) fibre filter followed by a 3-μm Nuclepore (polycarbonate) filter. After filtration, the fractions were acidified to pH 1. The 2-l fraction was used for the enrichment of Cd, Pb and Cu, and Zn was determined (in the 0.25-l fraction) directly with ICP-AES (using the TNS), as its concentrations were sufficiently high.

Although a significant fraction of the trace metals may be adsorbed on particulate matter, only the filtrate was analysed in this study.

Enrichment

Three river water fractions (each about 670 ml) were enriched on three separate columns as explained above. The mean recoveries for the six river water samples for Cd, Pb and Cu were 98.2, 103.5 and 86.2%, respectively.

Because the concentrations of matrix ions in the Samber and the Maas are much lower than in sea water (compare Tables 8 and 7), and as the same amount of resin was used as for the enrichment of sea water (*viz.*, 3 g), the removal of Ca and Mg in percentage terms was lower than in sea water, *viz.*, 72.3 and 83.4%, respectively. The method of standard additions was used for calibration.

Results with different techniques

The contents of Cd, Pb, Cu and Zn in the river water samples, obtained with the different techniques described earlier, are given in Tables 9–12, respectively. The ICP-AES results (using the TNS) were obtained after a 25-fold enrichment on Chelex-100 (apart from Zn). The uncertainties given on all results are the 95% confidence intervals corresponding with the measurement error only.

Table 9. Comparison of the Cd content (μg l^{-1}) in river water samples obtained with different techniques

River	ICP-AES (228.802 nm)	ICP-MS (^{114}Cd)
Samber—		
Thuin	0.09 ± 0.02	0.09 ± 0.02
Ham-sur-Sambre	0.13 ± 0.03	0.11 ± 0.04
Maas—		
Dinant	0.08 ± 0.02	0.07 ± 0.02
Namen	0.03 ± 0.01	0.08 ± 0.01
Flémalle	0.51 ± 0.03	0.67 ± 0.12
Visé	0.22 ± 0.02	0.25 ± 0.04

Table 10. Comparison of the Pb content (μg l^{-1}) in river water samples obtained with different analysis techniques

River	ICP-AES (220.353 nm)	ICP-MS (^{208}Pb)
Samber—		
Thuin	1.7 ± 0.5	1.1 ± 0.1
Ham-sur-Sambre	2.8 ± 0.5	2.3 ± 0.4
Maas—		
Dinant	0.7 ± 0.3	0.5 ± 0.1
Namen	1.2 ± 0.4	0.8 ± 0.3
Flémalle	0.9 ± 0.3	0.82 ± 0.04
Visé	2.2 ± 0.6	1.7 ± 0.1

Table 11. Comparison of the Cu content (μg l^{-1}) in river water samples obtained with different analysis techniques

River	ICP-AES (324.754 nm)	GFAAS (324.7 nm)
Samber—		
Thuin	2.1 ± 0.2	2.0 ± 0.2
Ham-sur-Sambre	2.7 ± 0.2	2.0 ± 0.1
Maas—		
Dinant	1.4 ± 0.2	1.4 ± 0.4
Namen	1.27 ± 0.04	1.6 ± 0.1
Flémalle	2.5 ± 0.1	2.7 ± 0.3
Visé	2.24 ± 0.06	2.2 ± 0.2

Table 12. Comparison of the Zn content (μg l^{-1}) in river water samples obtained with different analysis techniques

River	ICP-AES (213.856 nm) TNS	ICP-AES (213.856 nm) PNS	ICP-MS (^{66}Zn)
Samber—			
Thuin	25.6 ± 1.7	26.1 ± 1.7	23.8 ± 1.7
Ham-sur-Sambre	30.5 ± 1.3	32.4 ± 1.6	30.0 ± 3.2
Maas—			
Dinant	7.4 ± 0.5	7.1 ± 2.0	6.5 ± 0.3
Namen	10.5 ± 0.4	9.5 ± 1.6	9.8 ± 0.8
Flémalle	19.8 ± 1.0	19.4 ± 1.7	16.8 ± 1.4
Visé	46.4 ± 0.4	46.5 ± 1.8	42.8 ± 3.5

The agreement between the ICP-AES and ICP-MS results for Cd is satisfactory, except for the samples taken at Namen and Flémalle. The deviation for the Namen sample is analytically less significant, as the Cd content is close to the limit of detection with both methods (the detection limit for Cd with ICP-MS is about 0.04 μg l^{-1} for the measurement conditions used).

Although the results for Pb obtained with ICP-AES are systematically higher than those found with ICP-MS, they all agree with the latter within the 95% confidence intervals. The large uncertainty on the ICP-AES results is a consequence of the low levels of Pb and the poor sensitivity for Pb. The mean Pb content in the samples is only about three times the limit of detection, *viz.*, 0.4 μg l^{-1}.

For Cu, all ICP-AES results, except for the Ham-sur-Sambre sample, agree well with those found with GFAAS. The deviation for the Namen sample is not very significant, as the ICP-AES uncertainty for this determination was exceptionally low compared with the typical uncertainties, for instance on the sample taken at Dinant.

For Zn, the ICP-AES results obtained with the TNS and those found with the PNS, are in excellent agreement with each other. The measurement precision with the TNS for the lowest Zn concentrations is four times better than that achievable with the PNS. Further, the ICP-AES results in general, match well those obtained with ICP-MS.

Table 13. Analysis results (μg l^{-1}) obtained with ICP-AES for some other natural waters using the TNS

Element	Mineral water	Tap water
Pb	<0.04	4.0 ± 0.6
Cd	<0.02	0.17 ± 0.02
Cu	—	3.5 ± 0.2
Zn	—	252 ± 10

Results for Other Natural Waters

For the enrichment of the mineral water 1 g of Chelex-100 was used and Cd and Pb were determined with ICP-AES using the TNS. The tap water sample (also pre-concentrated on 1 g of Chelex-100) was taken at an end user, connected to the water supply system of Gent.

The analysis results are listed in Table 13. The uncertainties correspond with the 95% confidence interval associated with the measurement error only.

The results show that the concentrations of Cd and Pb in the mineral water Evian are at least one order of magnitude lower than those found in the tap water sample. The sensitivity of the proposed developed method is insufficient, but the sensitivities of ICP-MS and GFAAS are also insufficient for the direct determination of Cd and Pb in this mineral water.

Conclusions

It has been shown that Cd, Pb, Cu and Zn can be pre-concentrated almost quantitatively from different types of natural waters (mineral water, tap water, river water and sea water). To obtain an enrichment factor of 30 with the proposed method, a sample volume of 1.5 l is necessary. If pre-concentration with Chelex-100 is combined with ICP-AES using thermospray nebulisation, detection limits (except for Pb) of the order of 0.02 μg l^{-1} can be achieved. It has also been shown that the method of standard additions can be used to correct multiplicative interferences in the presence of a matrix. The results obtained for six river water samples were compared with those found by the analysis of the non-enriched sample with ICP-MS (Cd, Pb and Zn) or GFAAS (Cu). In all instances the agreement was satisfactory, showing the potential of the proposed method for accurate determinations of trace elements

The major drawback of the enrichment method is the large sample volume needed. As a consequence, the enrichment procedure is time consuming (several days). Clearly, some important modifications are required to adapt the method for routine analysis. The slow scanning monochromator of our ICP-AES instrumentation, which requires a large sample volume for the measurements, is indeed the limiting factor.

Grateful acknowledgement is made to H. Vanhoe for help with the ICP-MS measurements, to B. Desmet for technical assistance with the GFAAS measurements and to the National Fund for Scientific Research (Belgium) (NFWO) and Inter-university Institute for Nuclear Sciences (IIKW) for financial support. K. V. is a research assistant and C. V. a research director with the NFWO.

References

1. Thompson, M., Ramsey, M. H., and Pahlavanpour, B., *Analyst*, 1982, **107**, 1330.
2. Vermeiren, K. A., Taylor, P. D. P., and Dams, R., *J. Anal. At. Spectrom.*, 1987, **2**, 383.
3. Vermeiren, K. A., Taylor, P. D. P., and Dams, R., *J. Anal. At. Spectrom.*, 1988, **3**, 571.
4. Boniforti, R., Ferraroli, R., Frigieri, P., Heltai, D., and Queirazza, G., *Anal. Chim. Acta.*, 1984, **162**, 33.
5. Bio-Rad Laboratories, Chemical Division, Product Information, "Using Chelex-100 Chelating Resin," March, 1981.
6. Berman, S. S., Mclaren, J. W., and Willie, S. N., *Anal. Chem.*, 1980, **52**, 488.
7. Taylor, P., and Schutyser, P., *Spectrochim. Acta, Part B*, 1986, **41**, 81.
8. Rijks Institut voor Wateranalyse (RIWA), Annual report of the Maas (1983–1984) RIWA, The Netherlands.
9. Freiser, H., and Fernando, Q., "Ionic Equilibria in Analytical Chemistry," John Wiley, New York, 1963, Appendix (Table III), p. 306.
10. Sturgeon, R.E., Berman, S. S., Desaulniers, A., and Russell, D., *Talanta*, 1980, **27**, 85.
11. Rasmussen, L., *Anal. Chim. Acta*, 1981, **125**, 117.
12. Borowiec, J. A., Boorn, A. W., Dillard, J. H., Cresser, M. S., Browner, R. F., and Matteson, M. J., *Anal. Chem.*, 1980, **52**, 1054.
13. Kingston, H. M., Barnes, I. L., Brady, T. J., Rains, T. C., and Champ, M. A., *Anal. Chem.*, 1978, **50**, 2064.
14. Bevington, P. R., "Data Reduction and Error Analysis for the Physical Sciences," McGraw-Hill, New York, 1969, Chapter 4.

Paper 9/01911A
Received May 8th, 1989
Accepted August 2nd, 1989

Enrichment of Trace Amounts of Copper as Chelate Compounds Using a Finely Divided Ion-exchange Resin

Kunio Ohzeki, Masea Minorikawa, Fumihiko Yokota, Isoshi Nukatsuka and Ryoei Ishida
Department of Chemistry, Faculty of Science, Hirosaki University, Hirosaki 036, Japan

The enrichment of trace amounts of copper as complexes with various chelating agents was examined with the use of finely divided anion- and cation-exchange resins of the macroreticular type. Of the 16 chelating agents studied, bathocuproinedisulphonate (BCS) combined with the use of a finely divided anion-exchange resin was the most effective for the rapid enrichment of copper from large sample volumes. The resin particles holding the copper(I) - BCS complex were collected on a membrane filter and subsequently suspended in a small volume of 0.1 M hydrochloric acid. The resin suspension was then subjected to electrothermal atomisation atomic absorption spectrometry. The method was applied to the determination of copper in sea and river water samples and the results were compared with those obtained by densitometric measurement of the solid-state absorbance of the copper(I) - BCS complex in the resin phase.

Keywords: *Copper determination; bathocuproinedisulphonate; finely divided ion-exchange resin; electrothermal atomisation atomic absorption spectrometry; densitometry*

Finely divided ion-exchange resin particles are well suited for the rapid enrichment of ions from large volumes because, apart from being able to adsorb ions rapidly,[1] they can be dispersed throughout the bulk in a short time with sufficient stirring[2] and collected on a membrane filter by filtration under suction forming a thin layer.[3–5] The enrichment can be made selective with the use of complexing agents which react with the desired trace metal ions to form a complex having a high affinity for ion-exchange resins. Finely divided anion-exchange resins of the macroreticular type have been used for the pre-concentration of trace metal ions for their determination by solid-state spectrophotometry,[3–5] in which the metal ions are enriched as a coloured complex in the resin thin layer and determined directly by measuring the solid-state absorbance of the complex in the resin phase.

The application of atomic absorption spectrometry to the direct determination of metal ions enriched on an ion-exchange resin has been reported,[6–9] in which a single resin bead or the resin suspension was introduced directly into the graphite furnace for electrothermal atomisation atomic absorption spectrometry (ETAAS). Here also, a rapid and quantitative enrichment of the desired trace metal ions with small amounts of resin was required.

The aim of this work was to develop an effective method for the enrichment of trace amounts of copper by the combined use of finely divided ion-exchange resins and chelating agents. The strongly basic anion-exchange resins, Amberlyst A-27 and DIAION PA318, a weakly basic anion-exchange resin, DIAION WA30, and a strongly acidic cation-exchange resin, DIAION PK228, all of the macroreticular type, were selected as the adsorbents. The 16 chelating agents, including bathocuproinedisulphonate, were examined to determine the factors affecting the affinity of copper-(I) and -(II) chelates for the anion- and cation-exchange resins. In addition, the adsorption of the copper chelates on Amberlyst A-27 was compared with their adsorption on a cellulose nitrate membrane filter. The proposed enrichment method was applied to the determination of copper in water samples by solid-state spectrophotometry and ETAAS.

Experimental

Apparatus

A Nippon Jarrell-Ash atomic absorption spectrometer with an FLA-100 electrothermal atomiser was used for the measurement of the atomic absorption of copper. A Shimadzu CS-920 Chromatoscanner was used for the measurement of absorbance of the copper complex by reflective spectrophotometry. The densitometer has a function to linearise a convex calibration graph. A Toyo KG-25 filter holder was used for the collection of finely divided ion-exchange resins by filtration under suction. A Toyo KG-47 filter holder was used for the filtration of sea and river water samples. Yamato Model WAR-30 and WB-21 Auto-Stills were used to purify the water used; water passed through a reverse osmosis membrane was distilled twice. The glassware and plasticware were immersed in 1 + 1 nitric acid overnight and rinsed thoroughly with re-distilled water.

Reagents

All reagents used were of analytical-reagent grade. Chelating agents were obtained from Dojindo (Kumamoto, Japan) and Wako Pure Chemicals (Osaka, Japan) and used as received.

Copper(II) standard solution, 1000 p.p.m., *pH* 1. Prepared by dissolving 3.9293 g of copper(II) sulphate pentahydrate in dilute hydrochloric acid and diluting to 1000 ml. A working solution containing 1.00 μg ml^{-1} of copper was prepared from the stock solution by appropriate dilution, maintaining a pH of 1.

Bathocuproine (BC) (2,9-dimethyl-4,7-diphenyl-1,10-phenanthroline, BC) solution, 1 mM *in ethanol.*

Disodium bathocuproinedisulphonate (Na_2BCS) [disodium 2,9-dimethyl-1,10-phenanthrolin-4,7-diyldi(benzene-p-sulphonate), Na_2BCS] solution, 1 mM.

Bathophenanthroline (BP) (4,7-diphenyl-1,10-phenanthroline, BP) solution, 1 mM *in ethanol.*

Disodium bathophenanthrolinedisulphonate (Na_2BPS) [disodium 1,10-phenanthrolin-4,7-diyldi(benzene-p-sulphonate) Na_2BPS] solution, 1 mM.

Neocuproine (2,9-dimethyl-1,10-phenanthroline) solution, 1 mM *in* 10 mM *hydrochloric acid.*

1,10-*Phenanthroline (PHEN) solution*, 1 mM *in* 1 mM *hydrochloric acid.*

5,6-*Dimethyl-1,10-phenanthroline (DMPHEN) solution*, 1 mM *in* 2 mM *hydrochloric acid.*

2,2′-*Bipyridine solution*, 1 mM *in* 2 mM *hydrochloric acid.*

2,2′-*Biquinoline solution*, 1 mM *in ethanol.*

5,6-*Diphenyl-3-(2-pyridyl)-1,2,4-triazine (DPT) solution*, 1 mM *in ethanol.*

Disodium 3-(2-pyridyl)-1,2,4-triazin-5,6-diyldi(benzene-p-sulphonate) (Na_2PTBS) solution, 1 mM.

Ammonium pyrrolidinedithiocarbamate (APDC) solution, 0.4% *m/v*.

Disodium ethylenediaminetetraacetate (Na_2EDTA) solution, 10 mM.

trans-*Cyclohexane*-1,2-*diamine*-N,N,N′,N′-*tetraacetic acid (CyDTA) solution*, 10 mM, *pH* 6. Prepared by dissolving the acid (monohydrate) in sodium hydroxide solution.

3,6-*Dioxaoctane*-1,8-*diamine*-N,N,N′,N′-*tetraacetic acid (DODTA) solution*, 10 mM, *pH* 5. Prepared by dissolving the acid in sodium hydroxide solution.

8-*Hydroxyquinoline*, 10 mM. Prepared by dissolving 0.365 g of 8-hydroxyquinoline in 1 ml of acetic acid and diluting to 250 ml with water.

8-*Hydroxyquinoline*-5-*sulphonic acid solution*, 1 mM, *pH* 5. Prepared by dissolving the acid in sodium hydroxide solution.

Hydroxylamine hydrochloride solution, 10% *m/v*. A 250-ml portion of the solution was purified by adding 2.5 ml of 1 mM BC solution. The resulting copper(I) - BC complex was removed by filtration with a membrane filter of 0.45 μm pore size. When the removal of iron was required, 2.5 ml of 1 mM BP solution were added to the hydroxylamine hydrochloride solution and the resulting iron(II) - BP complex was removed by filtration.

Sodium acetate solution, 30% (3.66 M). A 1-l portion of the solution was purified by adding 4.0 ml of the purified hydroxylamine hydrochloride solution and 4.0 ml of 1 mM BC solution. The resulting copper(I) - BC complex was removed by filtration.

Ion-exchange Resin Suspensions

The macroreticular type ion-exchange resins used were the strongly basic anion-exchange resins, Amberlyst A-27 (Rohm and Haas) and DIAION PA318 (Mitsubishi Chemical Industry), a weakly basic anion-exchange resin of the $RN(CH_3)_2$ type, where R denotes the resin matrix, DIAION WA30, and a strongly acidic cation-exchange resin, DIAION PK228. The anion- and cation-exchange resins were conditioned in the usual way for preparing the chloride and hydrogen forms, respectively. Each wet resin was crushed in a PTFE mortar with a PTFE pestle to make a slurry, which was then diluted appropriately with water and the resulting resin suspension filtered through a G-3 glass filter with a nominal pore size ranging from 20 to 30 μm. The filtrate was stored in a polyethylene bottle and used for subsequent experiments. The anion- and cation-exchange resin suspensions thus obtained will be referred to as ARS and CRS, respectively. The ion-exchange capacities of ARS and CRS were determined by conductometric titration with standard solutions of silver nitrate and sodium hydroxide, respectively. The capacities of the resin suspensions of Amberlyst A-27, DIAION PA318, DIAION WA30, and DIAION PK228 were 8.15, 7.15, 14.79, and 6.99 μequiv. ml^{-1}, respectively.

Adsorption of Copper Chelates

Procedure A: fixation of copper complexes on an anion-exchange resin

An aliquot of a 50-ml solution containing 2.0 μg of copper(I) is placed in a 100-ml beaker and 0.8 ml of 6 M hydrochloric acid, 1.0 ml of 10% hydroxylamine hydrochloride solution, 1.0 ml of 1.0 mM chelating agent solution and 4.0 ml of 30% sodium acetate solution are added successively. When copper(II) complexes are to be prepared, the addition of the hydroxylamine hydrochloride solution is excluded and a 30% sodium acetate solution is used without purification. The pH of the resulting solution is about 4.8. The mixture is stirred for 10 min using a magnetic stirrer. A fixed amount of ARS having a capacity of 8.15 μequiv. is then added to the solution and the mixture is stirred for 5 min. The resin suspension is filtered under suction through a 0.45-μm membrane filter (diameter 25 mm). The anion-exchange resin is collected on the membrane filter as a thin circular layer *ca.* 17 mm in diameter and less than 0.05 mm thick. A blank thin layer is also prepared using the same procedure except that no copper(II) is added. The amounts of copper fixed on the anion-exchange resins were determined according to Procedures B and C as described below.

Procedure B: determination of copper fixed on an anion-exchange resin

The membrane filter holding the resin is removed from the filter support and the resin is transferred into a 100-ml beaker with the aid of a stream of water from a polyethylene wash bottle, *ca.* 30 ml of the resin suspension being obtained. A 1.0-ml portion of 6 M hydrochloric acid is added to the suspension which is allowed to stand for more than 1 h. The suspension is then diluted to 50 ml with water and 0.5 ml of 10 mM EDTA, 1.0 ml of 0.4% APDC solution, 4 ml of 30% sodium acetate solution and 2.5 ml of 2 M sodium perchlorate solution are added in that order. The mixture is stirred for 5 min and the resulting copper(II) - APDC complex is fixed on the resin. The resin is then collected on a 0.65-μm membrane filter (diameter 47 mm) as a thin circular layer *ca.* 17 mm in diameter. The integrated absorbance of the copper(II) - APDC complex in the resin phase is measured with the use of a Chromatoscanner at 436 nm by scanning the thin resin layer over an area of 30 × 24 mm. The blank value is also obtained.

Procedure C: determination of copper fixed on an anion-exchange resin

The membrane filter holding the thin layer of anion-exchange resin is placed in a 100-ml beaker and wetted with 1 ml of 6 M hydrochloric acid for more than 1 h. A 1-ml portion of 6 M nitric acid is used, in place of the hydrochloric acid, to decompose the copper(II) - BP and copper(II) - BPS complexes. The membrane filter is removed and the resulting resin suspension is diluted to 50 ml with water. The amount of copper is determined according to the method described in Procedure B.

Procedure D: fixation of copper complexes on a cation-exchange resin

The procedure for the fixation of the copper complex is the same as in Procedure A, except that 8.15 μequiv. of CRS are added in place of ARS. The determination of copper fixed on the resin is carried out according to Procedure B except that ultrasonic agitation is applied to remove the resin from the membrane filter.

Procedure E: extraction of copper complexes on a membrane filter

The extraction of the copper complex on a cellulose nitrate membrane filter is performed according to Procedure A but without the addition of ARS. The membrane filter holding the copper complex is then placed in a 100-ml beaker. A 1.0-ml portion of nitric acid is added to the beaker and the mixture is heated gently to decompose the copper complex together with the membrane filter. The resulting solution is diluted to 50 ml with water and a 1.0-ml portion of ARS prepared from Amberlyst A-27 is added. The amount of copper is then determined as the APDC complex according to Procedure B.

General Procedure for the Determination of Copper by ETAAS After Enrichment as the Copper(I) - BCS Complex on an Anion-exchange Resin

The enrichment of up to 0.2 μg of copper is carried out according to Procedure A with the combined use of 0.5 ml of 1 mM BCS and 1.0 ml of ARS (8.15 μequiv. ml^{-1}) prepared from Amberlyst A-27. The resulting membrane filter holding the thin resin layer is placed in a 10-ml beaker and exposed to

water vapour in a desiccator for more than 30 min to achieve a constant wetness. Then, 2.0 ml of 0.1 M hydrochloric acid are added to the beaker and the mixture is subjected to ultrasonic agitation for 1 min. A 20-μl portion of the resulting suspension is injected into the graphite furnace for the determination of copper by ETAAS.

General Procedure for the Determination of Copper by Densitometry After Enrichment as the Copper(I) - BCS Complex on an Anion-exchange Resin

The enrichment of up to 0.5 μg of copper as the BCS complex with the use of a finely divided anion-exchange resin, Amberlyst A-27, is carried out according to the general procedure for the determination of copper by ETAAS except that a 0.65-μm membrane filter (diameter 47 mm) is used. The resulting membrane filter holding the resin suspension is wetted with water and placed on a white plastic plate in the densitometer. The integrated absorbance of the copper(I) - BCS complex in the resin phase is measured at 485 nm by scanning the thin layer over an area of 30 × 24 mm.

Determination of Copper in Water Samples

The sea and river water samples are filtered, within 3 h of collection, through a 0.45-μm membrane filter (diameter 47 mm). The filtered samples are acidified by the addition of 2.5 ml of hydrochloric acid per litre of the sample and stored in polyethylene bottles. The amount of copper is determined by both ETAAS and densitometry from the respective calibration graphs obtained according to the general procedures, except that for the densitometric measurements the blank thin layer of the anion-exchange resin is prepared with the addition of 0.5 ml of 10 mM EDTA to the water sample before the addition of BCS in the general procedure. The addition of EDTA is effective for measuring the blank absorbance due to the coloured substances present in sea and river waters, as described later.

Results and Discussion

Determination of Copper Fixed on an Ion-exchange Resin

A simple and accurate method was required for the determination of copper fixed on the resins as complexes with different chelating agents. After many experiments, the method using APDC was found to be successful. This method was based on the conversion of the copper complex, fixed on the ion-exchange resin, to the APDC complex and the re-fixation of the resulting copper(II) - APDC complex on the resin phase. The addition of perchlorate ion to a final concentration of *ca.* 0.1 M was found to be effective for the fixation of the copper(II) - APDC complex on the resin phase. The APDC complex was determined subsequently by densitometry at 436 nm. The calibration graph of the copper(II) - APDC complex showed good linearity up to 2.2 μg of copper. This method was also applicable to the determination of copper fixed on the membrane filter as described in Procedure E.

Composition of Copper Complexes

The molar ratio method was applied to calculate the composition of the copper complexes formed under the experimental conditions. The complexation between 1.0-μg portions of copper and various amounts of BCS was carried out in 50-ml aliquots at pH 4.8 in the presence of hydroxylamine hydrochloride. The resulting copper(I) - BCS complex was fixed on the resin thin layer of Amberlyst A-27 and the absorbance of the complex in the resin phase was determined at 485 nm by densitometry.[10] On the other hand, the complexation between 2.0-μg portions of copper and various amounts of BP was carried out in the absence of hydroxylamine hydrochloride. The resulting copper(II) - BP complex was collected on a cellulose nitrate membrane filter and the amount of copper was determined according to Procedure E. The composition of the copper(I) - BCS complex was found to be 1 : 2 and that of the copper(II) - BP complex 1 : 3,[11] as shown in Fig. 1. It was postulated that BCS and the analogous chelating agents (L) react with copper(I) in the presence of hydroxylamine hydrochloride to form $Cu^{I}L_2$ complexes and that BP and the analogous chelating agents react with copper(II) in the absence of hydroxylamine hydrochloride to form $Cu^{II}L_3$ complexes.

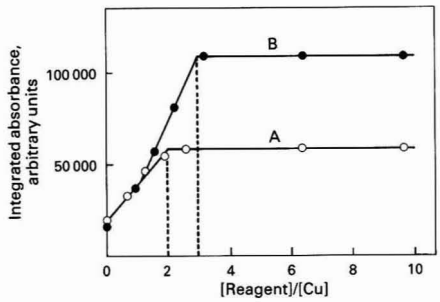

Fig. 1. Molar ratio method. A, Complexation between 1.0 μg of copper and various amounts of BCS in the presence of hydroxylamine hydrochloride. B, Complexation between 2.0 μg of copper and various amounts of BP in the absence of hydroxylamine hydrochloride

Table 1. Adsorption of 2.0 μg of copper as the copper(I) - BC complex on ion-exchange resins and a membrane filter from a 50-ml solution prepared with re-distilled water

Adsorbent	Procedure for determination*	Copper found/ μg†	Recovery, %
Amberlyst A-27	B	1.80	90
	C	2.04	102
DIAION PA318	C	1.98	99
DIAION WA30	B	1.78	89
	C	2.00	100
DIAION PK228	D	2.09	104
Membrane filter‡	E	2.04	102

* See text.
† Means of duplicate determinations.
‡ Cellulose nitrate, 0.45-μm pore size, 25 mm in diameter.

Recovery of the Copper(I) - BC Complex

The recovery of the copper(I) - BC complex from the solution on to the cation- and anion-exchange resins and a cellulose nitrate membrane filter was examined first. The recovery was found to be quantitative, except that the value obtained using Procedure B was 90%, as shown in Table 1. The recoveries obtained with Procedure B for the copper(I) - BCS and copper(II) - BPS complexes were found to be 87 and 90%, respectively (see Table 2). Consequently, the recovery loss was probably due to the fact that part of the resin (*ca.* 10%) remained on the membrane filter even after washing the filter to remove the resin in Procedure B. As described later, however, some copper complexes are fixed to the membrane filter in preference to the anion-exchange resin; hence Procedure B was required to calculate the amount of the copper complexes fixed on the anion-exchange resin alone. In subsequent experiments the recovery of each copper complex was calculated by taking the recovery of the copper(I) - BC complex to be 100%.

Table 2. Adsorption of 2.0 μg of copper on anion-exchange resins from a 50-ml solution prepared with re-distilled water in the presence of different chelating agents

Reagent	Copper adsorbed, %			
	Amberlyst A-27		DIAION PA318	DIAION WA30
	B*	C*	C*	B*
BC†	100	100	100	100
BCS†	98	99	100	101
2,2′-Biquinoline†	62			80
PTBS†	41	44	101	77
Neocuproine†	2			6
DPT†	2			2
BPS†	101			96
BPS	99	97	103	67
BP†	8			33
BP	9			20
DMPHEN†	1			2
DMPHEN	2			1
PHEN†	1			3
PHEN	2			0
2,2′-Bipyridine†	2			2
2,2′-Bipyridine	0			1
EDTA	0			
CyDTA	0			
DODTA	1			
8-Hydroxyquinoline-5-sulphonic acid	38			
8-Hydroxyquinoline	10			

* Procedure for the determination of copper, see text. Values are the means of duplicate determinations.

† Complexation was carried out in the presence of hydroxylamine hydrochloride.

Table 3. Adsorption of 2.0 μg of copper on a cation-exchange resin (DIAION PK228) from a 50-ml solution prepared with re-distilled water in the presence of different chelating agents

Reagent	Copper adsorbed, %*
BC†	100
BCS†	74
PHEN	87
BP	22
BPS	18

* Means of duplicate determinations.

† Complexation was carried out in the presence of hydroxylamine hydrochloride.

Table 4. Adsorption of 2.0 μg of copper on a membrane filter (cellulose nitrate, 0.45-μm pore size, 25 mm in diameter) from a 50-ml solution prepared with re-distilled water in the presence of different chelating agents

Reagent	Copper adsorbed, %*
BC†	100
DPT†	99
Neocuproine†	89
2,2′-Biquinoline†	80
BCS†	77
PTBS†	13
BP	97
DMPHEN	46
BPS	28
PHEN	23
2,2′-Bipyridine	6

* Means of duplicate determinations.

† Complexation was carried out in the presence of hydroxylamine hydrochloride.

Adsorption of Copper Complexes on Anion-exchange Resins

The results of the adsorption of copper on the anion-exchange resins in the presence of different chelating agents are shown in Table 2. In the complexation with *N,N*-donors, such as BC and BP, the charge on the Cu^{+} and Cu^{2+} ions could not be neutralised and hence there might be an electrostatic repulsion between the complexes and the ion-exchange sites of the resins. The copper(I) - BC and copper(I) - BCS complexes, however, were found to be fixed on both the strongly and weakly basic anion-exchange resins quantitatively. It was concluded that the copper(I) - BC complex is fixed on the resin as a result of hydrophobic interactions[12] between the complex and the matrices of the resin and that, with the copper(I) - BCS complex, the fixation due to ion-exchange adsorption by the sulphonate groups would predominate. The adsorption of the copper(II) - BC complex, however, was much lower than that of the copper(I) - BC complex. This was probably due to the fact that the 1 : 3 copper(II) - BP complex has an octahedral configuration[13] with two positive charges whereas the 1 : 2 copper(I) - BP complex has a tetrahedral configuration[14] with a single positive charge. In other words, the electrostatic repulsion of the anion-exchange resin would be much stronger for the copper(II) - BP complex than for the copper(I) - BC complex. Further, the hydrophobic interactions due to overlapping of the benzene rings of the complex with the matrices of the resin[12] would be much more favourable for the complex having a tetrahedral configuration than that with an octahedral configuration.

The fixation of the copper(II) - BPS complex on the anion-exchange resin was, therefore, mainly due to ion-exchange adsorption by the sulphonate groups of the complex. The adsorption of the copper(I) - PTBS complex on DIAION PA318 was found to be quantitative whereas the results obtained with the other resins were not as high; the reason for this difference is not clear. The weakly basic anion-exchange resin, DIAION WA30, appeared to be favourable for fixation of the copper complexes by hydrophobic interactions. The copper(II) - EDTA and analogous complexes were not fixed on Amberlyst A-27 at all. The recoveries of the copper(II) complexes with 8-hydroxyquinoline and 8-hydroxyquinoline-5-sulphonate were low, large amounts of the resin being necessary for quantitative collection of the 8-hydroxyquinoline-5-sulphonate complex.[15,16]

Adsorption of Copper Complexes on a Cation-exchange Resin

The adsorption of the copper-(I) and -(II) complexes on a cation-exchange resin was examined briefly using DIAION PK228. Except for the copper(I) - BC complex, the recoveries of the other complexes were unsatisfactory, as shown in Table 3. The copper(II) - BP complex having two positive charges and highly hydrophobic moieties was expected to be fixed on the resin effectively; however, the recovery was poor. The bulky octahedral configuration of the copper(II) - BP complex probably reduces both the electrostatic and hydrophobic interactions between the complex and the cation-exchange resin. The recovery of the copper(II) - BP complex was lower than that of the corresponding PHEN complex, which indicated that the affinity of the copper(II) - BP complex for the cation-exchange resin was reduced by the presence of the phenyl groups at the 9- and 10-positions of PHEN.

Adsorption of Copper Complexes on a Membrane Filter

The extraction of the copper-(I) and -(II) complexes with *N,N*-donors on a membrane filter was examined with the use of the cellulose nitrate filter. The complexes having highly hydrophobic moieties, such as the copper(I) - BC, copper(I) - DPT and copper(II) - BP complexes, were collected effectively on the filter, as shown in Table 4. The results may be useful for calculating the relative hydrophobicities of the

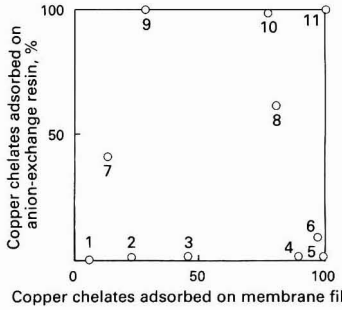

Fig. 2. Adsorption of copper chelates on the anion-exchange resin and membrane filter. Anion-exchange resin: Amberlyst A-27. Membrane filter: cellulose nitrate, 0.45-μm pore size, 25 mm in diameter. Copper(II) complexes with 1, 2,2′-bipyridine; 2, PHEN; 3, DMPHEN; 6, BP; and 9, BPS. Copper(I) complexes with 4, neocuproine; 5, DPT; 7, PTBS; 8, 2,2′-biquinoline; 10, BCS; and 11, BC

complexes. A comparison of the adsorption of the copper complexes on Amberlyst A-27 and the membrane filter is shown in Fig. 2.

Choice of Chelating Agent for Enrichment of Copper

It was concluded that BC, BCS, and BPS are useful reagents for the enrichment of copper with the use of Amberlyst A-27 and that BC, DPT and BP are useful for the enrichment of copper with the use of a cellulose nitrate membrane filter. Of the reagents studied, BC and BCS are superior to BPS and DPT as they are specific colour-producing reagents for copper.[14] Consequently, in subsequent experiments the enrichment of copper was carried out by the combined use of BCS and Amberlyst A-27, while BC was used to purify the hydroxylamine hydrochloride and sodium acetate solutions, *i.e.*, any copper ion in the solution was removed by filtration as the BC complex on the membrane filter.

Determination of Copper at ETAAS After Enrichment as the BCS Complex

Trace amounts of copper were fixed on the finely divided anion-exchange resin with the combined use of 0.5 ml of 1 mM BCS solution and 1.0 ml of ARS prepared from Amberlyst A-27 (8.15 μequiv. ml^{-1}). The resin was collected from the bulk solution on a membrane filter by filtration under suction and then suspended in a small volume of the appropriate medium (*i.e.*, water, 0.1 M hydrochloric acid or 0.1 M nitric acid) and 20-μl portions of the resulting suspension were subjected to ETAAS. The operating conditions of the apparatus are summarised in Table 5. A 0.1 M hydrochloric acid solution, 0.1 M nitric acid and water were examined as media for the preparation of the resin suspension for ETAAS. The regression equation of the calibration graph for copper obtained for each medium is summarised in Table 6. Hydrochloric acid was found to be superior to the other media in terms of sensitivity and reproducibility. The concentration of the acid was varied from 0.1 to 1.0 M; however, no significant difference was observed. The volume of the medium was also important. If the volume is too large the sensitivity of the method will be reduced whereas if it is too low the viscosity of the resulting resin suspension will increase and reproducible injections into the graphite furnace become difficult. After many experiments the volume of 0.1 M hydrochloric acid was fixed at 2.0 ml. Ultrasonic agitation was required to prepare the resin suspension; however, once formed, the resulting suspension was stable and reproducible injections into the graphite furnace were possible.

Table 5. Operating conditions for ETAAS. Wavelength, 324.8 nm; lamp current, 4 mA; argon flow-rate, 3 l min^{-1}; and peak hold, deuterium background corrector

Step	Current/A	Time/s	Mode	Final temperature/°C
Dry	18	50	Ramp	200
Ash I	40	15	Ramp	580
Ash II	40	6	Constant temperature	580
Atomise ..	200	10	Ramp	2350

Table 6. Selection of media for preparation of the resin suspension for ETAAS analysis

Medium	Regression equation of calibration graph*	Standard error of regression coefficient†
Water	$y = 42.2x + 1.24$	1.29
0.1 M hydrochloric acid ..	$y = 52.5x + 1.41$	1.02
0.1 M nitric acid	$y = 48.6x + 2.06$	1.49

* y = peak height including blank value in cm; x = amount of copper in μg, up to 0.2 μg.

† Calculated from $\sqrt{V_{y \cdot x}} / \sqrt{\Sigma(x_i - \bar{x})^2}$, where $V_{y \cdot x}$ is the mean square from the regression of y on x.

Table 7. Determination of copper in sea water; samples were taken from Fukaura, Japan Sea, on 25/1/89

Method	Sample volume/ml	Copper added/μg	Copper in sea water, p.p.b.	No. of analyses
ETAAS	150		0.18	1
	150	0.04	0.22*	1
	150	0.08	0.20*	1
	150	0.12	0.18*	1
	200		0.20	2
	250		0.19	2
			Mean: 0.20	8
			SD: ± 0.02	8
Densitometry ..	300		0.21	1
	400		0.19	1
			Mean: 0.20	2

* These values were calculated from: [total amount of copper found (ng) − amount of copper added (ng)] per 150 ml. When the recovery of copper from 150 ml of sea water was calculated from: {[total amount of copper found (ng)]/[(0.20 × 150) + amount of copper added (ng)]} × 100, the values were 104, 100 and 98% for 40, 80 and 120 ng of added copper, respectively.

Table 8. Determination of copper in river water; samples were taken from the Iwaki river on 15/2/89

Method	Sample volume/ml	Copper added/μg	Copper in river water, p.p.b.	No. of analyses
ETAAS	100		0.65	2
	100	0.04	0.67*	2
	100	0.08	0.64*	2
	100	0.12	0.67*	2
	150		0.65	2
	200		0.63	2
			Mean: 0.65	12
			SD: ± 0.03	12
Densitometry ..	100		0.64	2
	150		0.70	2
	200		0.68	2
			Mean: 0.67	6
			SD: ± 0.04	6

* These values were calculated from: [total amount of copper found (ng) − amount of copper added (ng)] per 100 ml. When the recovery of copper from 100 ml of river water was calculated from: {[total amount of copper found (ng)]/[(0.65 × 100) + amount of copper added (ng)]} × 100, the values were 102, 99 and 101% for 40, 80 and 120 ng of added copper, respectively.

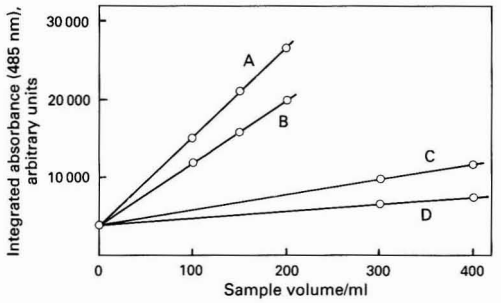

Fig. 3. Effect of sample volume on the determination of copper in river water (A and B) and sea water (C and D). A and C, Absorbance of the thin resin layer prepared from the acidified water sample with the addition of 0.5 ml of 1 mM BCS, 1.0 ml of 10% hydroxylamine hydrochloride solution, 4.0 ml of 30% sodium acetate solution and 1.0 ml of ARS with 8.15 μequiv. ml^{-1}. B and D, Absorbance of the thin resin layer prepared according to the same procedure as for A and C, except that a 0.5-ml portion of 10 mM EDTA was added before the addition of BCS

Effect of Sodium Chloride

The effect of the concentration of sodium chloride on the enrichment of copper as the BCS complex was examined following the general procedure for the determination of copper by ETAAS. A constant AAS signal for 0.12 μg of copper was obtained after the enrichment of copper from 50-ml solutions containing up to 0.8 M sodium chloride, which indicated that the proposed method is applicable to the determination of copper in water samples of high salinity.

Effect of Sample Volume

The enrichment of a 0.12-μg portion of copper as the BCS complex from various sample volumes was examined following the general procedure. A constant AAS signal for 0.12 μg of copper was obtained for the different sample volumes studied.

Effect of Foreign Ions

As reported previously,[10,17] the enrichment of copper as the BCS complex on an anion-exchange resin is not affected by the cations and anions normally present in water samples. Consequently, it is reasonable to expect that no foreign ions would interfere with the determination of copper by ETAAS. However, for the determination of copper by densitometry, the effects of humic substances in the water sample were serious because these substances were permanently fixed on the anion-exchange resin, producing a coloration in the same way as the copper(I) - BCS complex. The coloration due to the humic substances could be eliminated by the preparation of a blank thin layer of the anion-exchange resin in the presence of EDTA. With the addition of EDTA to the water sample before the addition of BCS, the formation of the copper(I) - BCS complex was suppressed completely and the blank absorbance, including that due to the humic substances, could be measured.

Determination of Copper in Water Samples

The pH values of the acidified sea and river water samples were 1.65 and 1.50, respectively. The results of the determination of copper by ETAAS and densitometry are summarised in Tables 7 and 8. The results obtained by ETAAS showed that the matrix effects of the water samples could be eliminated successfully by the enrichment of copper on an anion-exchange resin. The recovery of copper from sea and river waters, obtained by the addition of different amounts of copper, was found to be quantitative and the concentration of copper found in different sample volumes was constant. The effect of sample volume on the determination of copper by densitometry is shown in Fig. 3. The river water sample contained much larger amounts of naturally occurring coloured substances than the sea water sample. As the concentration of copper in the water samples was very low, the blank value should be accurately known, particularly for the determination of copper by densitometry. Consequently, the blank absorbance corresponding to each sample volume was calculated from the regression equation obtained for the experimentally observed blank values and the sample volumes, as shown by the solid lines, B and D, in Fig. 3. The results obtained by ETAAS and densitometry agreed closely with each other; however, some pre-treatment of the water samples such as UV irradiation[18,19] is recommended to reduce the blank value for densitometry.

Conclusion

It can be concluded that the degree of adsorption of copper chelates on the anion- and cation-exchange resins is dependent on the charge, hydrophobicity and configuration of the compounds and that the degree of adsorption of the chelates on a membrane filter is related to the hydrophobic properties of the compounds. The combined use of BCS and a finely divided anion-exchange resin has been shown to be extremely useful for the rapid and selective enrichment of trace amounts of copper followed by its determination by ETAAS or densitometry.

This work was supported in part by a Grant-in-Aid from the Ministry of Education, Science and Culture (Japan) and in part by a grant from Nihon Kagaku Kenkyu-kai (Sendai, Japan).

References

1. Boyd, G., E., Adamson, A. W., and Meyers, L. S., *J. Am. Chem. Soc.*, 1947, **69**, 2836.
2. Pinfold, T. A., and Karger, B. L., *Sep. Sci.*, 1970, **5**, 183.
3. Shriadah, M. M. A., Kataoka, M., and Ohzeki, K., *Analyst*, 1985, **110**, 125.
4. Shriadah, M. M. A., and Ohzeki, K., *Analyst*, 1985, **110**, 677.
5. Matsuhisa, K., and Ohzeki, K., *Analyst*, 1986, **111**, 685.
6. Isozaki, A., Soeda, N., Okutani, T., and Utsumi, S., *Nippon Kagaku Kaishi*, 1979, 549.
7. Nakano, K., Takeda, T., and Kakuta, T., *Bunseki Kagaku*, 1979, **28**, 325.
8. Takada, T., Okano, H., Koide, T., Fujita, K., and Nakano, K., *Nippon Kagaku Kaishi*, 1981, 13.
9. Koide, M., Lee, D. S., and Stallard, M. O., *Anal. Chem.*, 1984, **56**, 1956.
10. Ohta, M., and Ohzeki, K., *Bull. Chem. Soc. Jpn.*, 1984, **57**, 3571.
11. Akaiwa, H., Kawamoto, H., and Kinoshita, H., *Bunseki Kagaku*, 1987, **36**, 662.
12. Lundrungresn, J. L., and Schilt, A. A., *Anal. Chem.*, 1977, **49**, 974.
13. James, B. R., and Williams, R. J. P., *J. Chem. Soc.*, 1961, 2007.
14. Cheng, K. L., Ueno, K., and Imamura, T., "Handbook of Organic Analytical Reagents," CRC Press, Boca Raton, FL, 1982, p. 331.
15. Akaiwa, H., Kawamoto, H., Nakata, N., and Ozeki, Y., *Chem. Lett.*, 1975, 1049.
16. Abe, M., Ohzeki, K., and Kambara, T., *Bull. Chem. Soc. Jpn.*, 1978, **51**, 1090.
17. Takahashi, T., Imamura, T., and Fujimoto, M., *Mikrochim. Acta*, 1973, 69.
18. Moore, R. M., and Burton, J. D., *Nature (London)*, 1976, **264**, 241.
19. Itoh, J., Komata, M., and Oka, H., *Bunseki Kagaku*, 1987, **36**, 799.

Paper 9/02074H
Received May 17th, 1989
Accepted July 14th, 1989

Determination of Trace Impurities in Silicon and Chlorosilanes by Inductively Coupled Plasma Atomic Emission Spectrometry and Neutron Activation Analysis

C. C. Chu, P. Y. Chen and Mo H. Yang*
Institute of Nuclear Science, National Tsing Hua University, Hsinchu, Taiwan 30043, Republic of China
Zeev B. Alfassi*
Department of Nuclear Engineering, Ben Gurion University, Beer Sheva 84012, Israel

Methods are described for the determination of trace elements in Si and chlorosilanes by inductively coupled plasma atomic emission spectrometry (ICP-AES) and neutron activation analysis. The chlorosilanes were hydrolysed and Si was removed as SiF_4 by evaporation of an HF solution. The dependence of the ICP signal on several parameters was studied and the operating conditions were optimised. For the chlorosilane matrix the Si was removed by evaporation. Radiotracers were used to measure the recovery of the elements of interest following the established procedure for sample analysis. The reliability of the proposed methods was checked using the National Institute of Standards and Technology (formerly National Bureau of Standards) Standard Reference Material 57 Refined Silicon. The methods were applied to the determination of trace impurities in various Si-containing materials.

Keywords: *Inductively coupled plasma atomic emission spectrometry; trace impurity; silicon; chlorosilane*

Silicon is the most important basic semiconductor material. The purity of Si is important for the production of high-performance solid-state devices. It occurs naturally as silica and silicates. In the first step in the preparation of Si, SiO_2 is usually reduced by coke in a submerged electric furnace, a process which yields low-cost metallurgical-grade Si (MG-Si) with a purity of the order of 98%. To obtain semiconductor-grade (or electronic-grade) Si, MG-Si is reacted with hydrogen chloride in a fluidised-bed reactor to form trichlorosilane ($SiHCl_3$). The $SiHCl_3$ is purified carefully by distillation and the purified material is pyrolysed reductively and hyperpure Si is recovered by vapour deposition on the surface of polycrystalline seeds (Siemens process). This process, although used for electronic-grade Si, is too expensive for terrestrial photovoltaic applications. Several studies have been carried out on the preparation of less expensive Si which would be sufficiently pure for photovoltaic cells (solar-grade Si) but not for the electronics industry.[1–4] Throughout the development of processes for the preparation and purification of the materials, chemical analysis plays an important part in providing information on the concentration of impurities in the intermediates and final products. In this study we report on the development of analytical methods for the measurement of the concentration of trace elements in Si and chlorosilanes by the use of neutron activation analysis (NAA) and inductively coupled plasma atomic emission spectrometry (ICP-AES).

There is a large amount of literature on the analysis of Si, mainly by NAA,[5–10] but only a few studies have been reported on the analysis of chlorosilanes. Chlorosilanes have been studied previously by NAA (Cu, Sb, Cr, As, Hg and P) by Rausch *et al.*[11] They bound the impurities into a complex with $(C_6H_5)_3CCl$ and then evaporated the $SiHCl_3$; the residue was analysed by NAA. Martynov *et al.*[12] measured Cu in $SiCl_4$ by spectral and luminescence analysis. A sample of $SiCl_4$ was evaporated with CCl_4 to eliminate the Si and the hydrolysis products of the remaining sample were then treated with the minimum amount of HF. Dias *et al.*[13] determined P in $SiCl_4$ and $SiHCl_3$ by hydrolysing and extracting P as molybdophosphate into chloroform. Chang and co-workers[14,15] measured metal impurities in $SiHCl_3$ and Si (Ca, Cu, Fe, Mg, Mn and Ni) by atomic absorption spectrometric techniques; Al was measured by a spectrofluorimetric method and B and P by spectrophotometric methods using Methylene Blue and molybdophosphoric acid, respectively.

Experimental

Containers and Reagents

Polytetrafluoroethylene (PTFE), polyethylene and polypropylene containers were used throughout and were cleaned by immersing them in concentrated HNO_3 overnight and washing successively with de-ionised water.

All chemicals used were of analytical-reagent grade and were obtained from Merck (FRG). High-purity water with a resistivity of ≥ 10 MΩ cm, produced by reverse osmosis and de-mineralisation processes, was used.

Subsequently, it was found that the above procedure led to higher detection limits; hence the samples were prepared under more rigorous conditions in order to prevent contamination. All PTFE and quartz containers were immersed in nitric acid for 24 h and then cleaned by the vapour from boiling nitric acid followed by rinsing with ultrapure water prepared by sub-boiling distillation.[16] All liquid analytical reagents (HNO_3 and HF) were purified by sub-boiling distillation.

Sample Preparation

Chlorosilanes

Neither $SiHCl_3$ nor SiH_2Cl_2 can be used directly for NAA or ICP-AES. Owing to the low boiling-point of these compounds and the extensive radiolysis products formed, irradiation of quartz ampoules containing $SiHCl_3$ or SiH_2Cl_2 for long periods of time is likely to cause these ampoules to explode. The large amount of the Si matrix causes problems in the determination of trace elements by ICP-AES. The removal of most of the $SiHCl_3$ and SiH_2Cl_2 also has the advantage of pre-concentrating the trace elements. Owing to the high volatility of the chlorosilanes the simplest method would be to evaporate them to dryness. However, the chlorides of several elements (*e.g.*, As, B and Sb) are volatile and might be lost during this process. As the only volatile low-valent fluorides are those of Si and B it is preferable to remove the Si as

* To whom correspondence should be addressed.

$(HF)_2.SiF_4$. The volatility of BF_3 is only a problem for ICP-AES measurements because B cannot be measured by NAA followed by delayed gamma-ray spectrometry. To prevent the evaporation of BF_3 prior to ICP-AES measurements, mannitol should be added to the solution as it is known to form a non-volatile complex with BF_3. The chlorosilanes are hydrolysed in acidic aqueous solution and the HCl is evaporated. Owing to the large excess of H^+ in the aqueous solution, Cl is evaporated as HCl and not as the volatile $AsCl_3$ or $SbCl_3$. It is advantageous to be able to hydrolyse as large a sample of chlorosilanes as possible in order to obtain larger amounts of the impurities and to lower the detection limit; however, for practical purposes we used 10–20 ml of chlorosilanes.

The retention of the contaminants present in the $SiHCl_3$ was studied by using radiotracers of several of the elements; these were added together with the 20 ml of H_2O used for the hydrolysis of $SiHCl_3$. Table 1 gives the results of this study. As can be seen, the recovery of all the elements was greater than 96%, with the exception of As for which the recovery was only 90%. Similar results were obtained for SiH_2Cl_2. As there is no radiotracer for B, known amounts of a natural B compound (BBr_3) were added to the hydrolysing solution and the final concentration of B was measured by ICP-AES. Table 2 shows the recovery of B as a function of the amount of mannitol added. It can be seen that the addition of 1–2 mg of mannitol per microgram of B gives a recovery of greater than 99%.

Procedure. To 10 ml of $SiHCl_3$ or SiH_2Cl_2 kept in liquid N_2, 1 ml of 1% mannitol solution was added followed by 20 ml of water. The mixture was heated slowly to room temperature (25 °C) and then to dryness (80 °C). The dried material was dissolved in 10 ml of 40% HF (added dropwise) and the solution was evaporated to dryness on a water-bath (80 °C). As the ICP-AES measurements showed that not all the Si had been removed by this method and as the amount of Si remaining would interfere with the measurement of other elements by ICP-AES, two more cycles involving the addition of 1 ml of 40% HF to dissolve the solid residue and evaporation to dryness at 80 °C were carried out. Table 3 shows the amount of Si remaining from 10 g of $SiHCl_3$ after successive cycles of HF dissolution and evaporation to dryness. Three such cycles were carried out in this study and the dried material was dissolved in 0.5 ml of concentrated HNO_3. The concentration of Si remaining after the three cycles (5–20 μg ml^{-1}) was found not to interfere with the determination of the other elements.

Si

For NAA measurements the Si samples were sealed in quartz ampoules, irradiated and then analysed after cooling for a few hours as only short-lived activity is induced in Si itself. However, for ICP-AES measurements the Si sample must be dissolved and most of the Si removed. Hence Si samples (0.5 g) were dissolved in the minimum amount (about 6 ml) of HNO_3 - HF (2 + 1) and 1 ml of 1% mannitol was added and the solution was evaporated to dryness at 80 °C. This process was repeated twice and then the dried material was dissolved in 0.5 ml of 0.5 M HNO_3 and diluted to 10 ml for the ICP-AES measurements.

NAA

Dried samples were irradiated for 3 min and 2 h with a thermal neutron flux (ϕ) of 2×10^{12} n cm^{-2} s^{-1} and for 2 weeks with $\phi = 5 \times 10^{13}$ n cm^{-2} s^{-1}. The γ activity was measured with a 50 cm^{-3} Ge(Li) detector connected to a Tracor-Northern (TN-1170) 4096-channel analyser. The system has a resolution (full width at half maximum) of 1.84 keV at the ^{60}Co 1332-keV line and a photopeak to Compton ratio of 46.3. A multi-element standard containing all the elements studied in this work (Table 7) was irradiated with the samples. The amounts of the elements in the standard were 0.01–1.0 μg.

ICP-AES Measurements

A Kontron S-35 Plasmakon sequential-type ICP atomic emission spectrometer was used. The sensitivity and limits of detection depend on several parameters of the ICP instrument, which can be controlled. The optimisation is usually carried out to achieve the maximum signal to background ratio and to minimise the matrix effect.

It was decided to fix the photomultiplier voltage at 800 V and the observation height at 3.0 cm, and to optimise the other parameters. The flow-rate of the cooling gas chosen was high enough to cool the quartz wall of the ICP torch to ≤1000 °C while allowing a sufficiently high sensitivity for the determination of the trace elements, as the signal obtained decreases as the flow-rate of the cooling gas is increased. The minimum cooling gas flow-rate required to prevent the instrument from being damaged, 13 l min^{-1}, was used.

Using a constant cooling gas flow-rate (13 l min^{-1}), the flow-rates of the carrier and plasma gases were changed for various settings of the r.f. power and the signal to background ratio was measured for an aqueous solution containing 1 p.p.m. of B. For a high r.f. power (1.7 kW) the best choice was found to be a high carrier gas flow-rate and a low plasma flow-rate, whereas for 1.3 kW, the lowest power used, the best results were obtained with a medium carrier gas flow-rate. As a plasma gas flow-rate of less than 0.4 l min^{-1} is not sufficient to maintain a stable plasma, the following parameters were chosen: r.f. power, 1.5 kW; carrier gas flow-rate, 1.3 l min^{-1}; and plasma gas flow-rate, 0.4 l min^{-1}.

Table 4 shows the instrumental detection limit for various elements (defined as three times the standard deviation of the background[19]) obtained in this laboratory after optimisation and in three other laboratories. The very low detection limits

Table 1. Recovery of various radiotracers in the preparation of $SiHCl_3$ samples for analysis

Element	Radiotracer used	Activity/counts min^{-1} Added	In the final sample	Recovery, %
Cu	^{64}Cu	13 395	12 895	96
Zn	^{65}Zn	3541	3550	100
Sb	^{124}Sb	61 010	60 742	99
Fe	^{59}Fe	3983	3867	97
As	^{76}As	79 740	70 997	90
P	^{32}P	6198	6121	99
Mn	^{56}Mn	15 875	15 455	97

Table 3. Si content in the final residue from $SiHCl_3$ (10 g) after successive cycles of dissolution in HF and evaporation to dryness

No. of cycles	Si content in the residue/μg Experiment 1	Experiment 2
1	804	800
2	7.9	18
3	4.7	8.0

Table 2. Recovery of B in the hydrolysis and removal of $SiHCl_3$ as a function of mannitol added (B = 1 μg)

Amount of mannitol/mg	0	0.2	0.5	0.7	1.0	2.0
Recovery, %	29.9	77.0	94.5	98.6	99.4	99.6

Table 4. Instrumental detection limits obtained by four different laboratories using ICP-AES

Element	Detection limit, p.p.b. Boumans and de Boer[17]	Fassel and Knisley[18]	Kontron*	This work
B	0.1	5	5	0.4
P	15	40	76	11
Al	0.2	2	28	2
Cr	0.1	1	6	2
Cu	0.06	1	5	0.5
Fe	0.09	5	5	0.6
Mg	0.003	0.7	0.2	0.06
Mn	0.02	0.7	1	0.3
Co	—	3	6	1
Ti	0.03	3	4	0.3
Ca	0.0001	0.07	0.2	0.1
Ni	0.2	6	10	3

* Instrument manufacturer's data.

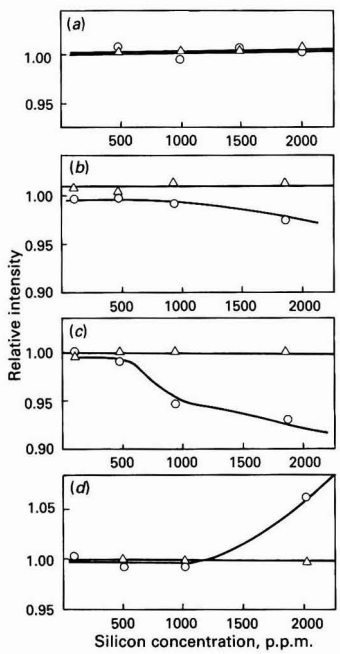

Fig. 1. Matrix effect caused by Si in the determination of (*a*) Cr (205.552 nm), (*b*) Ca (393.366 nm), (*c*) Al (309.271 nm) and (*d*) P (213.618 nm). Concentration of determinand: ○, 0.5; and △, 50 p.p.m.

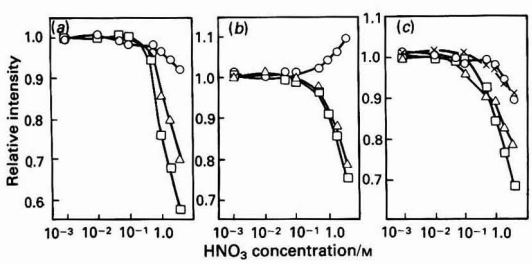

Fig. 2. Effect of the concentration of HNO_3 on the emission intensity of various elements at different concentrations and photomultiplier voltages. (*a*) Cr 250.552 nm, (*b*) P 213.618 nm, (*c*) Ca 393.366 nm (0.5 p.p.m.) and 317.933 nm (5.0 p.p.m.). □, 10 p.p.m. (5 p.p.m. for Ca), 400 V; △, 10 p.p.m. (5 p.p.m. for Ca), 800 V; ○, 0.5 p.p.m., 800 V; ×, 0.5 p.p.m., 400 V

for most elements obtained by Boumans and de Boer[17] (Table 4, second column) can mainly be attributed to the improved nebuliser performance (higher sample injection rate using an ultrasonic nebuliser). However, the improvement in our results compared with the manufacturer's data (compare the fifth column in Table 4 with the fourth) is significant. The detection limits reported here are similar to those attainable with modern equipment.[20,21]

The only element that can have a matrix effect on the determination of other elements is Si, which is the major element. In order to study the matrix effect of Si on the determination of several elements, solutions with various known concentrations of Si [prepared from 99.9999% Si dissolved in the minimum amount of concentrated HF - HNO_3 (1 + 1) and diluted further with ultrapure water] were prepared and known amounts of other elements were added. The results of the analysis of these solutions for Cr, Ca, Al and P by ICP-AES are shown in Fig. 1. As can be seen, up to 2000 p.p.m. of Si does not interfere with the determination of high concentrations (*ca.* 50 p.p.m.) of other elements. However, for lower concentrations of contaminants (*ca.* 0.5 p.p.m.) there is no effect for Cr, negative effects for Ca and Al and a positive effect for P. The fact that the shift in the matrix effect is not constant implies that of the usual causes of a matrix effect,[22,23] the only ones that might be significant here are either uncorrected background shifts or spectral coincidence. The former appears the more probable. The easiest way to overcome this problem is to reduce the Si concentration by repeated dissolution and evaporation. Fig. 1 shows that there is no interference for concentrations of Si of less than 500 p.p.m. and this can easily be obtained by an additional dissolution and evaporation cycle as can be seen in Table 3. However, as a precaution three dissolution and evaporation cycles were carried out.

The effect of the HNO_3 concentration on the determination of Cr, P and Ca was studied (Fig. 2). In all instances, except for 0.5 p.p.m. of P, increasing the HNO_3 concentration above 0.05 M leads to a decrease in the ICP signal. The usual explanation for the effect of acid[24–26] is that a variation in the acid concentration leads to a variation in the viscosity which results in changes in the transport properties of the sample and hence different uptake rates. However, the viscosity of 0.1 M HNO_3 is very close to that of pure water; moreover, if this explanation were correct, the same effect should be observed for all concentrations of the different elements. One possible explanation is that the matrix (HNO_3) hinders the volatilisation of the analyte atoms in the matrix during their passage through the ICP, *i.e.*, the matrix affects the spatial distribution pattern of the free analyte atoms and ions due to complex formation.[17,27] Fig. 2 shows that for concentrations of HNO_3 $\leq 5 \times 10^{-2}$ M this effect is within the experimental error of the method. In our experiments the HNO_3 concentration was only 0.01 and 0.025 M for the analysis of chlorosilanes and Si, respectively.

Linearity of the ICP-AES Response

The linearity of the ICP-AES response was measured both for pure aqueous solutions of the elements and by standard additions of the elements to the solution derived from the chlorosilanes.

Fig. 3 shows the results for Ca and P in a solution derived from $SiHCl_3$. As can be seen, the lines are parallel within experimental error (Ca slopes 4311 and 4180 mV p.p.m.$^{-1}$, P slopes 411 and 392 mV p.p.m.$^{-1}$) and the value of the concentration of Ca and P derived from the intercept is almost the same as that measured without the standard additions graphs (1.55 compared with 1.54 p.p.m. for Ca and 1.69 compared with 1.66 p.p.m. for P, respectively). This agreement indicates that the matrix does not interfere with the measurements.

Table 5. Detection limits for the determination of the various elements by NAA

Element	Ag	Al	As	Au	Co	Cr	Cu	Fe	Mn	Sb	Sm	V	Zn
Detection limit/ng	0.16	80	0.4	0.002	0.2	0.2	6.6	80	0.4	0.02	0.008	5	1.5

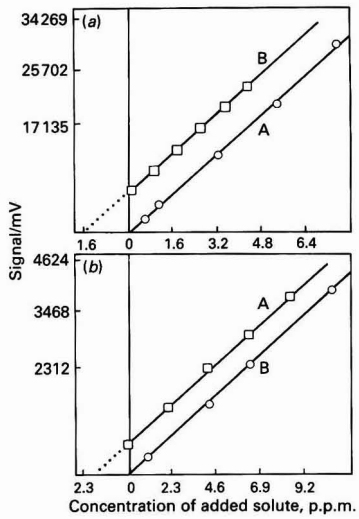

Fig. 3. A, Calibration graphs and B, standard additions graphs for (*a*) Ca and (*b*) P in a $SiHCl_3$ sample

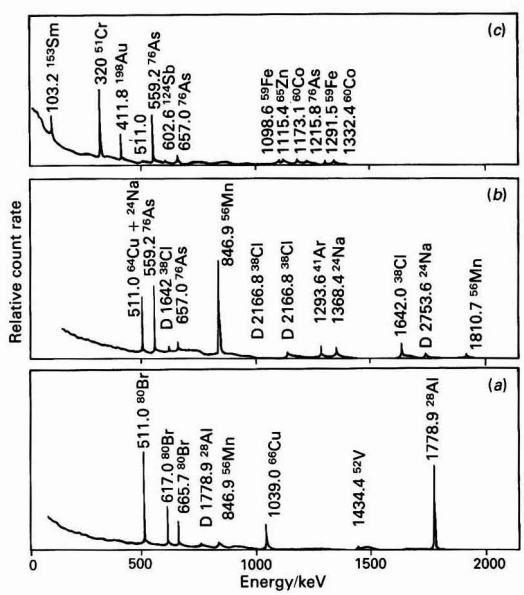

Fig. 4. Gamma-ray spectra of irradiated $SiHCl_3$ obtained for different irradiation, cooling and counting times. (*a*) t_i = 3 min, $t_{cooling}$ = 2 min, t_{count} = 5 min ($\phi = 2 \times 10^{12}$ n cm^{-2} s^{-1}); (*b*) t_i = 2 h, $t_{cooling}$ = 2 h, t_{count} = 20 min ($\phi = 2 \times 10^{12}$ n cm^{-2} s^{-1}); and (*c*) t_i = 14 d, $t_{cooling}$ = 7 d, t_{count} = 50 min ($\phi = 5 \times 10^{13}$ n cm^{-2} s^{-1})

Results

NAA

Fig. 4 shows the gamma-ray spectra measured for one of the $SiHCl_3$ samples after three different irradiation times. It can be seen that the elements present can easily be measured without interferences. The detection limits obtained are listed in Table 5. The detection limits are for the irradiation (t_i), cooling ($t_{cooling}$) and counting (t_{count}) times given in Fig. 4 ($\phi = 2 \times 10^{12}$ n cm^{-2} s^{-1}, t_i = 3 min, $t_{cooling}$ = 2 min, t_{count} = 5 min for Al and V; $\phi = 2 \times 10^{12}$ n cm^{-2} s^{-1}, t_i = 2 h, $t_{cooling}$ = 2 h, t_{count} = 20 min for Mn and Cu, $\phi = 5 \times 10^{13}$ n cm^{-2} s^{-1}, t_i = 14 d, $t_{cooling}$ = 7 d, t_{count} = 50 min for all other elements). The detection limit is defined as the amount that gives a peak equal to three times the square root of the background or 100 counts, whichever is the larger of the two criteria.

Table 6. Comparison of the certified values for NIST SRM 57 with results obtained by ICP-AES and NAA. The concentrations of some other elements determined by NAA are also given

Element	Certified value, p.p.m.	Found, p.p.m. ICP-AES	Found, p.p.m. NAA
Fe	6500	6570 ± 300	6000 ± 600
Al	6700	6460 ± 200	6300 ± 200
Ca	7300	7400 ± 100	—
Mn	340	311 ± 30	357 ± 38
Cr	250	240 ± 13	285 ± 4
Ni	20	22 ± 2	—
Ti	1000	955 ± 40	—
P	30*	31.8 ± 1.8	—
Cu	40*	39 ± 1.5	—
Sc	—	—	1.41 ± 0.03
Co	—	—	3.3 ± 0.02
La	—	—	60.9 ± 2.7
Sb	—	—	0.94 ± 0.05
V	—	—	28.0 ± 6.1

*Values for NIST SRM 57(A).

Verification of the Methods

In order to verify the analytical methods established, the results obtained here were compared with the certified values for the National Institute of Standards and Technology (NIST) [formerly National Bureau of Standards (NBS)] Standard Reference Material (SRM) 57 Refined Silicon [for P and Cu NIST SRM 57(A) was used]. Table 6 compares our results with the certified values and also gives the concentration of some elements for which there are no certified values. As can be seen, there is a reasonably good agreement between the measured and certified values of the elements tested. The method for the determination of B cannot be validated in this way as no certified value is given for B and as B can only be determined by ICP-AES and not by NAA. However, in order to check the proposed method the results of the ICP-AES measurements were compared with those obtained by spectrophotometry; the results agreed to within 6% (10.6 and 11.2 p.p.m.).

Applications

The proposed procedure was applied to the analysis of Si and chlorosilanes obtained from different purification stages of the processes currently under investigation in Taiwan.

Purification of chlorosilanes

Trichlorosilane is produced either by hydrochlorination of Si or by hydrogenation of $SiCl_4$. In the hydrochlorination of Si

the product is a mixture of 90% $SiHCl_3$ plus 10% $SiCl_4$. Table 7 gives the elemental concentration of the impurities in this mixture and the concentration in the separated $SiHCl_3$ for various stages of purification. The purification was carried out both by multi-fractional distillation and by chemical methods (reaction with Cr_2O_3 - NaOH, H_2O, Cu and Al_2O_3) followed by distillation. Table 7 shows that the chemical treatment followed by distillation leads to ultrapure $SiHCl_3$ in which none of the contaminants can be measured.

Table 7. NAA results for trace element concentrations in the various stages of purification of $SiHCl_3$. All values in p.p.b.

	Stage of purification			
Element	90% $SiHCl_3$ + 10% $SiCl_4$	Crude $SiHCl_3$	Distillation	Chemical treatment + distillation
Fe	15400	2600	<300	<20
Al	730	260	<20	<20
Cu	710	520	<2	<2
Zn	380	140	39	<0.6
Cr	23	22	<2	<0.05
Mn	9.8	11.1	0.7	<0.1
Co	2.3	1.4	1	0.05
Au	5.9	1.0	<0.002	<0.0005
Sb	1.8	1.3	<0.25	<0.005

Table 8. Concentration of trace elements in several samples of SiH_2Cl_2 measured by ICP-AES. All values in p.p.m.

	Sample No.		
Element	1	2	3
B	0.24	0.40	0.20
Fe	2.6	—	—
Al	2.5	3.5	2.8
Ca	1.1	2.5	1.7
Mg	0.30	0.80	0.50

Table 9. Concentration of impurities in MG-Si and their concentration after wet grinding as determined by ICP-AES. All values in p.p.m.

	Sample 1		Sample 2	
Element	Initial	After wet grinding	Initial	After wet grinding
Fe	4700	3100	4700	3500
Al	2100	1600	3100	2700
Ca	486	165	3100	2200
Mg	37	24	176	169
Mn	118	86	124	89
Cr	61	42	62	43
Ni	77	66	115	84
Cu	17	14	27	19
B	27	22	32	23
P	47	35	42	45

Contamination of SiH_2Cl_2

Dichlorosilane is produced by the disproportionation of $SiHCl_3$. The concentration of impurities in SiH_2Cl_2 produced from the disproportionation of crude $SiHCl_3$ as measured by ICP-AES is given in Table 8.

Refining of MG-Si by wet grinding

Metallurgical-grade Si is an inexpensive material produced by the reduction of SiO_2 with carbon in a furnace; it contains about 98% Si. Wet grinding is carried out to reduce the size of the grains in MG-Si. The process is important, not only because it reduces the physical size of the Si grains but also because it leads to removal of the impurities. Table 9 gives the impurities found in two samples of MG-Si before and after wet grinding. It can be seen that wet grinding removes part of the contamination but the improvement is less than a factor of two.

Upgrading of MG-Si by acid leaching and directional solidification

One of the simplest methods for upgrading MG-Si is by acid leaching together with magnetic separation. Table 10 gives the concentration of the impurities after a single leaching with HF (12%) + HCl (9%) at 80 °C for 1 h and after two leaching cycles in which the second cycle was carried out with a solution of HF (12%) + HCl (9%) + $C_2H_2O_4$ (10%) at 150 °C in an autoclave under its own pressure for 1 h. It can be seen that he level of contamination is reduced considerably; however, the purity is not sufficient for solar-grade Si. Further purification can be achieved by gas-assisted uni-directional solidification as shown in Table 10.

This work was supported by a grant from the National Science Council of the Republic of China.

References

1. McCormick, J. R., "Proceedings of the 16th IEEE Photovoltaic Specialist Conference," San Diego, 1982, pp. 57–61
2. Lerpold, M. H., "Proceedings of the 5th EC Photovoltaic Solar Energy Conference," Athens, 1983, p. 944.
3. Noda, T. "Proceedings of the Flat-plate Solar Array Project Workshop on Low-cost Polysilicon for Terrestrial Photovoltaic Solar Cell Applications," Las Vegas, 1985, pp. 213–230.
4. Aulich, H. A., "Proceedings of the Silicon Materials Research Symposium," Hsinchu, Taiwan, 1986, p. 18.
5. Wiehl, N., Herpers, U., and Weber, E., *J. Radioanal. Chem.*, 1982, **72**, 69.
6. Revel, G., Deschamps, N., Dardenne, C., Pastol, J. L., Hania, B., and Nguyen Dinh, H., *J. Radioanal. Nucl. Chem. Lett.*, 1984, **85**, 137.
7. Keenan, J. A., Genade, B. E., and White, J. B., *J. Electrochem. Soc.*, 1985, **132**, 2232.
8. Revel, G., *in* Roth, E., *Editor*, "Euroanalysis VI Conference Proceedings, Paris, September 7–11, 1987," Editions Physiques, Paris, 1988, p. 163.

Table 10. Concentration of elemental impurities in the various stages of upgrading MG-Si by chemical leaching/gas-assisted solidification methods

		Chemical leaching			Gas-assisted	
Element	MG-Si, p.p.m.	One cycle	Two cycles	Analytical method	solidification, p.p.b.	Analytical method
Al	6300	250	130	NAA, ICP-AES	<6	NAA
Fe	2800	32	2.5	ICP-AES	<4	NAA
Ca	2100	13	7.4	ICP-AES	<98	NAA
Cr	140	1.6	—	ICP-AES	<6	NAA
Co	77	—	—	ICP-AES	<1	NAA
Mn	0.5	0.5	—	ICP-AES	<1	NAA
Cu	37	—	—	ICP-AES	<1	NAA
B	25	29	19	ICP-AES	<81	ICP-AES

9. Verheijke, M. L., Jaspers, H. J. J., Hanssen, J. M. G., and Theunissen, M. J. J., *J. Radioanal. Nucl. Chem. Articles*, 1987, **113**, 397.
10. Haas, E. W., and Hofman, R., *Int. J. Solid State Elect.*, 1987, **30**, 329.
11. Rausch, H., Csada, G. I., and Szabo, E., *Chem. Zvesti*, 1967, **21**, 592.
12. Martynov, Y. M., Kreingold, E. A., and Maevskaya, B. M., *Zavod. Lab.*, 1965, **31**, 1443.
13. Dias, C. C., Jani, K. P., Murugaiyan, P., and Venkateswarlu, Ch., *Analyst*, 1975, **100**, 259.
14. Chang, M. M., Chen, C. C., Liu, C. S., Chang, C. T., and Shu, F. R., *J. Chin. Inst. Chem. Eng.*, 1974, **5**, 99.
15. Lu, C. L., Lin, K. N., and Chang, C. T., *Proc. Natl. Sci. Council (Taiwan)*, 1976, **9**, 913.
16. Zief, M., and Mitchell, J. W., "Contamination Control in Trace Element Analysis," Wiley, New York, 1976.
17. Boumans, P. W. J. M., and de Boer, F. J., *Spectrochim. Acta, Part B*, 1975, **30**, 309.
18. Fassel, V. A., and Knisley, R. N., *Anal. Chem.*, 1974, **46**, 1110A.
19. Currie, L. A., *Anal. Chem.*, 1968, **40**, 580.
20. Boumans, P. W. J. M., "Inductively Coupled Plasma Emission," Wiley, New York, 1987, p. 138.
21. Montaser, A., and Golightly, D. W., "Inductively Coupled Plasmas in Analytical Atomic Spectrometry," VCH, Weinheim, 1987, p. 178.
22. Fassel, V. A., *in* Fuwa, K., *Editor*, "Recent Advances in Analytical Spectroscopy," Pergamon Press, Oxford, 1982, pp. 1–15.
23. Haas, W. J., and Fassel, V. A., *in* "Elemental Analysis of Biological Materials," IAEA Technical Report Series No. 197, IAEA, Vienna, 1980, p. 167.
24. McQuaker, N. R., Kluckner, P. O., and Chang, G. N., *Anal. Chem.*, 1979, **51**, 888.
25. Dalquist, R. L., and Knoll, J. W., *Appl. Spectrosc.*, 1978, **32**, 1.
26. Greenfield, S., McGeachin, H. McD., and Smith, P. B., *Anal. Chim. Acta*, 1976, **84**, 67.
27. West, A. C., Fassel, V. A., and Knisley, R. N., *Anal. Chem.*, 1973, **45**, 1586.

Paper 9/00681H
Received February 13th, 1989
Accepted July 18th, 1989

Carbon Paste - Tetrathiafulvalene Amperometric Enzyme Electrode for the Determination of Glucose in Flowing Systems

Hari Gunasingham and Chin-Huat Tan
Department of Chemistry, National University of Singapore, Kent Ridge, Singapore 0511, Singapore

The development of a carbon paste - tetrathiafulvalene amperometric enzyme electrode for the determination of glucose in flowing streams is described. The enzyme electrode is operated in a flow-through detector based on the wall-jet configuration under flow injection (FI) and steady-state (SS) conditions. Under FI conditions, high precision (0.6%) and sample throughput (120 samples h^{-1}) are possible. Moreover no pre-conditioning of the electrode is required. The flow system is suitable for the determination of glucose in whole blood without sample dilution. With proper orientation of the jet with respect to the enzyme electrode, high accuracy can be obtained under SS conditions.

Keywords: *Amperometric enzyme electrode; tetrathiafulvalene; wall-jet electrode; glucose determination; flow injection*

Second generation amperometric enzyme electrodes employ a low relative molecular mass synthetic mediator as an electron shuttle between the enzyme redox centre and the electrode in place of naturally occurring oxygen.[1–16] Hence, a prerequisite of the mediator is its capacity for facile electron exchange with the active centre of the enzyme. Among other desirable characteristics are a low solubility in aqueous systems (this facilitates the immobilisation of the mediator on the electrode surface), high stability in both oxidised and reduced states (crucial for the stability of the enzyme electrode in practical applications) and fast heterogeneous electron-transfer kinetics at the electrode surface (allowing high sensitivity and fast response times).

In second generation glucose enzyme electrodes, a variety of mediators have been employed. These include ferrocenes,[3–7] quinones,[8–12] *N*-methylphenazine,[13] tetracyanoquinodimethane,[12] hexacyanoferrate(II)[14] and tetrathiafulvalene.[15,16] Of these, dimethylferrocene has been the most well developed and is the basis of a commercial monitor.[7]

The fabrication of a useful amperometric enzyme electrode requires consideration of the way in which the mediator - enzyme system is immobilised on the surface of the electrode. Simplicity and performance are the main guiding principles. For this reason, droplet evaporation of the mediator on to the surface of the electrode has been the most commonly applied technique.[3] Covalent binding has also been employed (via a polymer film) but has the disadvantage of the need for complicated organic chemistry; also, such systems have been found to be relatively unstable.[17] Another approach that qualifies on the grounds of its simplicity is to use a carbon paste electrode, where the mediator is mixed with the graphite-binder matrix making up the working electrode. However, for the purpose of an amperometric glucose sensor, only two types of system have to our knowledge been hitherto reported. One is based on quinone as the mediator[10,11] and the other on dimethylferrocene.[6]

As far as we are aware, the efficacy of carbon paste - mediator enzyme electrodes in flow systems has not been reported.

We are particularly interested in the analysis of undiluted whole blood under flow injection (FI) and steady-state (SS) conditions. In this paper a carbon paste - tetrathiafulvalene (TTF) enzyme electrode is employed, which has not been used previously in such studies. It is shown that the wall-jet cell configuration is well suited for the determination of glucose in whole blood under SS conditions. Although there is no need to dilute the sample, due consideration has to be given to the flow conditions in addition to the geometry, orientation and positioning of the jet inlet with respect to the enzyme electrode.

Experimental

Chemicals and Solutions

Tetrathiafulvalene (>99%) was obtained from Fluka Chemie (Buchs, Switzerland). Glucose oxidase (GOD) (E.C. 1.1.3.4, Type II from *Aspergillus niger*), bovine serum albumin (BSA) (Fraction V, 96–99% albumin), glutaraldehyde (GLA) (25% aqueous) and D(+)-glucose were obtained from Sigma (St. Louis, MO, USA). All other reagents used were of AnalaR grade. The carrier solution was 0.1 M sodium phosphate buffer (pH 7.4) containing 0.01% m/v sodium azide made up in Millipore Milli-Q grade water. All standards were also made up in this buffer. Glucose solutions were allowed to equilibrate overnight before use. For the pH studies, solutions were prepared by mixing with the appropriate amount of 0.1 M mono- or 0.1 M di-sodium phosphate solution. The pH was confirmed with a Corning pH meter and Model 150 ion analyser.

Construction of the Enzyme Electrode

A graphite rod (3 mm diameter) was obtained from Johnson Matthey (Royston, UK). A 2-mm thick disc was cut off from the rod and polished with abrasive paper. Electrical contact was made by a wire connected to one side of the disc with silver-loaded epoxy resin. The disc was then inserted into a PTFE holder and sealed with epoxy resin leaving a well of depth 1 mm. Prior to use, the electrode was cleaned successively with ethanol, nitric acid and ultrasonically in distilled water. The electrode was then oven dried at 80 °C.

The carbon paste was prepared by mixing the appropriate amount of TTF in acetone with graphite powder. The graphite powder was prepared by grinding a graphite rod into a fine powder using a pestle and mortar. The powder was refined further by passing it through a sieve screen (300 track per inch, Haver, FRG). The acetone was evaporated off by passing a stream of purified nitrogen into the mixture. Nujol (SpectrosoL, BDH, Poole, Dorset, UK), 20% m/m was then added to the graphite - TTF mixture, which was mixed with a stainless-steel spatula until a paste with an even consistency was obtained.

The enzyme electrodes were prepared by packing the carbon paste into the well of the electrode and then compressing and levelling it off with a flat spatula. The surface of the carbon paste was polished on an index card until a perfectly smooth surface was obtained. Glucose oxidase solution (10 μl) was deposited on the surface of the carbon paste and dried for 2 h at 4 °C. Then 2.5 μl of a freshly prepared solution of 5% BSA and 2.5% GLA were deposited

on top of the dried GOD and this was then covered with a polycarbonate membrane (0.03 μm pore size, Nucleapore, Pleasanton, CA, USA). The membrane was held in place with a PTFE cap. The enzyme electrode was allowed to set at 4 °C overnight.

Apparatus

Cyclic voltammetric measurements were performed with a PAR Model 273 potentiostat/galvanostat. Voltammograms and current - time plots were recorded with a Graphtec Model WX2400 *x* - *y* recorder. The reference electrode was a saturated calomel electrode (SCE) (Corning, Essex, UK) or Ag - AgCl and the counter electrode was glassy carbon. The water-bath was obtained from Hotech Instruments (Model 801, Taiwan).

Thin-layer Cell

A thin-layer cell with a working volume of 80 μl was used for the cyclic voltammetric studies. The counter electrode was graphite and the reference electrode was Ag - AgCl. The sample solutions were loaded into the loop of the manual injector valve (Valve V-7, Pharmacia Fine Chemicals, Uppsala, Sweden) and the working solutions were delivered with a peristaltic pump (Model MP-3, Eyela, Tokyo Rikakikai, Tokyo, Japan). The pump was calibrated prior to use on the basis of the time taken for a fixed volume to be delivered. Current - time plots were recorded with the Graphtec *x* - *y* recorder.

Automated Flow System

A large volume wall-jet cell was used for the SS and FI studies.[18] The reference electrode was Ag - AgCl and the counter electrode was graphite. A pneumatically actuated flow-injection valve (Model 5701, Rheodyne, Cotati, CA, USA) was employed with two peristaltic pumps to deliver the sample and carrier streams. The sample volume was 25 or 250 μl for the FI and SS measurements, respectively. The potential was controlled by a PAR 174A polarographic analyser. The entire system was under the control of an IBM compatible microcomputer, which allowed the automatic control of the flow system and the recording of current responses without user intervention.

Whole Blood Analysis

Blood from diabetic patients was obtained from the Diabetic Clinic of the National University Hospital. Blood samples were stored in heparinised phials and analysed within a few hours of collection. Blood glucose levels determined using the amperometric glucose sensor were compared against a Boehringer Reflolux Haemo-Glukotest 20-800R test strip that had been previously validated against a Beckman Astra Analyser.[19]

Results and Discussion

Cyclic Voltammetry

Tetrathiafulvalene undergoes two one-electron oxidation processes in aqueous solution leading to the formation of TTF^+ and TTF^{2+}.[20,21] The first oxidation process is reversible. In the GOD enzyme reaction it is the first redox process that is involved in the electron mediation given by:

$$\text{Glucose} + \text{GOD}_{ox} \longrightarrow \text{gluconolactone} + \text{GOD}_{red} \quad (1)$$

$$\text{GOD}_{red} + 2TTF^+ \longrightarrow \text{GOD}_{ox} + 2TTF + 2H^+ \quad (2)$$

$$2TTF \rightleftharpoons 2TTF^+ + 2e^- \quad (3)$$

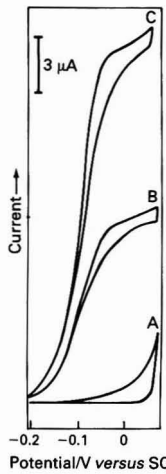

Fig. 1. Cyclic voltammograms at the carbon paste - TTF (20%) enzyme electrode. A, In 0.1 M phosphate buffer; B, in 6.45 mM glucose; and C, in 12.5 mM glucose. GOD loading, 0.4 mg; scan rate, 1 mV s^{-1}

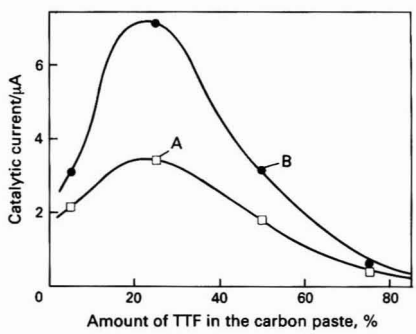

Fig. 2. Effect of the percentage of TTF in the carbon paste - TTF enzyme electrode. A, In 10 mM glucose; and B, in 20 mM glucose. GOD loading, 0.1 mg; operating potential, 180 mV *versus* Ag - AgCl

Fig. 1 shows cyclic voltammograms at the carbon paste - TTF enzyme electrode in the absence and presence of glucose. Although the cyclic voltammogram is not well defined in the absence of glucose, the catalytic current in the ensuing mediated enzyme reaction in the presence of glucose is distinct. Increasing the glucose concentration proportionately increases the catalytic current.

The ratio of the kinetically controlled catalytic current in the presence of glucose to the diffusion current in the absence of glucose gives an indication of the efficiency of TTF as a mediator. The typical ratio of the carbon paste - TTF system for 10 mM glucose is 1 : 20, which compares favourably with the dimethylferrocene enzyme electrode constructed by droplet evaporation of the ferrocene.[3] The TTF system also has the advantage that the operating potential is lower by about 50 mV *versus* SCE.

Effect of TTF Loading

Fig. 2 shows plots of the catalytic current against the percentage of TTF in the carbon paste. The catalytic current initially increases, reaching a maximum at a TTF loading of *ca.* 20%. Thereafter the catalytic current decreases rapidly reaching a negligible level as the TTF loading exceeds 80%.

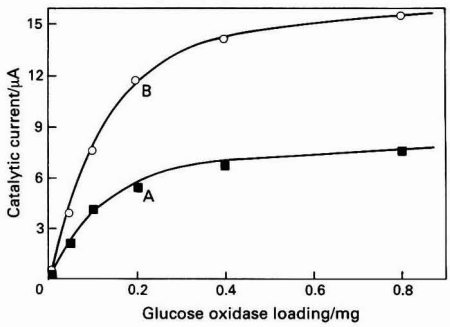

Fig. 3. Effect of GOD loading on the carbon paste - TTF (20%) enzyme electrode. A, In 6.45 mM glucose; and B, in 12.5 mM glucose. Catalytic current measured at 50 mV *versus* SCE

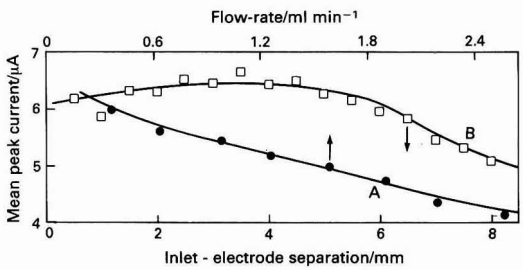

Fig. 4. Effect of A, flow-rate (inlet - electrode separation, 1 mm) and B, inlet - electrode separation (flow-rate, 1 ml min^{-1}) in the wall-jet detector on the carbon paste - TTF (20%) enzyme electrode. GOD loading, 0.4 mg; operating potential, 200 mV *versus* Ag - AgCl; glucose concentration, 10 mM; and sample volume, 25 μl

The observation of increasing catalytic current with TTF loading has been explained by Senda and co-workers[10,11] who have shown that the catalytic current is dependent on the concentration of the mediator. As the TTF loading increases beyond a point, the current decreases because of a lowering of the electrical conductivity with the reduction in graphite loading. There is, therefore, a trade-off between the TTF and graphite loadings. The optimum is a TTF loading in the range 20–30%.

Effect of GOD Loading

The effect of GOD loading is shown in Fig. 3. The catalytic current increases with the enzyme loading and reaches a limiting value at around 0.3 mg. The enzyme loading was therefore kept at 0.25 mg.

Effect of Flow-rate

The effect of flow-rate on the FI peak current is shown in Fig. 4 (curve A). The result is as expected for enzyme electrodes under FI conditions and is related to the residence time of the glucose at the surface of the enzyme electrode membrane.

Effect of Inlet - Electrode Separation

In conventional wall-jet electrodes where there is no reaction layer covering the surface of the working electrode, the practice is to optimise the inlet - electrode separation such that the inlet nozzle lies outside the wall-jet boundary layer.

Fig. 4 (curve B) shows the effect of inlet - electrode separation for the mediated enzyme electrode on the FI detection of a 10 mM glucose standard. The plot shows that, in contrast to conventional electrodes, the peak current response is constant up to a separation of *ca.* 5 mm.

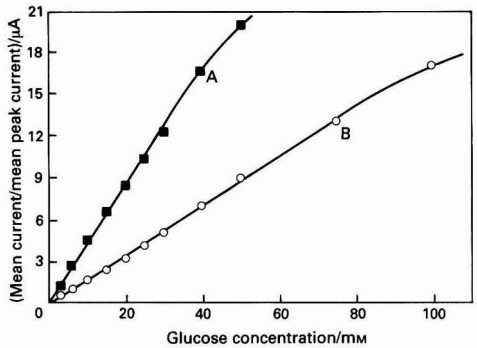

Fig. 5. Typical calibration graphs at the carbon paste - TTF (20%) enzyme electrode. GOD loading, 0.25 mg; operating potential, 200 mV *versus* Ag - AgCl. A, SS mode (flow-rate, 0.5 ml min^{-1}); and B, FI mode (sample volume, 25 μl; flow-rate, 1 ml min^{-1})

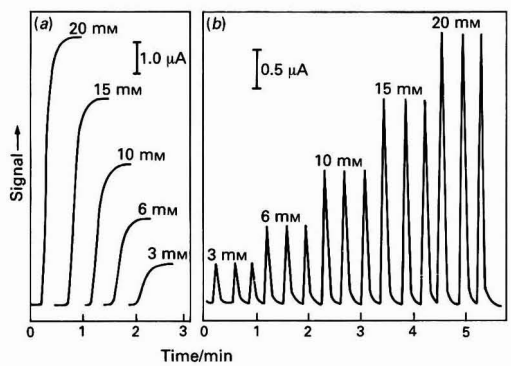

Fig. 6. Typical (*a*) SS and (*b*) FI profiles for the carbon paste - TTF (20%) enzyme electrode. Conditions as in Fig. 5

Linear Range

Fig. 5 shows the calibration graphs and Fig. 6 the actual responses obtained under SS and FI conditions. The calibration graphs show linearity under SS conditions up to *ca.* 35 mM and up to 80 mM under FI conditions. It is of interest that in both instances the plots pass through the origin. The upper limit of the linear range compares favourably with that reported by Cass *et al.*[3] for dimethylferrocene and by Cardosi[15] for TTF where the mediator was droplet evaporated on to the surface of the electrode.

The carbon paste - TTF electrode has a relatively fast response time. As shown in Fig. 6, the SS response is achieved within 30 s. In the FI mode, a sample throughput in excess of 120 samples h^{-1} is feasible.

Effect of pH

The effect of pH is shown in Fig. 7. A maximum is reached between 7.5 and 8.0. This is to be compared with the ferrocenes, which have been shown to be independent of pH.[3]

Effect of Temperature

Fig. 8 shows the effect of temperature on the SS current. The current response increases, reaching a maximum at about

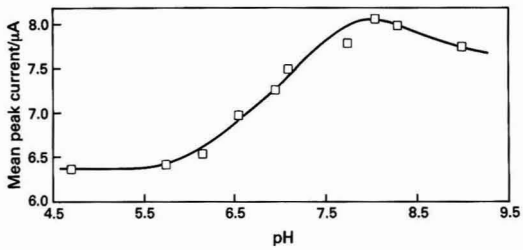

Fig. 7. Effect of pH on the carbon paste - TTF (20%) enzyme electrode. GOD loading, 0.25 mg; operating potential, 200 mV *versus* Ag - AgCl; glucose concentration, 10 mM; sample volume, 25 μl; and flow-rate, 1 ml min^{-1}

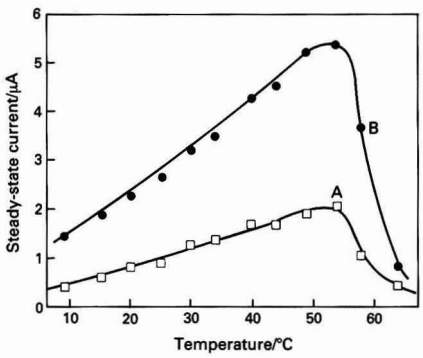

Fig. 8. Effect of temperature on the carbon paste - TTF (20%) enzyme electrode. A, 3.28 mM glucose; and B, 9.52 mM glucose. Operating potential, 200 mV *versus* Ag - AgCl

50 °C. Thereafter, the response declines rapidly presumably as a result of denaturing of the enzyme.

Stability

One of the advantages of the carbon paste - TTF enzyme electrode is the fact that pre-conditioning of the electrode is not necessary as in the ferrocene-based electrodes.[3,5] The electrode is highly stable as illustrated in Fig. 9 which shows successive injections of 10 mM glucose. The precision for 100 injections in terms of the relative standard deviation is 0.6%.

In terms of its long-term stability, the carbon paste electrode was used continuously for 2000 injections of a 10 mM glucose standard with only an 8% decline in the current response. The lifetime of the enzyme electrode is dictated more by degradation of the enzyme than by loss of TTF as the carbon paste provides a large reservoir of TTF. For this reason, the carbon paste - TTF enzyme electrode has a longer lifetime than an enzyme electrode prepared by droplet evaporation of TTF on to a solid electrode surface.

Interferences

One of the advantages of mediated enzyme electrodes is the ability to operate the electrode at a lower potential where the interfering effects of electroactive species that may be present in physiological species can be obviated. For the carbon paste - TTF electrode only ascorbic acid interferes in any significant way at the normal operating potential (150–200 mV *versus* Ag - AgCl) as shown in Fig. 10. Normal physiological levels of ascorbic acid are fairly low (*ca* 0.2 mM) and thus should not affect the results adversely.

Whole Blood Analysis

The analysis of whole blood in flowing systems requires careful consideration of matrix effects. The following are some of the important considerations. (i) Whole blood is more viscous than the aqueous glucose standards used to calibrate the electrode. (ii) Blood cells and other particles in blood tend to increase the residence time on the surface of the electrode. This is particularly a problem when the electrode membrane exposed to the flowing solution is roughened or not hydrophobic. (iii) Because of the higher viscosity and the density of blood cells and other particles in the blood, the orientation of the jet is critical. For the wall-jet cell it was necessary to work at a low flow-rate (0.5 ml min^{-1}) and orient the jet in such a way that it was vertical to the electrode surface. Also, the inlet - electrode separation had to be kept at about 0.5 mm.

Table 1 summarises levels of glucose in blood determined using the enzyme electrode compared with values obtained by

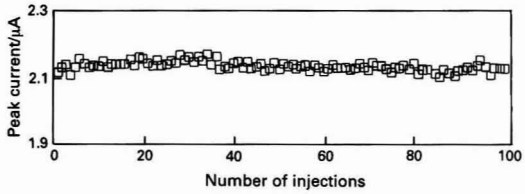

Fig. 9. Effect of successive injections of glucose on the carbon paste - TTF (20%) enzyme electrode. GOD loading, 0.25 mg; operating potential, 200 mV *versus* Ag - AgCl; glucose concentration, 10 mM; sample volume, 25 μl; and flow-rate, 1 ml min^{-1}

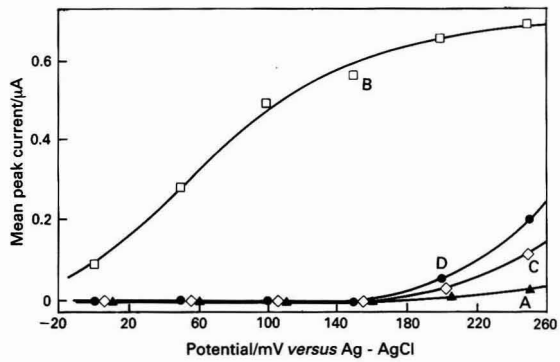

Fig. 10. Potential - peak current profile for A, H_2O_2; B, ascorbic acid; C, paracetamol; and D, uric acid at the carbon paste - TTF (20%) enzyme electrode. Concentration of each compound, 2 mM; sample volume, 25 μl; and flow-rate, 1 ml min^{-1}

Table 1. Determination of glucose (mM) in whole blood using the carbon paste - TTF (20%) enzyme electrode compared with a standard method. Operating potential, 200 mV *versus* Ag - AgCl; flow-rate, 0.5 ml min^{-1}

	Carbon paste - TTF electrode		
Sample	SS mode	FI mode	Reflolux method[19]
S1	10.3	12.1	10.5
S2	6.3	7.4	6.5
S3	8.7	11.1	8.2
S4	7.7	9.4	7.3
S5	7.7	8.7	7.7
S6	9.0	8.1	8.6
S7	7.5	5.8	7.5
S8	8.5	7.1	8.4
S9	8.9	9.1	8.4
S10	5.8	6.0	5.6

a standard reflectance technique.[19] The SS mode gives a good correlation whereas the FI mode generally gives higher values.

The award of grants from the Singapore Science Council and the National University of Singapore is gratefully acknowledged.

References

1. Aston, W. J., *in* Turner, A. P. F., Karube, I., and Wilson, G. S., *Editors*, "Biosensors Fundamentals and Applications," Oxford University Press, Oxford, 1987, p. 276.
2. Bartlett, P. N., and Whitaker, R. G., *Biosensors*, 1987/88, **3**, 359.
3. Cass, A. E. G., Davis, G., Francis, G. D., Hill, H. A. O., Aston, W. J., Higgins, I. J., Plotkin, E. V., Scott, L. D. L., and Turner, A. P. F., *Anal. Chem.*, 1984, **56**, 667.
4. Lange, M., and Chambers, J. Q., *Anal. Chim. Acta*, 1985, **175**, 89.
5. Green, M. J., and Hill, H. A. O., *J. Chem. Soc., Faraday Trans. 1*, 1986, **82**, 1237.
6. Dicks, J. M., Aston, W. J., Davis, G., and Turner, A. P. F., *Anal. Chim. Acta*, 1986, **182**, 103.
7. Matthews, D. R., Holman, R. R., Bown, E., Steemson, J., Watson, A., Hughes, S., and Scott, D., *Lancet*, 1987, **1**, 778.
8. Williams, D. L., Doig, A. R., and Korosi, A., *Anal. Chem.*, 1970, **42**, 118.
9. Ikeda, T., Katasho, I., Kamei, M., and Senda, M., *Agric. Biol. Chem.*, 1983, **48**, 1969.
10. Ikeda, T., Hamada, H., Miki, K., and Senda, M., *Agric. Biol. Chem.*, 1985, **49**, 541.
11. Senda, M., Ikeda, T., Miki, K., and Hasa, H., *Anal. Sci.*, 1986, **2**, 501.
12. Kulys, J. J., and Cenas, N. K., *Biochim. Biophys. Acta*, 1983, **744**, 57.
13. Jonsson, G., and Gorton, L., *Biosensors*, 1985, **1**, 355.
14. Ohura, H., Imato, T., Amasaki, S., and Ishibashi, N., *Anal. Sci.*, 1987, **3**, 453.
15. Cardosi, M. F., *Anal. Proc.*, 1987, **24**, 143.
16. Gunasingham, H., and Tan, C. H., *Electroanalysis*, in the press.
17. Foulds, N. C., and Lowe, C. R., *Anal. Chem.*, 1988, **60**, 2473.
18. Gunasingham, H., and Fleet, B., *Anal. Chem.*, 1983, **55**, 1409.
19. Gunasingham, H., Ang, K. P., Teo, P. Y. T., Tan, C. B., Tay, B., Aw, T. C., and Thai, A. C., *Anal. Chim. Acta*, 1989, **221**, 205.
20. Kamache, M., Menet, H., and Moradpour, A., *J. Am. Chem. Soc.*, 1982, **104**, 4520.
21. Kuo, K. N., Moses, P. R., Lenhard, J. R., Green, D. C., and Murray, R. W., *Anal. Chem.*, 1979, **51**, 745.

Paper 9/02112D
Received May 19th, 1989
Accepted July 4th, 1989

Determination of Nanomolar Levels of Histidine by Differential-pulse Adsorptive - Cathodic Stripping Voltammetry of its Copper(II) Complex

Josino C. Moreira and Arnold G. Fogg*
Chemistry Department, Loughborough University of Technology, Loughborough, Leicestershire LE11 3TU, UK

Histidine was determined at the 5×10^{-9}–1.6×10^{-7} M level by differential-pulse adsorptive stripping voltammetry at a hanging mercury drop electrode using the reduction peak of its copper(II) complex at −0.27 V *versus* Ag - AgCl obtained in pH 9.2 borate or hydrogen carbonate buffer: free copper(II) is reduced at −0.10 V. The copper(II) - tryptophan complex is also adsorbed, is reduced at −0.20 V and interferes when present at five times the concentration of the histidine complex. Other amino acids do not interfere. The copper(II) complexes of cysteine and cystine adsorb and are reduced at significantly more negative potentials than the histidine complex; these amino acids can be determined simultaneously with histidine. Surfactants interfere when present at high concentrations.

Keywords: *Histidine determination; adsorptive stripping voltammetry; copper(II) - histidine complex*

Histidine is a substance of biological importance owing to its ability to bind transition metals in biological systems.[1,2] Participation of histidine in complex formation has been proposed as part of the mode of action of many enzymes and metalloproteins including azurin, superoxide dismutase and haemocyanin. Histidine also appears to be involved in copper(II) transport in blood plasma.[3]

Many methods have been proposed for the determination of trace amounts of histidine, and several of these are electrochemical. A polarographic method has been developed that utilises a copper amalgam electrode,[4] while another uses a nickel(II) catalytic pre-wave.[5] Turbulent hydrodynamic voltammetry[6] and an indirect determination based on the use of the palladium(II) wave[7] have been used to determine histidine at relatively high levels (*ca.* 10^{-4} M).

Differential-pulse cathodic stripping voltammetry is a very sensitive method for the determination of substances that can be accumulated and then reduced at electrode surfaces. Synthetic food colours have been determined at the 1×10^{-9} M level in this laboratory after adsorptive accumulation at a hanging mercury drop electrode (HMDE).[8]

In the presence of an excess of Cu^{2+} ions, histidine is completely converted to a range of complexes whose stability constants and pH zones of stability have been reported.[9,10] In the present paper histidine is shown to be adsorbed at the surface of an HMDE in the presence of an excess of copper(II) and a method for determining histidine by differential-pulse adsorptive stripping voltammetry of the adsorbed copper species is proposed.

Experimental

Adsorptive stripping voltammetry was carried out with a Metrohm 626 Polarecord with a 663 VA stand using a multi-mode electrode in the HMDE mode. The three-electrode system was completed by means of a glassy carbon auxiliary electrode and an Ag - AgCl reference electrode. The cyclic voltammetric experiments were carried out by connecting the electrodes on the Metrohm 663 stand to a PAR 174A polarographic analyser (Princeton Applied Research): the multi-mode electrode (HMDE) was still activated by means of the Metrohm 626 Polarecord. The pH measurements were made with a Corning combined pH/reference electrode and a Radiometer PHM 64 pH meter, standardised with pH 7.00 phosphate buffer and pH 9.18 borate buffer.

Biochemicals were obtained from Sigma. L-Lysine hydrochloride, L-methionine and aspartic acid were Calbiochem A grade products. All solutions were prepared in de-ionised water from a LiquiPure system.

A 1.00×10^{-1} M solution of histidine was prepared by dissolving 0.1048 g of L-histidine hydrochloride monohydrate in 50 ml of de-ionised water in a calibrated flask. Stock standard solutions of copper(II), lead(II), cobalt(II), cadmium(II) and zinc(II) of suitable concentration were prepared by diluting SpectrosoL atomic absorption standard solutions (BDH).

Borate buffer solution (pH 9.2) was prepared by adjusting the pH of a sodium tetraborate solution with dilute hydrochloric acid or sodium hydroxide solution. The copper content of this buffer solution was determined to be 6×10^{-8} M by anodic stripping voltammetry.

The general procedure used for obtaining adsorptive stripping voltammograms was as follows. A 15-ml aliquot of 0.01 M pH 9.2 buffer solution was placed in a voltammetric cell and the required amounts of standard histidine and copper(II) solutions were added. The stirrer was switched on and the solution was purged with nitrogen for 6 min. Subsequently, deoxygenation was carried out for 15 s between adsorptive stripping cycles. After forming a new HMDE (maximum sized drop), a 2-min accumulation was effected at −0.15 V with stirring (maximum stirrer speed). At the end of the accumulation period the stirrer was switched off, and, after 20 s had elapsed to allow the solution to become quiescent, a negative potential scan was initiated between −0.15 and −0.60 V at 10 mV s^{-1} using the differential-pulse mode (pulse amplitude 50 mV).

Results and Discussion

When accumulation was effected at potentials more positive than −0.10 V the differential-pulse adsorptive stripping voltammograms obtained for histidine in the presence of an excess of Cu^{2+} ions exhibited two peaks, one at −0.12 V for free copper(II) and another at −0.27 V for the copper(II) - histidine complex. The height of the latter peak was shown to be dependent on the histidine and copper(II) concentrations, pH, accumulation potential and accumulation time. The effect of these parameters was investigated in order to optimise conditions for the determination of histidine.

The copper(II) concentration was varied from 5.0×10^{-8} to

* To whom correspondence should be addressed.

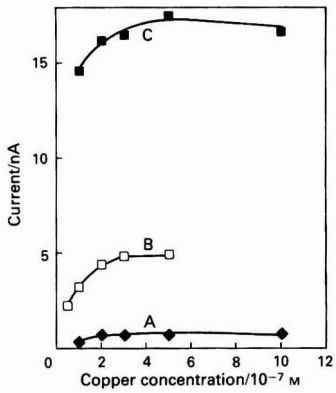

Fig. 1. Effect of added copper(II) concentration on the height of the differential-pulse adsorptive stripping voltammetric peak of the copper(II) - histidine complex. pH = 9.2; accumulation potential = −0.15 V; accumulation time = 120 s. Histidine concentration: A, 0; B, 1.5; and C, 7.0×10^{-8} M. Values for B and C are corrected for the blank

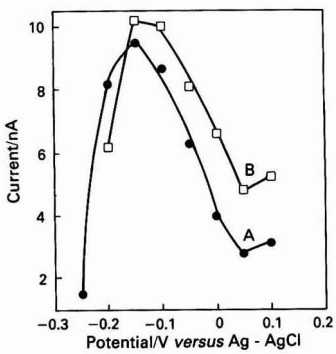

Fig. 2. Effect of accumulation potential on the height of the copper(II) - histidine peak. Histidine concentration = 4×10^{-8} M. Added copper(II) concentration = 5×10^{-7} M. A, In borate buffer; and B, in hydrogen carbonate buffer

Table 1. Effect of the pH on the height of the copper(II) - histidine peak. Added copper(II) concentration, 5×10^{-7} M; accumulation time, 120 s; accumulation potential, −0.15 V; histidine concentration, 2×10^{-8} M. Borate buffer

pH	8.5	9.0	9.2	9.3	9.4	9.6	9.8	10.3
Current/nA	2.4	3.8	4.3	4.6	4.4	4.0	3.8	3.9

1.0×10^{-6} M in the presence of 1.0×10^{-8}–1.2×10^{-7} M histidine. The reduction peak of the copper(II) - histidine complex increased with the copper(II) concentration up to about 5.0×10^{-7} M above which its size was limited by the histidine concentration. The effect of the copper(II) concentration on the height of the peak is shown in Fig. 1. The blank signal is caused by organic material in the de-ionised water.

Between pH 8 and 10 the main species present is the copper(II) - $(histidine)_2$ complex. The effect of pH on the height of the peak is shown in Table 1. The maximum height was observed at pH 9.3, but little difference in height was observed between pH 8.9 and 10.3. No adsorptive stripping signal was observed at pH < 8.0. The use of other buffers that cover this pH range was studied. Very poor signals were observed when Trizma was used; however, hydrogen carbonate buffer gave similar results to borate buffer and could be used up to pH 12.0 without loss of sensitivity.

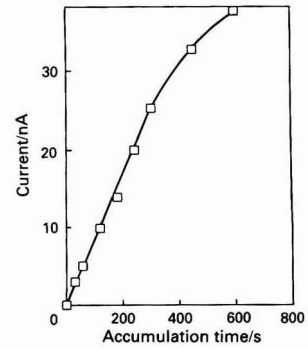

Fig. 3. Effect of accumulation time on the height of the copper(II) - histidine peak. Histidine concentration = 4×10^{-8} M. Added copper(II) concentration = 5×10^{-7} M

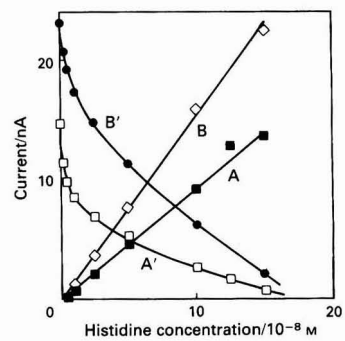

Fig. 4. Calibration graphs for the determination of A and B, histidine; and A′ and B′, effect of histidine concentration on the height of the free copper(II) peak. Drop size: A and A′, 1; and B and B′, 2

The effect of accumulation potential on the height of the copper(II) - histidine peak is shown in Fig. 2. An accumulation potential between −0.10 and −0.15 V is optimum. At more negative potentials the peak decreases rapidly as the reduction potential for the complex is approached. At more positive potentials the free copper(II) peak increases with a consequent general increase in the base line for the complex peak. The complex peak decreases in height as the free copper(II) peak increases. This may, in part, be an apparent decrease owing to the overlapping of the two peaks, but a decrease would be expected owing to competition between the two reactions for the electrode surface.

For optimum solution conditions the peak height of the complex increases rectilinearly with accumulation time up to about 5 min (see Fig. 3). At longer accumulation times rectilinearity is lost as a new peak (at a potential 70 mV more positive than the main peak), which may be due to the adsorption of a different copper(II) - histidine complex, appears.

Typical calibration graphs at two mercury drop sizes are shown in Fig. 4. Calibration is rectilinear up to at least 1.6×10^{-7} M histidine. The initial large decrease in the size of the free copper(II) peak with increasing histidine concentration is evident. Using a 2-min accumulation time, 5.0×10^{-9} M histidine could be determined readily. The precision was good: six determinations of histidine at the 4.0×10^{-8} M level gave a coefficient of variation of 3.6%.

Possible interferences in the determination of histidine as its copper(II) complex were investigated. The effect of other metal ions and amino acids, in particular, was examined.

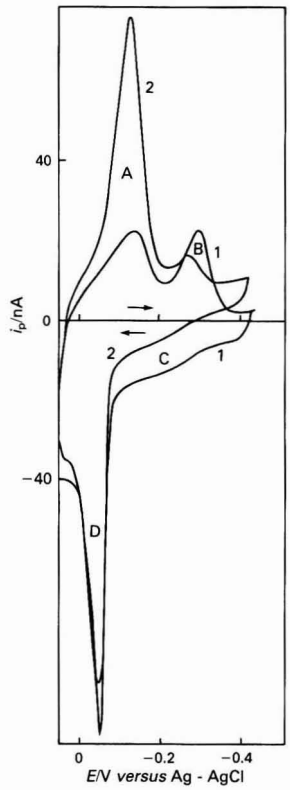

Fig. 5. Cyclic voltammogram of 1.0×10^{-7} M histidine at pH 9.2 in the presence of 5×10^{-7} M copper(II). Accumulation time = 120 s; accumulation potential = +0.05 V; scan rate = 10 mV s^{-1}. 1, First; and 2, second scan. Peaks A, B, C and D are identified in the text

Studies of interferences were carried out in a copper(II) solution in the presence and absence of 2.0×10^{-8} M histidine. Glycine, tyrosine, lysine, arginine, methionine, phenylalanine and aspartic acid did not interfere when present at the 1×10^{-7} M level. Tryptophan interfered at concentrations $>5.0 \times 10^{-8}$ M owing to the adsorption of its copper complex which was reduced at −0.20 V. Reduction peaks were observed for the copper(II) complexes of cysteine and cystine, but as these were at more negative potentials than that of the histidine complex, they did not interfere. As the determination is carried out in the presence of an excess of copper(II), and the histidine and cysteine/cystine peaks were completely resolved, it is possible to determine histidine and cysteine/cystine in mixtures. No significant difference (<10%) was observed when mixtures covering the range 1.0×10^{-8}–7.5×10^{-8} M were analysed. Cysteine and cystine were determined at the 2.0×10^{-9} M level under the conditions used.

Surface-active agents interfere by inhibiting adsorption of the copper(II) - histidine complex. In the presence of 0.5 mg l^{-1} of Triton X-100, the height of the copper(II) - histidine peak was reduced by 50%. Chelating agents, if present at sufficiently high concentrations, interfere by masking the added copper(II). This interference can be overcome by adding more copper(II). Lead(II), zinc(II), nickel(II), cadmium(II) and cobalt(II) did not interfere at the 1.0×10^{-6} M level. Nickel(II) and zinc(II) interfered at higher levels by competing with copper(II) for the histidine.

Cyclic voltammograms obtained for a solution 1.0×10^{-7} M in histidine and 5.0×10^{-7} M in copper(II) are shown in Fig. 5. The reduction processes due to the reduction of free copper(II) (peak A) and the copper(II) - histidine complex (peak B) can clearly be seen. On the reverse scan a partially developed oxidation process (peak C) associated with the copper(II) - histidine reduction peak was observed, in addition to a large peak due to the oxidation of copper (peak D). The histidine peaks (B and C) decreased markedly on subsequent cycles, whereas the free copper(II) peaks (A and D) increased. The cathodic peak B increased rectilinearly with scan rate as expected for the reduction of an adsorbed species,[11] and its peak potential was shifted 0.07 V in the negative direction when the scan rate was increased from 5 to 200 mV s^{-1}. The heights of peaks A and D are copper(II) concentration dependent, whereas those of peaks B and C are copper(II) - histidine dependent. These results are in agreement with those of Pena and Lopez[12] and Thomas and Zacharias[13,14] on similar systems, and are consistent with a one-electrode reduction process for the reduction of the copper(II) - histidine complex.

References

1. Freeman, H. C., *in* Eichorn, G. L., *Editor*, "Inorganic Biochemistry," Volumes 1 and 2, Elsevier, New York, 1973.
2. Hughes, M. N., "The Inorganic Chemistry of Biological Processes," Second Edition, Wiley, Chichester, 1981.
3. Lau, S. J., and Sarkar, B., *J. Biol. Chem.*, 1971, **246**, 5938.
4. Sanchez Perez, A., and Lucena Nobre, F., *J. Electroanal. Chem.*, 1976, **74**, 339.
5. Lopez Fonseca, J. M., and Arredondo, M. C., *An. Quim., Ser. A*, 1984, **80**, 377.
6. Varadi, M., and Pungor, E., *Magy. Kem. Foly.*, 1978, **84**, 58.
7. Jovanovic, D. A., *Acta Pharm. Jugosl.*, 1976, **26**, 229.
8. Fogg, A. G., Barros, A. A., and Cabral, J. O., *Analyst*, 1986, **111**, 831.
9. Freeman, H. C., and Martin, R. P., *J. Biol. Chem.*, 1969, **244**, 4823.
10. Kruck, T. P. A., and Sarkar, B., *Can. J. Chem.*, 1973, **51**, 3549.
11. Bard, A. G., and Faulkner, L. R., "Electrochemical Methods," Wiley, New York, 1980.
12. Pena, M. J., and Lopez, V., *An. Quim., Ser. A*, 1986, **82**, 28.
13. Thomas, G., and Zacharias, P. S., *Transition Met. Chem.*, 1984, **9**, 377.
14. Thomas, G., and Zacharias, P. S., *Polyhedron*, 1985, **4**, 811.

Paper 9/02397F
Received June 7th, 1989
Accepted August 2nd, 1989

Comparison of Stripping Methods at Thin-film Mercury Electrodes

Marina Mlakar and Milivoj Lovrić*
Center for Marine Research Zagreb, "Rudjer Bošković" Institute, POB 1016, Zagreb 41001, Yugoslavia

When a thin mercury film covered glassy carbon rotating disc electrode (TMFGCRDE) was used in square-wave anodic stripping voltammetric measurements, the highest sensitivity was obtained when the electrode was rotated slowly. The application of advanced analytical instrumentation to such measurements requires the addition of mercury ions to the sample.

Keywords: *Thin-film mercury electrode; glassy carbon electrode; rotating disc electrode; square-wave voltammetry; anodic stripping voltammetry*

The determination of toxic trace metals is an important problem in environmental research, marine and aquatic chemistry and clinical and food chemistry.[1] For trace metals capable of forming an amalgam, anodic stripping voltammetry is the most convenient analytical method.[1–4] The highest sensitivity is obtained if a thin mercury film covered glassy carbon rotating disc electrode[1,3,5–21] (TMFGCRDE) in combination with differential-pulse[1,9,12–17,19,20] (DPSV) or square-wave[16,17,21–23] stripping voltammetry (SWSV) is used. The advantages of the TMFGCRDE over a hanging mercury drop electrode are that it provides more effective and stable mass transfer during the accumulation step and very sharp anodic stripping peaks.[1,3,6,7,9,10,13,18,22,23] Pulse voltammetric stripping methods possess an advantage over linear scan stripping in that they discriminate effectively against charging current.[1,9,13,16,17,22–25] The theory of DPSV[26,27] indicates that, in contrast to DP polarography,[28] the sensitivity increases if the period between two successive pulses is equal to the duration of the pulse (*i.e.*, if the DPSV signal becomes similar to the SWSV signal). The theoretical treatment of SWSV at mercury film electrodes has shown that the sensitivity of the method increases proportionally within the square-wave frequency.[22,23] For these reasons, SWSV is superior to DPSV.[16,17,22,23]

In this paper the dependencies of the square-wave, differential-pulse, staircase and reverse-pulse stripping voltammetric peak currents on the rotation rate of the TMFGCRDE during the stripping period are demonstrated. This subject has been discussed several times in connection with linear scan[10,29–31] (LSSV), alternating current[8] (acSV), DPSV[9,13,32] and reverse-pulse[30,32] (RPSV) stripping voltammetric methods. Theoretically, if the rotation rate is very high and the scan rate (LSSV) or frequency (SWSV and DPSV) is low, the peak currents depend linearly on the square root of the rotation rate. On the other hand, if the rotation rate is low and the scan rate or frequency is high, the current is independent of the rotation rate.[8,30–32] In the practical application of the TMFGCRDE the use of forced mass transfer during the stripping period depends on the type of electrical contact on the RDE. If carbon brushes are used for the contact, the electrical noise is very high and the rotation of the RDE must be stopped before the stripping peaks are recorded.[9,10,14–19,29] The mercury contact provides a much lower noise level, so that the electrode can be allowed to rotate during stripping.[6,7,10,11–13,20,21] The rotation increases the LSSV peak currents.[5–7,10,11,20,30,31] The DPSV responses are usually recorded without rotation,[9,13–17,19] although some contrary examples are known.[12,20,21]

Experimental

The following chemicals were used: NaCl, concentrated $HClO_4$ (both Merck, Suprapur grade), $Pb(NO_3)_2$ and $Hg(NO_3)_2$ (both Merck, analytical-reagent grade). The water used for all the solutions was distilled four times, twice using quartz equipment.

The electrode system consisted of a glassy carbon rotating disc working electrode (GCRDE), an Ag - AgCl (saturated NaCl) reference electrode and a platinum wire counter electrode. The construction of the GCRDE has been described previously.[11,13] The glassy carbon disc (diameter 6 mm, surface area 0.283 cm^2; Tokai Electrode Manufacturing, Tokyo, Japan) was sealed in polycarbonate resin tubing and polished to a mirror finish. The tubing was fixed to a stainless-steel shaft which rotated inside an electrode holder. A noise-free mercury contact was used. The electrode was driven by a synchronous electric motor with a continuously changeable rotation rate of between 843 and 4402 rev min^{-1}. Each day, before the experiments, the GCRDE was cleaned by re-polishing with a soft tissue and conditioned by charging to +0.4 V *versus* Ag - AgCl for 30 s. The voltammetric cell (volume 100 ml) was made from PTFE. The reference and counter electrodes were isolated in separate compartments.

The solutions were de-aerated with extra-pure nitrogen for 20 min prior to measurements; a nitrogen atmosphere was maintained thereafter. The working electrode was rotated during the de-aeration period.

The TMFGCRDEs were formed as described previously.[6,7,10,13] Mercury(II) nitrate was added to the sample solution at a concentration of 4×10^{-5} M for *in situ* formation of the mercury film on the glassy carbon substrate. The initial film formation was performed by the accumulation of mercury at −0.9 V *versus* Ag - AgCl for 20 min. The electrode was rotated at a rate, ω_{acc}, of 2623 rev min^{-1} during this period. Thereafter, the film grew during each subsequent cathodic deposition stage. In situtations where the mercury film had to be maintained at a constant thickness during a series of measurements, the initial film formation was followed by the subsequent transfer of the TMFGCRDE into a sample solution containing no mercury ions.

Anodic stripping measurements of 5×10^{-8} M Pb^{2+} were performed in 0.55 M NaCl, pH 3 ($HClO_4$), supporting electrolyte. Lead amalgam was accumulated at an accumulation potential, E_{acc} of −0.8 V *versus* Ag - AgCl for an accumulation time, t_{acc}, of 2 min, during which the TMFGCRDE was rotated at 2623 rev min^{-1}. The anodic scan was preceded by a 30-s "rest" period (t_{rest}) during which the rotation of the electrode was decreased by reducing the rheostat or stopped by switching the motor off.

Princeton Applied Research (PAR) 384B and 174A polarographic analysers connected to a Bausch - Lomb DMP-40 digital plotter and a Hewlett-Packard 7045A x - y recorder, respectively, were used. The PAR 174A analyser was partially

* To whom correspondence should be addressed.

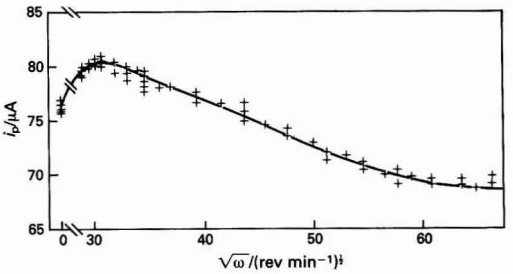

Fig. 1. Square-wave stripping voltammetry of 5×10^{-8} M Pb^{2+} in 0.55 M NaCl, pH 3 ($HClO_4$). Dependence of peak currents on the square root of the electrode rotation rate (ω) during the anodic stripping scan. Thin mercury film covered (*in situ*) glassy carbon rotating disc electrode (4×10^{-5} M Hg^{2+} added to the sample; initial accumulation of mercury for 20 min at −0.9 V). Lead amalgam accumulation: t_{acc} = 2 min; E_{acc} = −0.8 V *versus* Ag - AgCl; ω_{acc} = 2623 rev min^{-1}; t_{rest} = 30 s. Stripping conditions: square-wave frequency, f = 100 Hz; peak amplitude, a = 60 mV; dE = −2 mV

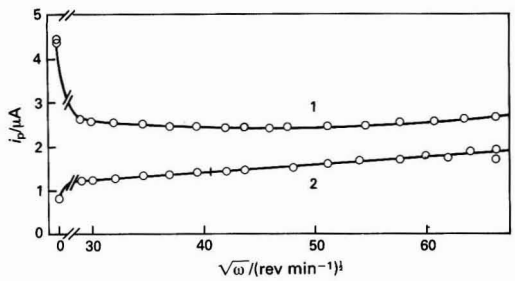

Fig. 2. 1, Differential-pulse and 2, staircase stripping voltammetry of lead. Dependence of peak currents on the square root of the electrode rotation rate during the anodic stripping scan. 1: t_d = 0.5 s; pulse duration, t_p = 57 ms; ΔE = 30 mV; dE = −2 mV. 2: dE = −4 mV; dt = 0.1 s (scan rate, v = 40 mV s^{-1}). All other parameters are as in Fig. 1

adapted to allow the drop time and pulse duration time to be varied.

Results and Discussion

The dependencies of the square-wave, differential-pulse, staircase (SSV) and reverse-pulse stripping peak currents on the square root of the TMFGCRDE rotation rate during the stripping period are shown in Figs. 1–3. The SWSV, DPSV and SSV measurements were performed using the PAR 384B polarograph, whereas the RPSV measurements were repeated with the PAR 174A analyser and identical results were obtained.

Apart from SSV, all the results are characterised by the adverse effect of the rotation on the stripping peaks. The staircase voltammetric results are similar to those obtained with LSV.[33–35] The SSV peaks (Fig. 2, curve 2) depend linearly on the square root of the TMFGCRDE rotation rate. This is in good agreement with LSSV theory.[31] In addition, the SSV peaks recorded at the stationary TMFGCRDE are smaller than those recorded at the rotating electrode. In contrast, the DPSV and RPSV peaks (Fig. 2, curve 1 and Fig. 3) are almost independent of the rotation rate, but the peaks recorded at the stationary electrode are much higher than the others. This fact cannot be explained by current theory.[32] In SWSV (Fig. 1), the peak currents decrease as the rotation rate increases. For a square-wave frequency of 100 Hz, the highest peaks appear when the electrode rotation rate is 1000 rev min^{-1}. Stopping the TMFGCRDE before stripping also causes a slight reduction in the height of the SWSV peaks.

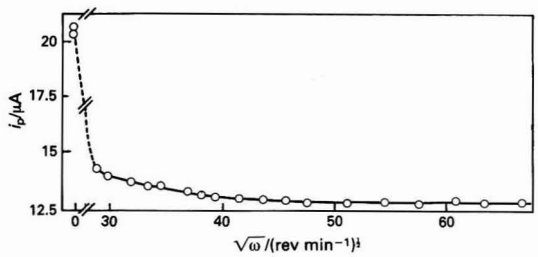

Fig. 3. Reverse-pulse stripping voltammetry of lead. Dependence of peak currents on the square root of the electrode rotation rate during the anodic stripping scan. t_d = 0.2 s; and t_p = 57 ms. All other parameters are as in Fig. 1

Residual currents detected by any of the four stripping methods do not depend significantly on the rotation rate.

The observed effects may be ascribed to the forced transport of Pb^{2+} ions during the stripping procedure. If during an anodic pulse a significant amount of amalgam is re-oxidised, the concentration of Pb^{2+} ions near the electrode surface will suddenly be increased. These ions are transported towards the bulk of the solution by diffusion and convection. The transport causes a decrease in the Pb^{2+} concentration at the mercury surface. In order to maintain a Nernst equilibrium, additional re-oxidation of the amalgam is required. Hence, the re-oxidation persists throughout the anodic pulse and a certain anodic current can be sampled when it ends. The current is higher if the pulse is shorter or if the convection is faster (the rotation rate is higher). When a cathodic pulse is applied, these Pb^{2+} ions are reduced (re-reduced). In DPSV and RPSV the periods between the anodic pulses may be regarded as cathodic pulses of longer duration. The re-deposition effect is more pronounced if the concentration of Pb^{2+} ions remaining in the vicinity of the electrode surface is higher, *i.e.*, if the convection is slower (the rotation rate is lower). The cathodic current caused by the re-reduction is also higher if the cathodic pulse duration, t_p, is shorter. In SWSV and DPSV, the cathodic current is subtracted from the anodic current (*i.e.*, their absolute values are summed). In SWSV both pulses are equally short and the stripping peaks decrease with an increase in the rotation rate because the cathodic components of the responses decrease as the re-deposition decreases. However, with a slowly rotating electrode the peaks are higher than at the stationary TMFGCRDE because moderate convection increases the anodic components without significantly decreasing the cathodic components. The anodic pulses in DPSV and RPSV are both sufficiently long (t_p = 57 ms); hence even moderate convection can decrease the concentration of Pb^{2+} ions in the vicinity of the electrode surface to such an extent that their re-deposition during the cathodic pulse is negligible. Hence, the stripping peaks become almost independent of the rotation rate in the range investigated. If the mass transfer is effected by diffusion only, the loss of Pb^{2+} ions during the anodic pulse is much smaller, hence their re-reduction can significantly enhance the response (particularly in RPSV). In SSV there are no cathodic pulses. The enhancement of the stripping peaks is caused by an increase in the anodic currents under conditions of forced convection.

That this is true is shown by the dependence of the RPSV peaks on the period between the pulses (Fig. 4). If the drop time (t_d, the period between the end of two successive pulses) is increased from 0.1 to 1.0 s, the peak currents become about twice as high because of the re-deposition effect. The results shown in Fig. 4 were obtained by anodic stripping at the stationary TMFGCRDE. Varying t_d has the opposite effect in DPSV: if t_d decreases, the peak currents increase. This is in agreement with theoretical[26,27] and experimental[13] observations. In both techniques the enhancement of the stripping

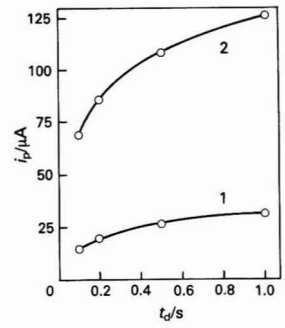

Fig. 4. Dependence of the reverse-pulse stripping peak currents of lead on drop time. The TMFGCRDE was not rotated during the anodic stripping scan. 1, t_p = 57 ms and 2, t_p = 27 ms. All other parameters are as in Fig. 1

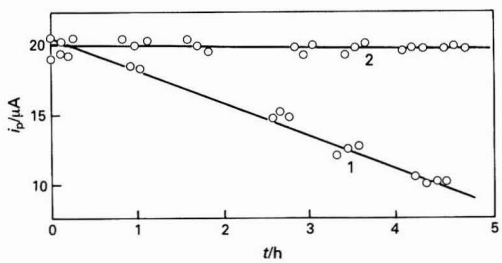

Fig. 5. Stability of the TMFGCRDE (no mercury added to the sample). The RPSV peak currents of lead were recorded repeatedly over a 4-h period and the electrode was not rotated during the anodic stripping scan: t_d = 0.2 s, t_p = 57 ms. 1, The cell was disconnected after each group of three subsequent anodic stripping cycles. 2, The working electrode was charged to −0.1 V *versus* Ag - AgCl between two successive recordings. All other parameters are as in Fig. 1

peaks can be achieved more effectively by decreasing the duration of the anodic pulse[9,13,36] (compare also curves 1 and 2 in Fig. 4).

Our results justify the practice of recording the differential- and reverse-pulse stripping voltammograms at a stationary TMFGCRDE.[9,13–17,19] The increased sensitivity obtained with this procedure is not due to the decreased noise level, as is sometimes stated,[9,29] but is caused by hydrodynamic factors. This practice is also recommended for SWSV, although higher peaks can be obtained if the stripping peaks are recorded at a slowly rotating electrode. However, it may be easier to switch the electric motor off at the end of the accumulation period (using the rest period for quiescing the solution), than to change the electrode rotation rate by altering the rheostat position during the first stage of the rest period.

The application of advanced analytical instrumentation (such as the PAR 384B analyser) to anodic stripping measurements with a TMFGCRDE imposes some restrictions on the choice of the analytical procedure. These instruments disconnect the electrolytic cell from the potentiostat after each anodic stripping cycle. It has been observed that a TMFGCRDE exposed to an open circuit may be ruined if mercury ions are not added to the sample.[19,37] To investigate the stability of a mercury film under open-circuit conditions, the cell was deliberately disconnected several times between RPSV measurements. The PAR 174A polarographic analyser was used. After the initial film formation by electrolysis of 4×10^{-5} M Hg^{2+} at −0.9 V for 20 min, the electrode was transferred into a mercury-free sample of Pb^{2+} ions. The RPSV peaks were measured several times over a period of 4 h; however, the electrolytic cell was disconnected after each measurement and connected again immediately before the next measurement. The stripping peaks were recorded at a stationary TMFGCRDE. The results are shown in Fig. 5, curve 1. The results of a control experiment are shown by curve 2. During this experiment, the working electrode was not disconnected, but was continuously charged to −0.1 V *versus* Ag - AgCl between two successive RPSV cycles. If mercury ions were also added to the sample, the RPSV peak currents were constant throughout the 4-h period regardless of whether or not the cell had been disconnected. The decrease in the peak currents, shown in Fig. 5, curve 1, may be explained by the fact that a film of mercury on glassy carbon consists of numerous very small drops.[38] If the glassy carbon surface is not charged to the controlled potential, but left in an open circuit, it is possible for some of these drops to unite forming larger drops, leaving part of the glassy carbon surface uncovered. It is known that the glassy carbon electrode surface consists of sites of variable activity.[38] Less than half of the geometric electrode surface consists of more active sites on which mercury droplets can be formed when mercury is deposited at low over-voltages. The remainder of the surface is less active and can be activated only if the deposition over-voltage and concentration of mercury ions are both high.[38] Hence it is possible that in an open circuit the droplets formed on the inactive sites become unstable and unite with more stable drops. Therefore, the active surface of the TMFGCRDE may decrease and the stripping peaks diminish. The actual volume of mercury on the glassy carbon surface remains the same after a supposed contraction of the thin layer but, on average, the layer becomes thicker while its active surface area decreases. During the accumulation period the reduction current is linearly proportional to the active area of the film, but not to its thickness. Hence the amount of accumulated amalgam decreases if the mercury film contracts. The stripping peak current depends linearly on the amount of accumulated amalgam.[22,23] The linear proportionality relationship is a function of the film thickness and decreases when the film becomes thicker.[29,39,40] For these reasons, the supposed film contraction would cause a reduction in the stripping peak current. If Hg^{2+} ions are present in the sample, the film of mercury regenerates during each cathodic deposition of the lead amalgam and hence the peak currents do not decrease even if the cell is disconnected. It is also possible that in an open circuit the mercury film is oxidised, but in a highly de-aerated solution, kept permanently under a nitrogen atmosphere, this possibility appears to be less probable. In any event if a TMFGCRDE is used with the PAR 384B analyser, the samples should contain mercury ions.

References

1. Wang, J., "Stripping Analysis," VCH Publishers, Deerfield Beach, 1985.
2. Kemula, W., Rakowska, E., and Kublik, Z., *J. Electroanal. Chem.*, 1959, **1**, 205.
3. Nürnberg, H. W., Valenta, P., Mart, L., Raspor, B., and Sipos, L., *Fresenius Z. Anal. Chem.*, 1972, **282**, 357.
4. Brainina, H. Z., "Stripping Voltammetry in Chemical Analysis," Wiley, New York, 1974.
5. Matson, W. R., Roe, D. K., and Carrit, D. E., *Anal. Chem.*, 1965, **37**, 1595.
6. Florence, T. M., *J. Electroanal. Chem.*, 1970, **27**, 273.
7. Florence, T. M., *J. Electroanal. Chem.*, 1972, **35**, 237.
8. Vydre, F., Štulikova, M., and Petak, P., *J. Electroanal. Chem.*, 1972, **40**, 99.
9. Copeland, T. R., Christie, J. H., Osteryoung, R. A., and Skogerboe, R. K., *Anal. Chem.*, 1973, **45**, 2171.
10. Batley, G. E., and Florence, T. M., *J. Electroanal. Chem.*, 1974, **55**, 23.
11. Sipos, L., Magjer, T., and Branica, M., *Croat. Chem. Acta*, 1974, **46**, 35.
12. Andrews, R. W., Larochelle, J. H., and Johnson, D. C., *Anal. Chem.*, 1976, **48**, 212.

13. Valenta, P., Mart, L., and Rützel, H., *J. Electroanal. Chem.*, 1977, **82**, 327.
14. Wang, J., and Ariel, M., *Anal. Chim. Acta*, 1978, **99**, 89.
15. Wang, J., and Ariel, M., *Anal. Chim. Acta*, 1978, **101**, 1.
16. Turner, J. A., Eisner, U., and Osteryoung, R. A., *Anal. Chim. Acta*, 1977, **90**, 25.
17. Barker, G. C., and Gardner, A. W., *J. Electroanal. Chem.*, 1979, **100**, 641.
18. Geineman, A. E., Kaplin, A. A., and Stromberg, A. G., *Zh. Anal. Khim.*, 1978, **33**, 1510.
19. Abdullah, M. I., Reusch Berg, B., and Klimek, R., *Anal. Chim. Acta*, 1976, **84**, 307.
20. Komorsky-Lovrić, Š., Lovrić, M., and Branica, M., *J. Electroanal. Chem.*, 1986, **214**, 37.
21. Komorsky-Lovrić, Š., *Anal. Chim. Acta*, 1988, **204**, 161.
22. Kounaves, S. P., O'Dea, J. J., Chandrasekhar, P., and Osteryoung, J., *Anal. Chem.*, 1986, **58**, 3199.
23. Kounaves, S. P., O'Dea, J. J., Chandrasekhar, P., and Osteryoung, J., *Anal. Chem.*, 1987, **59**, 386.
24. O'Dea, J. J., Osteryoung, J., and Osteryoung, R. A., *Anal. Chem.*, 1981, **53**, 695.
25. Osteryoung, J. G., and Osteryoung, R. A., *Anal. Chem.*, 1985, **57**, 101A.
26. Rifkin, S. C., and Evans, D. H., *Anal. Chem.*, 1976, **48**, 1616.
27. Aoki, K., Tokuda, K., and Matsuda, H., *J. Electroanal. Chem.*, 1984, **175**, 1.
28. Lovrić, M., and Branica, M., *J. Electroanal. Chem.*, 1985, **183**, 107.
29. de Vries, W. T., and van Dalen, E., *J. Electroanal. Chem.*, 1967, **14**, 315.
30. Levich, V. G., "Physicochemical Hydrodynamics," Prentice Hall, Englewood Cliffs, 1962.
31. Lovrić, M., and Osteryoung, J. G., *J. Electroanal. Chem.*, 1986, **197**, 63.
32. Myers, D. J., Osteryoung, R. A., and Osteryoung, J., *Anal. Chem.*, 1974, **46**, 2089.
33. Seralathan, M., Osteryoung, R. A., and Osteryoung, J. G., *J. Electroanal. Chem.*, 1987, **222**, 69.
34. Bilewicz, R., Osteryoung, R. A., and Osteryoung, J., *Anal. Chem.*, 1986, **58**, 2761.
35. Eisner, U., Turner, J. A., and Osteryoung, R. A., *Anal. Chem.*, 1976, **48**, 1608.
36. Varavko, T. N., and Kaplan, B. Y., *Zh. Anal. Khim.*, 1976, **31**, 429.
37. Peharac, Z., personal communication.
38. Štulikova, M., *J. Electroanal. Chem.*, 1973, **48**, 33.
39. de Vries, W. T., and van Dalen, E., *J. Electroanal. Chem.*, 1964, **8**, 366.
40. de Vries, W. T., *J. Electroanal. Chem.*, 1965, **9**, 448.

Paper 9/01686D
Received April 21st, 1989
Accepted June 22nd, 1989

Simultaneous Determination of Bismuth and Lead by Single-sweep Polarography of Their Glyoxalbis(2-hydroxyanil) Complexes

Mian Jiang, Fanchang Meng, Cheng Gong and Zaofan Zhao
Department of Chemistry, Wuhan University, Wuhan 430 072, People's Republic of China

Bismuth(III) and lead(II) can be reduced at −0.65 V (*versus* SCE) and −0.76 V (*versus* SCE), respectively, in a sodium hydroxide solution containing glyoxalbis(2-hydroxyanil) (GBHA) [2,2′-(ethanediylidenedinitrilo)diphenol] by using single-sweep polarography, based on their adsorptive GBHA complexes. Both waves are sensitive and selective and can be utilised for the simultaneous determination of these two elements. The linearity ranges for bismuth and lead are 7×10^{-8}–1×10^{-5} and 1×10^{-7}–6×10^{-6} M, respectively. The sensitivity for bismuth can be increased ten-fold by using cathodic stripping voltammetry with a static mercury electrode. The proposed procedure was applied to the simultaneous determination of bismuth and lead in some ore and alloy samples. The mechanism of the electrode process has also been studied.

Keywords: *Bismuth and lead determination; glyoxalbis(2-hydroxyanil); polarography*

The polarographic and voltammetric behaviour of bismuth and lead has been studied in detail.[1,2] Of the polarographic and voltammetric methods, anodic stripping voltammetry is the most sensitive approach; however, it is relatively time consuming and suffers from poor reproducibility for routine analysis.[3,4]

Glyoxalbis(2-hydroxyanil) (GBHA) [2,2′-(ethanediylidenedinitrilo)diphenol] (**I**) is a Schiff base.

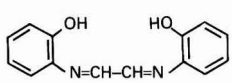

(I)

It can react with many cations to form coloured complexes. However, because of its poor selectivity and stability, this reagent is used mainly for the spectrophotometric determination of calcium in alkaline media after pre-separation of interfering ions. Nevertheless, considering its strong adsorptivity on an electrode surface and its strong complexing ability with many cations, GBHA might be useful for adsorptive stripping analysis and single-sweep polarography (SSP). We have found that, in sodium hydroxide solution, the Bi^{III} - GBHA and Pb^{II} - GBHA complexes can produce sensitive and selective peaks which can be used for the simultaneous determination of trace amounts of bismuth and lead. The proposed procedure was applied successfully to the analysis of several ores and alloys. Mechanistic studies show that the systems described are anion-induced adsorptive complex peaks.

Experimental

Chemicals and Apparatus

Glyoxalbis(2-hydroxyanil) (chemically pure, Third Chemical Reagent Factory of Shanghai, China) was purified by recrystallisation from aqueous ethanol. A 5.00×10^{-3} M stock solution was prepared by dissolving GBHA in ethanol and was kept in a dark place. The solution is stable for at least 1 week although it might darken slightly. The purity of solid GBHA was checked by its melting-point (210–213 °C, with decomposition) and UV absorption ($\varepsilon = 9800$ l mol^{-1} cm^{-1} at 294 nm). The 1.00×10^{-2} M standard solutions of bismuth and lead were prepared by dissolving pure metallic bismuth and lead (both of analytical-reagent grade) in 1 + 1 nitric acid. All other chemicals used were of analytical-reagent grade. Water was re-distilled in the presence of potassium permanganate.

A JP-2 oscillopolarograph (Chengdu Instrumental Factory, China) was used for SSP determinations. For derivative measurements, the conditions were: drop time, 7 s (standing time for pre-concentration, 5 s); scan rate, 250 mV s^{-1}; height of mercury head, 50 cm; and flow-rate, 2.0 mg s^{-1}. The three-electrode system used consisted of a dropping mercury electrode (DME), a platinum counter electrode and a saturated calomel reference electrode (SCE). The electrolytic cell was a 10-ml beaker. The same system, but with a static mercury drop electrode (Model 303) as the working electrode, was used for cyclic voltammetric measurements employing a PAR 174A system (Princeton Applied Research, Princeton, NJ, USA). All experiments were carried out at room temperature and all potentials quoted are relative to the SCE. It was not necessary to remove dissolved oxygen from the sample solutions except for the cyclic voltammetric studies.

Analytical Procedure

Single-sweep polarography

To the sample solution (7×10^{-8}–1×10^{-5} M Bi^{III} and 1×10^{-7}–6×10^{-6} M Pb^{II}), add 1 ml of 1×10^{-3} M GBHA and 1 ml of 2 M NaOH solution. Dilute the solution to 10 ml with water and mix thoroughly. After 30 min, record the derivative cathodic sweep polarogram from −0.40 to −0.90 V and measure the peak height of bismuth and lead at −0.65 and −0.76 V, respectively. The solution is stable for at least 1 h.

For the determination of bismuth and lead in bismutite ore and copper-base alloy samples, transfer 1 ml of the sample solution into a dry 10-ml beaker, add 1 ml of ammonia solution, 1 ml of 1×10^{-2} M 1,2-diaminocyclohexane-*N*,*N*,*N*′,*N*′-tetraacetic acid (DCTA), 1 ml of 1×10^{-3} M GBHA and 0.5 ml of 2 M NaOH solution. Dilute the solution to 10 ml and carry out the determination as described above.

Results and Discussion

Single-sweep Polarography

The normal and derivative (using a large capacitance in the circuit and a higher electronic amplifier factor) polarograms of the Bi^{III} - GBHA and Pb^{II} - GBHA complexes in sodium hydroxide solution are shown in Fig. 1. Two distinct peaks appear, at −0.65 V (for Bi^{III} - GBHA) and −0.76 V (for Pb^{II} - GBHA), during the cathodic sweep. It is clear that the derivative peak is easier to measure than the normal peak; hence the derivative mode was used for all measurements. The

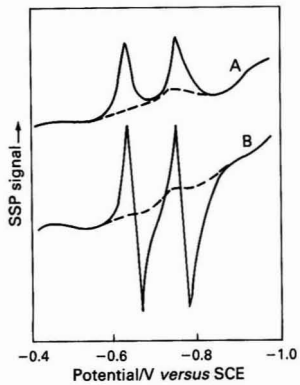

Fig. 1. Single-sweep polarograms of Bi^{III} and Pb^{II}: 0.1 M NaOH - 1×10^{-4} M GBHA, plus 5×10^{-6} M Bi^{III} and 5×10^{-6} M Pb^{II}. A, Normal SSP; and B, derivative SSP. The broken line represents the blank

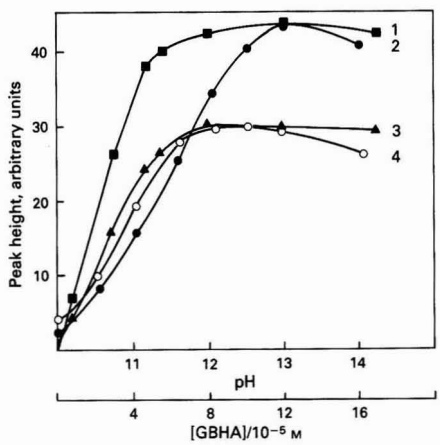

Fig. 2. 1, Effect of pH on the peak height of Bi^{III}; 2, effect of GBHA concentration on the peak height of Bi^{III}; 3, effect of pH on the peak height of Pb^{II}; and 4, effect of GBHA concentration on the peak height of Pb^{II}. Conditions: 0.1 M NaOH plus 5×10^{-6} M Bi^{III} or 5×10^{-6} M Pb^{II}

effect of pH and the concentration of GBHA on peak height is shown in Fig. 2. The optimum conditions for the determination are 1.00×10^{-4} M GBHA and 0.1 M NaOH.

Under the optimum conditions, the graphs of peak height *versus* concentration were linear in the range 7×10^{-8}–1×10^{-5} M for bismuth (correlation coefficient = 0.9991) and 1×10^{-7}–6×10^{-6} M for lead (correlation coefficient = 0.9986). The detection limit is 4×10^{-8} M (8.4 μg l^{-1}) for bismuth and 7×10^{-8} M (14.5 μg l^{-1}) for lead.

Spectrophotometric and Polarographic Studies of the Complexes

Ultraviolet spectrophotometric data showed that the Pb^{II} - GBHA complex exhibited an absorption maximum at 650 nm and the Bi^{III} - GBHA complex an absorption band with a broad shoulder in the range 460–590 nm. Because the absorption of the complexes is low, it is difficult to study them by spectrophotometry. The polarographic molar ratio method,[5] however, is very convenient for studying electrochemically active complexes. By using this method, the composition of the complexes was found to be 1 : 1 in both instances.

Properties of the Polarographic Peaks

Small amounts (<20 mg l^{-1}) of surfactants, such as sodium dodecyl sulphonate, cetylpyridinium bromide, hexadecyltrimethylammonium bromide and Triton X-100, suppress the peaks. The temperature coefficient for both peaks has a positive value in the range 10–28 °C whereas it has a negative value at temperatures higher than 30 °C. The peak height increases with the pre-concentration time at the static mercury drop electrode before the potential scan is carried out. All these phenomena demonstrate the adsorptive characteristics of the Bi^{III} - GBHA and Pb^{II} - GBHA complexes.

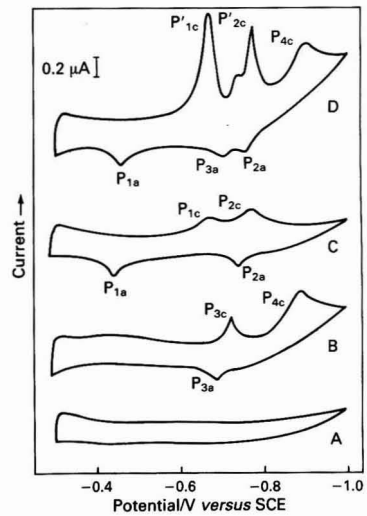

Fig. 3. Cyclic voltammograms: A, 0.1 M NaOH; B, as for A plus 3×10^{-4} M GBHA; C, as for A plus 1×10^{-5} M Bi^{III} and 1×10^{-5} M Pb^{II}; and D, as for C plus 3×10^{-4} M GBHA. Conditions: standing time for pre-concentration prior to the potential scan, t_i, 10 s; and scan rate, 100 mV s^{-1}

Fig. 3 shows the cyclic voltammograms of GBHA and its bismuth and lead complexes in sodium hydroxide solution. For curve B (GBHA), there are two cathodic peaks, P_{3c} (−0.72 V) and P_{4c} (−0.90 V), and an anodic peak, P_{3a} (−0.68 V). It appears that redox couple 3 is reversible whereas couple 4 is irreversible. The peak height of peak P_{3c} increases with the standing time before the potential scan is carried out, but peaks P_{4c} and P_{3a} remain unchanged. The last two peaks are directly proportional to the square root of the potential scan rate ($v^{\frac{1}{2}}$) in the range 2–22 (mV $s^{-1})^{\frac{1}{2}}$. These results indicate that peak P_{3c} is controlled by adsorption whereas peaks P_{4c} and P_{3a} are controlled by diffusion.

Fig. 3, C shows the cyclic voltammogram of Bi^{III} and Pb^{II} in the absence of GBHA. As expected, the redox reaction of Bi^{III} (P_{1a}/P_{1c}) is irreversible whereas that of Pb^{II} (P_{2a}/P_{2c}) is reversible.

Fig. 3, D shows that, in the presence of GBHA, peaks P_{1c} and P_{2c} increase markedly (denoted by P'_{1c} and P'_{2c}, respectively), whereas peaks P_{3c}, P_{4c}, P_{1a}, P_{2a} and P_{3a} remain unchanged.

Fig. 4 indicates that the peak current of peak P_{1c} is directly proportional to $v^{\frac{1}{2}}$ whereas that of peak P'_{1c} deviates towards the current axis, showing conclusively that peak P'_{1c} is an adsorptive peak. The same result can be obtained for peaks P_{2c} and P'_{2c}.

Mechanism of the Electrode Process

Anson and Barcley[6] have studied the iodide-induced adsorption in the reduction of Cd^{II} species. The following mechansim was proposed:

$$CdI_2 + 2I^- + Hg \rightarrow I_2Cd \left\langle \begin{matrix} I^- \\ I^- \end{matrix} \right\rangle Hg$$

Bond and Helfter[7] also investigated the effect of anion-induced adsorption on the polarographic half-wave potential

Table 1. Results of the determination of bismuth and lead in several samples

Sample	Proposed method, %*		Certified value, %	
	Bismuth	Lead	Bismuth	Lead
Copper-base alloy(I)†	0.00099 ± 0.00006	0.058 ± 0.002	0.00093	0.054
Copper-base alloy(II)†	0.00085 ± 0.00003	0.052 ± 0.004	0.00087	0.054
Copper-base alloy(III)†	0.00052 ± 0.00002	0.089 ± 0.004	0.00052	0.092
Ore(I)‡	0.095 ± 0.02	—	0.096	—
Ore(II)‡	0.074 ± 0.02	—	0.078	—

* Mean ± standard deviation of six determinations.
† Copper-base alloy samples and their certified values were provided by the Wuhan Institute of Iron and Steel.
‡ Ore samples (ore type: bismutite mineral) and their certified values were obtained from the Yichang Institute of Geology.

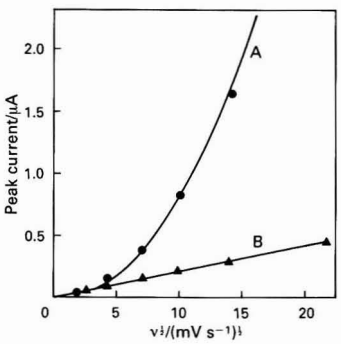

Fig. 4. Relationship between peak current and $v^{\frac{1}{2}}$. A, For peak P'_{1c}, conditions as in Fig. 3, D; B, for peak P_{1c}, conditions as in Fig. 3, C

and showed that the reduction of metal ions would not be affected if the concentration of the ligand was less than 10^{-3} M. It is obvious that the reduction of Bi^{III} - GBHA and Pb^{II} - GBHA is very similar to that of Cd^{II} - I^-. In a strongly basic medium, GBHA can be adsorbed strongly on the electrode in an anionic form, which induces the adsorption of the Bi^{III} and Pb^{II} complexes.

In a weakly basic solution (pH 8–9), however, neither GBHA nor its complexes can be adsorbed because GBHA is in the undissociated form. This has been shown experimentally.

Taking into consideration the above-mentioned studies, the mechanism giving rise to the polarographic peaks may be represented as follows:

$$Bi(OH)^{2+} + GBHA^{2-} \rightleftharpoons [Bi(OH)(GBHA)]^0 \quad \text{(in solution)}$$

$$[Bi(OH)(GBHA)]^0 + Hg \rightleftharpoons Bi(OH)^{2+} \text{ - } GBHA^{2-} \text{ - } Hg \quad \text{(on the electrode)}$$

$$Bi(OH)^{2+} \text{ - } GBHA^{2-} \text{ - } Hg + 3e^- \xrightarrow{-0.65\ V} Bi \text{ - } Hg + GBHA^{2-} + OH^- \quad (\text{peak } P'_{1c})$$

$$Pb(OH)_3^- + GBHA^{2-} \rightleftharpoons [Pb(GBHA)]^0 \quad \text{(in solution)}$$

$$[Pb(GBHA)]^0 + Hg \rightleftharpoons Pb^{2+} \text{ - } GBHA^{2-} \text{ - } Hg \quad \text{(on the electrode)}$$

$$Pb^{2+} \text{ - } GBHA^{2-} \text{ - } Hg + ne^- \xrightarrow{-0.76\ V} Pb \text{ - } Hg + GBHA_{red}^{2-} \quad (\text{peak } P'_{2c})$$

Effect of Co-existing Substances on the Determination

More than 30 foreign ions in solution were examined for their possible influence on the determination of bismuth and lead. The results showed that large amounts of the anions typically found in natural samples and up to a 5000-fold (mol : mol) excess of Al^{3+} or NH_4^+ did not interfere with the simultaneous determination of bismuth and lead. For Bi^{III}, there were no effects from a 600-fold excess of Be^{2+}, MoO_4^{2-}, Fe^{3+} or WO_4^{2-}, a 50-fold excess of Zn^{2+}, Ni^{2+}, Mn^{2+}, Sr^{2+}, Sb^{3+}, Cd^{2+}, Mg^{2+}, Ba^{2+} or As^{III} and a ten-fold excess of Ca^{2+}, Co^{2+} or Cr^{3+}. For Pb^{II}, a 200-fold excess of Fe^{3+}, WO_4^{2-} or Be^{2+}, a 50-fold excess of Ni^{2+}, Mn^{2+}, Mg^{2+}, Sr^{2+}, Ba^{2+}, Ca^{2+}, Cd^{2+}, Cr^{3+}, MoO_4^{2-}, Sb^{3+} or As^{III} and a ten-fold excess of Co^{2+} or Zn^{2+} did not interfere.

A 20-fold excess of Cu^{2+} interfered seriously with the determination of bismuth and lead. However, Cu^{2+} could be masked with 10^{-3} M DCTA in the presence of ammonia solution after which at least a 200-fold excess could be tolerated.

Application

The proposed procedure was applied to the determination of bismuth and lead in copper-base alloys and ores. For the analysis of copper-base alloys, 0.2 g of the sample was treated with 20 ml of 1 + 1 nitric acid. After decomposition had been completed, the solution was diluted to about 100 ml with water. To the solution, 5 g of solid NH_4Cl and 5 ml of 0.1 M $AlCl_3$ solution (as co-precipitation carrier) were added. The solution was heated to 60–70 °C, then sufficient ammonia solution was added dropwise to precipitate $Al(OH)_3$ and also bismuth, lead and other hydrolysable ions. The precipitate was filtered off and washed in the usual way, then dissolved in 1 + 2 hydrochloric acid and the solution diluted to 25 ml with water. An aliquot of the sample solution was used for the determination of bismuth and lead by the SSP procedure (from the calibration graph) described above. The results are given in Table 1.

For the analysis of bismuth-containing ores, 0.1 g of the sample was treated with 5 ml of 1 + 1 hydrochloric acid and heated at 60–70 °C for 5 min. Then, 15 ml of nitric acid were added to decompose the sample completely. After the addition of small amounts of 0.1 M hydrochloric acid, the solution was filtered and washed with 0.05 M hydrochloric acid. The filtrate and washings were collected and diluted to 25 ml with water. An aliquot of the sample solution was used for the determination of bismuth by the procedure given above. These results are also presented in Table 1.

This work was supported by the National Natural Science Foundation of China.

References

1. Sharpe, T. F., *in* Bard, A. J., *Editor*, "Encyclopedia of Electrochemistry of the Elements," Volume 1, Marcel Dekker, New York, 1978, p. 235.
2. Filipovic, L., *Arh. Kem.*, 1951, **23**, 159.
3. Florence, T. M., *J. Electroanal. Chem.*, 1974, **49**, 255.
4. Florence, T. M., and Batley, G. E., *Talanta*, 1976, **23**, 179.
5. Luo, Z., "Ternary Complexes and Their Applications in Analytical Chemistry," People's Educational Press, Beijing, 1981, p. 84.
6. Anson, F. C., and Barcley, D. J., *Anal. Chem.*, 1968, **40**, 1791.
7. Bond, A. M., and Helfter, G., *J. Electroanal. Chem.*, 1973, **42**, 1.

Paper 9/02101I
Received May 18th, 1989
Accepted July 13th, 1989

Computational Algorithms in Ion-selective Electrode Potentiometry by the Two Standard Additions Method

Jirong Wang
Department of Modern Chemistry, University of Science and Technology of China, Hefei, Anhui, People's Republic of China

Until now, the various computing equations for standard additions methods have been empirical. Workers have used their own judgement to decide whether a solution existed to a given equation and selected an iterative equation and an initial approximation accordingly. If the computed results were wrong, it was not apparent whether this was caused by using the wrong computational method or incorrect experimental processes. Clearly, this situation is unsatisfactory. In this paper, the existence theorems of solutions and the "non-local" convergence equations are given. On the basis of these, rapid algorithms and programs are recommended. Some computed results are listed to prove the accuracy of the programs. These programs not only handle data, but are also suitable for incorporation in the read only memory of a microcomputer ion meter.

Keywords: *Ion-selective electrode; computational algorithm*

Various computational methods exist for the standard additions method, but all are empirical. In this paper, optimum equations are given and are analysed in detail by the theory of algorithms.

Theory

For the two standard additions method, we can obtain the following three equations according to Nernst's equation:

$$E_x = E^\circ + S\log c_x \quad .. \quad .. \quad .. \quad .. \quad (1)$$

$$E_1 = E^\circ + S\log\left(\frac{c_xV_x + c_sV_s}{V_x + V_s}\right) \quad .. \quad .. \quad (2)$$

$$E_2 = E^\circ + S\log\left(\frac{c_xV_x + 2c_sV_s}{V_x + 2V_s}\right) \quad .. \quad .. \quad (3)$$

where E_x, E_1 and E_2 are the measured electrode potentials, E° is the standard potential, S is the slope [usually close to the Nernstian value (RT/nF)], V_x and c_x are the volume and unknown concentration of the solution, respectively and V_s and c_s are the volume and concentration of the standard solution, respectively.

By subtracting equation (1) from both equation (2) and equation (3)

$$E_1 - E_x = S\log\left[\frac{c_xV_x + c_sV_s}{c_x(V_x + V_s)}\right] \quad .. \quad .. \quad (4)$$

and

$$E_2 - E_x = S\log\left[\frac{c_xV_x + 2c_xV_s}{c_x(V_x + 2V_s)}\right] \quad .. \quad .. \quad (5)$$

If $R = (E_1 - E_x)/(E_2 - E_x)$, $V = V_s/V_x$ and $X = c_s/c_x$ then, on dividing equation (4) by equation (5), we obtain

$$R = \frac{\ln[(1 + VX)/(1 + V)]}{\ln[(1 + 2VX)/(1 + 2V)]} = \frac{\ln(1 + VX) - \ln(1 + V)}{\ln(1 + 2VX) - \ln(1 + 2V)} \quad (6)$$

Then, if

$$f(X) = \frac{\ln(1 + VX) - \ln(1 + V)}{\ln(1 + 2VX) - \ln(1 + 2V)}$$

we obtain

$$f(X) - R = 0 \quad .. \quad .. \quad .. \quad (7)$$

Typically, c_s/c_x is in the range 25–200 and V_s/V_x in the range 0.01–0.05. For the two standard additions method, as $c_s > c_x > 0$, then $1 < c_s/c_x < +\infty$.

Theorem 1. If $X \in (1, +\infty)$ and $V \in (0, +\infty)$, then $\frac{1}{2} < f(X) < 1$.

Proof. The function $h(X) = (1 + 2VX)/(1 + VX) = 2 - 1/(1 + VX)$ is strictly increasing. Hence,

$$\frac{1 + 2V}{1 + V} < \frac{1 + 2VX}{1 + VX}, \quad \frac{1 + VX}{1 + V} < \frac{1 + 2VX}{1 + 2V}$$

and

$$\ln[(1 + VX)/(1 + V)] < \ln[(1 + 2VX)/(1 + 2V)]$$

therefore

$$f(X) < 1$$

As

$$\frac{V}{1 + V} < \frac{VX}{1 + VX}, 1 - \left(\frac{V}{1 + V}\right)^2 > 1 - \left(\frac{VX}{1 + VX}\right)^2,$$

$$\left(\frac{1 + VX}{1 + V}\right)^2 > \frac{1 + 2VX}{1 + 2V}$$

then

$$2\ln[(1 + VX)/(1 + V)] > \ln[(1 + 2VX)/(1 + 2V)]$$

that is,

$$f(X) > \tfrac{1}{2}$$

Theorem 2. If $X \in (1, +\infty)$ and $V \in (0, +\infty)$, then

(i) $\lim_{X \to 1^+} f(X) = \dfrac{1 + 2V}{2 + 2V} = a$ and (ii) $\lim_{X \to +\infty} f(X) = 1$.

Proof.

$$\text{(i)} \lim_{X \to 1^+} f(X) = \lim_{X \to 1^+}\left(\frac{1}{2} \cdot \frac{1 + 2VX}{1 + VX}\right) = \frac{1}{2} \cdot \frac{1 + 2V}{1 + V} = a$$

$$\text{(ii)} \lim_{X \to +\infty} f(X) = \lim_{X \to +\infty}\left(\frac{1 + 2VX}{1 + VX} \cdot \frac{V}{2V}\right) = 1.$$

Theorem 3. If $X \in (1, +\infty)$ and $V \in (0, +\infty)$, then (i) $g(X) = (1 + 2VX)\ln[(1 + 2VX)/(1 + 2V)] - 2(1 + VX)\ln[(1 + VX)/(1 + V)] > 0$ and (ii) $f(X)$ is strictly increasing.

Proof. (i) As $g'(X) = 2V\{\ln[(1 + 2VX)/(1 + 2V)] - \ln[(1 + VX)/(1 + V)]\} > 0$, and $\lim_{X \to 1^+} g(X) = 0$, then

$$g(X) > 0$$

(ii) As $f'(X) = [g(X)V]/\{(1 + VX)(1 + 2VX)[\ln(1 + 2VX)/(1 + 2V)]^2\} > 0$, then $f(X)$ is strictly increasing.

Theorem 4. If $V \in (0, +\infty)$ and $R \in (a, 1)$, then there is a unique solution $X^* \in (1, +\infty)$ to equation (6); if $V \in (0, +\infty)$ and $R \notin (a, 1)$, then there is no solution to equation (6) in the interval $(1, +\infty)$.

Proof. Using theorems 2 and 3, the proof of theorem 4 is easy. Using theorem 4, equations (1), (2) and (3) can be solved as follows:

$$c_x = c_s/X^* \quad .. \quad .. \quad .. \quad .. \quad .. \quad .. \quad .. \quad (8)$$

$$S = (E_1 - E_x)/\log\{(c_xV_x + c_sV_s)/[c_x(V_x + V_s)]\} \quad .. \quad (9)$$

$$E^\circ = E_x - S\log c_x \quad .. \quad .. \quad .. \quad .. \quad .. \quad .. \quad (10)$$

On the basis of theorem 4, we do not only solve equation (7) with the bisection method (*i.e.*, the method of halving the interval), but also check on errors in the experimental data.

The experimental data obtained in the determination of fluorine with a fluorine electrode by two standard additions were $V_x = 100$ ml; $V_s = 5$ ml; $V = V_s/V_x = 0.05$; $E_x = 110.2$ mV; $E_1 = 98.3$ mV; and $E_2 = 87.2$ mV.

Because $R < a$, equation (7) has no solution in the interval $(1, +\infty)$. It indicates that errors exist in the experimental process. The cause of the errors must be sought.

If $V \in (0, +\infty)$ and $R \in (a, 1)$, the equation

$$X = F(X), F(X) = \frac{1+V}{V}\left(\frac{1+2VX}{1+2V}\right)^R - \frac{1}{V} \quad .. \quad (11)$$

has the same solution, X^*, as equation (6) in the interval $(1, +\infty)$.

Theorem 5. If $X \in (1, +\infty)$, $V \in (0, +\infty)$ and $R \in (a, 1)$, then $|F'(X^*)| < 1$.

Proof. Using theorem 3(i) and theorem 4, we obtain

$$|F'(X^*)| = \left[2R(1+V)\left(\frac{1+2VX}{1+2V}\right)^R \frac{1}{1+2VX}\right]_{X=X^*} < 1$$

Theorem 6: contraction mapping theorem.[1] If $X \in (1, +\infty)$, $V \in (0, +\infty)$ and $R \in (a, 1)$, then the sequence $\{X_n\}$ $(n = 0, 1, 2, 3, \ldots)$ such that

$$X_{n+1} = \frac{1+V}{V}\left(\frac{1+2VX_n}{1+2V}\right)^R - \frac{1}{V}, \quad n = 0, 1, 2, 3, \ldots \quad (12)$$

converges to X^*, the solution of equation (6), for any initial approximation $X_0 \in [X^* - \delta, +\infty)$, where δ is a suitable small, positive, real number.

Proof. As $|F'(X^*)| < 1$ and $|F'(X)|$ is a continuous function, there exists an interval $[X^* - \delta, X^* + \delta]$ such that for any $X \in [X^* - \delta, X^* + \delta]$, $|F'(X)| < L < 1$, where L is a suitable small positive number.

As $|F'(X)|$ is strictly decreasing, for $X \in [X^* - \delta, +\infty)$ we have $|F'(X)| < L < 1$ for a suitable choice of L. Hence $\lim_{n \to +\infty} X_n = X^*$.

If the volumes (V_{s_1}, V_{s_2}) and concentrations (c_{s_1}, c_{s_2}) of the standard solution are different, then we obtain the following series of equations:

$$E_x = E^\circ + S\log c_x \quad .. \quad .. \quad .. \quad .. \quad .. \quad (13)$$

$$E_1 = E^\circ + S\log\left(\frac{c_xV_x + c_{s_1}V_{s_1}}{V_x + V_{s_1}}\right) \quad .. \quad .. \quad (14)$$

$$E_2 = E^\circ + S\log\left[\frac{c_xV_x + c_{s_1}(V_{s_1} + V_{s_2})}{V_x + V_{s_1} + V_{s_2}}\right] \quad .. \quad (15)$$

and

$$E_x = E^\circ + S\log c_x \quad .. \quad .. \quad .. \quad .. \quad .. \quad (16)$$

$$E_1 = E^\circ + S\log\left(\frac{c_xV_x + c_{s_1}V_{s_1}}{V_x + V_{s_1}}\right) \quad .. \quad .. \quad (17)$$

$$E_2 = E^\circ + S\log\left(\frac{c_xV_x + c_{s_1}V_{s_1} + c_{s_2}V_{s_2}}{V_x + V_{s_1} + V_{s_2}}\right) \quad .. \quad (18)$$

Similarly, we obtain

$$\left(\ln\frac{1+V_1X}{1+V_1}\right)\Big/\left[\ln\frac{1+(V_1+V_2)X}{1+V_1+V_2}\right] = R \quad .. \quad (19)$$

and

$$\left(\ln\frac{1+V_1X}{1+V_1}\right)\Big/\left[\ln\frac{1+(V_1+\theta V_2)X}{1+V_1+V_2}\right] = R \quad .. \quad (20)$$

where $R = (E_1 - E_x)/(E_2 - E_x)$, $V_1 = V_{s_1}/V_x$, $V_2 = V_{s_2}/V_x$, $X = c_{s_1}/c_x$ and $\theta = c_{s_2}/c_{s_1}$. Let

$$p = \frac{V_1(1 + V_1 + V_2)}{(V_1 + V_2)(1 + V_1)}$$

then we have the following theorems.

Theorem 7. If $X \in (1, +\infty)$, V_1 and $V_2 \in (0, +\infty)$ and $R \in (p, 1)$, then equation (19) has a unique solution, $X^* \in (1, +\infty)$, and the sequence $\{X_n\}$ $(n = 0, 1, 2, 3, \ldots)$ such that

$$X_{n+1} = \frac{1+V_1}{V_1}\left[\frac{1+(V_1+V_2)X_n}{1+V_1+V_2}\right]^R - \frac{1}{V_1}, \quad n = 0, 1, 2, 3, \ldots \quad (21)$$

converges to the solution X^* of equation (19) for any initial approximation $X_0 \in [X^* - \delta, +\infty)$, where δ is a suitable, small, positive, real number.

Theorem 8. If $X \in (1, +\infty)$, V_1 and $V_2 \in (0, +\infty)$, $\theta > 1$ and $R \in (0,1)$, then equation (20) has a unique solution, $X^* \in (1, +\infty)$, and the sequence $\{X_n\}$ $(n = 0, 1, 2, 3, \ldots)$ such that

$$X_{n+1} = \frac{1+V_1}{V_1}\left[\frac{1+(V_1+\theta V_2)X_n}{1+V_1+V_2}\right]^R - \frac{1}{V_1}, \quad n = 0, 1, 2, 3, \ldots \quad (22)$$

converges to the solution X^* of equation (20) for any initial approximation $X_0 \in [X^* - \delta, +\infty)$, where δ is a suitable small, positive, real number.

Proof. The basis of the proofs for theorems (7) and (8) is the same as that for theorem 6; hence the details are omitted.

Theorem 6 is called a "non-local" or "large-range" convergence theorem because it specifies a fixed, known interval, $I = [X^* - \delta, +\infty)$, and displays convergence for any $X_0 \in I$. Often it is not possible to specify such an interval in advance, but we might still hope that the iteration would converge if we could manage to make the initial guess, X_0, "sufficiently close" to the point X^*. Any theorem which states that "if the initial guess is very close to the solution, then the method will converge," is called a "local" or "point-field" convergence theorem, because it does not specify beforehand precisely how close X_0 must be to X^*.

Equations (21) and (22) are also called the "non-local" convergence equations.

Because X_0 generally is not greater than 300, we can let $X_0 = 300$.

Brand and Rechnitz[2] gave the well known iterative method for the two standard additions method. According to this, the iterative process is at times divergent.[3] What are the causes of divergence? What are the conditions for convergence? Is the initial approximation $c_x^{(0)} = 0$ M optimum? Is there an optimum initial approximation? What is a direct iterative equation? How do we decide the solution to the equation?

Table 1. Experimental data and numerical results. (The results of the bisection and iteration methods are the same)

Ion	I*	V_x/ml	c_x/M	c_s/M	V_s/ml	E_x,E_i†/mv	Results
F^-	1	0	0	0	0	299.9	$c_x = 1.05 \times 10^{-5}$ M
	2	25.00	1.00×10^{-5}	1.00×10^{-3}	1.0	192.0	$E^\circ = -53.7$ mV
	3	25.00	1.00×10^{-5}	1.00×10^{-3}	1.0	178.5	$S = -57$ mV decade^{-1}
Cl^-	1	0	0	0	0	161.8	$c_x = 1.02 \times 10^{-3}$ M
	2	50.00	1.00×10^{-3}	1.00×10^{-1}	1.00	135.0	$E^\circ = -12.8$ mV
	3	50.00	1.00×10^{-3}	1.00×10^{-1}	2.00	108.5	$S = -58.4$ mV decade^{-1}
I^-	1	0	0	0	0	−89.1	$c_x = 0.99 \times 10^{-5}$ M
	2	50.00	1.00×10^{-5}	1.00×10^{-4}	5.00	−104.2	$E^\circ = -377.62$ mV
	3	50.00	1.00×10^{-5}	1.00×10^{-3}	2.00	−130.9	$S = -57.7$ mV decade^{-1}
NO_3^-	1	0	0	0	0	214.5	$c_x = 1.01 \times 10^{-4}$ M
	2	50.00	1.00×10^{-4}	1.00×10^{-2}	1.00	187.4	$E^\circ = -18.1$ mV
	3	50.00	1.00×10^{-4}	1.00×10^{-2}	2.00	167.0	$S = -58.2$ mV decade^{-1}
CN^-	1	0	0	0	0	−171.4	$c_x = 9.88 \times 10^{-5}$ M
	2	50.00	1.00×10^{-4}	1.00×10^{-2}	2.50	−215.5	$E^\circ = -403.4$ mV
	3	50.00	1.00×10^{-4}	1.00×10^{-2}	2.50	−229.6	$S = -57.9$ mV decade^{-1}
Ag^+	1	0	0	0	0	249.1	$c_x = 1.03 \times 10^{-4}$ M
	2	50.00	1.00×10^{-4}	1.00×10^{-2}	1.00	276.5	$E^\circ = 486.3$ mV
	3	50.00	1.00×10^{-4}	1.00×10^{-2}	1.00	289.1	$S = 59.5$ mV decade^{-1}
K^+	1	0	0	0	0	−173.5	$c_x = 1.02 \times 10^{-4}$ M
	2	50.00	1.00×10^{-4}	1.00×10^{-2}	2.00	−134.6	$E^\circ = 58.9$ mV
	3	50.00	1.00×10^{-4}	1.00×10^{-2}	3.00	−116.3	$S = 57.7$ mV decade^{-1}
Pb^{2+}	1	0	0	0	0	−224.6	$c_x = 1.61 \times 10^{-6}$ M
	2	100.00	2.0×10^{-6}	2.00×10^{-4}	1.00	−214.8	$E^\circ = -60.5$ mV
	3‡	100.00	2.0×10^{-6}	2.00×10^{-4}	1.00	−209.5	$S = 28.3$ mV decade^{-1}
Ca^{2+}	1	0	0	0	0	−22.5	$c_x = 0.978 \times 10^{-3}$ M
	2	50.00	1.00×10^{-3}	1.00×10^{-1}	0.25	−17.8	$E^\circ = 57.3$ mV
	3§	50.00	1.00×10^{-3}	1.00×10^{-1}	0.25	−14.5	$S = 26.5$ mV decade^{-1}
Cd^{2+}	1	0	0	0	0	−214.2	$c_x = 0.95 \times 10^{-5}$ M
	2	50.00	1.00×10^{-5}	1.00×10^{-3}	1.00	−199.0	$E^\circ = -56.4$ mV
	3	50.00	1.00×10^{-5}	1.00×10^{-3}	1.00	−192.2	$S = 31.4$ mV decade^{-1}

* I = Ith measurement of the electrode potential.
† i = 1 or 2.
‡ Results from reference 2.
§ Results from reference 3.

According to the computational process[2] and equations (16), (17) and (18), we obtain

$$c_x = \mathrm{BR}(c_x),$$

$$\mathrm{BR}(c_x) = \left[\frac{(c_xV_x + c_{s_1}V_{s_1})(V_x + V_{s_1} + V_{s_2})}{(V_x + V_{s_1})(c_xV_x + c_{s_1}V_{s_1} + c_{s_2}V_{s_2})}\right]^{\frac{E_x - E_2}{E_1 - E_2}} \times \frac{c_xV_x + c_{s_1}V_{s_1} + c_{s_2}V_{s_2}}{(V_x + V_{s_1} + V_{s_2})} \quad \ldots \quad (23)$$

where $\mathrm{BR}(c_x)$ is a function of c_x.

Theorem 9. If V_{s_1}, V_{s_2}, $V_x > 0$ ml, $c_{s_2} \geqslant c_{s_1} > c_x > 0$ M and

$$0 < \frac{E_1 - E_2}{E_x - E_2} < \frac{V_{s_2}}{V_{s_1} + V_{s_2}} \cdot \frac{V_x}{V_x + V_{s_1}}, \quad c_{s_1} = c_{s_2} \quad \ldots \quad (24)$$

$$0 < \frac{E_1 - E_2}{E_x - E_2} < 1, \quad c_{s_1} < c_{s_2} \quad \ldots \quad (25)$$

then there is a unique solution $c_x^* \in (0, +\infty)$ to equation (23). The sequence $\{c_x^{(n)}\}$ such that

$$c_x^{(n+1)} = \mathrm{BR}[c_x^{(n)}], \quad n = 0, 1, 2, 3, \ldots \quad \ldots \quad (26)$$

converges to the solution c_x^*, for $c_x^{(0)} \in [0, c_x^* + \delta]$, $\delta > 0$.

Proof. The details of this proof are troublesome and hence they are omitted.

On the basis of the direct iterative equation, equation (26), there is no need to compute E° and S repeatedly. There is no need to fix $c_x^{(0)} = 0$ M as $c_x^{(0)} \in [0, c_x^* + \delta]$. The optimum initial approximation should be the limit of the linear range of the working curve, for example $c_x^{(0)} = 10^{-7}$ M. If equation (24) or (25) does not hold, then the iterative process is divergent and there is no solution to equation (23) in the interval $(0, +\infty)$.

Because the values of $\{c_x^{(n)}\}$ are smaller than the values of $\{X_n\}$, rounding-off errors affect the values of $\{c_x^{(n)}\}$ more.

When c_x^* is obtained, we have

$$S = (E_1 - E_x)/\log\{(c_x^*V_x + c_{s_1}V_{s_1})/[c_x^*(V_x + V_{s_1})]\} \quad \ldots \quad (27)$$

$$E^\circ = E_x - S\log c_x^* \quad \ldots \quad (28)$$

The program is written on the basis of equations (26), (27) and (28). The computational results obtained for many sets of experimental data are satisfactory.

The mathematical methods discussed in this paper are suitable not only for the two standard additions method but also for the two standard subtractions method, the two sample additions (subtractions) method and various standard additions (subtractions) methods through ionic strength calibration.[4,5]

Experimental

All reagents were of analytical-reagent grade and the electrodes used were obtained from Jiangsu Electroanalytical Factory Instrument, Jiangsu, China. The electrode potential was measured with respect to a saturated mercury(I) electrode using a Model PXJ-1B digital ion activity meter (Jiangsu Electric Analytical Instruments).

Careful attention was required with respect to the volume of ionic strength adjustment buffer added.

The experimental data were processed on an Apple-II microcomputer.

Results and Discussion

With equation (12) as the basis, the computer program IM1, in BASIC, was written for use with the Apple-II microcomputer.

When $X_0 = 300$ and $\varepsilon = 10^{-7}$, where ε is a small positive real number, convergence was achieved in 1 s. It is possible to prove that the order of convergence was 1.

According to theorem 4, the bisection method is highly satisfactory. The program BM1 is also written in BASIC. Usually $A = 1$ or 2 and $B = 200$ or 300, so the initial interval $[A, B]$ contains X^*, *i.e.*, $X^* \in [A, B]$. When $\varepsilon = 10^{-7}$, convergence is achieved in 1 s. The convergence rate of the bisection method is the same as the geometric progression, which has a common ratio of 1/2.

On the basis of equations (21) and (22), programs IM2 and IM3 were written in BASIC and, according to theorems 7 and 8, the bisection programs BM2 and BM3 were also written in BASIC.

The results obtained for each set of data are shown in Table 1 together with experimental data from other sources. From Table 1, we can compare each result with the original concentration. Obviously, high accuracy has been achieved by the programs as the theory and numerical results show.

It is very easy to select $[A, B]$ and X_0. These are common for various ion-selective electrodes, the programs being "non-local" convergent. In conclusion, these programs are suitable for incorporation in the ROM of the microcomputer ion meter.

References

1. Wang, J., *Chem. J. Chin. Univ.*, 1985, **6**, 487 (in Chinese).
2. Brand, M. J. D., and Rechnitz, G. A., *Anal. Chem.*, 1970, **42**, 1172.
3. Xuan, J., *Ion-Sel. Electrode Lett.*, 1981, **1**, 37 (in Chinese).
4. Wang, J., *Chem. World*, 1986, **27**, 310 (in Chinese).
5. Wang, J., *Comput. Appl. Chem.*, 1984, **1**, 305 (in Chinese).

Paper 8/04733B
Received November 11th, 1988
Accepted July 17th, 1989

Accuracy and Sensitivity of the Potentiometric Determination of Total Sulphur in Petroleum*

Sabri M. Farroha and Albertine E. Habboush†
Department of Chemistry, College of Science, University of Baghdad, Jadriya, Baghdad, Iraq

A potentiometric method is described for the determination of total sulphur in crude oil and its fractions over all concentration ranges. The method involves the quantitative conversion of sulphur to sulphate using an oxygen flask method followed by potentiometric titration using lead nitrate as titrant with a lead-selective indicator electrode. The sensitivity, accuracy and reproducibility of the method were investigated by analysing a series of standard sodium sulphate solutions and synthetic standards. The limits of detection ranged from 3.2×10^{-4} to 1.6×10^{-6} g ml^{-1}. The results were plotted on Gran plots and showed an error ranging from 0.51 to 3.0%, while the relative standard deviation did not exceed 3.13%. The method was applied successfully to the determination of total sulphur in crude oil and its fractions, before and after treatment, in addition to premium and super gasoline with and without tetraethyllead (TEL). The results showed that the amount of sulphur present in these fractions ranged from 0.035% m/m in super gasoline with TEL to 0.73% m/m in gas oil, and amounted to 1.99% m/m in crude oil with a relative standard deviation of between 0.9 and 5.17%.

Keywords: *Total sulphur determination; crude oil; petroleum; potentiometric titration; oxygen flask*

In spite of the large number of methods available for the determination of total sulphur in crude oil and its fractions, there is still no simple single procedure that is applicable to all fractions in all concentration ranges. The lamp method[1–3] with different detection techniques such as volumetric titration, turbidimetry or gravimetry has been used for volatile products, and the bomb combustion method[4–6] with similar detection techniques for heavy products including kerosene. Selig[7] determined sulphur in organic compounds by potentiometric titration with lead perchlorate; the procedure was subsequently extended to petroleum products by Heistand and Blake.[8] However, obscure and poor end-points were obtained if the sulphate level was less than 100 μg of sulphur. All these methods suffer from various difficulties, such as lack of sensitivity, and have a limited range of detection.

The aim of this investigation[9] was to develop a single, rapid, sensitive and accurate method for the determination of total sulphur in crude oil and its fractions in all concentration ranges.

Experimental and Results

Apparatus

The oxygen flask was a 1-l Pyrex conical flask with a ground-glass stopper cut to the appropriate length, into which 4–5 cm of platinum wire about 1 mm in diameter had been sealed. To the end of the wire was attached an oblong shaped piece of platinum gauze, which acted as a hinge to clamp the sample container.

Ashless filter-paper, Whatman No. 544, 1 × 1 cm, with a 5-cm long fuse, and pure gelatin capsules, No. 2, Lilly, USA, were used as sample carriers.

A Beckman Model 4500 digital pH meter, an Ingold 157200 lead-selective electrode and a Beckman saturated calomel electrode were used.

A 2-ml calibrated glass syringe, a 10-ml burette fitted with a tapered plastic tube and a magnetic stirrer were also used.

Chemicals

The following reagents were obtained from Fluka in the highest available purity: lead nitrate, sodium nitrite, sulphur (pure, sublimed), methanol, sodium sulphate and sodium nitrate.

Procedures

Determination of sulphate by potentiometric titration using a lead-selective electrode

The sensitivity, accuracy and precision of the potentiometric determination of sulphur were determined by titrating samples of standard sodium sulphate solutions with concentrations in the range 1.0×10^{-2}–5.0×10^{-5} M, corresponding to 3.20×10^{-3}–1.60×10^{-5} g of sulphur. Each 10 ml of the standard sulphate solutions was transferred quantitatively into a 250-ml beaker and 40 ml of methanol containing 1 ml of 0.1 M $NaNO_3$ solution were added. The pH was adjusted to between 6 and 7. The cell was assembled and the solution was titrated potentiometrically against lead nitrate solution in the range 1.0×10^{-2}–1.0×10^{-4} M using a lead-selective electrode and a double-junction saturated calomel electrode. The results were plotted as Gran plots and the amount of sulphate was calculated, Tables 1 and 2.

Preparation and measurement of a synthetic standard solution

Amounts of pure sublimed sulphur in the range 2.45×10^{-3}–1.96×10^{-4} g were weighed accurately in a gelatin capsule and combusted in an oxygen flask containing 0.015–0.010 g of sodium nitrite in 20 ml of distilled water as an absorbent. The flask was shaken gently, then left for 30–45 min after which the contents were transferred quantitatively into a 150-ml beaker and boiled to expel carbon dioxide, destroy excess of sodium nitrite and reduce the volume to about 20 ml. The solution was cooled to room temperature and its pH was adjusted to 6–7. Then, 1 ml of 0.1 M sodium nitrate solution was added, the volume was made up to 100 ml with methanol and the solution was titrated potentiometrically following the same procedure described above for the standard sulphate solutions. The results are summarised in Table 3.

* Presented at the Pittsburgh Conference and Exposition on Analytical Chemistry and Applied Spectroscopy, Atlanta, GA, USA, 6–10 March, 1989.

† To whom correspondence should be addressed.

Table 1. Summary of the results for the accuracy of the potentiometric determination of sulphur in sodium sulphate solution with lead nitrate as titrant

Sample No.	Sulphate/ M	Titrant/ M	Theoretical sulphur content*/g	Sulphur found*/g	Error, %
1	1.0×10^{-2}	1.0×10^{-2}	3.2×10^{-3}	3.28×10^{-3}	2.50
2	1.0×10^{-3}	1.0×10^{-3}	3.2×10^{-4}	3.14×10^{-4}	1.87
3	2.5×10^{-4}	2.5×10^{-3}	8.0×10^{-5}	7.36×10^{-5}	8.00

* For a 10-ml sample.

Table 2. Summary of the results for the accuracy of the potentiometric determination of sulphur in sodium sulphate solution with lead nitrate as titrant using Gran plots

Sample No.	Sulphate/ M	Titrant/ M	Theoretical sulphur content*/g	Sulphur found*/g	Error, %
1	5.0×10^{-4}	1.0×10^{-3}	1.60×10^{-4}	1.62×10^{-4}	1.25
2	2.5×10^{-4}	2.5×10^{-3}	8.00×10^{-5}	7.87×10^{-5}	1.63
3	5.0×10^{-5}	1.0×10^{-3}	1.6×10^{-5}	1.63×10^{-5}	1.87
4	5.0×10^{-5}	1.0×10^{-4}	1.60×10^{-5}	1.55×10^{-5}	3.13

* For a 10-ml sample.

Table 3. Summary of the results for the accuracy of the potentiometric determination of sulphate in synthetic standard samples

Sample No.	Amount of sulphur/g	Amount of sulphur recovered/g	Error, %
1	1.96×10^{-4}	1.97×10^{-4}	0.51
2	1.666×10^{-3}	1.616×10^{-3}	3.00
3	1.764×10^{-3}	1.735×10^{-3}	1.64
4	2.450×10^{-3}	2.398×10^{-3}	2.12

Determination of total sulphur in crude oil and petroleum fractions

A 0.10-ml amount of crude oil or petroleum fraction was measured with a syringe and dropped on to a filter-paper or on to a piece of filter-paper placed in a gelatin capsule and the procedure described above for the standard sulphate solutions and synthetic standards was followed. The results are summarised in Table 4.

Blank corrections

Methanol (100 ml) containing 1 ml of 0.1 M sodium nitrate solution was titrated using a similar procedure to that described above.

Four gelatin capsules were combusted and the solutions were titrated potentiometrically in the usual manner. The amount of sulphur per capsule was as follows: 5.23×10^{-5}, 5.16×10^{-5}, 5.10×10^{-5} and 5.07×10^{-5} g; 5.14×10^{-5} g was taken as the average and used throughout in the calculations involving the experiments with petroleum fractions in gelatin capsules.

Discussion

The conditions for the quantitative conversion of total sulphur to sulphate were investigated carefully; these included selection of a suitable absorbing solution, the type of sample carrier, the size and atmosphere of the oxygen flask and the time required for complete absorption of the combustion products.

The conditions for the oxygen flask combustion experiments were well suited for the combustion of the crude oil and the petroleum fractions. The flask size chosen (1 l) was in accordance with the size of the samples (0.1 ml), which usually contained amounts of sulphur in the range 1.68×10^{-3}–2.5×10^{-5} g. Increasing the flask size, and hence the amount of sample taken, would increase the sensitivity, but decrease the ease and simplicity with which the combustion could be performed. The atmosphere in the flask was at least 95% oxygen to ensure complete combustion. The use of filter-paper as a sample carrier was satisfactory and gelatin capsules were necessary for the volatile fractions. Sodium nitrite was found to be a suitable absorbent and the time required for complete absorption was about 30 min. Excess of sodium sulphite was completely destroyed by boiling, and no adverse effect on the lead-selective electrode was observed. To decrease the solubility of lead sulphate, methanol was chosen as the solvent as it has a low dielectric constant and has no effect on the electrode body.

Sensitivity, Accuracy and Precision of the Potentiometric Measurements

Table 1 shows that titrating 1.0×10^{-2} and 1.0×10^{-3} M sulphate solutions, which contain 3.2×10^{-3} and 3.2×10^{-4} g of sulphur, gave a 2.5 and 1.87% error, respectively, and that when a 2.5×10^{-4} M solution containing 8.0×10^{-5} g of sulphur was titrated a poor titration curve was obtained with an error of 8%. Table 2 shows the results of the potentiometric titration using a Gran plot for the standard sulphate solutions with concentrations of between 5.0×10^{-4} and 5.0×10^{-5} M, containing 1.60×10^{-4}–1.6×10^{-5} g of sulphur. The error does not exceed 3.13%. Further, Table 2 shows that when a sulphate sample of concentration 5×10^{-5} M containing 1.6×10^{-5} g of sulphur was titrated with 10^{-3} M lead nitrate solution, the error was 1.87%. However, when a similar sulphate sample was titrated with 1.0×10^{-4} M lead nitrate solution, the error increased to 3.13%.

Synthetic Standards

The results presented in Table 3 show that the conversion of sulphur to sulphate was quantitative and that the amounts of sulphur recovered were in good agreement with the theoretical values.

Table 3 shows the results for amounts of sulphur in the range 2.45×10^{-3}–1.96×10^{-4} g, which corresponds to 2.45×10^{-5}–1.96×10^{-6} g ml^{-1}; the average error is between 0.51 and 3.0%.

Table 4 shows that the proposed method can be applied successfully to the determination of total sulphur in crude oil and its fractions, both before and after treatment, in addition to premium and super gasoline with and without tetraethyllead (TEL). The amount of sulphur could be detected directly

Table 4. Summary of the results for the determination of total sulphur in crude oil and its fractions before and after treatment. Numbers in parentheses are sample numbers

Cut	Amount of sulphur/g per 100 ml: Proposed method	Amount of sulphur/g per 100 ml: Standard additions method	Sulphur content, % m/m	Mean sulphur content, % m/m	Relative standard deviation, %
Light naphtha	(1) 0.2044 (2) 0.2004 (3) 0.2052 (4) 0.2036	(5) 0.2020	(1) 0.305 (2) 0.299 (3) 0.306 (4) 0.304 (5) 0.301	0.303	0.962
Heavy naphtha	(1) 0.2373 (2) 0.2309 (3) 0.2325	(4) 0.2373	(1) 0.330 (2) 0.321 (3) 0.323 (4) 0.330	0.326	1.438
Kerosene	(1) 0.3319 (2) 0.3287 (3) 0.3207 (4) 0.3142 (5) 0.3287	(6) 0.3297	(1) 0.420 (2) 0.416 (3) 0.406 (4) 0.398 (5) 0.416 (6) 0.416	0.412	2.013
Gas oil	(1) 0.6173 (2) 0.5948 (3) 0.6413	(4) 0.6012	(1) 0.734 (2) 0.708 (3) 0.763 (4) 0.716	0.730	3.340
Treater outlet	(1) 0.0244 (2) 0.0231	(3) 0.02	(1) 0.036 (2) 0.034 (3) 0.035	0.035	2.857
Reformate	(1) 0.0577 (2) 0.0596 (3) 0.0628	(4) 0.0571	(1) 0.080 (2) 0.083 (3) 0.087 (4) 0.079	0.082	4.369
Hydro treater kerosene	(1) 0.0398 (2) 0.0410 (3) 0.0404	(4) 0.0423	(1) 0.050 (2) 0.052 (3) 0.053 (4) 0.053	0.052	2.505
Premium gasoline without TEL	(1) 0.0385 (2) 0.0394 (3) 0.0372	(4) 0.03837	(1) 0.056 (2) 0.057 (3) 0.054	0.056	2.744
Super gasoline without TEL	(1) 0.0423 (2) 0.0398 (3) 0.0407	(4) 0.0407	(1) 0.060 (2) 0.057 (3) 0.058	0.058	2.619
Premium gasoline with TEL	(1) 0.0333 (2) 0.0321	(3) 0.0289	(1) 0.047 (2) 0.045 (3) 0.041	0.044	6.891
Super gasoline with TEL	(1) 0.0260 (2) 0.0231 (3) 0.0266		(1) 0.037 (2) 0.032 (3) 0.037	0.035	5.170
Crude oil	(1) 1.6674 (2) 1.6931 (3) 1.6835	(4) 1.7379 (5) 1.6033 (6) 1.6898	(1) 1.976 (2) 2.006 (3) 1.995 (4) 2.002 (5) 2.059	1.990	2.609

Table 5. Methods used for the determination of total sulphur in volatile petroleum fractions (light and heavy naphtha)

Method	Type of determination	Range of concentrations	Comments	Reference
Lamp method (ASTM D-1266-64)	Volumetric	0.2–0.005% (200–50 p.p.m.)	Not useful for concentrations of sulphur higher than 4%	1,2
	Gravimetric	Not useful for concentrations lower than 5×10^{-3} g l^{-1} (5 p.p.m.)	Requires at least 18 h for a single determination	—
	Turbidimetric	Not useful for concentrations higher than 5×10^{-2} g l^{-1} (50 p.p.m.)	—	—
Modified lamp method (ASTM D-1266-70)	Volumetric, gravimetric and turbidimetric	Not useful for concentrations lower than 4×10^{-3} g l^{-1} (4 p.p.m.)	Not useful for very volatile fractions	3

for the different fractions of petroleum, in which the sulphur content varied from 1.99% m/m in crude oil to 0.035% m/m in super gasoline with TEL, with a relative standard deviation not exceeding 5.17%. These results are in good agreement with those obtained using the standard additions method.

The effect of the addition of TEL to gasoline on the amount of sulphur present was also studied. Table 4 shows that the amount of sulphur decreased from 0.056 to 0.044% m/m in premium gasoline and from 0.058 to 0.035% m/m in super gasoline after the addition of TEL as an antiknock agent. It is apparent from Table 5 and from the literature[1–4] that there is no single sensitive and accurate method available that is applicable to the determination of total sulphur in crude oil and its fractions in all concentration ranges.

The results presented in Table 4 demonstrate that the proposed method is sensitive, accurate and can be applied to the determination of total sulphur in crude oil and its fractions regardless of the degree of volatility of the fraction and the percentage of sulphur that it contains, as the sensitivity of the method was below the minimum amount of sulphur in any of the fractions.

References

1. "ASTM Standards, D-1266-64, Part 17," American Society for Testing and Materials, Philadelphia, PA, 1966, p. 456.
2. "IP Standards for Petroleum and Its Products," Part 1, Section 1, Institute of Petroleum, London, 1971, p. 374.
3. "ASTM Standards, D-1266-70 (re-approved 1975), Part 23," American Society for Testing and Materials, Philadelphia, PA, 1979, p. 650.
4. "ASTM Standards, D-129-64 (re-approved 1978), Part 23," American Society for Testing and Materials, Philadelphia, PA, 1979, p. 99.
5. "ASTM Standards, D-1552-79, Part 23," American Society for Testing and Materials, Philadelphia, PA, 1979, p. 828
6. Franks, M. C., and Gilpin, R. L., *J. Inst. Petr.*, 1962, **48**, 464.
7. Selig, W., *Mikrochim. Acta*, 1970, 168.
8. Heistand, R. N., and Blake, C. T., *Mikrochim. Acta*, 1972, 212.
9. Michael, M. N., *MSc Thesis*, Baghdad University, 1980.

Paper 9/01213C
Received March 21st, 1989
Accepted August 10th, 1989

Micro-technique for the Identification of Food Hydrocolloids

F. Olga Flint
Procter Department of Food Science, University of Leeds, Leeds LS2 9JT, UK

A simple technique is described for the identification of 13 hydrocolloid powders including pectin, seed gums, gum exudates, seaweed extracts, gelatin and pre-gelled starch. The method is based on the microscopical appearance of the different hydrocolloid particles when treated with aqueous Toluidine Blue under neutral and acid conditions. The reaction with iodine solution provided a confirmatory test for eight of the hydrocolloids. The technique relies on the combined physical and chemical properties of the individual hydrocolloids and gives results that are easy to interpret even for workers with limited experience of optical microscopy.

Keywords: *Microchemical test for food gum; seed gum; gum exudate; agar and carrageenan; gelatin and pre-gelled starch*

Hydrocolloids are widely used as emulsifiers and stabilisers in the food industry. Most of these, including seed gums (guar and locust bean), gum exudates (acacia, ghatti, karaya and tragacanth) and the seaweed extracts agar and carrageenan are imported in a powdered form; the identification of these natural gums can be difficult for both importer and user.

The limitations of the methods currently available were discussed by Morley *et al.*[1] in a paper which described a technique for separating the individual components of hydrocolloid mixtures. Their technique included confirmatory tests for a number of hydrocolloids but starch, gelatin, karaya, ghatti and xanthan gums were not included and guar and locust bean were found to be chemically indistinguishable. Microscopical methods for food hydrocolloids are described by Czaja[2] but these are all of an empirical nature.

The proposed method depends on the physical appearance of individual hydrocolloid particles when these are treated with specific aqueous stains. Hydrocolloid powders respond to water in characteristic ways; some, *e.g.*, pectin and gum acacia dissolve rapidly, others, *e.g.*, tragacanth and karaya gum first absorb water and swell before eventually dispersing. This affects the microstructure of gums stained with aqueous reagents.

All the anionic hydrocolloids are coloured by aqueous solutions of the basic dye Toluidine Blue, the microscopical appearance of the stained particles allowing several of them to be identified instantly. When the gum is pre-acidified only the sulphate-containing hydrocolloids, *e.g.*, agar and carrageenan are coloured.

Pre-gelled starches which lack anionic groups do not react with Toluidine Blue. Their presence is shown by an iodine solution, which also acts as a confirmatory test for several of the gums.

Experimental

Materials Examined

Powdered Irish Moss was supplied by Red Carnation Gums (London, UK); all other gums tested were obtained from Sigma (Poole, Dorset, UK). The pre-gelatinised starch (Clearjel) was supplied by National Starch and Chemical (Manchester, UK).

Reagents

Aqueous Toluidine Blue, 0.1%. Prepared by dissolving 110 mg of Biological Stain Commission certified Toluidine Blue (dye content, 91%) in 100 ml of distilled water.

Oxalic acid, 0.2 M. Prepared by dissolving 2.52 g of oxalic acid hydrate in distilled water and diluting to 100 ml.

Stock solution of iodine in aqueous potassium iodide (Lugol's Iodine). Prepared by dissolving 1 g of iodine in 100 ml of 2% m/v aqueous potassium iodide.

Working solution of iodine. Prepared by diluting 5 ml of Lugol's Iodine to 100 ml with distilled water just before use.

Toluidine Blue Staining Procedure on Hydrated Gum

Sprinkle 2–3 mg of the powdered gum on to a microscope slide. Tap the slide to give an even layer of the powder about 1 cm in diameter. Add 1 drop of distilled water, leave to hydrate for 1 min and then add 1 drop of 0.1% aqueous Toluidine Blue. Leave to stain for 1 min, add a coverslip, invert and blot firmly on fluff-free blotting paper to remove excess of stain. Examine the slide by bright-field illumination and between crossed polarising filters using a 10× objective.

All gums except pectin, gum arabic and pre-gelled starches yield a positive test. For these three hydrocolloids, add the drop of 0.1% Toluidine Blue to the gum powder on the slide without tapping to give an even layer, quickly add a coverslip, blot and examine promptly. Pectin and gum arabic will now give a positive test; pre-gelled starches remain uncoloured.

Toluidine Blue Staining Procedure on Acidified Gum

Sprinkle 2–3 mg of the powdered gum on to a microscope slide. Tap the slide to give an even layer of the powder about 1 cm in diameter. Add 1 drop of 0.2 M oxalic acid, leave for 1 min and then add 1 drop of 0.1% aqueous Toluidine Blue. Leave to stain for 1 min, add a coverslip, blot and examine as for the stained hydrated gum.

Iodine Staining Procedure

Sprinkle 2–3 mg of the gum and tap out as before. Add 1 drop of freshly diluted iodine solution, leave for 1 min, add a coverslip, invert and blot firmly. Examine as in the previous procedures. Pre-gelled starches, gelatin, tragacanth, guar, locust, agar and Irish Moss powder give well defined staining. Carrageenan stains very weakly and the colour is best seen by the naked eye when the slide is viewed against a white background.

Results

The results are summarised in Table 1 and illustrated in Figs. 1–4 (magnification, ×150).

Table 1. Microstructure of stained gum particles

Gum	Appearance of hydrated gum stained with Toluidine Blue	Appearance of acidified gum stained with Toluidine Blue	Appearance of gum stained with iodine reagent
Guar	Pink cells with dark purple contents	Colourless cells with pale contents	Colourless cells with yellow contents
Locust (carob)	Pink "foam-like" structure containing irregular dark-purple bodies	Colourless "foam-like" structure containing irregular pale blue bodies	Colourless structure with irregular yellow bodies
Tragacanth	Pink, blue and purple swollen particles containing small intact starch granules (unstained) which show well defined Maltese crosses between crossed polars	Unstained swollen particles starch granules prominent. Crossed polars show well defined Maltese crosses	Unstained swollen particles containing heavily stained blue - black starch granules (staining masks birefringence)
Karaya	Pink, dark magenta "puffy" swollen granules (cumulus cloud shape). Shows bright polarisation colours	Unstained	Unstained
Ghatti	Dull purple angular particles showing parallel striations. Weakly birefringent	Unstained	Unstained
Arabic (acacia)	Pale purple pink angular particles "melt and disperse." Not birefringent	Unstained	Unstained
Pectin	Deep magenta pink rounded particles, fast dispersing, contain tiny birefringent particles	Unstained	Unstained
Gelatin	Pale pink angular particles	Unstained	Pale yellow angular particles
Agar	Dark magenta purple staining outer layers of angular particles. Particle interiors unstained, brightly birefringent	Same staining as hydrated gum	Patchy deep red - brown angular particles. Birefringent
Irish Moss (crude powder)	Bright magenta dispersion showing darker stained "folds." Rounded groups of cells enclosed. Shows bright polarisation colours	Same staining as hydrated gum	Unstained matrix enclosing strongly stained red - brown filled cells
Carrageenan	Intensely stained magenta dispersion showing dark stained "folds." Shows bright polarisation colours	Same staining as hydrated gum	Viewed without microscope, slide appears pale purple - brown
Xanthan	Intensely stained magenta dispersion showing dark stained "folds" very similar to carrageenan. Bright polarisation colours	Unstained	Unstained
Pre-gelatinised starch	Unstained	Unstained	Red stained swollen gum particles containing blue starch granules (not birefringent)

Discussion

The results summarised in Table 1 show that many of the gums tested were positively identified by Toluidine Blue staining. The staining effects seen in Figs. 1–4 are not empirical and they can be explained in terms of the chemical and physical nature of the gums. Almost all food hydrocolloids are anionic in nature and different hydrocolloids have different dye-binding properties. Hence, when stained with the metachromatic basic dye Toluidine Blue they exhibit different shades of blue, purple and pink according to the density of the stain bound by the different gums. When carboxyl containing gums are acidified they no longer bind Toluidine Blue but the sulphate-rich hydrocolloids retain their anionic charge and staining properties at the pH given by the oxalic acid treatment (<2). Further differentiation is achieved by the characteristic ways in which different hydrocolloids swell in aqueous media and this pattern of staining was found to be constant for the same gums obtained from different suppliers.

Many of the gums could be identified without the iodine test but the test is required to distinguish gelatin and gum arabic and is useful as a confirmatory test for powdered Irish Moss, carrageenan, agar, guar, locust and tragacanth gums.

The metachromatic staining of Toluidine Blue is adversely affected by the presence of inorganic salts[3] and a dye sample of approximately 90% purity is recommended for this procedure. The photomicrographs (Figs. 1–4) were taken with a modern research microscope (Nikon Optiphot) but similar results can be obtained with any routine microscope which has a good light source. The use of polarising filters is helpful but not essential for the identification of the different gums.

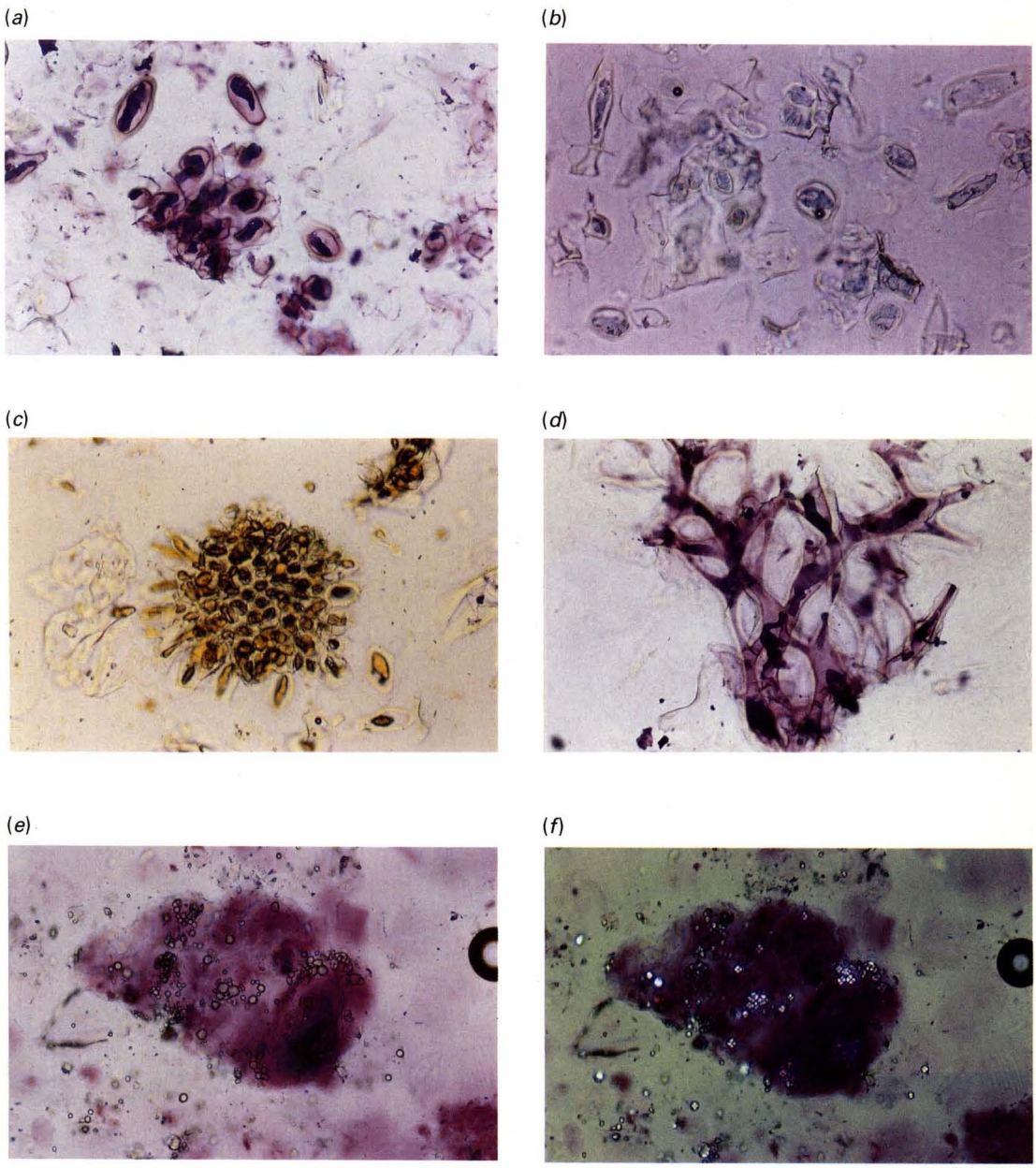

Fig. 1. (*a*) Hydrated guar gum stained with Toluidine Blue; individual endosperm cells stained pink with dark purple contents. (*b*) Acidified guar gum stained with Toluidine Blue; endosperm cells colourless with pale blue contents. (*c*) Guar gum stained with iodine; endosperm cell contents yellow. (*d*) Hydrated locust bean gum stained with Toluidine Blue; pink foam-like structure with dark purple inclusions. (*e*) Hydrated tragacanth gum stained with Toluidine Blue; swollen gum particles stained pink and purple containing unstained starch granules (bright-field illumination). (*f*) Same field as (*e*) viewed between partially crossed polarising filters, starch granules show well defined Maltese crosses

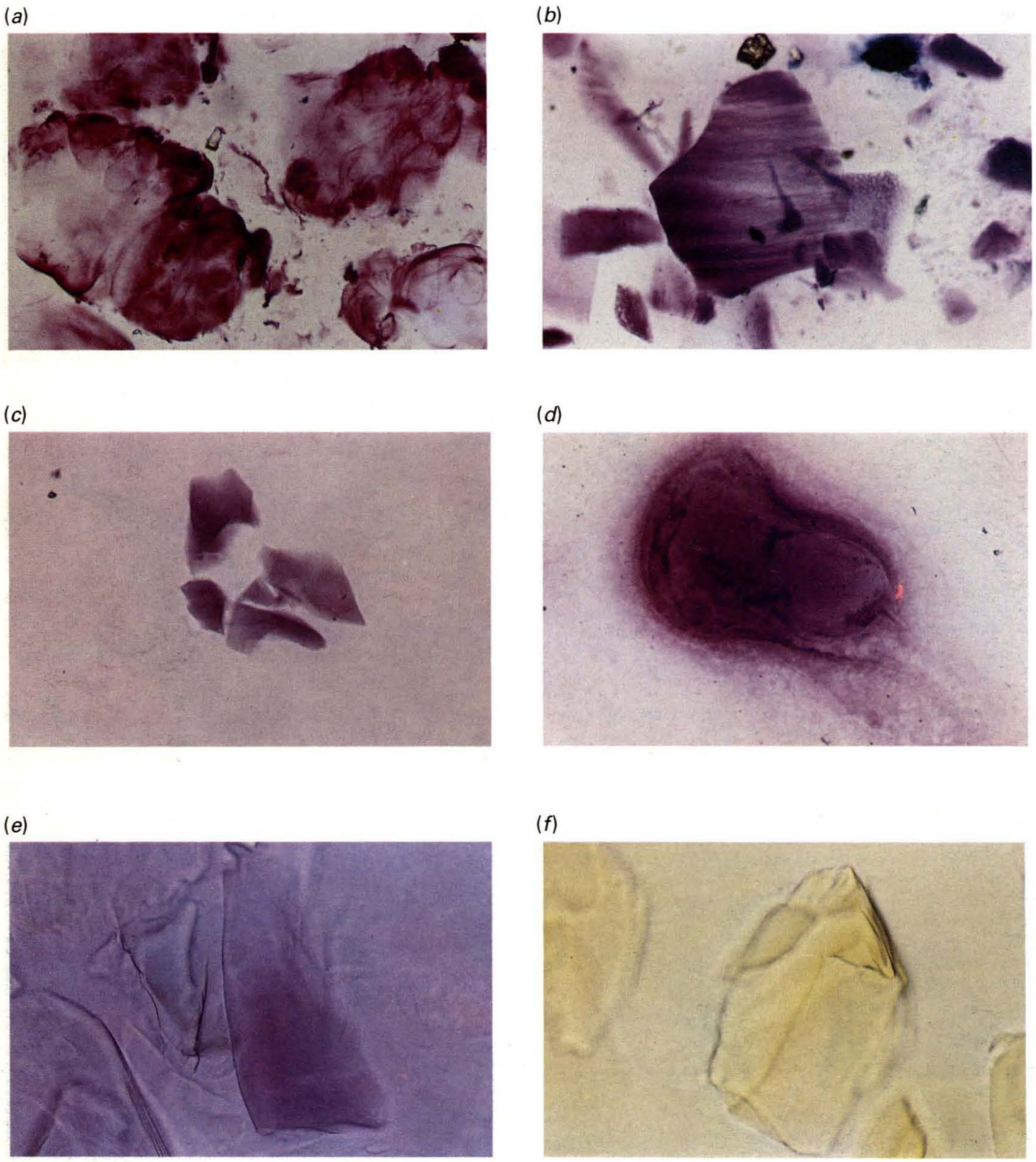

Fig. 2. (*a*) Hydrated Karaya gum stained with Toluidine Blue, cumulus shaped swollen granules, pink to dark purple. (*b*) Hydrated Ghatti gum stained with Toluidine Blue, dull purple angular particles, larger granules show well defined parallel striations. (*c*) Gum acacia treated directly with Toluidine Blue, purplish pink angular particles which soon disperse. (*d*) Citrus pectin treated directly with Toluidine Blue, bright magenta rounded particles, fast dispersing. (*e*) Hydrated gelatin stained with Toluidine Blue, pale pink particles similar to gum acacoa. (*f*) Gelatin stained with iodine reagent, pale yellow angular particles

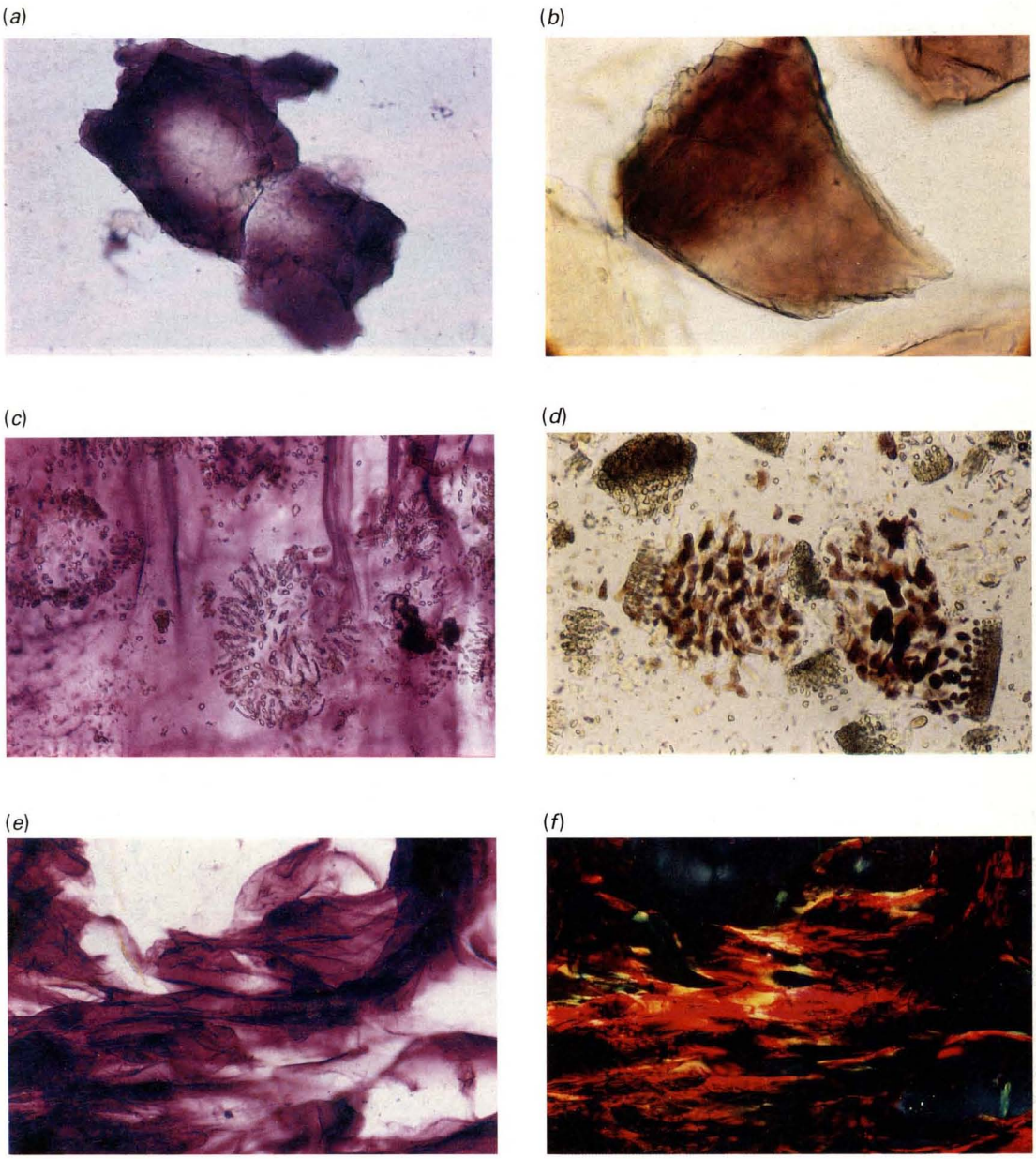

Fig. 3. (*a*) Agar, acidified before Toluidine Blue staining. Outer layers of angular particles dark magenta purple. (*b*) Agar stained with iodine reagent, unevenly stained red - brown angular particles. (*c*) Irish Moss powder acidified before Toluidine Blue staining showing stained "folds" (see Carrageenan), matrix encloses rounded clumps of cells. (*d*) Irish Moss powder stained with iodine reagent, matrix unstained, contains aggregates of red - brown filled cells. (*e*) Carrageenan acidified, stained with Toluidine Blue, magenta dispersion showing darker coloured folds (bright-field illumination). (*f*) Same field as (*e*) viewed between crossed polarising filters. Bright polarisation colours (red, orange and green) showing aligned dye molecules

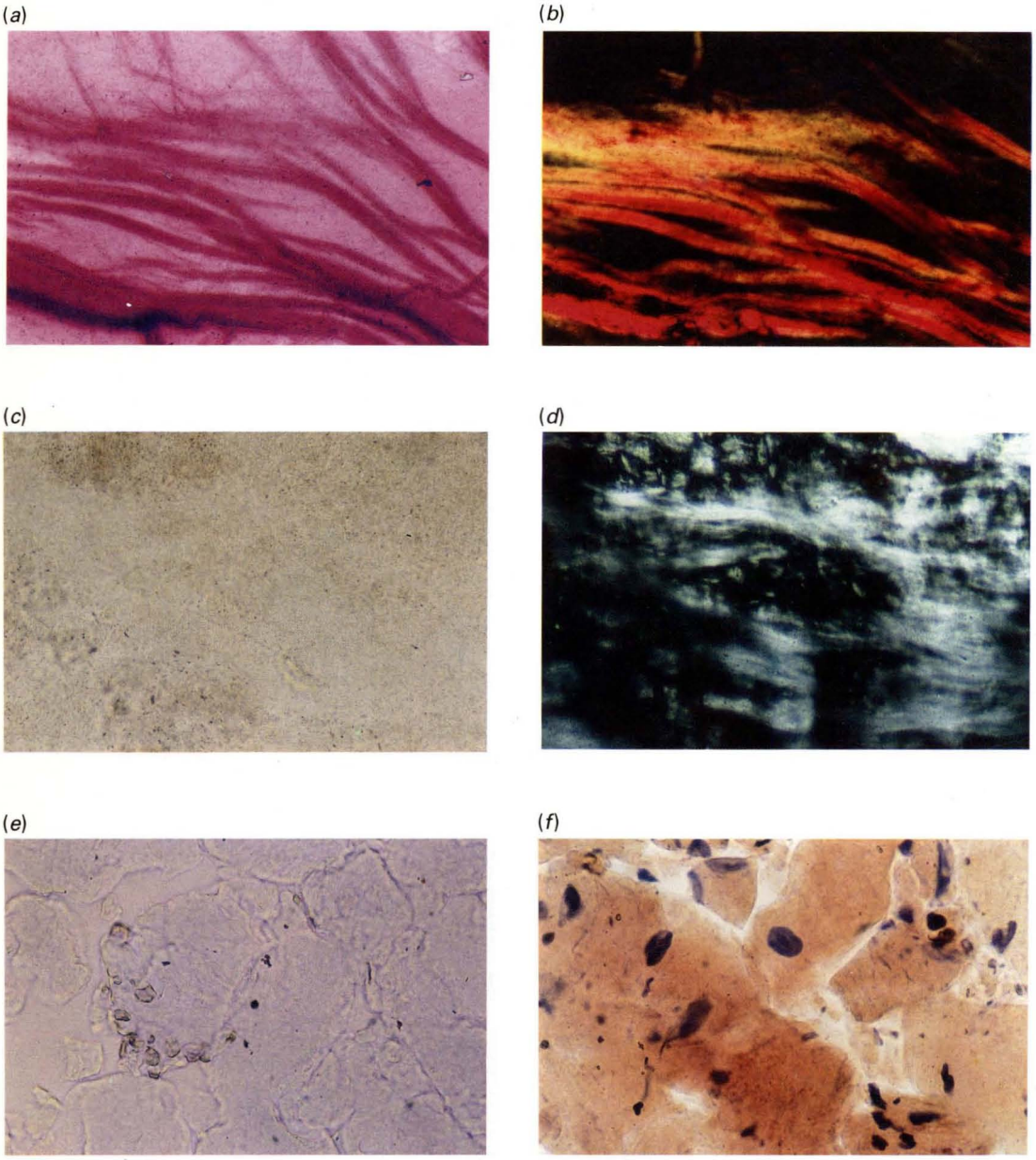

Fig. 4. (*a*) Xanthan hydrated and stained with Toluidine Blue, magenta dispersion showing darker coloured folds similar to carrageenan. (*b*) Same field as (*a*) viewed between crossed polarising filters showing similar polarisation colours to carrageenan. (*c*) Xanthan acidified, stained with Toluidine Blue. Complete absence of staining [*cf.* Fig. 3(*e*)]. (*d*) Same field as (*c*) viewed between crossed polarising filters showing white birefringence caused by unstained gum [*cf.* Fig. 3(*f*)]. (*e*) Pre-gelatinised starch hydrated and stained with Toluidine Blue, swollen particles unstained. (*f*) Pre-gelatinised starch stained with iodine reagent, swollen particles, red, contain individual dark blue staining starch granules

Thanks are due to the Laboratory of the Government Chemist and Red Carnation Gums Ltd., for materials and financial help and to Barry M. Firth for technical assistance.

References

1. Morley, R. G., Phillips, G. O., and Powder, D. M., *Analyst*, 1972, **97**, 315.
2. Czaja, A. Th., "Methoden der Lebensmittel-mikroscopie und Lebensmittel-uberwachung," Umschau Verlag, Frankfurt am Main, 1971, p. 71.
3. Flint, F. O., and Firth, B. M., *Analyst*, 1988, **113**, 365.

Paper 9/03167G
Received July 26th, 1989
Accepted August 11th, 1989

Determination of Orthophosphate in Waters and Soils Using a Flow Analyser

David J. Malcolme-Lawes and Koon Hung Wong
Centre for Research in Analytical Chemistry and Instrumentation, King's College London, Strand, London WC2, UK

A high-performance continuous flow analyser has been used for the determination of orthophosphate ion in potable waters and soil extracts by the heteropolymolybdenum blue method. Interference from a number of common ionic species has been examined and found to be small at the levels encountered in potable waters. The limit of detection for PO_4^{3-} was calculated to be 14.5 p.p.b. (4.8 p.p.b. of P), a linear calibration range of up to 0–100 p.p.m. was demonstrated and the sample throughput was better than 120 samples h^{-1} using the calibration range 0–4 p.p.m. and above, and 50 samples h^{-1} using the range 0–0.5 p.p.m.

Keywords: *Orthophosphate; flow injection*

In recent papers[1–3] a novel approach to non-segmented continuous flow analysis has been described in which a computer-controlled valve-switching system was used to permit precise mixing of sample and reagents for selective reaction analysis. An improved version of the apparatus, which employed a computer-controlled colorimeter provided excellent sample throughput and sensitivity, and results obtained in analyses of nitrate, nitrite and ammonium ions in waters were presented.[3] In this work we undertook some analyses of orthophosphate in water and soil extracts, the latter for comparison with analyses carried out at ICI, Jealotts Hill Research Station. The principal aim of the work was to determine whether the sensitivity, sample throughput rate and range of linearity for the determination of orthophosphate using this method offered improvements compared with previously reported methods.

The instrument[1,2] used in these experiments has remained much as described previously[3] for the sequential determination of nitrate, nitrite and ammonium, although in the present analyses the reducing column was not used. The reagent mixture was allowed to fill the manifold for a pre-determined time period, referred to as the fill time ($t_{fill.}$). At this point the sample loop circuit was switched out of the manifold and filled with sample using a solenoid-operated syringe pump. The sample loop was then switched back into the manifold and the reagent/sample segments passed into the controlled temperature reaction coil. At the end of the reaction time ($t_{reac.}$) the reaction mixture passed from the reaction coil towards the detector for a specified time (t_{wash}). However, the mixture flow could be diverted to waste for a time period $t_{dil.}$ (which we refer to as the dilution time) and only the tail portion of the reaction mixture passed through the detector and the product absorbance was recorded. This approach was useful for high-concentration samples, where either the product absorbance or the depletion of reagent would be very large and would result in operation outside the linear range of normal operation. It also has an advantage over the in-line dilution technique[2] in that the refractive index effects observed in a reagent - carrier - sample pattern are greatly reduced.

Experimental

Orthophosphate was determined by the heteropolymolybdenum blue method. "Conventional" flow injection methodology[4] relied on the reaction of ammonium molybdate with orthophosphate to form a yellow complex under strongly acidic conditions; the latter would subsequently be reduced downstream by merging with a reductant such as ascorbic acid to form the heteropolymolybdenum blue complex, which could then be monitored at 670 nm.

Our methodology differed in that the reagents were pre-mixed in the manifold and orthophosphate samples were then injected downstream. After passing through the temperature-controlled reaction coil, the absorbance of the blue complex was also measured at 670 nm. The acidity of the carrier was found to be crucial. This is quite understandable considering the reaction would "normally" be a two-stage process. Conditions had to be arranged so that the blue complex would not be formed when the two reagents were first mixed together; it should only be formed after the injection of orthophosphate. This provides a significant improvement over conventional methods. The tolerance limit between formation of the blue complex when only the reagents were mixed and no reaction occurring at all (owing to too much acid in the carrier) was very small. Consequently, careful adjustment of the acidity of the carrier was required, and the carrier solutions used were made up using water and acid volumes measured to an estimated accuracy of 1%. The NaCl present in the carrier is used primarily to minimise refractive index effects within the flow cell, so the precise NaCl concentration is less critical.

Chemicals

Ammonium molybdate (AM), AnalaR, BDH.
L-Ascorbic acid (AA), Biochemical, BDH.
Potassium antimonyl tartrate (PAT), Aldrich.
Potassium dihydrogen orthophosphate, AnalaR, BDH.
Nitric acid (sp. gr. 1.42), AnalaR, BDH.
Sodium chloride, Analytical Reagent, FSA Laboratory Supplies.

Analyte Standards

Standard solutions of 10 and 1000 p.p.m. of PO_4^{3-} were prepared by the dissolution of weighed amounts of potassium dihydrogen orthophosphate in distilled water. On subsequent dilution, five orthophosphate standards in each of the following concentration ranges were prepared for calibration purposes: 0–0.5, 0–4, 0–20 and 0–100 p.p.m. of PO_4^{3-}.

Carrier

Sodium chloride (15.0 g) was dissolved and made up to 1000 cm^3 in 0.12 M nitric acid.

Reagents

(1) Ammonium molybdate (8.0 g) + potassium antimonyl tartrate (1.8 g) in 1000 cm^3 of distilled water; the latter acts as a catalyst[4] for the reaction.

Table 1. Examples of linear calibration parameters for orthophosphate calibrations

Range, p.p.m.	Experimental conditions: t_{fill}/ s	$t_{reac.}$/ s	$t_{dil.}$/ s	Coil temperature/ °C	Derived parameters: Slope/ A p.p.m.$^{-1}$	Intercept/ A	Correlation coefficient ($n = 5$)
0–0.5	3	40	1	35	0.3282	0.2939	0.9998
0–4	3	10	1	35	0.2768	0.1196	0.9988
0–20	3	0	7	35	0.0539	0.1763	0.9995
0–100	2	0	14	20	0.0200	0.1168	0.9999

(2) L-Ascorbic acid (12.0 g) in 1000 cm^3 of distilled water.

Both reagents were stored in the dark and at 4 °C when not in the instrument.

Conditions

The following conditions were used: t_{wash} = 25.0 s; and monitoring wavelength = 670 nm. Other conditions were as described below.

Results

The absorbance peaks generated by the injection of a blank (distilled water) and five orthophosphate standards were recorded and linear calibration parameters evaluated for the calibration ranges described above. The results are shown in Table 1.

The reproducibility of peak heights recorded for successive injections was examined for a number of calibration standards, blanks and diluted standards using the conditions of the appropriate calibration range. The relative standard deviation (RSD) of peak heights for ten injections of an approximately 3-p.p.m. sample was 1.08%, that for a 65-p.p.m. sample 1.10%, that for a 0.5-p.p.m. sample 0.98% and that for a 40-p.p.b. sample 1.97%. The RSD for a blank recorded under the conditions of the 0–4 p.p.m. calibration range was 1.13% and that for a blank recorded under the conditions of the 0–0.5 p.p.m. calibration was 1.38%. The limits of detection (evaluated as twice the standard deviation of a blank divided by the sensitivity) evaluated from the reproducibility results were calculated to be 93.2 p.p.b. of PO_4^{3-} (30.4 p.p.b. of P) for the conditions of the 0–100 p.p.m. calibration range (see Table 1), 16.1 p.p.b. of PO_4^{3-} (5.25 p.p.b. of P) for the conditions of the 0–4 p.p.m. calibration range and 14.5 p.p.b. of PO_4^{3-} (4.8 p.p.b. of P) for the 0–0.5 p.p.m. calibration range. The RSD for computed concentrations of PO_4^{3-} from ten injections of a 40-p.p.b. sample was 9.19%.

Interference Studies

The interferences caused by foreign ions in the determination of orthophosphate are said to be high unless extraction procedures are used.[5,6] Our instrumental method has been developed primarily for use with potable and environmental water samples, so our investigations of interferences were limited largely to those species which are to be expected in potable waters.[7–9]

Our studies were basically directed towards confirming what levels of added ions did not cause interference, in the sense that the instrument reported results for orthophosphate in the presence of the added ion which were within 1% of results reported in the absence of added ion. In most instances the added ion was mixed with the sample solution, although for Na and Cl the high levels were also administered to the carrier, as the saline carrier was used to balance refractive index effects. For 5 p.p.m. of PO_4^{3-}, the sample was not observed to suffer interference from 9000 p.p.m. of Cl^-, 7000 p.p.m. of Na^+, 900 p.p.m. of Ca^{2+}, Cd^{2+}, K^+, Br^- and HCO_3^-, 500 p.p.m. of SO_4^{2-}, 200 p.p.m. of Mg^{2+}, 100 p.p.m. of NH_4^+, Ni^{2+}, CO_3^{2-}, NO_3^- and disodium ethylenediaminetetraacetate (Na_2EDTA), 90 p.p.m. of NO_2^-, 20 p.p.m. of Zn^{2+}, 10 p.p.m. of Mn^{2+}, $CH_3CO_2^-$ and phenol, 1 p.p.m. of Al^{3+} or 0.1 p.p.m. of Cr^{6+}, Pb^{2+}, Sn^{2+} and AsO_4^{3-}.

Interferences due to Fe^{3+} and SiO_3^{2-} were observed at levels of 10 and 100 p.p.m., respectively, although the addition of 1 g of citric acid per litre of carrier effectively removed interferences at these levels. Similarly, Cu^{2+} levels of 10 p.p.m. caused interference and 1 g of Na_2EDTA per litre of carrier was found to overcome this effect.

It is important to note that the levels at which the potential interferents were added far exceeded the concentrations that would normally be encountered in potable water supplies.[7–9] Hence in normal circumstances interferences from the ions studied should not present a problem.

Table 2. Determination of orthophosphate in soil extracts

Sample No.	Phosphate concentration (as PO_4^{3-}), p.p.m.: Present results	Manual results
1	1.17 ± 0.04	0.95
2	8.80 ± 0.10	7.84
3	3.36 ± 0.09	3.06
4	12.71 ± 0.05	11.09
5	5.29 ± 0.04	4.07
6	17.44 ± 0.18	15.11
7	10.15 (5) ± 0.27	9.59
8	2.77 ± 0.06	2.42
9	6.23 ± 0.11	6.13
10	2.24 ± 0.16	1.38
11	8.96 ± 0.13	8.64
12	4.82 ± 0.05	4.90

Determination of Orthophosphate in Soil Extracts

The method detailed above was applied to the determination of orthophosphate in soil extracts. The extracts were prepared[10] by shaking 2.5 cm^3 of dried, ground soil with 50 cm^3 of 0.5 M sodium hydrogen carbonate solution (pH 8.5) for 30 min at 20 °C. The mixture was then filtered and the filtrate neutralised with 0.5 M nitric acid in the ratio of 1:1. The destruction of the excess of hydrogen carbonate prior to analysis was carried out to prevent bubble formation within the manifold when the samples were injected into the carrier. No further manipulation of the samples was required before analysis. The results, expressed as p.p.m. of PO_4^{3-} with corresponding standard ($n = 3$), are given in Table 2 together with results obtained by manual analysis (based on the same extraction procedure and analysis reaction) of the same samples at an independent laboratory.[7] Bearing in mind that the independent results are for single analyses and are expected to be accurate to within 10%, the results indicate that the proposed method produces somewhat higher concentrations of orthophosphate than the manual method, possibly as a result of different pH levels in the larger volume samples and standards used in the manual method. The use of the method of standard additions, as reported previously,[3] confirmed that our results were not affected by the sample matrix.

Discussion

Růžička and Hansen[11] used the reduction of phosphomolybdate to molybdenum blue and the "conventional" flow injection technique to determine orthophosphate using a residence time of 6 s to provide a sensitivity of 0.0064 A p.p.m.$^{-1}$ of PO_4^{3-} and a linear range of 7.7–76.7 p.p.m. of PO_4^{3-} at a sampling rate of 120 samples h^{-1}. Yoza *et al.*[12] used a different chemistry and established a linear range of 1.9–9.5 p.p.m. of PO_4^{3-}, but at a sensitivity of 0.003 A p.p.m.$^{-1}$ of PO_4^{3-} and a residence time of 65 s. By overlapping injections they maintained a sample throughput of 120 samples h^{-1}.

Johnson and Petty[13] used the molybdenum blue test in reversed flow injection to achieve a very high sensitivity (0.1404 A p.p.m.$^{-1}$ of PO_4^{3-}) with a residence time of 15 s (at 50 °C) and a sample throughput rate of 90 samples h^{-1}, and achieved a limit of detection of 5 p.p.b. of PO_4^{3-} (1.7 p.p.b. of P), which is three times lower than ours, but at the cost of a vastly different sample size. Worsfold *et al.*[14] also used a reversed flow injection approach to achieve a stated limit of detection of 12 p.p.b. of P (36 p.p.b. of PO_4^{3-}). Janse *et al.*[4] used the reduction of phosphomolybdate with both ascorbic acid and tin(II) chloride, and achieved a limit of detection of 30.6 p.p.b. of PO_4^{3-} with a linear range of 0.12–7.67 p.p.m. of PO_4^{3-} and a sampling rate of 180 samples h^{-1}. Motomizu *et al.*[15] used malachite green and ammonium heptamolybdate as a complexing agent to develop a very sensitive assay with a very low limit of detection ("several ng ml^{-1}"), but with a limited linear range (0.01–0.8 p.p.m. of PO_4^{3-}) and a limited sample throughput (40 samples h^{-1}).

The results of this study indicate that this new instrument is capable of a combination of precision, sensitivity, reproducibility and sample throughput at least as good as those obtained previously for phosphate determinations with samples of a comparable size, and with the added flexibility of improved ranges of linearity. Hence the system used as described can determine orthophosphate ion with a sensitivity adjustable up to 0.328 A p.p.m.$^{-1}$ of PO_4^{3-}, and a calculated limit of detection of 16 p.p.b. of PO_4^{3-} (5.25 p.p.b. of P) for 120 0.3-ml samples h^{-1}, or 14.5 p.p.b. of PO_4^{3-} (4.8 p.p.b. of P) for 50 0.3-ml samples h^{-1}. The linear range is very good and we have demonstrated this through linear calibrations over the ranges 0–0.5 p.p.m. to 0–100 p.p.m., although we have not determined an upper limit for this range because the flexibility of the slicing and in-line dilution[2] techniques allows this to be varied considerably.

An additional attraction of the present instrument is that it can be, and in our laboratory is routinely, programmed to carry out the phosphate analysis sequentially with the analyses for nitrate, nitrite and ammonium ion reported earlier,[3] or indeed with any other analysis for which a suitable procedure can be defined. The limit to such sequential analyses is determined by the number of reagent bottles available, which is eight on our "laboratory-built" prototype instrument and currently 16 on the commercial version. This flexibility can be valuable in situations where a rapid result for several analytes is required from a single sample, such as in medical diagnosis or the determination of water quality. Further, the concentration of the analytes might be dramatically different because the procedure for each analysis can be programmed to incorporate an independent dilution factor ($t_{dil.}$) as described above (or to use the in-line dilution technique described previously[2]).

Some aspects of this work were performed with the aid of support from the Royal Society. The authors are also grateful for the advice of R. Newton of Biotech Instruments and for the cooperation of N. B. Coombe of ICI Jealotts Hill Research Station in providing samples and the results of reference analyses. Commercial versions of an autosampling version of the instrument described are available as the Biostar Chemical Analyser from Biotech Instruments Ltd, 183 Camford Way, Luton LU3 3AN, UK.

References

1. Malcolme-Lawes, D. J., Milligan, G. A., and Newton, R., *J. Autom. Chem.*, 1987, **9**, 179.
2. Malcolme-Lawes, D. J., and Pasquini, C., *J. Autom. Chem.*, 1988, **10**, 25.
3. Malcolme-Lawes, D. J., and Pasquini, C., *J. Autom. Chem.*, 1988, **10**, 192.
4. Janse, T. A. H., van der Wiel, P. F. A., and Kateman, G., *Anal. Chim. Acta*, 1983, **155**, 89.
5. American Public Health Association, American Water Works Association and Water Pollution Control Federation, "Standard Methods for the Examination of Water and Wastewater," Fifteenth Edition, American Public Health Association, New York, 1981, pp. 445–452.
6. Williams, W. J., "Handbook of Anion Determination," Butterworths, London, 1979.
7. Tecator, *In Focus*, 1987, **10**, 1.
8. "International Standard for Drinking Water," Second Edition, World Health Organisation, Geneva, 1963.
9. Bond, R. G., Straub, C. P., and Prober, R., "CRC Handbook of Environmental Control, Volume 3: Water Supply and Treatment," CRC Press, Cleveland, Ohio, 1973.
10. Coombe, N. B., personal communication.
11. Růžička, J., and Hansen, E. H., *Anal. Chim. Acta.*, 1975, **78**, 145.
12. Yoza, N., Kurokawa, Y., Hirai, Y., and Ohashi, S., *Anal. Chim. Acta*, 1980, **121**, 281.
13. Johnson, K. S., and Petty, R. L., *Anal. Chem.*, 1982, **54**, 1185.
14. Worsfold, P. J., Clinch, J. R., and Casey, H., *Anal. Chim. Acta.*, 1987, **197**, 43.
15. Motomizu, S., Wakimoto, T., and Toei, K., *Talanta*, 1980, **30**, 333.

Paper 9/01465I
Received April 10th, 1989
Accepted August 16th, 1989

Determination of Oxonium Ion in Strongly Ionisable Inorganic Acids and Determination of Substituted Acetic Acids Using Flow Injection and Chemiluminescence Detection

Issam M. A. Shakir and Azad T. Faizullah
Chemistry Department, College of Science, University of Salahaddin, Arbil, Iraq

A method is described for the determination of oxonium ion in strongly ionisable inorganic acids such as sulphuric (0.015–0.16 M), hydrochloric (0.03–0.18 M), perchloric (0.03–0.14 M), nitric (0.03–0.16 M) and phosphoric (0.02–0.09 M) acids. In addition, halogeno-substituted acetic acids such as chloroacetic (0.02–0.08 M), trichloroacetic (0.03–0.16 M) and trifluoroacetic (0.03–0.14 M) acids can be determined. Formic acid can be detected at the 0.1 M level but acetic acid could not be detected up to 0.2 M. The method is based on the *in situ* generation of bromine from the $BrO_3^- - Br^- - H_3O^+$ reaction; the bromine is then reacted with H_2O_2 to liberate oxygen for the oxidation of luminol. A sample size of 60 μl was used with a flow-rate of 2 ml min^{-1}. The reproducibility of the determination at all the concentrations studied was close to zero. Linear regression of the log-log plot of concentration (M) *versus* chemiluminescence intensity [peak height (mV)] gave a correlation coefficient of 0.98–0.99 for all the acids studied, except for phosphoric and sulphuric acids which gave a correlation coefficient of 0.93 in the concentration range studied. Various parameters were optimised such as the concentration of the reactants. Electronegativity can be demonstrated using this method.

Keywords: *Chemiluminescence; flow injection; inorganic acid; halogeno-substituted acetic acid; oxonium ion*

The chemiluminescence from the oxidation of luminol by hydrogen peroxide in alkaline medium has, so far, been the most attractive system for determining many inorganic and organic species.[1,2] However, an alternative procedure for generating luminol chemiluminescence has recently been described,[3] based on the homogeneous catalysis of the *in situ* generation of bromine using bromate-bromide-acid for the decomposition of hydrogen peroxide. In addition to not being dependent on the presence of metal ions, the reaction has been applied successfully to the determination of bromide ion[4] over a wide dynamic range. The fact that the chemiluminescence intensity of the reaction is related to the oxonium ion concentration suggests that it could be used for the determination of the oxonium ion concentration of many acids and α-substituted acetic acids. The determination of acids by flow injection-chemiluminescence has not yet been reported. This paper describes the determination of some inorganic acids, and chloro- and fluoro-substituted acetic acids.

Experimental

Apparatus

A multi-channel peristaltic pump (Desaga), a six-way injection valve with a 60-μl sample loop, silicone rubber tubing (0.5 mm i.d.), a reaction cell (spiral, 100 μl), a laboratory-built detector,[4] a high radiance monochromator (1200 nm mm^{-1}) with an inlet slit width of 20 nm and an outlet slit width of 5 nm, an EMI IP28 photomultiplier tube, wavelength scanning facilities covering the range 100 nm per 4.5 s–100 nm per 4.5 d and an *x-t* potentiometric recorder (1 mV–5 V) were used.

Reagents

Potassium bromate solution, 0.4 M. Dissolve 133.6080 g of $KBrO_3$ in 2 l of water.

Potassium bromide solution, 1 M. Dissolve 238.02 g of KBr in 2 l of water.

Hydrogen peroxide solution, 100 mM. Dilute 19.44 ml of 35% m/v H_2O_2 to 2 l with water.

Sodium carbonate solution, 0.5 M. Dissolve 105.99 g of Na_2CO_3 in 2 l of water. From this solution 1 l of 100 mM Na_2CO_3 solution was prepared.

Luminol solution, 1 mM. Dissolve 0.17716 g of luminol in 1 l of 100 mM Na_2CO_3 solution.

Nitric acid, 1 M. Dilute 128 ml of 70% m/m HNO_3 (sp.gr. 1.42) with water to 2 l in a calibrated flask.

Sulphuric acid, 1 M. Dilute 111 ml of 96% m/m H_2SO_4 (sp. gr. 1.84) with water in a 2-l calibrated flask.

Hydrochloric acid, 1 M. Dilute 176.50 ml of 35% m/m HCl (sp. gr. 1.18) with water in a 2-l calibrated flask.

Perchloric acid, 1 M. Dilute 173 ml of 70% m/m $HClO_4$ (sp. gr. 1.66) with water in a 2-l calibrated flask.

Phosphoric acid, 1 M. Dilute 136.5 ml of 85% m/m H_3PO_4 (sp. gr. 1.69) with water in a 2-l calibrated flask.

Acetic acid, 1 M. Dilute 115 ml of 99.5% m/m CH_3COOH (sp.gr. 1.05) with water in a 2-l calibrated flask.

Formic acid, 1 M. Dilute 76.3 ml of 99% m/m HCOOH (sp. gr. 1.22) with water in a 2-l calibrated flask.

Monochloroacetic acid, 1 M. Dissolve 23.625 g of $CH_2ClCOOH$ (98% pure) in water in a 250-ml calibrated flask.

Trichloroacetic acid, 1 M. Dissolve 40.8475 g of CCl_3COOH (98% pure) in water in a 250-ml calibrated flask.

Trifluoroacetic acid, 1 M. Dilute 19.14 ml of CF_3COOH (sp. gr. 1.49) with water in a 250-ml calibrated flask.

General Procedure

Fig. 1 shows a schematic diagram of the system used in which an acidic solution (60 μl) is injected through the sample loop into a stream of distilled water and the signal is recorded as a single symmetrical peak. A flow-rate of 2 ml min^{-1} was found to be optimum with respect to peak profile and the time for a single measurement. A 2-s output filter rise time was used, as this gave a better, smoother profile compared with a rise time of 20 or 200 ms.

Results

Effect of Reactant Concentrations

The reactants involved in this procedure include bromate, bromide, luminol and hydrogen peroxide. After a series of experiments, we chose the set-up shown in Fig. 1 in which a distilled water stream was employed at the acid injection

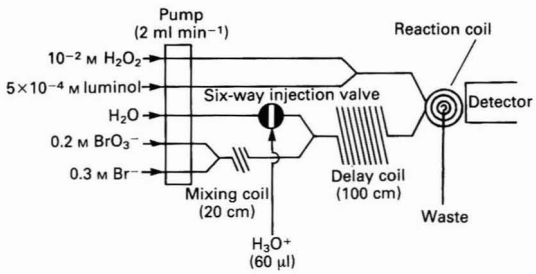

Fig. 1. Schematic diagram of the flow injection system used for the determination of oxonium ion based on chemiluminescence

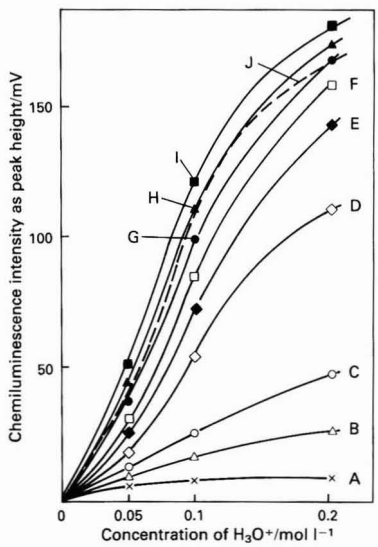

Fig. 2. Effect of bromide ion concentration on the chemiluminescence intensity. [H_2O_2], 1×10^{-2} M, [luminol], 1×10^{-5} M; and [$KBrO_3$], 100 mM. [Br^-]: A, 1; B, 5; C, 10; D, 50; E, 100; F, 150; G, 200; H, 250; I, 300; and J, 500 mM

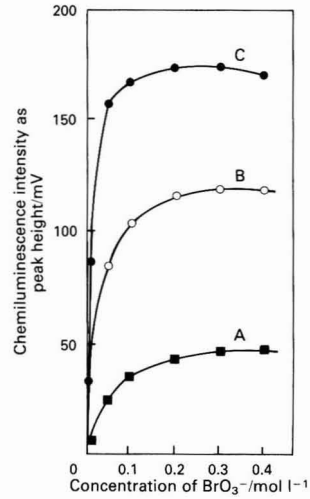

Fig. 3. Effect of bromate ion concentration on the chemiluminescence intensity. [KBr], 300 mM; [luminol], 1×10^{-5} M; and [H_2O_2], 1×10^{-2} M. Acid concentration: A, 50; B, 100; and C, 200 mM

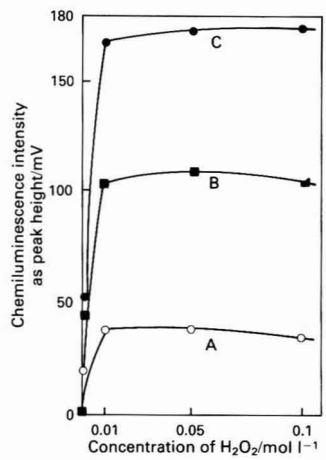

Fig. 4. Effect of H_2O_2 concentration on the chemiluminescence intensity. [KBr], 300 mM; [luminol], 1×10^{-5} M; and [$KBrO_3$], 200 mM. Acid concentration: A, 50; B, 100; and C, 200 mM

point. The reason for this was to overcome the inhomogeneity produced when the acid was injected directly into the BrO_3^- - Br^- stream. Therefore, the acid sample was injected into the distilled water line and was then mixed with the BrO_3^- - Br^- stream to produce bromine, allowing a delay time through the 100-cm coil. Three different acid concentrations were used, *viz.*, 50, 100 and 200 mM HNO_3, prepared by appropriate dilution of the stock solution. Each measurement was repeated four times at each reactant concentration. Polytetrafluoroethylene tubing (0.5 mm i.d.) was used throughout, except for the pump tubing which was made from silicone rubber.

Effect of bromide ion concentration

Solutions containing 1×10^{-2} M H_2O_2, 1×10^{-5} M luminol, 100 mM $KBrO_3$ and different bromide ion concentrations (1, 5, 10, 50, 100, 150, 200, 250, 300 and 500 mM) were prepared in 50-ml calibrated flasks. Distilled water produced no significant response. Fig. 2 shows the variation of chemiluminescence intensity, expressed as peak height in mV (average of four measurements), with the acid concentration at different bromide concentrations. A KBr concentration of 300 mM was chosen for optimum sensitivity and reproducibility. The broken line in Fig. 2 indicates the result obtained with 500 mM KBr, which was not chosen because of the deviation of the graph and the high concentration involved.

Effect of bromate ion concentration

Using 300 mM KBr (see above) and keeping the luminol and hydrogen peroxide concentrations at 1×10^{-5} and 1×10^{-2} M, respectively, solutions containing different bromate ion concentrations (10, 50, 100, 200, 300 and 500 mM) were prepared in 50-ml calibrated flasks. Higher concentrations were not studied owing to the low solubility of $KBrO_3$ in water. Fig. 3 shows the variation of chemiluminescence intensity, expressed as peak height in mV (average of four measurements), for each acid and bromate ion concentration. It can be seen that 200 mM $KBrO_3$ is the optimum concentration, taking into account the difficulty of dissolving higher concentrations of $KBrO_3$ with no increase in sensitivity.

Effect of hydrogen peroxide concentration

Using 300 mM KBr, 200 mM $KBrO_3$ and a luminol concentra-

tion of 1×10^{-5} M, solutions containing different H_2O_2 concentrations (10, 50 and 100 mM) were prepared in 50-ml calibrated flasks. Fig. 4 shows the variation of chemiluminescence intensity, expressed as peak height in mV (average of four measurements), with the H_2O_2 concentration. A zero concentration of H_2O_2 produced no signal. A 100 mM concentration of H_2O_2 was used.

Effect of luminol concentration

Using 300 mM KBr, 200 mM $KBrO_3$ and 100 mM H_2O_2, solutions containing different luminol concentrations (10^{-6}, 10^{-5}, 5×10^{-5}, 10^{-4}, 5×10^{-4} and 10^{-3} M) were prepared in 50-ml calibrated flasks using 100 mM Na_2CO_3 solution to complete the prepared solutions. Fig. 5 shows the variation of chemiluminescence intensity, expressed as the average peak height in mV ($n = 4$), with the luminol concentration using different acid solutions. The optimum sensitivity was obtained at 5×10^{-4} M luminol.

From these experiments the optimum reactant concentrations were found to be 300 mM KBr, 200 mM $KBrO_3$, 100 mM H_2O_2 and 5×10^{-4} M luminol in 100 mM Na_2CO_3 (see Fig. 1).

Effect of Delay Reaction Coil Length on the *in situ* Generation of Bromine

Delay reaction coil lengths (Fig. 1) of 100 and 60 cm gave successive increases in the chemiluminescence intensity of 200 and 160%, respectively, compared with direct attachment. Therefore, a 100-cm delay reaction coil was used for the complete generation of bromine in the first reaction.

Determination of Acids

Solutions containing various acid concentrations were prepared covering the range 0–200 mM (*viz.*, 0, 1, 5, 10, 15, 20, 25, 30, 35, 40, 45, 50, 60, 70, 80, 90, 100, 120, 140, 160, 180 and 200 mM). Each solution was prepared in a 50-ml calibrated flask using a 500 mM solution of each acid prepared by appropriate dilution of the acid stock solutions. Each concentration measurement was repeated four times, using different amplification settings and with 300 mM KBr, 200 mM $KBrO_3$, 5×10^{-4} M luminol prepared in 100 mM Na_2CO_3, 100 mM H_2O_2, a flow-rate of 2 ml min^{-1}, a 2-s output filter rise time at 417 nm, a 20-nm inlet slit width, a 5-nm outlet slit width and a 100-cm delay reaction coil. Fig. 6 shows the variation of chemiluminescence intensity, expressed as peak height in mV (average of four measurements), with the acid concentration over the range 0–0.2 M. Phosphoric, perchloric, nitric, sulphuric and hydrochloric acids gave an almost S-shaped curve. Results for concentrations greater than 200 mM are not included; it was found that peak broadening occurred at concentrations above 200 mM; hence the concentration was restricted to 0–0.2 M. Fig. 7 shows the results obtained for formic, acetic, α-chloroacetic, trichloroacetic and trifluoroacetic acids. Acetic acid showed no response in the range

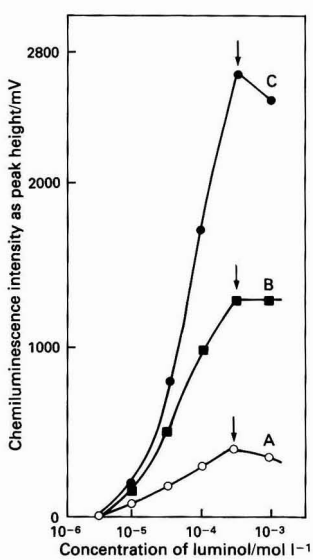

Fig. 5. Effect of luminol concentration on the chemiluminescence intensity. [KBr], 300 mM; [$KBrO_3$], 200 mM; [H_2O_2], 100 mM. Acid concentration: A, 50; B, 100; and C, 200 mM. The arrows indicate optimum concentrations

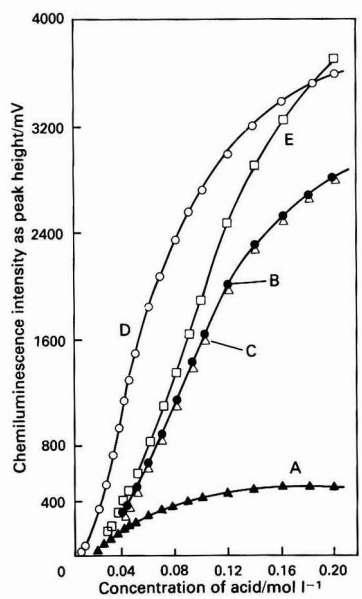

Fig. 6. Chemiluminescence intensity expressed as average peak height (mV) *versus* acid concentration (M). Acid: A, phosphoric; B, nitric; C, perchloric; D, sulphuric; and E, hydrochloric

Table 1. Linear regression analysis of the linear part of the calibration graph of log concentration (M) *versus* log chemiluminescence intensity (peak height in mV)

Linear regression analysis*	Acid							
	$CH_2ClCOOH$	H_3PO_4	CF_3COOH	HNO_3	H_2SO_4	HCl	$HClO_4$	CCl_3COOH
Linear range/M	0.02–0.08	0.02–0.09	0.03–0.14	0.03–0.16	0.015–0.16	0.03–0.18	0.03–0.14	0.03–0.16
Correlation coefficient	0.99	0.93	0.98	0.99	0.93	0.99	0.99	0.98
Slope/mV mol^{-1} l	1.52	2.02	1.05	1.73	1.68	1.58	1.82	2.05
Intercept	3.73	4.88	4.59	4.90	5.28	4.82	5.01	5.22

* Log chemiluminescence intensity (average peak height in mV) = slope × log concentration (M) + intercept.

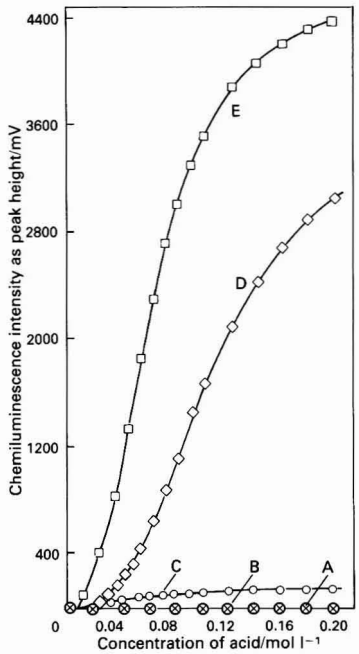

Fig. 7. Chemiluminescence intensity expressed as peak height (mV) *versus* acid concentration (M). Acid: A, formic; B, acetic; C, monochloroacetic; D, trichloroacetic; and E, trifluoroacetic

studied, whereas formic acid gave a weak response for concentrations of 100–200 mM [average response (x) = 6.0 mV (n = 4), coefficient of variation (CV) <0.5% for 100 mM; x = 7.2 mV (n = 4), CV <0.4% for 200 mM]. A graph of the logarithm of the chemiluminescence intensity *versus* the logarithm of the concentration was plotted for each acid. Table 1 gives the range of linearity for each acid together with the slopes and correlation coefficients obtained by linear regression analysis.

Discussion

The method described here is based on two reactions (Fig. 1). The first involves the *in situ* generation of bromine from $BrO_3^- - Br^- - H_3O^+$ in which the reaction is completed or almost completed in the delay reaction coil (dynamic system). The second involves the reduction of bromine by H_2O_2 to liberate oxygen, which is then used to oxidise luminol in alkaline medium (the main reaction), the reaction occurring before the solution reaches the detector. In this way the acid concentration is completely or almost completely consumed by the release of bromine; hence the oxidation of luminol in alkaline medium can be performed successively even though acids are initially involved in the reaction. Strongly ionisable acids can be determined rapidly and with good precision. Each acid gives a characteristic chemiluminescence intensity (single symmetrical peak) *versus* concentration graph; this can be attributed to the degree of ionisation of the acids used, *i.e.*, to the number of H_3O^+ ions produced by each acid. For example, nitric and perchloric acids give similar results, which also shows that ClO_4^- and NO_3^- ions have no effect on the emission intensity. Sulphuric acid contributes two hydrogen ions, *i.e.*, a first, strong ionisation followed by a second, weak ionisation ($K_a = 1.2 \times 10^{-2}$). For weakly ionisable acids the profile of the rise in the curves in Fig. 6 is inversely proportional to their pK_a values. For example, acetic acid ($pK_a = 4.75$) shows no response up to 200 mM, whereas formic acid ($pK_a = 3.75$) shows a weak response over the range 100–200 mM. Chloroacetic acid ($pK_a = 2.85$) shows a slight rise in the curve, whereas phosphoric acid ($pK_{a1} = 2.12$) shows an even greater rise in the profile of the curve, greater than that of chloroacetic acid. α-Substituted acetic acids show a rise in the curve (an increase in acidity) that is inversely proportional to the size of the halogen atom (the chlorine atom is larger than the fluorine atom) and to the bond length (C–F = 1.36 ± 0.03 Å; C–Cl = 1.766 ± 0.03 Å). This rise is directly proportional to the electronegativity (*e.g.*, $F^- : Cl^- : H^+ = 4 : 3 : 2.1$) and to the inductive effect. The effect of the fluorine atom on the ionisation of substituted acetic acids is greater than that of the chlorine atom. It was found that repeated determinations over a period of up to 4 months showed no change in the chemiluminescence intensity or shape of the curve for each acid. The reproducibility of all the measurements at the various concentrations tested is close to zero. All measurements were performed at 18 °C. During the preparation of the solutions, sufficient time was allowed for the heat of dilution to be dissipated. This ensured that there was no temperature effect on the rate of the reaction. Almost 90 successive measurements (injections) can be performed per hour. The minimum detectable concentrations in mM (peak heights in mV in parentheses) of the acids studied were as follows: HNO_3, 10 (8); $HClO_4$, 10 (4); H_2SO_4, 5 (7.2); HCl, 10 (8.0); H_3PO_4, 20 (12); $CH_2ClCOOH$, 20 (11.2); CCl_3COOH, 15 (10); and CF_3COOH, 4 (4.8). These values are relative to distilled water, which shows zero response using a 60-μl sample for each injection.

The authors thank the Arbil military hospital for their assistance and Dr. Farouk M. A. Shakir for helpful discussions.

References

1. Isacsson, U., and Wettermark, G., *Anal. Chim. Acta*, 1974, **68**, 339.
2. Paul, D. B., *Talanta*, 1978, **25**, 377.
3. Shakir, I. M. A., and Faizullah, A. T., *J. Univ. Kuwait (Sci.)*, submitted for publication.
4. Shakir, I. M. A., and Faizullah, A. T., *Analyst*, 1989, **114**, 951.

Paper 9/02043H
Received May 16th, 1989
Accepted July 26th, 1989

Supersonic Jet - Synchronous Scan Luminescence Spectrometry of Naphthalene Derivatives

Totaro Imasaka, Isao Maeno and Nobuhiko Ishibashi*
Faculty of Engineering, Kyushu University, Hakozaki, Fukuoka 812, Japan

Supersonic jet - synchronous scan luminescence (SSJ - SSL) spectrometry provides a simple spectrum, as a single component gives a single peak in most instances. In this approach resonance fluorescence from the zero-point level of the S_1 state is assumed to be dominant. However, there are some exceptions to this assumption. For example, naphthalene, the electronic transition of which is forbidden, provides strong vibronic bands in the spectrum. Even for a molecule such as naphthalene, SSJ - SSL spectrometry is considered to be useful for simplification of the spectrum, as only one or two major peaks are obtained. The method was applied to a dimethylnaphthalene mixture and a heat-exchange oil, which were supplied as unknown samples.

Keywords: *Supersonic jet spectrometry; synchronous scan luminescence spectrometry; laser fluorimetry; naphthalene derivative; heat-exchange oil*

Supersonic jet (SSJ) spectrometry provides sharp spectral features and is advantageous for the identification of chemical species.[1-3] However, it gives many spectral lines, making it very difficult to resolve each component in the spectrum of a mixture. The combination of SSJ spectrometry with gas or liquid chromatography (CHR) has been reported elsewhere[4-11]; however, the time in which the sample is flowing through the detector is limited to several seconds. Unfortunately, it is difficult to measure the excitation spectrum over such a short period of time. Therefore, only a molecule the excitation wavelength of which is known prior to the measurement, can be detected. This prevents the application of SSJ spectrometry to unknown chemical species.

Recently, supersonic jet - synchronous scan luminescence (SSJ - SSL) spectrometry was developed as an alternative to the CHR - SSJ technique.[12] This is simply a combination of two spectrometric methods, SSJ and SSL; however, it offers many advantages. Firstly, the spectrum is simple, as a single component gives a single peak corresponding to a 0-0 transition in most instances. This behaviour is similar to chromatography, but the separation/resolution is better by a factor of 10^4 in a theoretical plate. Secondly, the SSJ - SSL spectrum can be measured without any prior knowledge of the sample, as the excitation and fluorescence wavelengths are scanned simultaneously by adjusting them to the same value. On the other hand the excitation wavelength should be carefully adjusted in conventional SSJ spectrometry to one of the narrow spectral lines for recording the fluorescence spectrum. However, the excitation spectrum should be measured to determine the optimum excitation wavelength by adjusting the monochromator wavelength to one of the narrow lines in the fluorescence spectrum. Hence a trial and error approach is inevitable in conventional SSJ spectrometry, making it more difficult to apply this technique to an unknown sample.

However, SSJ - SSL spectrometry also has a disadvantage. In this approach the 0-0 transition peak is assumed to be strong. This assumption is correct for a rigid molecule in most instances, but is incorrect for a non-rigid molecule. There are, however, some exceptions. For example, naphthalene has a rigid structure, but the 0-0 transition peak is extremely small and strong vibronic transition peaks occur.[13-16] This is due to the forbidden nature of the S_1 - S_0 transition.[17,18] The first and third excited singlet states have a $^1B_{3u}$ symmetry and the S_1 - S_0 transition moment disappears with configuration interaction, *i.e.*, the mixing of electronic states with the same symmetry group to produce different symmetries. This is known as accidental cancellation of the transition moment, as this transition is originally symmetry allowed. Further configuration interaction results in a non-zero S_1 - S_0 transition moment ($f = 0.001$, where f is the oscillator strength) and vibronically induced bands of b_{1g} or a_{1g} symmetry appear; band b_{1g} gains intensity by vibronic coupling with the nearby S_2 $^1B_{2u}$ ($f = 0.26$, $\Delta E = 3900$ cm^{-1}, where ΔE is the energy separation between the electronic states) and band a_{1g} from S_3 ($f = 2$, $\Delta E = 16\,000$ cm^{-1}).[18] Therefore, vibronic bands are dominant in the spectrum of naphthalene. Hence there is a need to re-investigate the advantages of SSJ - SSL spectrometry to determine whether this technique is useful for such a molecule.

In this work the SSJ - SSL spectra and conventional excitation spectra of naphthalene and eight methyl-substituted naphthalenes have been measured. The spectral features, particularly the intensity of the 0 - 0 transition relative to the other vibronic transitions, were compared for these molecules. The correlation between the spectral features and the molecular structure is also discussed. In addition, the application of SSJ - SSL spectrometry to real samples, such as a dimethylnaphthalene mixture and a heat-exchange oil, is described.

Experimental

Apparatus

A schematic diagram of the apparatus is shown in Fig. 1. The sample is placed in the reservoir and the temperature is controlled by housing the arrangement in the chamber of a gas chromatograph (Shimadzu, GC-8A). The vaporised sample is

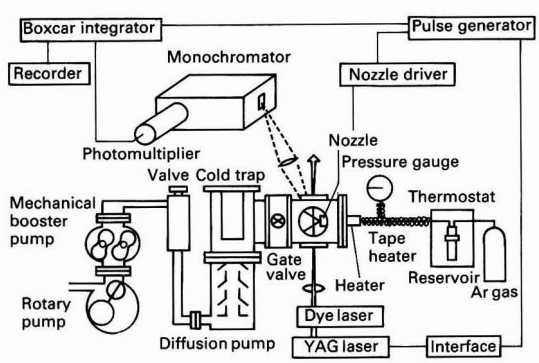

Fig. 1. Schematic diagram of the experimental apparatus

* To whom correspondence should be addressed.

introduced from a pulsed supersonic jet nozzle[19] into a 6-in chamber, which is evacuated using a vacuum system described elsewhere.[20] The chemical species in the supersonic jet is excited by a dye laser (Quantel, TDL50) pumped by the second harmonic of an Nd:YAG laser (Quantel, YG581C-20). The dye laser frequency is doubled by an autotracking system (Quantel, UVX-2, DCC-2). The harmonic emission is separated from the fundamental beam by a quartz prism, and the beam walk-off, caused by a change in the wavelength, is corrected by a laboratory-built prism autotracking system.[21] The laser beam is focused 10 mm away from the supersonic jet nozzle and the fluorescence is measured by a monochromator (CT-100) equipped with an optional grating (400 grooves mm^{-1}, 300-nm blaze). The monochromator wavelength is synchronised with the dye laser wavelength using a stepping motor attached to the monochromator, which is driven by a laboratory-built pulse generator. The fluorescence signal from a photomultiplier (Hamamatsu, R928) is fed to a boxcar integrator (Stanford Research Systems, SR250).

Naphthalene derivatives have fairly long lifetimes and a time-resolved fluorescence detection system was used for rejection of light scatter from the exciting source. The delay and gate times were adjusted to 0.2 and 1 μs, respectively.

Reagents

Naphthalene was obtained from Kanto Chemicals, 1-methylnapthalene, 2-methylnaphthalene, 1,2-dimethylnaphthalene and 2,6-dimethylnaphthalene from Tokyo Kasei Kogyo and 1,3-dimethylnaphthalene, 1,4-dimethylnaphthalene, 1,5-dimethylnaphthalene and 1,8-dimethylnaphthalene from Wako Pure Chemical Industries. The dimethylnaphthalene mixture, the composition of which was unknown, was purchased from Tokyo Kasei Kogyo. The heat-exchange oil was a gift from Soken Kagaku, and was known to be a mixture of naphthalene derivatives. The laser dye used in most of the experiments was 4-dicyanomethylene-2-methyl-6-(*p*-dimethylaminostyryl)-4*H*-pyran (DCM), which was supplied by Exciton Chemical as a laser-grade dye.

Results and Discussion

Naphthalene

The SSJ - SSL spectrum of naphthalene is shown in Fig. 2, together with an excitation spectrum for comparison. A single peak appears in the SSJ - SSL spectrum, which corresponds to the $\bar{8}_0^1$ transition of naphthalene, according to the notation given by Stockburger *et al.*[22] On the other hand several peaks are present in the conventional excitation spectrum. It can be seen that the signal intensity for the 0 - 0 peak is extremely small for naphthalene in the SSJ - SSL spectrum; this is in contrast to other large planar molecules such as anthracene derivatives.[12] This spectral feature is ascribed to a small transition moment between the S_1 and S_0 states and to the necessity for vibronic coupling for the signal to appear. It can also be seen that the SSJ - SSL spectrum is somewhat simpler than the conventional SSJ spectrum even for a molecule such as naphthalene which gives strong vibronic bands. This might be attributed to "a double filter effect" in SSJ - SSL spectrometry; a small signal peak observed in the excitation spectrum is reduced further by a fluorescence isolation process, due to a small Franck - Condon factor.

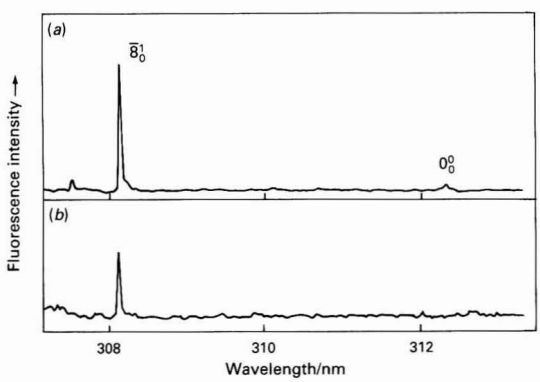

Fig. 2. Supersonic jet spectra of naphthalene. (*a*) Conventional excitation spectrum ($\lambda_{em.}$ = 317.3 nm); and (*b*) synchronous scan luminescence spectrum

Monomethylnaphthalenes

Spectral simplification is more clearly demonstrated for the monomethylnaphthalenes, as shown in Figs. 3 and 4. Basically, only a single peak is observed in the SSJ - SSL spectrum, whereas many signal peaks appear in the conventional SSJ excitation spectrum. It can be seen that the signal corresponding to the 0 - 0 transition is predominant only in the spectrum of 2-methylnaphthalene. On the other hand a strong vibronic transition is seen in the spectrum of 1-methylnaphthalene. Mirror symmetry breakdown is known to occur for 2-methylnaphthalene, which is ascribed to the Duschinsky effect and to vibronically induced anharmonicity.[23–25] The simplicity of the SSJ - SSL spectrum of 2-methylnaphthalene can be partly attributed to this effect.

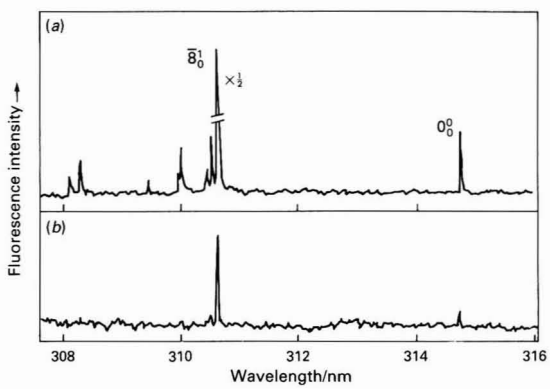

Fig. 3. Supersonic jet spectra of 1-methylnaphthalene. (*a*) Conventional excitation spectrum ($\lambda_{em.}$ = 320.0 nm); and (*b*) synchronous scan luminescence spectrum

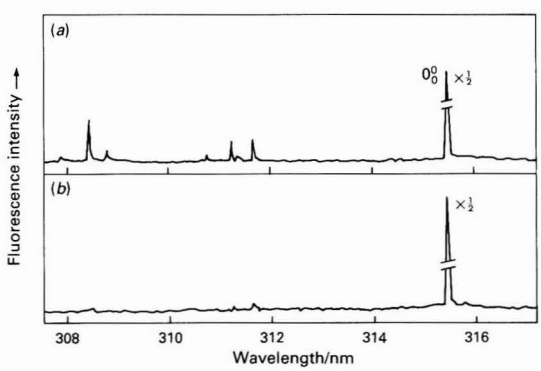

Fig. 4. Supersonic jet spectra of 2-methylnaphthalene. (*a*) Conventional excitation spectrum ($\lambda_{em.}$ = 330.0 nm); and (*b*) synchronous scan luminescence spectrum

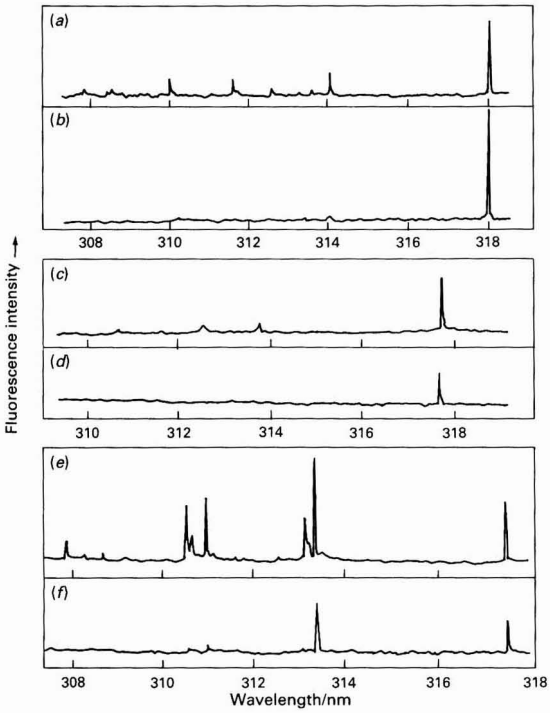

Fig. 5. Supersonic jet spectra. (*a*) Conventional excitation spectrum ($\lambda_{em.}$ = 332.1 nm) and (*b*) synchronous scan luminescence spectrum of 1,2-dimethylnaphthalene. (*c*) Conventional excitation spectrum ($\lambda_{em.}$ = 331.7 nm) and (*d*) synchronous scan luminescence spectrum of 1,3-dimethylnaphthalene. (*e*) Conventional excitation spectrum ($\lambda_{em.}$ = 321.9 nm) and (*f*) synchronous scan luminescence spectrum of 1,4-dimethylnaphthalene

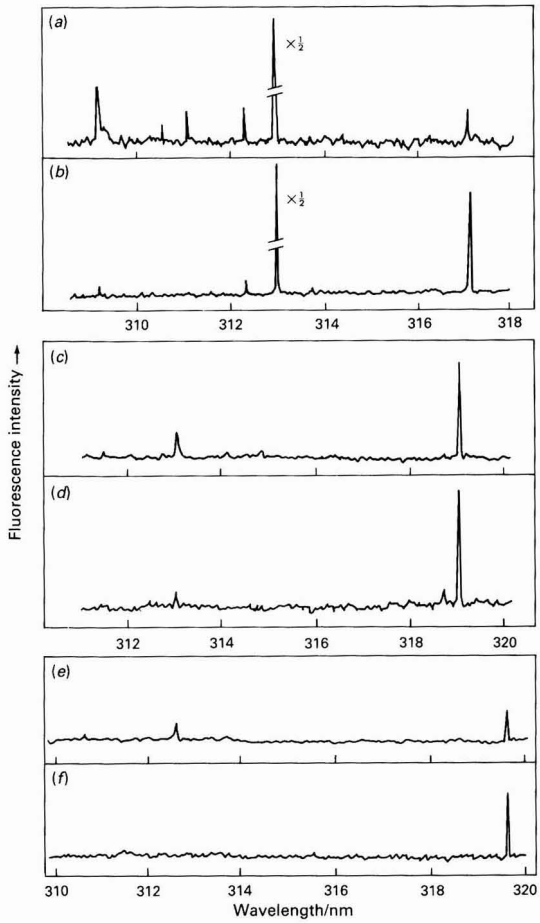

Fig. 6. Supersonic jet spectra. (*a*) Conventional excitation spectrum ($\lambda_{em.}$ = 322.1 nm) and (*b*) synchronous scan luminescence spectrum of 1,5-dimethylnaphthalene. (*c*) Conventional excitation spectrum ($\lambda_{em.}$ = 324.7 nm) and (*d*) synchronous scan luminescence spectrum of 1,8-dimethylnaphthalene. (*e*) Conventional excitation spectrum ($\lambda_{em.}$ = 334.1 nm) and (*f*) synchronous scan luminescence spectrum of 2,6-dimethylnaphthalene

Dimethylnaphthalenes

Supersonic jet spectra of the dimethylnaphthalenes are shown in Figs. 5 and 6. Only one or two major peaks appear in the SSJ - SSL spectrum, and the spectral features are much simpler than those in the conventional SSJ excitation spectrum. It should be noted that the ratio of the 0 - 0 peak to the 8_0^1 peak is strongly affected by the position of the methyl substituents in the naphthalene ring. The ratio increases in the order 1,3-, 2,6- > 1,2-, 1,8- > 1,4- > 1.5-dimethylnaphthalene. The structures of the spectra are shown schematically in Fig. 7. It is interesting to note that a molecule with a methyl group in the β-position gives a strong 0 - 0 peak. This is most clearly shown in the spectrum of 2,6-dimethylnaphthalene. However, there is an exception, *i.e.*, 1,8-dimethylnaphthalene. The reason is unknown at present, but a possible explanation might be provided by the planar symmetry of the molecule; the naphthalene derivatives with a methyl group at the β-position are planar and non-symmetrical in the ground state and this situation is identical in 1,8-dimethylnaphthalene because of the repulsion between the two methyl groups. However, further investigations might be necessary to confirm this possibility.

Real Samples

The SSJ - SSL spectrum of a dimethylnaphthalene mixture was measured to ascertain the advantages of SSJ - SSL spectrometry. The spectrum is shown in Fig. 8. Three dimethylnaphthalene isomers can clearly be seen, and 1- and 2-methylnaphthalene are present as impurities. Several unassigned peaks are also present in the spectrum. It should be noted that these unassigned peaks do not originate from the weak signals observed in the standard spectra; this was confirmed by careful comparison of the peak positions with the standards. Hence these peaks must be due to other chemical species. As 1,6-, 1,7-, 2,3- and 2,7-dimethylnaphthalene are not commercially available, a firm conclusion is difficult at present. However, these peaks are probably not due to 2,3- and 2,7-dimethylnaphthalene, as these compounds have two methyl groups at the β-position, *cf.* 2,6-dimethylnaphthalene, which would give a strong 0 - 0 peak above 319 nm. It is also difficult to envisage that the peaks are due to 1,6- and 1,7-dimethylnaphthalene. These compounds have a methyl group at the α-position and would give a weak resonance fluorescence peak at *ca.* 315 nm; however, they should give a stronger 0 - 0 transition peak at *ca.* 318 nm simultaneously. Therefore, these peaks are considered to originate from other chemical species, *e.g.*, tri- or tetramethylnaphthalenes.

A database is very useful in SSJ - SSL spectrometry because it yields only one or two spectral peaks the parameters of

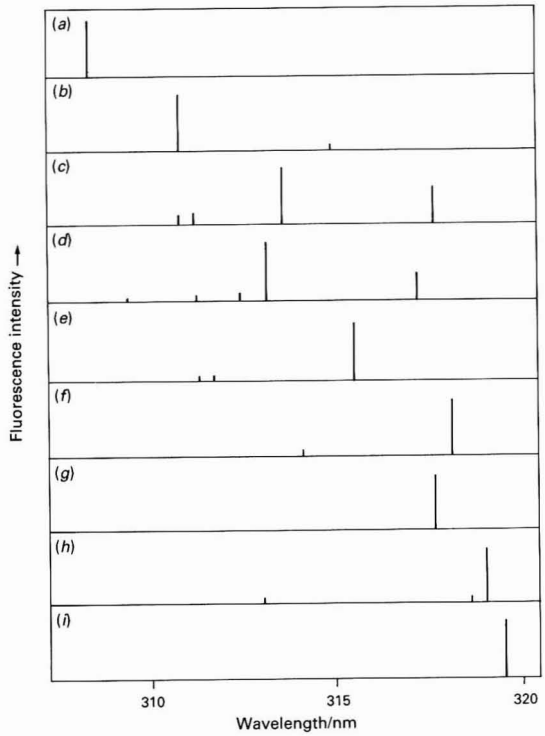

Fig. 7. Schematic SSJ - SSL spectra of the naphthalene derivatives obtained by simplifying the results shown in Figs. 2–6. (*a*) Naphthalene; (*b*) 1-methylnaphthalene; (*c*) 1,4-dimethylnaphthalene; (*d*) 1,5-dimethylnaphthalene; (*e*) 2-methylnaphthalene; (*f*) 1,2-dimethylnaphthalene; (*g*) 1,3-dimethylnaphthalene; (*h*) 1,8-dimethylnaphthalene; and (*i*) 2,6-dimethylnaphthalene

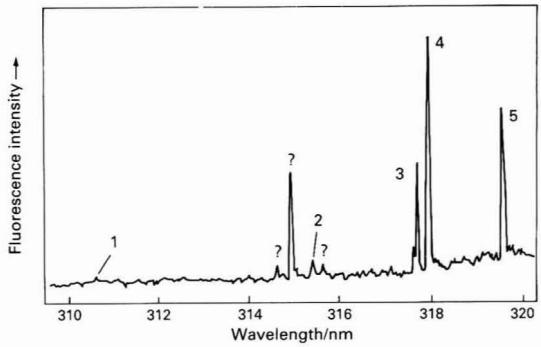

Fig. 8. SSJ - SSL spectrum of a mixture of dimethylnaphthalenes. 1, 1-Methylnaphthalene; 2, 2-methylnaphthalene; 3, 1,3-dimethylnaphthalene; 4, 1,2-dimethylnaphthalene; and 5, 2,6-dimethylnaphthalene. The peaks marked ? represent unassigned peaks

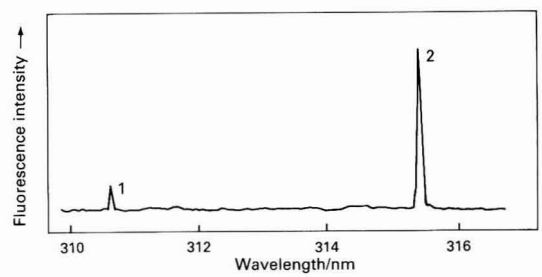

Fig. 9. SSJ - SSL spectrum of a heat-exchange oil. 1, 1-Methylnaphthalene; and 2, 2-methylnaphthalene

which are accurately determined. Once such a database has been compiled in tabular form, the unknown signal peaks in Fig. 8 should easily be assigned. The wavelengths for the 0 - 0 transition have been summarised in tabular form.[26] However, our results indicate that resonance fluorescence from high vibrational levels of the excited state is sometimes dominant, particularly when the S_1 - S_0 electronic transition is originally forbidden and partly vibronically allowed. Therefore, care must be taken in constructing the database.

The application of SSJ - SSL spectrometry to a heat-exchange oil is shown in Fig. 9. The spectrum consists of two sharp peaks, which are readily assigned to 1- and 2-methylnaphthalene from the data for the standards.

Application to Other Chemical Species

Supersonic jet - synchronous scan luminescence spectrometry has a distinct advantage over conventional SSJ spectrometry with respect to spectral simplicity. This is useful in the analysis of a sample containing many isomers, as demonstrated above. For example, polychlorinated biphenyls (PCBs) are highly carcinogenic, like the dioxins, and occur at levels two orders of magnitude higher in the environment.[27] Many SSJ studies have already been performed on biphenyl and its derivatives using a combination of SSJ spectrometry with multi-photon ionisation, fluorescence and phosphorescence detection.[28–31] As PCB has 207 isomers and their carcinogenicities are very different, this might offer a means of demonstrating the advantages of SSJ - SSL spectrometry. However, it is difficult to observe the SSJ - SSL spectrum of unsubstituted and *para*-substituted PCBs due to a large configurational change between the ground (twisted) and excited (planar) states.[32] As described above, the SSJ - SSL technique is useful for a rigid molecule. However, it should be noted that highly chlorinated PCBs with an even higher carcinogenicity have a coplanar structure. Hence it is possible to determine harmful PCBs selectively by SSJ - SSL spectrometry, although the rate of inter-system crossing might increase with an increase in the number of chlorine atoms in the molecule. However, this work was not carried out because of the highly carcinogenic nature of PCB.

Polychlorinated naphthalenes (PCNs) are also known to be highly carcinogenic compounds. A group of these isomers might be measured by SSJ - SSL spectrometry, as monochlorinated naphthalenes have already been measured by SSJ spectrometry[18] and have a rigid and planar structure. However, PCNs are extremely toxic and are not commercially available; therefore, they were not used in this work. For application to real samples, the development of an instrument or procedure that is applicable to highly toxic samples is required. Such a spectrometric approach should allow spectral measurements using a limited amount of sample and the safe recovery of the remaining chemicals in the nozzle or reservoir. A recently proposed method using a laser ablation technique might be useful for overcoming this problem.[33]

This research was supported by a Grant-in-Aid for Scientific Research from the Ministry of Education, Japan, and by the Nissan and Kurata Foundations.

References

1. Hayes, J. M., and Small, G. J., *Anal. Chem.*, 1983, **55**, 565A.
2. Johnston, M. V., *Trends Anal. Chem.*, 1984, **3**, 58.

3. Lubman, D. M., *Anal. Chem.,* 1987, **59**, 31A.
4. Imasaka, T., Shigezumi, T., and Ishibashi, N., *Analyst,* 1984, **109**, 277.
5. Imasaka, T., Okamura, T., and Ishibashi, N., *Anal. Chem.,* 1986, **58**, 2152.
6. Imasaka, T., Tashiro, K., and Ishibashi, N., *Anal. Chem.,* 1986, **58**, 3242.
7. Hayes, J. M., and Small, G. J., *Anal. Chem.,* 1982, **54**, 1202.
8. Pepich, B. V., Callis, J. B., Danielson, J. D. S., and Gouterman, M., *Rev. Sci. Instrum.,* 1986, **57**, 878.
9. Pepich, B. V., Callis, J. B., Burnes, D. H., Gouterman, M., and Kalman, D. A., *Anal. Chem.,* 1986, **58**, 2825.
10. Stiller, S. W., and Johnston, M. V., *Anal. Chem.,* 1987, **59**, 567.
11. Imasaka, T., Tanaka, K., and Ishibashi, N., *Anal. Sci.,* 1988, **4**, 31.
12. Imasaka, T., Tsukamoto, A., and Ishibashi, N., *Anal. Chem.,* 1988, **60**, 1362.
13. Beck, S. M., Powers, D. E., Hopkins, J. B., and Smalley, R. E., *J. Chem. Phys.,* 1980, **73**, 2019.
14. Beck, S. M., Hopkins, J. B., Powers, D. E., and Smalley, R. E., *J. Chem. Phys.,* 1981, **74**, 43.
15. Behlen, F. M., and Rice, S. A., *J. Chem. Phys.,* 1981, **75**, 5672.
16. Behlen, F. M., McDonald, D. B., Sethuraman, V., and Rice, S. A., *J. Chem. Phys.,* 1981, **75**, 5685.
17. Dewar, M. J. S., and Longuet-Higgins, H. C., *Proc. Phys. Soc. London, Sect. A.,* 1954, **67**, 795.
18. Jacobson, B. A., Guest, J. A., Novak, F. A., and Rice, S. A., *J. Chem. Phys.,* 1987, **87**, 269.
19. Imasaka, T., Okamura, T., and Ishibashi, N., *Anal. Chem.,* 1986, **58**, 2152.
20. Imasaka, T., Fukuoka, H., Hayashi, T., and Ishibashi, N., *Anal. Chim. Acta,* 1984, **156**, 111.
21. Kawasaki, S., Imasaka, T., and Ishibashi, N., *Opt. Commun.,* 1988, **66**, 285.
22. Stockburger, M., Gattermann, H., and Klusmann, W., *J. Chem. Phys.,* 1975, **63**, 4519.
23. Warren, J. A., Hayes, J. M., and Small, G. J., *J. Chem. Phys.,* 1984, **80**, 1786.
24. Warren, J. A., Hayes, J. M., and Small, G. J., *Chem. Phys.,* 1986, **102**, 313.
25. Ichimura, T., Auty, A. R., Jones, A. C., and Phillips, D., *J. Spectrosc. Soc. Jpn.,* 1985, **34**, 83.
26. Imasaka, T., Sakaki, K., and Ishibashi, N., *Chemometrics Intell. Lab. Syst.,* in the press.
27. Tachikawa, R., *Kagaku (Kyoto)*, 1986, **41**, 540.
28. Murakami, J., Ito, M., and Kaya, K., *J. Chem. Phys.,* 1981, **74**, 6505.
29. Takei, Y., Yamaguchi, T., Osamura, Y., Fuke, K., and Kaya, K., *J. Phys. Chem.,* 1988, **92**, 577.
30. Suzuki, T., Sato, M., Mikami, N., and Ito, M., *Chem. Phys. Lett.,* 1986, **127**, 292.
31. In, H., and Bernstein, E. R., *J. Chem. Phys.,* 1988, **88**, 7337.
32. Imamura, A., and Hoffmann, R., *J. Am. Chem. Soc.,* 1968, **90**, 5379.
33. Imasaka, T., Tashiro, K., and Ishibashi, N., *Anal. Chem.,* 1989, **61**, 1530.

Paper 9/01207I
Received March 21st, 1989
Accepted July 17th, 1989

Titrimetric Determination of Gold in Some Pharmaceutical Preparations*

Biljana F. Abramović
Institute of Chemistry, Faculty of Sciences, University of Novi Sad, Dr. Ilije Djuričića 4, YU-21000 Novi Sad, Yugoslavia

Mitar M. Marinković
Military Medical Centre, YU-21000 Novi Sad, Yugoslavia

Ferenc F. Gaál†
Institute of Chemistry, Faculty of Sciences, University of Novi Sad, Dr. Ilije Djuričića 4, YU-21000 Novi Sad, Yugoslavia

Two titrimetric methods based on derivative potentiometry and catalytic controlled-current potentiometry were developed to determine the content of some gold compounds as gold in pharmaceutical preparations using potassium iodide solution as titrant. A negatively polarised glassy carbon indicator electrode, and the Ce^{IV} - As^{III} system in the presence of sulphuric acid as an indicator reaction, served to monitor the catalytic titrations. The same glassy carbon electrode was also used in the derivative potentiometric titrations. Particular attention was paid to sample decomposition. Contents of gold of about 30 μg ml^{-1} were determined with a relative standard deviation of less than 1.4%. The results showed satisfactory agreement with those of comparative methods.

Keywords: *Gold pharmaceutical preparation; catalytic titration; derivative potentiometric titration; potassium iodide as titrant; cerium(IV) - arsenic(III) indicator reaction*

In the last 30 years, organic compounds of gold have been used increasingly in the treatment of rheumatoid arthritis.[1] For this purpose in Yugoslavia, the following gold compounds are used: gold(I) thioglucose [(1-thio-D-glucopyranosato)gold(I), $C_6H_{11}AuO_5S$, relative molecular mass, M_r, 392.18], gold(I) sodium thiomalate [(disodium mercaptosuccinato)gold(I), $C_4H_3AuNa_2O_4S$, M_r 390.12] and auranofin [(1-thio-β-D-glucopyranosato)(triethylphosphine)gold(I) 2,3,4,6-tetraacetate, $C_{20}H_{34}AuO_9PS$, M_r 678.48].

Several methods have been reported for the determination of the content of organic gold compounds in pharmaceutical preparations, namely neutron activation analysis,[2,3] spectrophotometry[4] and gravimetry.[5,6] However, the procedures are either time consuming[4–6] or require sophisticated equipment.[2,3] For this reason, and as part of a wider study of the determination of metals in pharmaceuticals,[7,8] the present work was aimed at developing a fast, simple method for the determination of the above-mentioned gold compounds as gold in pharmaceutical preparations. For this purpose a titrimetric method with potassium iodide as titrant was employed, using derivative potentiometry and catalytic controlled-current potentiometry to follow the course of the titration. These titrimetric methods have been used effectively for the analysis of pure gold-containing compounds.[9]

In these catalytic titrations, a solution of gold(III) is titrated with a solution of potassium iodide in the presence of components of the indicator reaction Ce^{IV} - As^{III}.[9] In the course of the titration, the following reactions take place almost simultaneously:

$$Au^{III} + 3I^- \rightleftharpoons AuI(s) + I_2 \quad .. \quad .. \quad (1)$$

$$I_2 + As^{III} \rightleftharpoons 2I^- + As^V \quad .. \quad .. \quad (2)$$

Obviously, the iodide and gold(III) react in a ratio of 1 : 1. In parallel with these reactions the reaction catalysed by iodide takes place.

$$2Ce^{IV} + As^{III} \rightleftharpoons 2Ce^{III} + As^V \quad .. \quad .. \quad (3)$$

As the iodide concentration in the titrated solution before the equivalence point is very small, the rate of reaction (3) is very slow. However, after the equivalence point the titrant reacts catalytically; hence a small excess of titrant produces large changes in the rate of the indicator reaction. As a result, abrupt changes in the concentration of the indicator reaction components, *i.e.*, in the potential, take place, which can easily be detected by controlled-current potentiometry.

On the other hand, in the derivative potentiometric titrations, which are carried out in the absence of the indicator reaction components, the iodide and gold(III) react in a ratio of 3 : 1 [only reaction (1) takes place].

Experimental

Reagents and Samples

All chemicals used were of analytical-reagent grade. Solutions were prepared with doubly distilled water.

The gold content was determined in the following pharmaceutical preparations: Auropan tablets (Krka, Novo Mesto, Yugoslavia), 3 mg of auranofin per tablet; Tauredon ampoules (Byk Gulden, Konstanz, FRG), 50 mg of gold(I) sodium thiomalate per injection; and Solganol B oleosum ampoules (Schering, Berlin, FRG), 0.1 and 1.0 g of gold(I) thioglucose per injection.

Standard potassium iodide solution, 6.0×10^{-3} M. Standardised by automatic potentiometric titration with silver nitrate obtained by dissolving metallic silver in nitric acid. A silver electrode was used as the indicator electrode.

Arsenic(III) solution, 0.15 M *and cerium(IV) solution*, 8×10^{-2} M. Prepared as described previously.[9]

Apparatus

The course of the catalytic titrations was monitored by controlled-current potentiometry ($I = 2$ μA) with a negatively polarised glassy carbon (GC) indicator electrode (Sigri Elektrographit 2400, with a laboratory-made disc of surface area 0.07 cm^2) in conjunction with an Iskra saturated calomel electrode (SCE). After each measurement the electrode was polished with alumina powder wetted with water.

* Presented in part at the XI Meeting of the Chemists of Croatia, Zagreb, Yugoslavia, February 13–15, 1989.

† To whom correspondence should be addressed.

In the derivative potentiometric titrations the same pair of electrodes coupled to a Radiometer PHM62 standard pH meter through a suitable resistance - capacitance (*RC*) circuit (R = 10 kΩ, C = 440 μF) served as the indicator electrode.

The titrant was added continuously from a Radiometer ABU 12 automatic piston burette at an optimum rate of 0.142 ml min^{-1} (for catalytic titration) and 0.284 ml min^{-1} (for derivative potentiometric titration). Titration curves were recorded by means of a chart recorder (Goerz-Electro Servogor S RE-541 and Servogor 2S RE-571). The reaction vessel and electrodes were washed with doubly distilled water.

Recommended Procedure

The procedure was the same for both catalytic and derivative potentiometric titrations, except that in the latter instance no indicator reaction components were added.

Auropan tablets

After homogenisation of 50 Auropan tablets by grinding in a mortar, the following procedure was used. Weigh about 0.3 g (to an accuracy of 0.01 mg) of the homogenised powder, which corresponds to the mass of one Auropan tablet, and place in a 50-ml reaction vessel. Add 0.5 ml of aqua regia and 1.0 ml of water. After evaporation (water-bath) to half of the initial volume add 4.0 ml of 4 M sulphuric acid, 1.0 ml of Ce^{IV} solution and 0.4 ml of As^{III} solution and dilute the contents to 30 ml with water. Titrate the reaction mixture with the standard solution of potassium iodide.

Tauredon ampoules

Two solutions of the preparations were made.

Solution I. The contents of two ampoules, each containing 50 mg of gold(I) sodium thiomalate, were transferred quantitatively into a 50-ml calibrated flask and diluted to volume with water.

Solution II. A 10.00-ml aliquot of solution I was placed in a 50-ml calibrated flask and diluted to volume with water.

The titration procedure was as follows. Place 5.00 ml of solution II in a 50-ml beaker and evaporate on a water-bath to dryness. After dissolving the dry residue in 0.3 ml of aqua regia and heating the solution for a short time (about 1 min) on a water-bath, add 4.0 ml of 4 M sulphuric acid, 1.0 ml of Ce^{IV} solution and 0.4 ml of As^{III} solution and dilute the contents to 30 ml with water. Titrate the reaction mixture with the standard solution of potassium iodide.

Solganol B oleosum ampoules

Four solutions of the preparation were prepared.

Solution III. After de-oiling with acetone,[6] the contents of one ampoule [5 ml of a 20% suspension of gold(I) thioglucose] were transferred quantitatively into a 250-ml calibrated flask and diluted to volume with water.

Solution IV. A 25.00-ml aliquot of solution III was placed in a 250-ml calibrated flask and diluted to volume with water.

Solution V. The contents of two ampoules [5 ml of a 2% suspension of gold(I) thioglucose] (after de-oiling) were transferred quantitatively into a 200-ml calibrated flask and diluted to volume with water.

Solution VI. A 20.00-ml aliquot of solution V was placed in a 50-ml calibrated flask and diluted to volume with water.

The titration procedure was as follows. Take 5.00 ml of solution IV, or solution VI, in a 50-ml beaker and evaporate on a water-bath to dryness. Then proceed as described above for the Tauredon ampoules.

Solutions I, III and V are employed in the gravimetric determinations.

The end-point of the catalytic titration was determined graphically from the intersection of straight-line extrapolations before and after the equivalence point or from the maximum of the derivative titration curve. The results were corrected for the blank.

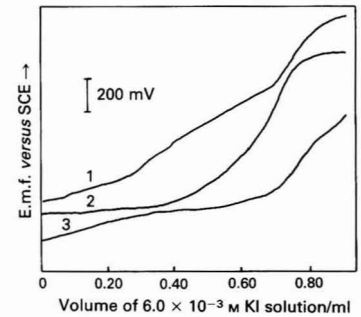

Fig. 1. Effect of HNO_3 concentration on the shape of the catalytic potentiometric [GC(−) - SCE(+)] (I = 2 μA) titration curves in the determination of the auranofin content as Au^I in Auropan tablets: 1, 2.3 M HNO_3 (mass of auranofin 2.866 mg); 2, 1.4 M HNO_3 (mass of auranofin 2.751 mg); and 3, 0.46 M HNO_3 (mass of auranofin 2.747 mg)

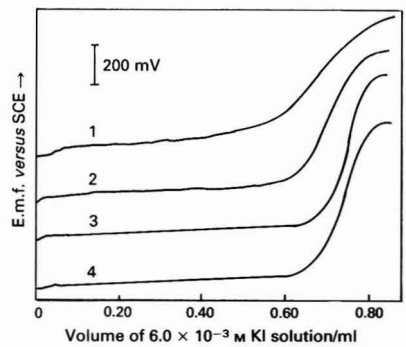

Fig. 2. Effect of volume of aqua regia on the shape of the catalytic potentiometric [GC(−) - SCE(+)] (I = 2 μA) titration curves in the determination of the auranofin content as Au^I in Auropan tablets. Volume of aqua regia: 1, 5.0 ml (mass of auranofin 2.866 mg); 2, 1.0 ml (mass of auranofin 2.864 mg); 3, 0.5 ml (mass of auranofin 2.654 mg); and 4, 0.3 ml (mass of auranofin 2.577 mg)

Results and Discussion

Optimisation of Conditions

It was found that mineralisation of all three samples before titration was necessary. The titration of samples that had not been mineralised resulted in titration curves that could not be used because of their poor reproducibility (in the analysis of Auropan tablets and Tauredon ampoules) and because of the completion of the Ce^{IV} - As^{III} indicator reaction at the beginning of the titration (in the analysis of Solganol B oleosum ampoules), so that a blank was almost obtained. For this reason, the first step was to find the best procedure for mineralisation of each of the three samples. For example, in the analysis of Auropan tablets it was found that the mineralisation of auranofin with nitric acid (in the concentration range 0.46–2.3 M HNO_3) did not give satisfactory results (Fig. 1, curves 1–3) as the shape of the titration curve obtained was not suitable for the determination of the end-point. In addition, it can be seen that the changes in potential before the equivalence point were more pronounced for the higher concentrations of nitric acid. If, however, the mineralisation was carried out with hydrogen peroxide followed by evapora-

tion to dryness, there was no change in potential during the titration. For this reason the possibility of mineralisation of auranofin with aqua regia was investigated. It was found that the effect of mineralisation at room temperature was negligible as the shape of the titration curve was almost identical with that obtained with no mineralisation of the sample. However, if the reaction mixture was heated to reduce the volume by half, the shape of the titration curve obtained was much more suitable for the determination of the end-point (Fig. 2). Further, it was observed that the amount of aqua regia added influenced the shape and length of the titration curve; hence the volume of aqua regia used had to be optimised. As can be seen from Fig. 2, if this volume was larger than 1.0 ml (curve 1), the shape and length of the titration curve were not suitable for the determination. Further, if the volume of aqua regia was greater than 0.5 ml (curve 2), the results were lower than expected; hence 0.5 ml was chosen as the optimum volume (curve 3).

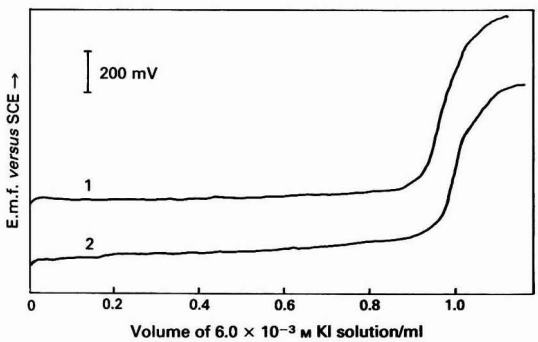

Fig. 3. Typical catalytic potentiometric [GC(−) - SCE(+)] (I = 2 μA) titration curves obtained in the determination of 1, 2.079 mg of gold(I) thiomalate in Tauredon ampoules; and 2, 2.154 mg of gold(I) thioglucose in Solganol B oleosum ampoules as Au^{I}

Similar results were obtained for the optimisation of the mineralisation procedure for gold(I) thioglucose and gold(I) sodium thiomalate. Typical titration curves are shown in Fig. 3. It should be noted that almost identical titration curves were obtained irrespective of whether the solution was evaporated to half its original volume before or after the addition of aqua regia, or whether the aqua regia was added after evaporation of the reaction mixture to dryness. The third possibility was chosen as it gave the most well defined reaction conditions.

The same mineralisation procedure was also used in the derivative potentiometric titrations.

Further, as described previously,[9] two procedures for derivative potentiometric titration were employed [(*i*) titration in the absence of both components of the indicator reaction; and (*ii*) in the absence of Ce^{IV} only]. In the present work, we tested these procedures for the determination of gold in pharmaceutical preparations. In the first instance, the shape of the titration curves obtained made them suitable for the determination of the end-point (Fig. 4). In the second

Table 1. Results of the determination of auranofin as gold in Auropan tablets (n = 8)

	Catalytic titration	HPLC method	Derivative potentiometric titration
Mean Au content/μg	830	835	824
Standard deviation/μg	6	7	9
Relative standard deviation, %	0.7	0.8	1.1
Standard deviation of mean/μg	2.1	2.5	3.2
Content of auranofin/μg	2858	2875	2839
Relative error, %	4.7	4.2	5.4
$t_{0.05;14}$ = 2.14; $t_{0.01;14}$ = 2.98		1.46 2.57	
$F_{0.05;7;7}$ = 3.79		1.37 1.62	

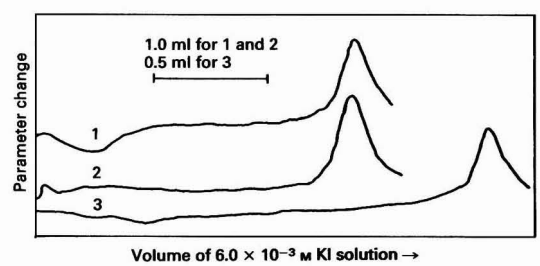

Fig. 4. Typical derivative potentiometric (GC - SCE) titration curves obtained in the determination of the Au^{I} content in 1, 2.079 mg of gold(I) thiomalate in Tauredon ampoules; 2, 2.154 mg of gold(I) thioglucose in Solganol B oleosum ampoules; and 3, 2.715 mg of auranofin in Auropan tablets

Table 2. Results of the determination of gold(I) sodium thiomalate as gold in Tauredon ampoules

	Catalytic titration					Derivative potentiometric titration					Official BP method[5]				
Sample No.	1	2	3	4	5	1	2	3	4	5	1	2	3	4	5
Mean Au content/mg	26.12	26.32	26.33	26.10	26.19	26.22	25.92	26.62	26.01	25.85	26.24	26.42	26.06	26.23	26.44
n	4	4	4	4	4	4	4	4	4	4	1	1	1	1	1
Standard deviation/mg	0.28	0.07	0.07	0.15	0.26	0.12	0.11	0.22	0.15	0.12	—	—	—	—	—
Relative standard deviation, %	1.08	0.27	0.25	0.58	0.99	0.45	0.42	0.83	0.59	0.45	—	—	—	—	—
Standard deviation of mean/mg	0.14	0.04	0.03	0.08	0.13	0.06	0.05	0.11	0.08	0.06	—	—	—	—	—
Content of gold(I) sodium thiomalate	51.72	52.12	52.14	51.69	51.86	51.93	51.33	52.71	51.51	51.19	51.97	52.33	51.61	51.95	52.37
Relative error, %	3.44	4.24	4.27	3.37	3.72	3.86	2.66	5.43	3.03	2.38	3.95	4.66	3.23	3.90	4.71
$t^{*}_{0.05;6}$ = 2.45; $t_{0.01;6}$ = 3.71	0.69	6.22	2.51	0.82	2.38	—	—	—	—	—	—	—	—	—	—
$F^{*}_{0.05;3;3}$ = 9.28; $F_{0.01;3;3}$ = 29.46	5.77	2.32	10.99	1.02	4.86	—	—	—	—	—	—	—	—	—	—

* Comparison of catalytic and derivative potentiometric titrations.

instance, owing to the presence of As^{III}, two maxima were observed in the derivative potentiometric titration curves. However, none of the maxima were suitable for the determination of the end-point; the first peak was very small, while the second peak appeared after the equivalence point when 20% excess of titrant was added. For this reason, the first procedure, involving no components of the indicator reaction, was chosen for the determination.

Accuracy and Precision of the Determination

For clarity, the results are given for each preparation separately.

Auropan tablets

Selected results are presented in Table 1. The results obtained using the proposed titrimetric methods were compared with those obtained by high-performance liquid chromatography (HPLC) (the recommended procedure of the manufacturer). The gravimetric method, which was used for the determination of gold in the other two pharmaceutical preparations,[5,6] could not be applied because of the necessity to use between 50[5] and 100[6] tablets, which would not only be time consuming, but also very expensive.

According to a one-way analysis of variance there was a significant difference between the above-mentioned methods [the calculated F-value was found to be 3.88 for $f_1 = 2$ and $f_2 = 21$; the theoretical values are 3.47 ($p = 0.05$) and 5.78 ($p = 0.01$)]. Therefore, these methods are biased and give different estimates for the gold content in the sample. At the 95% confidence level, the intervals were 830 ± 6.2 for catalytic titration, 824 ± 6.2 for derivative potentiometric titration and 835 ± 6.2 μg of Au for the HPLC method. The dispersion of the mean values due to the methods used was 13.1.

The significance test was applied to check whether there was a significant difference between the accuracy and precision of the proposed titrimetric methods with respect to the HPLC method. As can be seen from Table 1, the difference in precision is not significant. As regards accuracy, the results of the derivative potentiometric titrations, in contrast to those of the catalytic titrations, showed a significant difference.

The results obtained with catalytic titration and with the HPLC method were in agreement with the declared content of auranofin per tablet (3 mg ± 5%), while derivative potentiometric titration gave lower results.

In order to investigate the uniformity of contents, a series of analyses of individual tablets (with no prior homogenisation) was carried out. It was found that the difference in contents was small, *i.e.*, the standard deviation was 1.84% ($n = 8$).

Tauredon ampoules

Selected results obtained using the proposed titrimetric methods and the BP gravimetric method[5] are compared in Table 2. The gravimetric procedure described in the United States Pharmacopeia (USP)[6] could not be applied because of the need to use a 5-fold excess of the sample, *i.e.*, 0.5 g. According to a two-way analysis of variance (Table 3) there was no significant difference between any of the above-mentioned methods and between samples ($F < 1$); hence the experimental data form a general set. Therefore, the confidence interval of the general mean value is 26.20 ± 0.11 mg of gold at the 95% confidence level and $0.14 < \sigma < 0.33$. It should be noted that the two-way analysis of variance was carried out only for $n = 1$, because (due to a shortage of sample) only one measurement was carried out in the gravimetric determination. On comparing the accuracy and precision of catalytic and derivative potentiometric titrations (Table 2) it can be concluded that, for a larger number of samples, there was no significant difference.

However, the results obtained were higher than the declared content of gold in the sample (23.00 ± 1.15 mg).[5] This can be explained by the fact that the sample was prepared by transferring the contents of the ampoule into the calibrated flask quantitatively, whereas the ampoule had been filled to the "declared filling volume."

Solganol B oleosum ampoules

Selected results are given in Table 4. The results obtained using the proposed titrimetric methods were compared with those given by the pharmacopoeial gravimetric methods.[5,6] According to a two-way analysis of variance (Table 5), there

Table 3. Analysis of variance ($n = 1$)

Source of variation	Sum of squares	No. of degrees of freedom	Mean squares	F-ratio
Method	0.061	2	0.0305	0.55
Sample	0.083	4	0.0208	0.37
Residual	0.446	8	0.0558	—
Total	0.590	14	0.0420	—

Table 4. Results of the determination of gold(I) thioglucose as gold in Solganol B oleosum ampoules

Parameter	Catalytic titration					Derivative potentiometric titration				
Sample No.	1	2	3	4	5	1	2	3	4	5
Mean Au content/mg	540	540	52.7	52.9	52.8	538	539	52.0	52.0	52.2
n	6	9	4	4	4	6	5	4	4	4
Standard deviation/mg	2.4	3.6	0.22	0.50	0.55	7.7	7.0	0.32	0.38	0.37
Relative standard deviation, %	0.4	0.7	0.43	0.95	1.05	1.4	1.3	0.61	0.74	0.71
Standard deviation of mean/mg	1.0	1.2	0.11	0.25	0.28	3.2	0.3	0.16	0.19	0.19
Content of gold(I) thioglucose/mg	1075	1076	105.0	105.3	105.2	1071	1073	103.5	103.5	103.9
Relative error, %	7.5	7.7	5.0	5.3	5.2	7.1	7.3	3.5	3.5	3.9

Parameter	Official USP method[6]					Official BP method[5]	
Sample No.	1	2	3	4	5	1	2
Mean Au content/mg	541	542	52.1	52.8	52.7	541	542
n	3	2	1	1	1	1	1
Standard deviation/mg	0.7	0.4	—	—	—	—	—
Relative standard deviation, %	0.1	0.1	—	—	—	—	—
Standard deviation of mean/mg	0.4	0.3	—	—	—	—	—
Content of gold(I) thioglucose/mg	1076	1080	103.8	105.1	104.9	1077	1079
Relative error, %	7.6	8.0	3.8	5.1	4.9	7.7	7.9

Table 5. Analysis of variance ($n = 1$)

Source of variation	Sum of squares	No. of degrees of freedom	Mean squares	F-ratio
Method	11.95	3	3.98	34.14 ($F_{0.05;3;3} = 9.28; F_{0.01;3;3} = 29.46$)
Samples 1 and 2	1.85	1	1.85	15.86 ($F_{0.05;1;3} = 10.13; F_{0.01;1;3} = 34.12$)
Residual	0.35	3	0.12	
Total	14.15	7	—	
Method	0.897	2	0.448	12.55
Samples 3–5	0.178	2	0.089	2.39 ($F_{0.05;2;4} = 6.94; F_{0.01;2;4} = 18.00$)
Residual	0.143	4	0.036	
Total	1.218	8	—	

was a significant difference between the above-mentioned methods at the 0.01 level for the determination of gold in samples 1 and 2 and at the 0.05 level in samples 3–5. Also, there was a significant difference between samples 1 and 2 at the 0.05 level, whereas there was no significant difference between samples 3–5 at this level. It should be mentioned that these results should be viewed with a certain amount of caution because of the relatively small number of samples used. In addition, the two-way analysis of variance was again carried out only for $n = 1$ (*cf.* above). Further, from the one-way analysis of variance (carried out separately for samples 1 and 2) it follows that there is no significant difference between the proposed titrimetric methods and the USP gravimetric method[6] at $p = 0.05$ (taking into account the value of n). Also, as regards the precision of the determination, there was no significant difference between the two proposed titrimetric methods, or between the catalytic titration and the official USP method,[6] whereas the difference between the derivative potentiometric method and the official USP method[6] was significant.

In this instance the results were also higher than the declared content of gold (50.3 ± 2.5, *i.e.*, 503 ± 25 mg), which can be explained in the same way as above.

Conclusion

The proposed titrimetric methods for the determination of gold in pharmaceutical preparations have certain advantages over the official pharmacopoeial and manufacturer's (HPLC) methods.[5,6] By comparison with the HPLC method, simple equipment is used instead of relatively expensive (and hence not always available) instrumentation. Also, when compared with the gravimetric methods,[5,6] the proposed titrimetric methods are much simpler, faster and more economical. Of the two proposed titrimetric methods, catalytic titration has certain advantages because of the better agreement of the results with those of the official pharmacopoeial methods.[5,6]

The authors thank the Research Fund of Vojvodina for partial financial support of this work.

References

1. Brown, D. H., and Smith, W. E., *Chem. Soc. Rev.*, 1980, **9**, 217.
2. Pijck, J., *J. Pharm. Belg.*, 1962, **17**, 323; *Chem. Abstr.*, 1964, **61**, 8136.
3. Schiller, P., *Kernenergie*, 1963, **6**, 514.
4. Weyers, J., and Gárniak, H., *Acta Pol. Pharm.*, 1968, **25**, 25.
5. "British Pharmacopoeia 1973," HM Stationery Office, London, 1973, p. 423.
6. "The United States Pharmacopeia XXI," Mack, Easton, PA, 1985, pp. 81 and 469.
7. Gaál, F. F., and Abramović, B. F., *Mikrochim. Acta*, 1982, **I**, 465.
8. Abramović, B. F., Marinković, M. M., and Gaál, F. F., *Acta Pharm. Jugosl.*, 1989, **39**, 129.
9. Abramović, B. F., Gaál, F. F., Cservenák, R. I., and Varga, A. Gy., *Microchem. J.*, 1984, **30**, 1962.

Paper 9/01198F
Received March 20th, 1989
Accepted June 16th, 1989

Studies on Inorganic Ion Exchangers

Part 5.* Preparation, Properties and Application of Antimony(III) Arsenate and Antimony(III) Molybdate

C. Janardanan and S. Madhavankutty Nair†
Department of Chemistry, University of Calicut, Kerala 673 635, India

Two inorganic ion-exchange materials, antimony(III) arsenate and antimony(III) molybdate, have been synthesised and characterised. The distribution coefficients of 12 metal ions in de-mineralised water were determined. The order of selectivity was found to be $Cd^{2+} < Ca^{2+} < Mg^{2+} < Pb^{2+} < Cu^{2+} < Th^{4+} < Hg^{2+}$ for antimony(III) arsenate and $Mg^{2+} < Th^{4+} < Ni^{2+} < Zn^{2+} < Co^{2+} < Ca^{2+} < Hg^{2+} < Cd^{2+} < Cu^{2+} < Pb^{2+} < Bi^{3+} < Sn^{2+}$ for antinomy(III) molybdate; Zn^{2+}, Co^{2+} and Ni^{2+} were not adsorbed by antimony(III) arsenate. The effects of temperature and of the size and charge of the exchanging ion on the exchange capacity were determined and successful separations of Hg^{2+} from Zn^{2+}, Ni^{2+} and Cd^{2+}, and Pb^{2+} from Zn^{2+}, Cu^{2+} and Mg^{2+} were carried out on columns of antimony(III) arsenate and antimony(III) molybdate, respectively.

Keywords: *Inorganic ion exchanger; binary separation; distribution coefficient; antimony(III) arsenate; antimony(III) molybdate*

Many useful inorganic ion-exchange materials that have found application in the areas of analytical chemistry, radiochemistry, environmental chemistry and biochemistry have been synthesised during the last two decades. The rapid development of nuclear energy, hydrometallurgy of rare elements, preparation of high-purity materials, water purification, etc., has necessitated the synthesis of new, highly selective ion-exchange materials that are resistant to chemicals, temperature changes and radiation and which are more suitable than commercial organic or natural (soils, clay minerals, etc.) ion exchangers. Inorganic ion exchangers possessing high selectivity for certain ions or groups of ions[1] have been utilised for the chromatographic separation of many elements. Acidic salts of tetravalent metal ions have been the most extensively studied group of synthetic ion exchangers. Among the metals studied have been zirconium, thorium, titanium, cerium(IV), tin(IV), etc. Exchangers of trivalent metal ions have not been studied extensively, although exchangers based on aluminium, iron, chromium, bismuth and cerium have been reported.[2–6] The known antimony-based ion exchangers include antimonic acid,[7] antimony(V) silicate[8] and antimony pentoxide.[9] However, an exchanger based on antimony(III) has not yet been reported.

This paper describes the synthesis and ion-exchange properties of antimony(III) arsenate and antimony(III) molybdate both of which are obtained as amorphous substances. The amorphous nature of these exchangers prompted us to conduct a more detailed study. The amorphous precipitates have a greater surface area than the crystalline compounds and, therefore, have higher exchange capacities. However, amorphous precipitates are more soluble than crystalline compounds and hence it is desirable to have a certain degree of crystallisation; this can be achieved by heating or refluxing the precipitate. For antimony(III) arsenate and antimony(III) molybdate, refluxing has no effect on the nature of the precipitate.

Experimental

Reagents

Antimony(III) chloride (BDH), sodium arsenate (Riedel de Häen) and sodium molybdate (V/o SOJUZCHIMEXPORT) were used. All other chemicals were of AnalaR grade.

* For part 4 of this series see Janardanan, C., and Nair, S. M. K., *Indian J. Chem.*, in the press.

† To whom correspondence should be addressed.

Table 1. Conditions for synthesis and IECs of antimony(III) arsenate and antimony(III) molybdate

	Concentration of reagent/M*				
	Sb^{III}	YO_4	pH	Colour	IEC/ mequiv. g^{-1}
Y = As—					
1	0.05	0.05	0.85	White	0.7
2	0.05	0.01	0.74	White	0.6
3	0.1	0.1	1	White	0.3
Y = Mo—					
1	0.1	0.1	0	Dull white	1.02
2	0.05	0.05	1	White	0.6

* Mixing ratio 1 : 1.

Apparatus

A glass column (5 × 1.1 cm i.d.) was used for the separations. A 1-g amount of the exchanger in the H^+ form was placed in the column and the flow-rate was initially maintained at 1 ml min^{-1}. A Global pH meter, Model DPH-500, was used for pH measurements.

Synthesis of Antimony(III) Arsenate and Antimony(III) Molybdate

Antimony(III) arsenate was prepared by adding an aqueous solution of sodium arsenate to an acidic solution of antimony(III) chloride at different concentrations, pH and mixing ratios (Table 1). Antimony(III) molybdate was prepared by mixing an acidic solution of 0.1 M antimony(III) chloride and 0.1 M sodium molybdate in a volume ratio of 1 : 1 at different pH values. Details are given in Table 1. The mixture was stirred well and the pH was adjusted to the desired value with HCl or NaOH solution. The resulting product was allowed to stand for 24 h at room temperature after which it was filtered and washed with 1.0 M HCl followed by de-mineralised water. Antimony(III) arsenate was dried at room temperature and antimony(III) molybdate at 50 °C. Both exchangers were broken and sieved to the required mesh size (60–100 mesh) and were converted into the H^+ form by immersing them in 1.0 M HNO_3.

Table 2. Effect of size and charge of the exchanging ion on the IEC

Exchanging ion	Hydrated ionic radius/Å	IEC/mequiv. g^{-1} Antimony(III) arsenate	IEC/mequiv. g^{-1} Antimony(III) molybdate
Li^{I}	3.40	0.30	0.56
Na^{I}	2.76	0.70	1.02
K^{I}	2.32	0.76	1.20
Mg^{II}	7.00	0.59	0.96
Ca^{II}	6.30	0.79	1.40
Ba^{II}	5.90	0.82	1.60

Determination of Ion-exchange Capacity

The Na^+ ion-exchange capacity (IEC) was determined by the column method. A 1-g amount of the ion-exchange material in the H^+ form was placed in a glass tube with an i.d. of 1.1 cm plugged with glass-wool at the bottom. A 250-ml volume of 1.0 M sodium chloride solution was then passed through the column at a low flow-rate (1 ml min^{-1}) and the eluate was titrated with 0.1 M NaOH solution. The strong acid capacities were expressed in units of mequiv. g^{-1} (Table 1). The effect of the hydrated ionic radii on the exchange capacity of various bivalent cations is given in Table 2.

Determination of Optimum Mole Ratio

Mole ratios of antimony(III) arsenate and antimony(III) molybdate were determined by dissolving 100 mg of the exchanger in concentrated HCl. Antimony was determined by the pyrogallate method,[10] arsenic by the magnesium ammonium arsenate method[11] and molybdate by the oxinate method.[12]

Stability in Various Solvents

Antimony(III) arsenate was stable in 1.0 M H_2SO_4, 1.0 M HNO_3, ethanol and 0.01 M NaOH whereas antimony(III) molybdate was stable in HCl, H_2SO_4, HNO_3 (all 2.0 M), ethanol and 0.01 M NaOH. The exchangers did not lose their IEC at these solvent concentrations.

Effect of Heat

The samples were heated at different temperatures in a thermostatically controlled oven for 6 h and the IECs were determined. The results are given in Table 3.

Distribution Coefficients

Distribution coefficients (K_d) for 12 metal ions at concentrations of 0.005 M were determined by the batch process in the usual manner[13] by equilibrating 100 mg of the ion exchanger with 20 cm^3 of the metal ion solution for 6 h at room temperature (30 ± 1 °C). Each solution was then analysed for the metal ion by complexometric titration with ethylenediaminetetraacetic acid (EDTA). The K_d values for the metal ions were calculated using the following equation:

$$K_d\,(\text{ml g}^{-1}) = \frac{V_i - V_f}{V_f} \times \frac{V}{m}$$

where V_i and V_f are the initial and final volumes of EDTA, respectively, V is the volume of the metal ion solution and m is the mass of the exchanger taken. The K_d values of the metal ions are given in Table 4.

Column Operation

For separation studies 1 g of the exchanger was used in the column (5 × 1.1 cm i.d.). The flow-rate was 0.4 ml min^{-1}. The eluate was titrated with EDTA solution. Quantitative separation of Hg^{2+} - Zn^{2+}, Hg^{2+} - Ni^{2+} and Hg^{2+} - Cd^{2+} was achieved on a column of antimony(III) arsenate and that of Zn^{2+} - Pb^{2+}, Cu^{2+} - Pb^{2+} and Mg^{2+} - Pb^{2+} on a column of antimony(III) molybdate. The results are summarised in Table 5.

Table 3. Properties of antimony(III) arsenate and antimony(III) molybdate (both in the H^+ form) heated at different temperatures

Temperature/ °C	Colour	IEC/mequiv. g^{-1} Antimony(III) arsenate	IEC/mequiv. g^{-1} Antimony(III) molybdate
50	Dull white	0.68	1.02
150	Dull white	0.55	0.86
200	White	0.30	0.52
300	Dirty white	0.024	0.15

Table 4. K_d values of metal ions on antimony(III) arsenate and antimony(III) molybdate

Cation	Taken as	K_d/ml g^{-1} Antimony(III) arsenate	K_d/ml g^{-1} Antimony(III) molybdate
Zn^{II}	Sulphate	0	115.38
Mg^{II}	Chloride	4.10	76.19
Ca^{II}	Chloride	3.10	139.50
Pb^{II}	Nitrate	10.50	800.00
Hg^{II}	Chloride	157.89	150.00
Cd^{II}	Chloride	1.96	163.64
Sn^{II}	Chloride	Precipitated	1760.00
Cu^{II}	Chloride	12.20	212.50
Co^{II}	Chloride	0	120.32
Ni^{II}	Chloride	0	106.15
Bi^{III}	Nitrate	Precipitated	845.70
Th^{IV}	Nitrate	58.66	97.30

Table 5. Binary separations on antimony(III) arsenate and antimony(III) molybdate columns

Separation (eluent)	Amount loaded/ mg	Amount recovered/ mg
Antimony(III) arsenate—		
Zn^{II} (very dilute HNO_3, pH 3)	1.92	1.92
Hg^{II} (0.05 M NH_4NO_3 + 0.05 M HNO_3)	4.90	4.80
Ni^{II} (very dilute HNO_3, pH 3)	1.30	1.30
Hg^{II} (0.05 M NH_4NO_3 + 0.05 M HNO_3)	4.90	4.85
Cd^{II} (very dilute HNO_3, pH 3)	2.81	2.80
Hg^{II} (0.05 M NH_4NO_3 + 0.05 M HNO_3)	4.90	4.88
Antimony(III) molybdate—		
Zn^{II} (0.1 M HNO_3 + 0.1 M NH_4NO_3)	1.92	1.88
Pb^{II} (0.3 M HNO_3 + 0.5 M NH_4NO_3)	6.50	6.39
Cu^{II} (0.1 M HNO_3 + 0.1 M NH_4NO_3)	1.30	1.27
Pb^{II} (0.3 M HNO_3 + 0.5 M NH_4NO_3)	6.50	6.50
Mg^{II} (0.1 M HNO_3 + 0.1 M NH_4NO_3)	0.62	0.61
Pb^{II} (0.3 M HNO_3 + 0.5 M NH_4NO_3)	6.50	6.40

Results and Discussion

Both antimony(III) arsenate and antimony(III) molybdate were obtained in the form of a hard mass that was amorphous in nature and could easily be sieved to the desired particle size. Both exchangers are stable in acids and solutions of sodium chloride but dissolve to a considerable extent in bases, particularly in NaOH solution. The ion exchangers can be regenerated twice without any appreciable decrease in the IEC. The exchangers gradually lose their exchange properties when used repeatedly.

The ratios of Sb : As and Sb : Mo in the exchangers were found to be 1 : 1 and 1 : 2, respectively, with a variation of 0.01% for repetitive determinations (n = 3).

The maximum IEC of antimony(III) arsenate was found to be 0.7 mequiv. g^{-1} whereas that of antimony(III) molybdate was 1.02 mequiv. g^{-1}. The values decreased on drying the compounds at higher temperatures (Table 3). These results indicate that antimony(III) molybdate retains some IEC even on heating at 300 °C.

The effect of the size and charge of the exchanging ion on the IEC of the two exchangers is shown in Table 2. For the alkali and alkaline earth metal ions the IEC of both exchangers is as follows: $K^{I} > Na^{I} > Li^{I}$; and $Ba^{II} > Ca^{II} > Mg^{II}$. This in agreement with theoretical considerations.[14]

The uptake of metal ions by antimony(III) arsenate is in the order $Hg^{2+} > Th^{4+} > Cu^{2+} > Pb^{2+} > Mg^{2+} > Ca^{2+} > Cd^{2+}$ and by antimony(III) molybdate in the order $Sn^{2+} > Bi^{3+} > Pb^{2+} > Cu^{2+} > Cd^{2+} > Hg^{2+} > Ca^{2+} > Co^{2+} > Zn^{2+} > Ni^{2+} > Th^{4+} > Mg^{2+}$ (Table 4); Zn^{2+}, Co^{2+} and Ni^{2+} were not adsorbed by antimony(III) arsenate. The high uptake of certain ions demonstrates not only the ion-exchange properties but also the adsorption and ion-sieve characteristics of the exchangers.[15]

The quantitative separation of Hg^{2+} from Zn^{2+}, Ni^{2+} and Cd^{2+} (0.005 M each) was carried out successfully on a small column of antimony(III) arsenate and the separation of Zn^{II} - Pb^{II}, Cu^{II} - Pb^{II} and Mg^{II} - Pb^{II} on antimony(III) molybdate. The metal ions were eluted in the order indicated, using the eluents given in parentheses (Table 5). In all instances the recovery ranged from 95 to 100%, with a variation of 3% for successive determinations.

Conclusion

It is evident from the results that the quantitative and efficient separation of various metal ions such as Hg from Zn, Ni and Cd, and Pb from Zn, Cu and Mg is feasible with antimony(III) arsenate and antimony(III) molybdate.

References

1. Vesely, V., and Pakarek, V., *Talanta*, 1972, **19**, 219.
2. Kobayshi, E., and Goto, T., *Kogyo Kagaku Zasshi*, 1970, **73**, 692.
3. Thind, P. S., and Singh, H., *J. Indian Chem. Soc.*, 1981, **58**, 1187.
4. Szirtes, L., and Zsinka, L., *Chem. Zvesti*, 1967, **21**, 620.
5. Rawat, J. P., and Mukkawat, K. P. S., *Chromatographia*, 1978, **11**, 513.
6. Akilamali, K., Luma, B., and Mwamb, W., *Anal. Chem.*, 1979, **51**, 165.
7. Abe, M., and Ito, T., *Bull. Chem. Soc. Jpn.*, 1968, **51**, 2360.
8. Varshney, K. G., Agrawal, S., Varshney, K., Sharma, U., and Rani, S., *J. Radioanal. Nucl. Chem.*, 1984, **82**, 299.
9. Abe, M., *J. Inorg. Nucl. Chem.*, 1979, **41**, 83.
10. Vogel, A. I., "A Textbook of Quantitative Inorganic Analysis," Fourth Edition, The English Language Book Society and Longmans, London, 1982, p. 451.
11. Vogel, A. I., "A Textbook of Quantitative Inorganic Analysis," Third Edition, The English Language Book Society and Longmans, London, 1968, p. 501.
12. Vogel, A. I., "A Textbook of Quantitative Inorganic Analysis," Fourth Edition, The English Language Book Society and Longmans, London, 1982, p. 472.
13. Qureshi, M., Varshney, K. G., and Israilli, A. H., *J. Chromatogr.*, 1971, **54**, 141.
14. Vogel, A. I., "A Textbook of Quantitative Inorganic Analysis," Fourth Edition, The English Language Book Society and Longmans, London, 1982, p. 170.
15. Janardanan, C., Nair, S. M., and Savariar, C. P., *Analyst*, 1988, **113**, 1141.

Paper 9/01466G
Received April 10th, 1989
Accepted July 4th, 1989

Sequential Extraction - Spectrofluorimetric Determination of Lead and Cadmium Using Cryptands

Domingo Blanco Gomis and Elena Andres Garcia
Departamento de Quimica Fisica y Analitica, Facultad de Quimica, Universidad de Oviedo, Oviedo, Spain

A spectrofluorimetric method for the determination of ultratrace amounts of lead and cadmium is described based on the sequential extraction of the ternary ion-association complexes formed between the cation, a cryptand as the ligand and eosin as a counter ion. A linear working range from the detection limit (0.5 ng ml^{-1}) to 250 ng ml^{-1} of lead and to 150 ng ml^{-1} of cadmium was obtained. The relative standard deviation was 2–4%. The proposed method has been applied successfully to the determination of lead and cadmium in zinc metals and soft drinks.

Keywords: *Lead; cadmium; spectrofluorimetry; cryptand ether; ion-pair extraction*

The toxic heavy metals lead and cadmium are two of the most important environmental pollutants. Lead is amongst the oldest metals known to man and its modern uses include storage batteries, ammunition, solder, pigments and anti-knock compounds in petrol. Cadmium has a much more recent history, but is widely used in metallurgical, nuclear and electrical engineering, and the paint and plastics industries. The industrial use of both elements has ensured that they are now dispersed throughout large parts of the environment. Man ingests lead and cadmium from food and drink and inhales them from aerosols and particulates in the atmosphere. Because lead and cadmium accumulate in the organs of the body, only being excreted very slowly, the inhalation or ingestion of small amounts of both metals over long periods of time can lead to some form of lead and cadmium intoxication. Moreover, there is evidence that lead and cadmium have additive effects.[1,2] Consequently, regulatory standards have been proposed with the aim of limiting general exposure or ingestion. The determination of trace amounts of lead and cadmium are therefore important in the quality control of many different industrial processes. For these reasons, highly sensitive and reliable methods of determination are needed.

Many analytical techniques are available for the determination of these inorganic substances in industrial and food chemistry; namely, atomic absorption spectrometry, emission spectrometry, spectrophotometry, electrochemical techniques, neutron activation analysis, etc., but when the elements are present at very low levels, pre-concentration is often required before analysis. Fluorescence is one of the more sensitive and selective methods of chemical analysis, which is normally applied in solution. The methods usually employed for the determination of lead and cadmium consists in the formation of a highly fluorescent binary or ternary complex. Hence, lead has been determined with 1,10-phenanthroline plus eosin or morin, and cadmium with 8-hydroxyquinoline-5-sulphonic acid or calcein.[3]

A recent approach has been to use macrocyclic (crown ethers) or macrobicyclic (cryptands) compounds as ligands in solvent extraction. We have described the sensitive and selective fluorimetric determination of lead with 18-crown-6,[4] cryptand 2.2.2[5] and cryptand 2.2.1[6] using eosin as a counter ion. The lead complexes formed were extracted into dichloromethane, chloroform or 1,2-dichloroethane by forming extractable ion-association species with the fluorescent eosinate anion. From this work we concluded that extraction improves the selectivity: for example, the selectivity (as expressed by the difference between the logarithms of the corresponding complexation constants, $\Delta \log K_s$) for Pb^{2+} over Cd^{2+} with 18-crown-6 is 4.27 − 5.31 = −1.04, with cryptand 2.2.2 it is 12.72 − 7.10 = 5.62 and with cryptand 2.2.1 (optimum for lead) it is 13.12 − 10.04 = 3.08.[7,8] Therefore the best choice of ligand for the extraction of lead in the presence of cadmium is cryptand 2.2.2, and a poorer choice is 18-crown-6. Cadmium, however, is not extracted by the 18-crown-6 - dichloromethane system or by the cryptand 2.2.2 - chloroform system, in spite of its high stability constants, but it is extracted easily by the cryptand 2.2.1 - 1,2-dichloroethane system. Selectivity also depends, therefore, upon the type of ligand and the nature of the solvent and counter ion. This provides opportunities for selectivity control and opens up the possibility of simultaneous sequential extraction and determination of these cations in the same sample. In this paper, we describe the extraction - spectrofluorimetric determination of trace amounts of lead and cadmium by using the cryptands 2.2.2 and 2.2.1 and eosin as a counter ion. The proposed method has been applied successfully to the determination of lead and cadmium in zinc metals and soft drinks.

Experimental

Reagents

All reagents used were of analytical-reagent grade. Doubly distilled and de-mineralised water was used throughout.

Stock solutions of Pb^{II} and Cd^{II} (1000 p.p.m.) were prepared by dissolving lead or cadmium nitrate in acidified water. The solutions were standardised by precipitation of lead sulphate and complexometric titration, respectively.[9,10] All working standard solutions were prepared fresh by dilution of the appropriate stock solution with acidified water.

Solutions of cryptands 2.2.2 and 2.2.1 were prepared by dissolving the commercial products (Kryptofix, Merck) in water to which perchloric acid had been added and through which argon had been passed in order to remove carbon dioxide and avoid carbonation of the cryptands. The ligand concentrations used when the solutions were stored in polyethylene flasks were 10^{-3} and 10^{-4} M, respectively, and the perchloric acid concentration used was 1.5 times that of the ligand. Acidic eosin solution (10^{-4} M) was prepared by dissolving pure eosin (synthesised by reaction of Br^- - BrO_3^- with fluorescein in acidified aqueous acetone[11]) in alkaline water (pH 8–9).

Buffer solutions (pH 7.8) were prepared with 0.5 or 0.1 M tris(hydroxymethyl)aminomethane - HCl.

Apparatus

Fluorescence intensity measurements and spectra were obtained with a Perkin-Elmer LS-5 spectrofluorimeter equipped with a Model 3600 data station. The excitation and emission slit widths were both 2.5 nm and standard 1-cm silica cells were used. The temperature of the sample cell was kept

constant within 1 °C by using a Julabo (Paratherm III) thermostat system.

For the determination of lead and cadmium in real samples a Perkin-Elmer ICP/5000 emission spectrometer and a Perkin-Elmer 3030 graphite furnace atomic absorption spectrometer were used.

Procedure

Pipette standard lead and cadmium solutions (containing up to 1.25 μg of lead and 0.75 μg of cadmium) into a 50-ml separating funnel or a 10-ml centrifuge tube. Add 0.12 ml of the cryptand 2.2.2 stock solution, 0.5 ml of buffer solution, 0.72 ml of eosin solution and dilute to 5 ml with doubly distilled de-mineralised water (final pH 7.8 ± 0.1). After mixing, add 5 ml of chloroform and extract the lead complex by shaking for 5 min. Allow the phases to separate and transfer 4 ml of the aqueous phase into a separating funnel or a centrifuge tube, add 0.63 ml of the cryptand 2.2.1 stock solution and dilute to 5 ml with water. After mixing, add 5 ml of 1,2-dichloroethane and extract the cadmium complex by shaking for 5 min. The organic phases were previously equilibrated with buffered aqueous phase. Measure the fluorescence intensity, I_F, of the chloroform and 1,2-dichloroethane phases at 552 nm (excitation wavelength, 536 nm).

Run a reagent blank in the same way and subtract its fluorescence from that of the sample.

Results and Discussion

Optimisation of Extraction Conditions

In previous papers,[4–6] where we tested different acidic fluorescent dyes [fluorescein, dichlorofluorescein, dichlorotetraiodofluorescein, tetrabromofluorescein (eosin) and tetraiodofluorescein] as counter ions and different solvents (benzene, chlorobenzene, dichloromethane, 1,2-dichloroethane, carbon tetrachloride and chloroform) for the extraction of heavy metals with macrocyclic compounds, it was shown that eosin invariably gave the best fluorescence signal and the organic solvent used depended on the nature of the metal cation and macrocyclic compound employed. From these results we selected cryptand 2.2.2, eosin and chloroform for the extraction of lead and cryptand 2.2.1, eosin and 1,2-dichloroethane for the extraction of cadmium.

The excitation and emission spectra of the blank and the lead and cadmium complexes extracted into chloroform and 1,2-dichloroethane, respectively, from an aqueous medium at pH 7.8 are shown in Fig. 1. The absorption spectra have maxima at 536 nm, and the fluorescence maxima are at 552 nm for both complexes. A spectral band pass of 2.5 nm was used for both absorption and fluorescence.

The pH of the aqueous phase is an important factor for the ion-pair extraction. The pH dependence of the ion-association lead and cadmium ternary complexes is complicated owing to the possible secondary reactions affecting the cations, the ligands and/or the counter ion. The conditional stability constants for the cryptate complexes in aqueous solution at different pH values were calculated from the stability constants of the cryptates,[8] the pK_a values of the mono- and di-protonated cryptands[8,12] and the stability constants of lead and cadmium hydroxide.[13] A maximum value of the conditional stability constant was observed at pH 8.7 and 10 for the lead and cadmium complexes, respectively.

The influence of pH on the extraction of the lead and cadmium complexes for the pH range 5–12, fixed by the addition of tetramethylammonium hydroxide or nitric acid (ionic strength was kept constant at 0.01 M), was studied by measuring the fluorescence intensity. The relationship

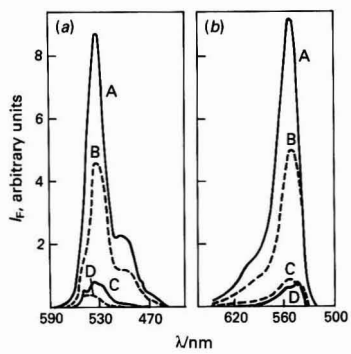

Fig. 1. (*a*) Excitation and (*b*) emission spectra of A and B, ion-association lead and cadmium complexes and C and D, blank. Solid line, Pb; and dashed line, Cd

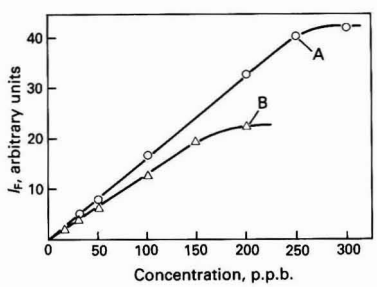

Fig. 2. Calibration graphs for the spectrofluorimetric determination of lead and cadmium. A, Pb; and B, Cd

Table 1. Effect of foreign ions (M) on the determination of 0.4 μg of lead and 0.5 μg of cadmium

Cation or anion	M: Cd,Pb molar ratio	Apparent recovery, %
Li^+	1000	100.0
Na^+	500	95.6
K^+	1000	101.4
Cs^+	1000	96.9
NH_4^+	500	103.0
Tl^+	500	100.8
Ag^+	10*	138.5
	5	103.5
Mg^{2+}	500	98.4
Ca^{2+}	5	111.0
	1	96.7
Sr^{2+}	5*	210.0
	0.5	96.5
Ba^{2+}	500	97.1
Cu^{2+}	150*	107.0
	100	103.5
Hg^{2+}	5	106.5
	1	102.1
Ni^{2+}	500	104.5
Zn^{2+}	500	97.3
Co^{2+}	1000	100.8
Fe^{3+}	10	107.4
	5	104.2
Al^{3+}	500	103.6
Cr^{3+}	10*	108.8
	5	105.2
NO_3^-	15000	100.6
Cl^-	15000	98.1
PO_4^{3-}	5000	97.0
SO_4^{2-}	5000	101.1

* Tolerance limit for the extraction of the lead complex.

Table 2. Determination of lead and cadmium in zinc metals and soft drinks

Sample	ICP-AES	GFAAS	Proposed method
Commercial zinc—			
Pb/mg g^{-1}	28.0 ± 0.2	—	28.4 ± 0.3
Cd/mg g^{-1}	4.34 ± 0.04	—	4.47 ± 0.27
High-purity zinc—			
Pb/μg g^{-1}	7.0 ± 0.4	—	6.9 ± 0.2
Cd/μg g^{-1}	15.8 ± 0.6	—	15.9 ± 0.4
Cola drink—			
Pb/μg l^{-1}	—	13.8 ± 2.2	15.1 ± 1.6
Cd/μg l^{-1}	—	2.6 ± 0.6	2.9 ± 0.3
Lemon juice—			
Pb/μg l^{-1}	—	33.6 ± 3.7	37.9 ± 1.9
Cd/μg l^{-1}	—	8.9 ± 0.4	9.1 ± 1.4

between pH and I_F showed a maximum at pH 7–9 for both cryptate complexes. For subsequent studies, the pH was fixed at 7.8 by the addition of tris(hydroxymethyl)aminomethane.

In previous work,[5,6] it was verified that the minimum cryptand and eosin : lead or cadmium molar ratio was 3–5 : 1. For this reason, a 10-fold molar excess of cryptands and eosin was used. The ionic strength must be kept constant because an ionic strength of >0.15 M produces a sharp decrease in the signal of the cadmium ion-association complex.

Calibration Graph

The calibration graph, shown in Fig. 2, was linear from the detection limit (0.5 ng ml^{-1}, determined as twice the standard deviation of the blank) up to 250 ng ml^{-1} of lead and 150 ng ml^{-1} of cadmium. The relative standard deviation was 2–4%.

Effect of Foreign Ions

The effect of several metal ions, selected from those capable of forming stable complexes with cryptands and those most commonly associated with lead and cadmium, and some common anions was studied. Table 1 shows the tolerance limits of the complex most affected by the presence of foreign ions, which was generally the cadmium complex. No significant interference from large amounts of alkali metals was observed. The possible interference of iron and chromium is attributed to the relatively high working pH, which results in the precipitation of hydroxides, which would hinder the formation and extraction of the complexes. It is possible to minimise this effect as described previously[4] or reduce the pH of the extraction. Among the cations tested, strontium, calcium and mercury interfered. If these cations are present in the sample at an intolerably high ratio, then they should be removed or the standard additions method should be applied.

Determination of Lead and Cadmium in Real Samples

To examine the applicability of the proposed method, lead and cadmium were determined in four samples of industrial and toxicological interest.

For the analysis of commercial and high-purity zinc metals sample solutions were prepared by dissolving 0.025 g of a finely ground sample of commercial zinc and 0.25 g of high-purity zinc in a small volume of dilute hydrochloric acid (1 + 1) and diluting to 50 ml with doubly distilled and de-mineralised water. Portions of the commercial (0.1 ml) and high-purity (3.2 ml) zinc samples were then extracted as described under Procedure. For the analysis of soft drinks, 4 ml of the sample were extracted, previously degassed if necessary, and 0.1 ml of 0.5 M buffer solution was added instead of 0.5 ml of 0.1 M buffer solution. The results, shown in Table 2, are in good agreement with those obtained by inductively coupled plasma atomic emission spectrometry (ICP-AES) and graphite furnace atomic absorption spectrometry (GFAAS).

Conclusion

The sensitivity, selectivity and applicability that can be achieved by using cryptands in the extraction of toxic metals has been shown. The selectivity depends upon the stability constants of the cryptate complexes and the nature of the extraction system. This enables the sequential extraction and determination of different toxic cations in a variety of samples such as water, foods, chemicals, metals, etc., to be performed with minimum sample handling. Unfortunately, owing to the lack of knowledge on the extraction of ternary ion-association complexes, the most appropriate extraction method must be obtained by using empirical procedures.

References

1. Ferm, V. H., *Experientia,* 1969, **25**, 56.
2. Challop, R. S., *New Eng. J. Med.,* 1971, **285**, 970.
3. Schulman, S. G., "Molecular Luminescence Spectroscopy: Methods and Applications," Part 1, Wiley, New York, 1985.
4. Medel, A. S., Gomis, D. B., Fuente, E., and Jimeno, S. A., *Talanta,* 1984, **31**, 515.
5. Gomis, D. B., Fuente, E. A., and Medel, A. S., *Talanta,* 1985, **32**, 915.
6. Gomis, D. B., Abrodo, P. A., Lobo, A. P., and Medel, A. S., *Talanta,* 1988, **35**, 553.
7. Izatt, R. M., Terry, R. E., Haymore, B. L., Hansen, L. D., Dalley, N. K., Avondet, A. G., and Cristensen, J. J., *J. Am. Chem. Soc.,* 1976, **98**, 7620.
8. Neu, F. A., Spiess, B., and Weill, M. J. S., *Helv. Chim. Acta,* 1977, **60**, 2633.
9. Charlot, G., "Les Méthodes de la Chimie Analytique, Analyse Quantitative Minérale," Masson, Paris, 1961.
10. Kinnunen, J., and Mericanto, B., *Chemist-Analyst,* 1952, **41**, 76.
11. Fempeydic, D., Dnur, F., and Sevillain, P., *Bull. Soc. Chim. Fr.,* 1982, II-5.
12. Lehn, J. M., and Sauvage, J. P., *J. Am. Chem. Soc.,* 1975, **97**, 6700.
13. Ringbom, A., "Complexation in Analytical Chemistry," (Spanish translation), Alhambra, Madrid, 1979.

Paper 9/01271K
Received March 28th, 1989
Accepted June 21st, 1989

Extraction, Separation and Spectrophotometric Determination of Cadmium and Mercury Using Triphenylphosphine Oxide and its Application to Environmental Samples

B. Raman and V. M. Shinde
Analytical Laboratory, Department of Chemistry, The Institute of Science, 15 Madam Cama Road, Bombay 400 032, India

A method is proposed for the solvent extraction of cadmium and mercury from salicylate media using triphenylphosphine oxide as extractant. The optimum extraction conditions were evaluated from a critical study of the effect of pH, sodium salicylate concentration and the concentration of triphenylphosphine oxide. The probable composition of the species has been deduced from log - log data and an extraction mechanism is suggested. The method has been used to separate zinc, cadmium and mercury from binary and ternary mixtures and for the spectrophotometric determination of mercury or cadmium in environmental samples.

Keywords: *Cadmium(II); mercury(II); solvent extraction; salicylate solution; triphenylphosphine oxide*

Heavy metals such as mercury and cadmium are widely distributed throughout the environment as a result of soil erosion and a broad spectrum of industrial and agricultural processes. Inhalation of cadmium fumes produces emphysema followed by bronchitis. Similarly, mercury poisoning results in severe nausea, vomiting, abdominal pain and kidney damage. It is important to study these elements as they are potent metabolic poisons and members of the group of non-essential toxic trace elements consisting of Cd, Hg, Pb, Tl, Te and As.

An extensive literature study showed that a large number of reagents are useful for the extraction of cadmium and mercury. Among neutral extractants, tributyl phosphate,[1,2] trioctylphosphine oxide,[3] bis(2-ethylhexyl) phosphate[4] and mesityl oxide[5,6] have been used for the extraction of cadmium. Reagents such as n-alkylarsonic acid[7] and dioctylarsinic acid[8] have also been used for the extraction of cadmium. High relative molecular mass amines such as *N*-phenyl-*N*-thiobenzoylhydroxylamine,[9] tribenzylamine,[10] Aliquat 336,[11–13] Alamine 336,[12–14] trioctylamine[15] and Primene JMT[13] have had considerable use for the extraction of cadmium. Similarly, as reported previously, a large number of extractants such as diethyl ether,[16] mesityl oxide,[5] dioctylarsinic acid,[8] and caproic acid[17] have been used for the extraction of mercury. High relative molecular mass amines such as Amberlite LA-1,[18] tribenzylamine,[10] trioctylamine,[15,19] Alamine 304,[20] Alamine 336[21] and Primene JMT[21] have also been used. These methods, however, suffer from drawbacks such as longer extraction periods,[3,6,9,15,16] multi-stage extractions under different conditions[10] and interference from common anions.[1] Most of these methods were not applied for analytical purposes.

This paper reports a method for the extraction of cadmium and mercury from salicylate solution using triphenylphosphine oxide as extractant. The metal ions from the organic phase were back-stripped and determined complexometrically. The spectrophotometric determination was possible in the organic phase itself. The proposed method allows the mutual separation of zinc, cadmium and mercury from binary and ternary mixtures and is applicable to the determination of cadmium and mercury in industrial effluents, biological samples and commercial products.

Experimental

Chemicals and Reagents

Stock solutions of cadmium and mercury were prepared by dissolving 2.85 g of cadmium sulphate and 1.67 g of mercury(II) chloride, respectively, in 250 ml of distilled water containing a minimum amount of the appropriate acid to prevent hydrolysis. The solutions were standardised by standard methods[22,23] and test solutions of the required concentration were prepared by suitable dilution. A 5% solution of triphenylphosphine oxide (Fluka grade, m.p. 156–158 °C) in toluene was used for the extractions. Buffer solution (pH 9.2) was prepared by dissolving 4.767 g of borax (0.05 M) in 250 ml of distilled water and a buffer solution of pH 10 was prepared from 0.01 M sodium carbonate and 0.01 M sodium hydrogencarbonate. Another buffer solution of pH 4.7 was prepared from 0.1 M sodium acetate and 0.1 M acetic acid. A 0.1% methanolic solution of 1-(2-pyridylazo)-2-naphthol (PAN) was used for the spectrophotometric determinations of cadmium and mercury. All chemicals were of analytical-reagent grade.

General Extraction Procedure

To an aliquot of solution containing 1 mg of cadmium or mercury, were added, 1.6 g (for cadmium) and 2.4 g (for mercury) of sodium salicylate in a total volume of 25 ml to give final concentrations of 0.4 and 0.6 M, respectively. The solution pH was adjusted to 6.8–9.2 and 5.5–5.8 for cadmium and mercury, respectively, using hydrochloric acid and sodium hydroxide solutions. The solutions were then transferred into separating funnels and shaken for 2 min with two 5-ml portions of 5% triphenylphosphine oxide. Cadmium was stripped with distilled water and mercury was stripped with acetate buffer (pH 4.7) and determined complexometrically.[22,23]

For microgram amounts of cadmium (2–10 μg) and mercury (10–50 μg), extractions were performed with a single 5-ml aliquot of 5% triphenylphosphine oxide solution and subsequently the metal ions were determined spectrophotometrically in the organic phase itself, as described below.

To the organic phase containing cadmium, 5 ml of borax buffer solution (pH 9.2) were added followed by 1 ml of 0.1% PAN solution. The mixture was shaken for 2 min and the orange organic layer was diluted to 10 ml using toluene. The absorbance of the complex was measured at 555 nm against a reagent blank prepared analogously. The extraction of the metal ion was determined from a previously constructed calibration graph in the concentration range 2–10 μg of cadmium per 10 ml of the organic phase. To calculate the mercury extracted into the organic phase, 5 ml of the sodium hydrogencarbonate buffer (pH 10) were added followed by 1 ml of 0.1% PAN solution. After separation of the orange organic layer, this layer was diluted to 10 ml with toluene and the absorbance of the complex was measured at 555 nm

against a reagent blank prepared in the same manner, commencing with the extraction. This method obeys Beer's law in the concentration range 10–50 μg of mercury per 10 ml of the organic phase and the complete analysis, from extraction to determination, takes about 20 min.

Results and Discussion

Extraction Conditions

By varying the pH (4.5–10.0) and the concentrations of salicylate (0.05–0.8 M) and triphenylphosphine oxide (1–5% with toluene as diluent), it was found that a double extraction (each, 2-min shaking) with 5 ml of 5% triphenylphosphine oxide solution was essential for milligram amounts of metal ions. However, at the microgram level, a single extraction with 5 ml of 5% triphenylphosphine oxide solution was adequate for the quantitative extraction of cadmium or mercury in the concentration ranges 0.2–1.0 and 1.0–5.0 μg ml^{-1}, respectively. Various stripping agents such as water, hydrochloric acid, sodium hydroxide solution and acetate buffer were tried. Water strips cadmium; however, only acetate buffer of pH 4.7 was effective for the quantitative stripping of mercury. The optimum extraction conditions are given in Table 1 and Figs. 1 and 2.

Nature of Extracted Species

The nature of the extracted species was investigated by a single extraction of a fixed amount of cadmium or mercury with varying concentrations of salicylate and triphenylphosphine oxide. The log-log plots of distribution ratio *versus* salicylate concentration (at fixed pH and concentration of triphenylphosphine oxide) and *versus* triphenylphosphine oxide concentration (at fixed pH and concentration of salicylate) indicated a molar ratio of 1:2 with respect to both extractant and salicylate ion (Figs. 3 and 4). The probable extracted species is $M(sal)_2.2TPPO$, where M is cadmium(II) or mercury(II), sal is the salicylate ion and TPPO, triphenylphosphine oxide. Hence, the extraction of metal involves solvation of the metal salicylate salt. The probable extraction mechanism is as follows:

$$M(H_2O)_2^{2+} + 2HOC_6H_4COO^- \rightleftharpoons \underset{\text{Metal salicylate}}{M(HOC_6H_4COO)_2.2H_2O}$$

$$M(HOC_6H_4COO)_2.2H_2O + 2TPPO \rightleftharpoons \underset{\text{Extracted species}}{M(HOC_6H_4COO)_2.2TPPO} + 2H_2O$$

Spectral Characteristics

It is feasible to determine cadmium and mercury spectrophotometrically with PAN in the organic phase itself, hence eliminating the stripping step. Both Cd-PAN and Hg-PAN complexes in TPPO have maximum absorbance at 555 nm and the concentration ranges over which they conform to Beer's law are 0.2–1.0 μg ml^{-1} and 1.0–5.0 μg ml^{-1}, respectively. The colour of the complex is stable for 24 h. The molar absorptivity of the Cd-PAN complex is 5.3×10^4 l mol^{-1} cm^{-1} and that of the Hg-PAN complex is 2.4×10^4 l mol^{-1} cm^{-1}. The coefficient of variation in the determination of 4 μg of cadmium is 1.59%, whereas for 20 μg of mercury it is 1.52% (both in 10 ml of the organic phase). The spectrophotometric data for the determination of cadmium and mercury in triphenylphosphine oxide with PAN as the chromogenic agent are given in Table 2.

Effect of Possible Interfering Ions

The extractions of cadmium and mercury were carried out according to recommended procedures to examine the effect

Table 1. Optimum conditions for the extraction of cadmium and mercury

Metal ion	Concentration	Salicylate concentration/ M	5% TPPO in toluene/ml	pH	Stripping solution
Cadmium(II) . .	1–5 mg	0.4	2 × 5	6.8–9.2	Water
	2–10 μg*	0.4	5	6.8–9.2	—
Mercury(II) . .	1–5 mg	0.6	2 × 5	5.5–5.8	Acetate buffer
	10–50 μg*	0.6	5	5.5–5.8	—

* Determined in the organic phase with PAN as the chromogenic agent.

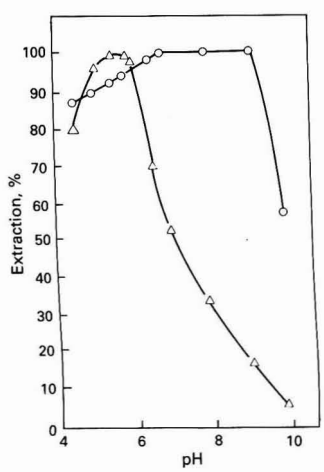

Fig. 1. Extraction of ○, Cd^{II} and △, Hg^{II} as a function of pH

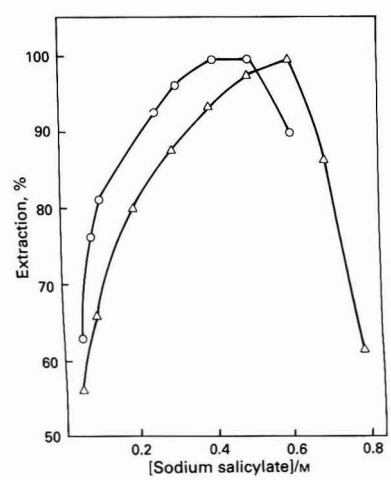

Fig. 2. Extraction of ○, Cd^{II} and △, Hg^{II} as a function of the concentration of salicylate

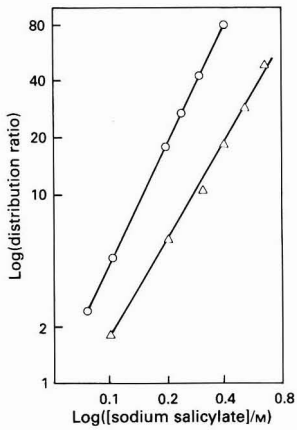

Fig. 3. Log - log plot of the distribution ratio of ○, Cd^{II} and △, Hg^{II} as a function of the concentration of sodium salicylate

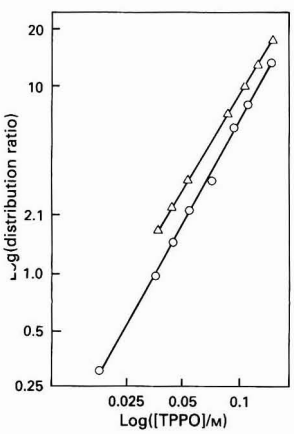

Fig. 4. Log - log plot of the distribution ratio of ○, Cd^{II} and △, Hg^{II} as a function of the concentration of triphenylphosphine oxide

Table 2. Spectrophotometric data for the determination of cadmium and mercury in triphenylphosphine oxide with PAN

Metal ion	Standard concentration/ $\mu g\ l^{-1}$	Absorbance* at 555 nm	RSD,† %
Cadmium . .	Sample blank	—	—
	200	0.105	3.00
	400	0.207	1.59
	600	0.315	1.42
	700	0.364	1.35
	800	0.418	0.98
	1000	0.526	1.09
Mercury	Sample blank	—	—
	1000	0.119	3.2
	2000	0.239	1.6
	2500	0.298	2.0
	3000	0.357	1.1
	4000	0.482	1.1
	5000	0.599	1.2

* Mean of six readings.
† RSD = relative standard deviation.

of interference from foreign ions. The tolerance limit was set as being the amount required to cause a 2% error in the recovery of cadmium or mercury. The results in Table 3 show

Table 3. Effect of possible interfering ions on the extraction of 4 μg of cadmium(II)* and 20 μg of mercury(II)*

Metal ion	Tolerance limit of foreign ion/μg
Cadmium(II) . .	F^-, 80; Cl^-, 80; Br^-, 80; I^-, 80; SO_4^{2-}, 40; SO_3^{2-}, 60; ascorbate, 60; NO_3^-, 80; PO_4^{3-}, 80; $S_2O_3^{2-}$, 80; tartarate, 80; thiourea, 80; citrate, 40; SCN^-, 40; CN^-, 20; As^{III}, 80; Sb^{III}, 80; Bi^{III}, 80; Ba^{II}, 40; Ca^{II}, 40; Sr^{II}, 60; Al^{III}, 80; Mg^{II}, 40; Au^{III}, 80; Pb^{II}, 20; Fe^{III}, 80; Te^{IV}, 80; Se^{IV}, 60; Th^{IV}, 40; Ti^{IV}, 20; Zr^{IV}, 20; Mn^{II}, none; Zn^{II}, none; Cu^{II}, none; Cr^{VI}, 80; V^{V}, 80; Pd^{II}, 80
Mercury(II) . .	F^-, 400; Cl^-, 400; I^-, 400; Br^-, 200; SO_4^{2-}, 200; ascorbate, 60; NO_3^-, 100; PO_4^{3-}, 200; $S_2O_3^{2-}$, none; thiourea, none; tartarate, 400; citrate, 400; NO_2^-, 400; SCN^-, 200; CN^-, 200; Mg^{II}, 400; Ca^{II}, 200; Ba^{II}, 200; Pb^{II}, 200; Pd^{II}, 200; As^{III}, 400; Cr^{VI}, 400; Bi^{III}, 100; Fe^{III}, 400; Se^{IV}, 400; Te^{IV}, 400; Ti^{IV}, 200; Zr^{IV}, 200; Th^{IV}, 100; V^{V}, 100; W^{VI}, 200, Cu^{II}, none; Zn^{II}, none; Sb^{III}, none; Mo^{VI}, 100

* Spectrophotometric detection.

Table 4. Mutual separation of zinc, cadmium and mercury from binary mixtures

Sample No.	Composition/mg	Recovery,* %
1	Cd^{II}, 1; Zn^{II}, 1	Cd^{II}, 99.7; Zn^{II}, 99.9
2	Cd^{II}, 2; Zn^{II}, 1	Cd^{II}, 99.7; Zn^{II}, 99.8
3	Hg^{II}, 1; Zn^{II}, 1	Hg^{II}, 99.6; Zn^{II}, 99.8
4	Hg^{II}, 2; Zn^{II}, 1	Hg^{II}, 99.6; Zn^{II}, 99.8
5	Hg^{II}, 1; Cd^{II}, 1	Hg^{II}, 99.6; Cd^{II}, 99.8
6	Hg^{II}, 1; Cd^{II}, 2	Hg^{II}, 99.4; Cd^{II}, 99.6

* Mean of six results.

that a large number of cations and anions are tolerated. The notable interferences are due to Mn^{II}, Zn^{II} and Cu^{II} for cadmium and Zn^{II}, Sb^{III}, Cu^{II}, thiourea and $S_2O_3^{2-}$ for mercury. The interferences due to zinc and copper in the extraction of mercury were eliminated by washing the organic phase with water. Subsequently, the mercury was complexed with PAN to develop colour in the organic phase.

Separation of Cadmium(II), Mercury(II) and Zinc(II) from Binary Mixtures

From 0.4 M sodium salicylate solution, adjusted to pH 9.2, cadmium shows quantitative extraction into 5% triphenylphosphine oxide dissolved in toluene. Under these conditions, however, zinc remains in the aqueous phase. This has been used for the mutual separation of zinc and cadmium from binary mixtures. Under the extraction conditions for cadmium, mercury shows partial extraction (≈ 8%). From the organic phase, cadmium is scrubbed off with distilled water and determined complexometrically.[22] After the removal of cadmium from the organic phase, partially extracted mercury is stripped with acetate buffer (pH 4.7) and this is combined with the aqueous phase containing the major amount of unextracted mercury. In the combined aqueous phase mercury is finally determined complexometrically.[23]

The mutual separation of zinc and mercury is accomplished by selective stripping. Both zinc and mercury extract quantitatively in triphenylphosphine oxide from a 0.6 M sodium salicylate solution of pH 5.5. Zinc from the organic phase is first stripped with water and determined as described earlier; subsequently, mercury is scrubbed with acetate buffer and determined complexometrically. The separation of zinc and mercury is quantitative. The results for the binary separations are given in Table 4.

Mutual Separation of Zinc(II), Cadmium(II) and Mercury(II) from Ternary Mixtures

Zinc(II), cadmium(II) and mercury(II) were separated from a ternary mixture by the scheme shown in Fig. 5. The recoveries of all three metals were ≥99.0%. The results are given in Table 5.

Analytical Performance

The proposed method has good precision; this is indicated in terms of the RSDs for the two metal ions (Table 2). The values of Sandell's sensitivity for the cadmium and mercury complexes are 0.002 and 0.008 μg cm^2, respectively.

Determination of Cadmium and Mercury in Environmental, Biological and Commercial Samples

1. *Industrial effluents*

The wastewater generated by industrial operations is composed of both industrial and domestic effluents. For the treatment of domestic effluent, the wastewater is pumped inside the factory and after treatment it is mixed and, therefore, diluted, with industrial effluent, which results in its dilution.

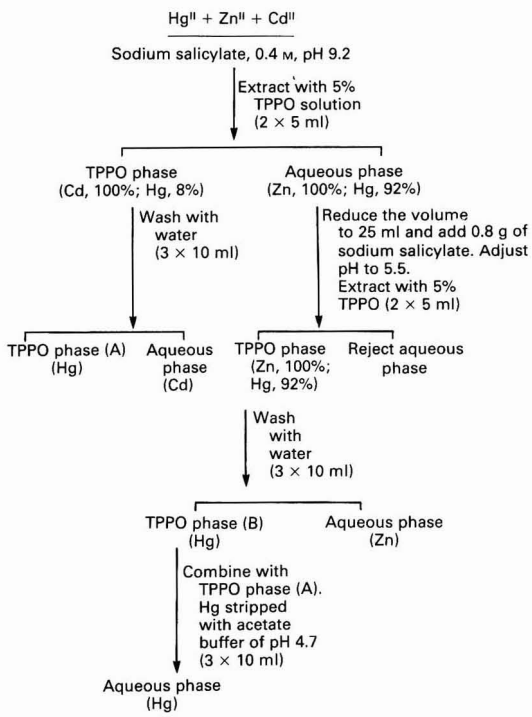

Fig. 5. Flow sheet for the separation of Zn^{II}, Cd^{II} and Hg^{II} in their ternary mixtures

Two types of effluent (treated and untreated) from two different industries were analysed for their content of mercury. One of the effluents (I) was generated from the industrial manufacture of different categories of products such as rayon textile yarn, rayon fabric, sulphuric acid, caustic soda, carbon disulphide and liquid chlorine, and the other industrial effluent (II) was generated in the manufacture of caustic soda, hydrochloric acid and liquid chlorine.

The process of manufacture of caustic soda involves the use of an electrode consisting of brine and mercury. The wastewater from this plant is an alkaline medium containing trace amounts of mercury. The specific parameter prescribed by the statutory agencies for industrial effluent I is mercury, whereas for effluent II the parameters are mercury and zinc.

Untreated effluent (I and II; 100 ml each) and treated effluent (I, 1 l; II, 500 ml) were evaporated on a hot-plate to reduce the respective volumes to about 15 ml. They were digested with 2 ml of concentrated sulphuric acid for 10 min and subsequently, the solutions were diluted to 25 ml and used for the extraction of mercury by the recommended procedure. The results were found to be in good agreement with the results obtained by the Central Laboratory, Maharashtra Pollution Control Board (Bombay, India) using a mercury analyser.

2. *Fish*

Fish belonging to the genus *Mugil* (found dead in Thane-Belapur creek, New Bombay, India; cause of death water pollution) was analysed for the presence of heavy metals such as cadmium and mercury. The muscle, tissues and other visceral parts of the fish were dried in an oven at 105 °C for 5 min to remove the moisture content. The dried sample (500 mg) was digested with 2–3 ml of concentrated sulphuric acid. The acid extract was diluted to approximately 25 ml and filtered. The filtrate was diluted to 50 ml and an aliquot of this solution was used for the determination of cadmium and mercury by the recommended extraction procedure.

3. *Kidney stone sample*

Three different samples of kidney stones were finely ground and 100 mg of each was dissolved in 2–3 ml of concentrated sulphuric acid. The solutions were evaporated to dryness and the residue was taken up with water. (Calcium sulphate was filtered off and microgram amounts of calcium were masked with sodium pyrophosphate.) The solution was diluted to 100 ml and from this an aliquot portion was taken for the extraction and determination of cadmium by the proposed method.

4. *Cigarette (Golden Flair Delux Filter)*

The tobacco contents of two cigarettes were dissolved in 2 ml of concentrated sulphuric acid and heated on a hot-plate for 20 min. The black residue obtained after diluting with water was eliminated by filtration. This solution was used for the extraction and determination of cadmium by the proposed method.

The results for the analysis of mercury and cadmium in the above-mentioned samples were also comparable with the known analytical methods.[1,24] The results for the determina-

Table 5. Mutual separation of zinc, cadmium and mercury from ternary mixtures

	Amount taken/mg			Amount found*/mg			Recovery,* %		
Sample No.	Zn	Cd	Hg	Zn	Cd	Hg	Zn	Cd	Hg
1	1.0	1.5	1.0	0.997	1.49	0.992	99.7	99.3	99.2
2	2.0	1.0	1.5	1.99	0.994	1.49	99.5	99.4	99.3
3	1.0	2.0	1.0	0.998	1.99	0.995	99.8	99.5	99.5

* Mean of six results.

Table 6. Determination of mercury in environmental samples

Sample	Composition, p.p.m.	Recovery data: Amount of Hg^{II} added, p.p.m.	Total amount of Hg^{II} recovered by the proposed method, p.p.m.	Amount of Hg^{II} found in the effluent sample by difference (mean of six determinations), p.p.m.	RSD, %	Amount of Hg^{II} found in the effluent sample using a mercury analyser,‡ p.p.m.
1. *Industrial effluent I*—						
Treated	Dissolved O_2, 6.7; BOD* (after 5 d at 20 °C), 26.0; COD,† 24.2; suspended solids, 20.2; albuminoid, 0.4; residual chlorine, nil; zinc, nil; mercury, 0.037; pH, 8.71	0.03	0.069	0.039	3.02	0.037
Untreated	—	0.04	0.139	0.099	2.95	0.083
2. *Industrial effluent II*—						
Treated	Dissolved O_2, 3.2; BOD (after 5 d at 20 °C), 24.0; COD, 35.2; suspended solids, 42.0; albuminoid, 0.38; mercury, 0.013; pH, 9.95	0.05	0.063	0.013	6.90	0.013
Untreated	—	0.06	0.168	0.108	2.86	0.109

* BOD = biological oxygen demand.
† COD = chemical oxygen demand.
‡ Analysis performed at the Maharashtra Pollution Control Board (Bombay, India) using a mercury analyser. The fish sample was found to contain 200 p.p.m. (mean of six determinations; RSD, 1.4%) of mercury.

Table 7. Determination of cadmium in biological and commercial samples

Sample	Proposed method: Cadmium(II),* p.p.m.	Proposed method: RSD, %	PAR method[1]: Cadmium(II), p.p.m.
1. Fish	40.0	1.4	41.2
2. Kidney stone			
Sample a	22.5	1.2	22.4
Sample b	42.8	1.1	43.0
Sample c	60.0	1.2	59.8
3. Cigarette	3.46	1.8	3.4

* Mean of six determinations.

tion of mercury in the environmental samples are shown in Table 6 and those for cadmium in Table 7.

Interpretation of Results

According to the effluent standards laid down by statutory agencies for pollution control, for the effluents released into saline water, the level of mercury should not exceed 0.01 p.p.m. In the untreated effluent samples analysed, the mercury level was found to be more than the permitted limit. In the treated sample of effluent I, the mercury level exceeded the above tolerable limit. However, in the treated sample of effluent II, the mercury level seemed to be within the permissible limit.

Very high levels of both cadmium and mercury in the sample of dead fish indicates a higher level of pollution than is perhaps advisable.

The content of cadmium in one particular brand of cigarette was found to be 3.46 p.p.m. As cadmium is a cumulative kidney poison, the levels of cadmium in tobacco should be monitored.

Conclusions

1. The proposed method has been successfully applied to the separation and determination of zinc(II), cadmium(II) and mercury(II), both in binary and ternary mixtures.
2. The method is rapid and the operation of one complete analysis takes about 20 min.
3. The separation and determination of cadmium(II) and mercury(II) in environmental samples is possible using the proposed method.
4. The method has good precision.

The authors thank the Council of Scientific and Industrial Research, New Delhi, India for financing this project and also the Maharashtra Pollution Control Board for providing the samples.

References

1. Kalyanaraman, K., and Khopkar, S. M., *J. Ind. Chem. Soc.*, 1979, **56**, 203.
2. Kish, P. P., and Balog, I. S., *Zh. Anal. Khim.*, 1979, **34**, 2326.

3. Matsui, M., Doe, H., Hirade, T., and Shigematsu, T., *Anal. Lett.* 1979, **12A**, 1385.
4. Rico Selas, M. I., Climent Morato, M. D., and Jimenez Gomez, S., *An. Quim.*, 1978, **74**, 919.
5. Mudshingikar, V. V., and Shinde, V. M., *Talanta*, 1983, **30**, 405.
6. Otomo, M., and Singh, R. B., *Anal. Sci.*, 1985, **1**, 165.
7. Pietsch, R., and Gilani, P. T., *Anal. Chim. Acta*, 1975, **75**, 385.
8. Dominguez, R. J. G., and Irgolic, K. J., *Anal. Chim. Acta*, 1976, **84**, 109.
9. Uhlemann, E., Maack, B., and Raab, M., *Anal. Chim. Acta*, 1980, **116**, 403.
10. Nakamura, K., and Ozawa, T., *Anal. Chim. Acta*, 1976, **86**, 147.
11. McDonald, C. W., and Sheng, L. T., *Sepn. Sci.*, 1975, **10**, 499.
12. de Jong, G. J., Brinkman, U. A. T., and Kok, W. T., *J. Radioanal. Chem.*, 1977, **35**, 245.
13. Singh, O. V., and Tandon, S. N., *J. Radioanal. Chem.*, 1977, **36**, 331.
14. McDonald C. W., and Hussein, P. G., *Sepn. Sci.*, 1977, **12**, 271.
15. Patil, P. S., and Shinde, V. M., *Chem. Anal. (Warsaw)*, 1977, **22**, 1067.
16. Bock, R., and Pulf, H. S., *Z. Anal. Chem.*, 1971, **14**, 255.
17. Singh, J. M., Singh, O. V., and Tandon, S. N., *Indian J. Chem., Sect. A*, 1978, **16**, 1001.
18. De, A. K., Ray, U. S., and Parhi, N., *Indian J. Chem., Sect. A*, 1984, **231**, 140.
19. McClellan, B. E., Meredith, M. K., Parmelae, R., and Beck, P. J. P., *Anal. Chem.*, 1974, **46**, 306.
20. McDonald, C. W., and Hussein, P. G., *Mikrochim. Acta*, 1982, **II**, 77.
21. Singh, O. V., and Tandon, S. N., *Radiochem. Radioanal. Lett.*, 1974, **19**, 371.
22. Vogel, A. I., "A Textbook of Quantitative Inorganic Analysis," Longmans, London, 1961, p. 444.
23. Welcher, F. J., "The Analytical Uses of Ethylenediamine Tetraacetic Acid," Van Nostrand, New York, 1961, p. 164.
24. Eshwar, M. C., and Sharma, C. D., *Ind. J. Technol.*, 1986, **24**, 161.

Paper 8/03336F
Received August 17th, 1988
Accepted July 7th, 1989

Spectrophotometric Determination of Hydrogen Peroxide Using Tris(1,10-phenanthroline)iron(II)

Hüseyin Afşar
Department of Chemistry, Faculty of Science, Yıldız University, Şişli, Istanbul, Turkey
Reşat Apak* and İzzet Tor
Department of Chemistry, Faculty of Engineering, Istanbul University, Vezneciler, Istanbul, Turkey

Hydrogen peroxide reacts with iron(II) in acidic medium, and the unreacted iron(II) forms a stable complex with 1,10-phenanthroline that absorbs at 508 nm. This indirect spectrophotometric method, based on the absorbance reduction of tris(1,10-phenanthroline)iron(II) was utilised for the determination of hydrogen peroxide. The effective molar absorptivity for H_2O_2 is 2.22×10^4 l mol^{-1} cm^{-1}. The proposed procedure is sensitive and has been applied to the analysis of commercial peroxide samples. Possible interferences are discussed.

Keywords: *Hydrogen peroxide determination; visible spectrophotometry; 1,10-phenanthroline; tris(1,10-phenanthroline)iron(II)*

The methods reported for the spectrophotometric determination of H_2O_2 involve reactions based on the production of coloured peroxy compounds, the oxidation of reducing dyes, the formation of organometallic complexes or the reduction of hexacyanoferrate(III). In this regard, the colorimetric procedures using thiocyanate,[1–3] molybdate,[4] iodide,[5–7] peroxytitanate,[8–11] Indigo Carmine,[12,13] hexacyanoferrate(III),[14] *p*-dimethylaminobenzaldehyde,[15] sulphosalicylate,[16] metal chelates of benzohydroxamic acid,[17] metavanadate,[18,19] manganate(VI),[20] phenolphthalein[21,22] and the copper(II) complex of *p*-toluidine (*p*-aminotoluene)[23] could be mentioned.

Recent procedures for the determination of H_2O_2 and organic hydroperoxides at the micromolar level were classified[24] as follows: the formation of phenolphthalein or triiodide; catalytic dye bleaching; the coupled oxidation of reduced nicotinamide adenine dinucleotide phosphate; and horseradish peroxidase coupled oxidations. However, the linearity of the absorbance - concentration graphs of the first two methods was not satisfactory.

The decrease in the molar absorptivity of the vanadium(V) - Xylenol Orange reagent due to peroxy complex formation has been used to determine H_2O_2[25]; however, the magnitude of this decrease depended on the ratio of vanadium to Xylenol Orange in addition to the pH. The titanium(IV) - 4-(2-pyridylazo)resorcinol monosodium salt (PAR) method had a narrow linear range[26] and turbidity problems were encountered for food samples.[27] The methods based on the formation of a quinoid dye by 4-aminoantipyrine and *N,N*-diethylaniline,[28–30] or the peroxidase-catalysed oxidation of the leuco forms of basic dyes,[31] which are sensitive, were not highly selective for H_2O_2.

The sensitive method based on the tris(1,10-phenanthroline)iron(II) complex, which was reported by Bailey and Boltz,[32] leads to serious error. Hence a method using 1,10-phenanthroline for the indirect determination of H_2O_2 has been established and tested for inorganic and organic peroxide samples.

Experimental

Except for ethyl methyl ketone peroxide (EMKP) (2-butanone peroxide) (Fluka) all reagents were supplied by Merck and were of analytical-reagent grade. The aqueous stock solutions were prepared as follows.

Iron(II) sulphate, 0.1 M. Prepared from $FeSO_4.7H_2O$ in 2% H_2SO_4 solution and standardised with disodium ethylenediaminetetraacetate.

Hydrogen peroxide, 0.1 M. Prepared from commercial hydrogen peroxide and standardised with permanganate solution.

1,10-*Phenanthroline* (*phen*), 0.1 M. Prepared from 1,10-phenanthroline monohydrate ($C_{12}H_8N_2.H_2O$) in 0.25 M HCl.

Sodium perborate, 0.1 M. Prepared from $NaBO_2.H_2O_2.3H_2O$ in a 0.025 M solution of citric acid.

Water, doubly distilled over permanganate was used in all experiments. Working solutions were prepared from the corresponding stock solutions and the absorption spectra were recorded with a Perkin-Elmer 554 UV - visible spectrophotometer. An Oxford Analytical Instruments (Abingdon, Oxford, UK) automatic pipette was used for the kinetic studies and pH adjustments were made using a Wiss-Techn. digital 510 pH meter.

Procedure for Construction of the Calibration Graph

To establish the calibration graph of concentration of H_2O_2 *versus* absorbance, 0.5–5.0-ml aliquots (in 0.5-ml increments) of a 1×10^{-3} M solution of H_2O_2 were added to ten 100-ml calibrated flasks, each containing 1 ml of a 1×10^{-2} M solution of Fe^{II}. The flasks were agitated for 10 min at room temperature. Subsequently 4 ml of a 1×10^{-2} M solution of phen were added to each flask, the solutions diluted to the mark with distilled water and the absorbances were recorded at 508 nm *versus* distilled water. Similar experiments were carried out with ammonium peroxydisulphate by using 1×10^{-3} M $(NH_4)_2S_2O_8$ solution in place of the H_2O_2 solution.

Procedure for Determining the Optimum pH Interval and Time

Buffer solutions of pH 1.1, 1.5, 2.5 and 3.5 were prepared by mixing solutions of 0.1 M HCl and 0.1 M glycine and 0.1 M NaCl in the appropriate proportions.

To 11 100-ml calibrated flasks, 25 ml of the buffer solution and 1 ml of 0.01 M Fe^{II} solution were added. The first flask received 4 ml of 0.01 M phen and was diluted to the mark with water. To each of the remaining ten flasks were added 2 ml of 1×10^{-3} M H_2O_2. The flasks were stoppered and agitated. Each minute, up to the tenth minute after H_2O_2 addition, 4-ml aliquots of 0.01 M phen solution were added to each flask, respectively, and the solutions were diluted to the mark with distilled water.

* To whom correspondence should be addressed.

The contents of the flask not containing H_2O_2 were transferred into the sample cell. The reference cell was filled with each of the H_2O_2-containing solutions and the absorption differences at 508 nm were recorded.

Procedure for Determining EMKP

Starting from a 50% technical sample of EMKP, *i.e.*, a sample containing 50% plasticiser, a 0.27 M solution was prepared by dilution with ethyl methyl ketone (EMK). A 0.1-ml aliquot of this solution was transferred into a 100-ml flask and 5 ml of 0.1 M $FeSO_4$ were added. Dilute H_2SO_4 was added dropwise until a clear solution was obtained and the contents of the flask were diluted to the mark with water. This solution (5 ml) was pipetted into a 100-ml flask, 2 ml of 0.05 M phen were added and the mixture was diluted to the mark with water. The corresponding concentration of EMKP, calculated for the final solution, was 1.35×10^{-5} M. With the EMKP solution in the reference cell and the reagent blank in the sample cell, the absorption difference was measured directly at 508 nm.

Results and Discussion

Critical Evaluation of Previous Work

In the work reported by Bailey and Boltz,[32] H_2O_2 was reacted with an excess of ammonium iron(II) sulphate and the unoxidised Fe^{II} was determined colorimetrically by measuring the absorbance of its complex with phen. However, the optimum conditions of analysis were not specified and the concentration of H_2O_2 was calculated[32] by the use of the following equation, which is erroneous:

$$A = \varepsilon l(c_{Fe_0} - 0.5c_{H_2O_2}) \quad .. \quad .. \quad (1)$$

where A is the decrease in the absorption of the solution at 508 nm, l is the optical cell thickness, c_{Fe_0} is the initial molar concentration of Fe^{II}, $c_{H_2O_2}$ is the molarity of H_2O_2 and ε represents the molar absorptivity of tris(1,10-phenanthroline)iron(II).

$$2Fe^{2+} + H_2O_2 + 2H^+ \rightarrow 2Fe^{3+} + 2H_2O \quad .. \quad (2)$$

equation (1) is wrong and the redox valency of H_2O_2 is 2, not 1/2. With the initial and final (following the reaction with H_2O_2) concentrations of Fe^{II} defined as c_{Fe_0} and c_{Fe}, respectively, and substituting 1/2 $(c_{Fe_0} - c_{Fe})$ for $c_{H_2O_2}$, then, according to equation (2), the absorbance difference, ΔA, would be given by

$$\Delta A = \varepsilon l(c_{Fe_0} - c_{Fe}) = \varepsilon l(2c_{H_2O_2}) = \varepsilon' l c_{H_2O_2} \quad .. \quad (3)$$

where ε', the molar absorptivity of H_2O_2, is twice that of the tris(1,10-phenanthroline)iron(II) complex.

Recognising that the molar absorptivity of the phen - iron(II) complex is $\varepsilon = 1.11 \times 10^4$ l mol^{-1} cm^{-1},[33] the actual value of ε' for H_2O_2 is 2.22×10^4 l mol^{-1} cm^{-1}, four times that reported[32] previously. In addition, the working pH for Bailey and Boltz's studies[32] was 4 and the reaction is slow at this pH as the work decribed here shows. If all the H_2O_2 has not reacted by the time phen is added, the possibility still exists for the phen - Fe^{III} complex to be reduced to the phen - Fe^{II} complex in weakly acidic/neutral solution, where the rate of this (reverse) reaction would be favourable.[34,35] For example, the oxidation of H_2O_2 by tris(2,2′-bipyridyl)iron(III), *i.e.*,

$$2[Fe(bipy)_3]^{3+} + H_2O_2 \rightarrow 2[Fe(bipy)_3]^{2+} + O_2 + 2H^+$$

was reported to proceed to the right quantitatively, the rate constant displaying an inverse dependence on acid in neutral solution.[34] Therefore, the possibility of incomplete reaction in the method described in reference 32 further reduces the likelihood of obtaining quantitative results.

From Fig. 1, A, it can be seen that 1 μmol of Fe^{II} plus 4 μmol of phen in 10 ml of solution would give a maximum absorbance of 1.12 at 508 nm against a phen blank or distilled water. This absorbance was halved ($A_{508} = 0.56$) when 0.25 μmol of H_2O_2 was added to 1 μmol of Fe^{II} in the pH range 2–4, followed by the addition of 4 μmol of phen after 10 min of agitation, with the total volume being kept constant at 10 ml (Fig. 1, B). Apparently, 0.25 μmol of H_2O_2 oxidised 0.50 μmol of Fe^{II}, confirming the validity of equation (2), and only half of the original Fe^{II} iron remained in solution to form the coloured phen chelate. The Fe^{II}, Fe^{III}, phen and H_2O_2 did not absorb against water in the spectral region of interest (Fig. 1, C–F).

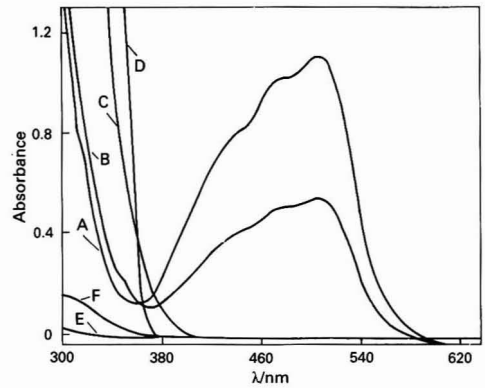

Fig. 1. Absorption spectra: A, 10^{-4} M Fe^{II} + 4×10^{-4} M phen; B, 0.25 μmol of H_2O_2 added to 1 μmol of Fe^{II} at pH 2–4; 4 μmol of phen added after 10 min (total volume, 10 ml); C, 10^{-4} M Fe^{II}; D, 10^{-4} M Fe^{III}; E, 4×10^{-4} M phen; and F, 2.5×10^{-5} M H_2O_2

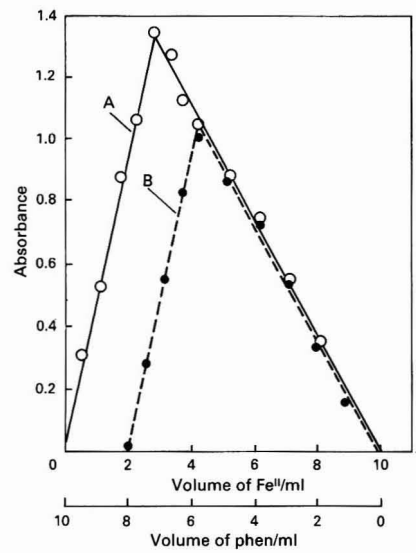

Fig. 2. Job plot for the Fe^{II} - phen complex in the presence and absence of H_2O_2. Concentrations of isomolar solutions mixed, 5×10^{-3} M; total volume, 100 ml; λ, 508 nm. A, Fe^{II} - phen; and B, Fe^{II} - H_2O_2 - phen. H_2O_2 (5 μmol) was added to each Fe^{II} solution of the series 10 min before the addition of phen (total volume, 100 ml)

Job's method of continuous variations[36] was applied to the isomolar series of 5×10^{-3} M solutions of Fe^{II} and phen in a total volume of 100 ml and the absorbances were recorded at 508 nm against water. Fig. 2, A shows the Job plot for 1 mol of Fe^{II} with 3 mol of ligand. When 2 ml of 2.5×10^{-3} M (5 μmol) H_2O_2 were added to each solution of Fe^{II} in the series and stirred for 10 min, Fig. 2, B was obtained following the

Table 1. Results of the regression analysis of the absorbance - concentration data

Substance	Linear correlation coefficient	Intercept on A-axis ($c = 0$)/A	Slope (dA/dc)/ A l mol^{-1}
H_2O_2	−0.9983	1.102	-2.16×10^4
$(NH_4)_2S_2O_8$	−0.9994	1.111	-2.19×10^4
$NaBO_2.H_2O_2.3H_2O$	−0.9995	1.142	-2.26×10^4

addition of phen as before; the total volume was kept constant at 100 ml. The maximum absorbance for the latter series was obtained for 4 ml of Fe^{II} - 6 ml of phen, indicating that 10 μmol of Fe^{II} remained after H_2O_2 oxidation, *i.e.*, one-third of the amount of phen. Again, this showed that 5 μmol of H_2O_2 reacted with 10 μmol of Fe^{II}. The observation that Fe^{II} (2 ml) - phen (8 ml) did not absorb after the addition of H_2O_2 was further confirmation that the reacting mole ratio of Fe^{II} : H_2O_2 was 2 : 1.

Calibration Graph

For constructing a concentration *versus* absorbance graph, a standard solution of H_2O_2, or substances that are known to hydrolyse to H_2O_2 in aqueous solution, *e.g.*, ammonium peroxydisulphate or sodium perborate, could be used. The $(NH_4)_2S_2O_8$ and $NaBO_2.H_2O_2.3H_2O$ each yield 1 mol of H_2O_2 per mol of substance in aqueous solution in acidic medium.[37,38]

The concentrations of Fe^{II} and phen were maintained at 1.0×10^{-4} and 4.0×10^{-4} M, respectively. The calibration graphs were linear for the three substances tested and regression analysis by the least-squares approximation yielded the data given in Table 1.

From the data in Table 1 the following line equation (to two significant figures) was obtained:

$$A = -2.2 \times 10^4 c + 1.1 \quad .. \quad .. \quad (4)$$

where A is the absorbance at 508 nm and c is the initial concentration of peroxide. The molar absorptivity for peroxide is 2.2×10^4 l mol^{-1} cm^{-1}.

Effect of Iron(II) Concentration

For the determination of peroxide, an excess of Fe^{II} should be taken so that the final (unoxidised) Fe^{II} would remain measurable spectrophotometrically. For six constant concentrations of H_2O_2, the absorbances were plotted as a function of the concentration of Fe^{II}; an Fe^{II} : phen mole ratio of 1 : 4 was maintained in all solutions (Fig. 3). The lines obtained had a constant slope $dA/d[Fe^{II}] = 1.11 \times 10^4$ A l mol^{-1} and a graph of slope *versus* concentration of H_2O_2 yielded a straight line, showing that the rate of change of absorbance with the concentration of Fe^{II} was not a function of the concentration of H_2O_2. Similarly, for three constant concentrations of Fe^{II}, plots of A *versus* $[H_2O_2]$ were linear with constant slopes, and, therefore, the absorbance was independent of the concentration of Fe^{II}, *i.e.*, $dA/d[H_2O_2] = -2.22 \times 10^4$ A l mol^{-1} (Fig. 4).

Working pH

The choice of the appropriate pH should be made by considering the effect of pH on the reaction of Fe^{II} with H_2O_2, and on the reactions of Fe^{II} and Fe^{III} with phen. Moreover, the hydrolytic precipitation pH values of Fe^{II} and Fe^{III} should not be exceeded.

Knowing the equilibrium constant for the reaction[39]

$$Fe(OH)_3 + 3phen \rightleftharpoons [Fe(phen)_3]^{3+} + 3OH^-, \quad K = 10^{-14}$$

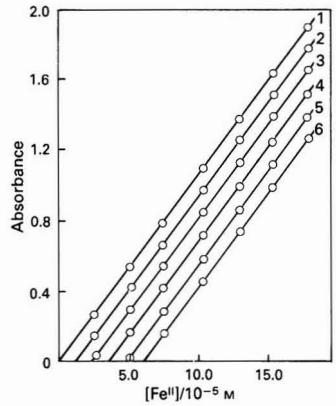

Fig. 3. Variation of A_{508} with Fe^{II} concentration. Fe^{II}: phen mole ratio, 1 : 4 (constant). $dA/d[Fe^{II}]$, 1.11×10^4 A l mol^{-1}. $[H_2O_2]$: 1, 0; 2, 0.6×10^{-5}; 3, 1.2×10^{-5}; 4, 1.8×10^{-5}; 5, 2.4×10^{-5}; and 6, 3.0×10^{-5} M

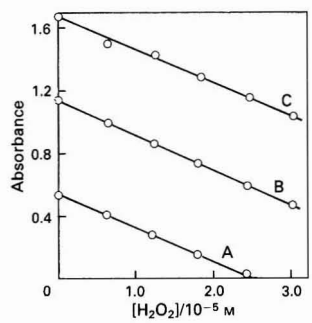

Fig. 4. Variation of A_{508} with H_2O_2 concentration. Fe^{II}: phen mole ratio, 1 : 4 (constant). $dA/d[H_2O_2] = -2.22 \times 10^4$ A l mol^{-1}. $[Fe^{II}]$: A, 5×10^{-5}; B, 10×10^{-5}; and C, 15×10^{-5} M

the maximum allowable concentration of OH^- to prevent hydrolytic precipitation of Fe^{III} can be calculated from

$$[OH^-]_{max.} = (L_T - 3M_T)\left[\frac{K}{M - (A/\varepsilon)}\right]^{\frac{1}{3}} \quad .. \quad (5)$$

where L_T and M_T are the total concentrations of phen and Fe^{II} and A is the final absorbance. Precautions should be taken to ensure that a pH of 6.5 is not exceeded for colour development.

Optimum pH Interval for the Oxidation of Fe^{II} With H_2O_2

Although a neutral medium would allow colour development in the presence of excess of phen without hydrolytic precipitation of Fe^{III}, the oxidation of Fe^{II} by H_2O_2 [equation (2)] would require an acidic medium, as the rate of this oxidation is decreased by an increase in pH. If all of the H_2O_2 has not reacted by the time phen is added, its reaction with Fe^{II} might not proceed further as the pH is shifted from acid to neutral. The $[Fe(phen)_3]^{3+}$ - $[Fe(phen)_3]^{2+}$ redox couple has a standard potential of 1.06 V, which is higher than that of the Fe^{3+} - Fe^{2+} couple, *i.e.*, 0.77 V. In acidic and basic media H_2O_2 has standard potentials of 1.77 and 0.88 V, respectively. Therefore, if the H_2O_2 reaction has not gone to completion at the time of addition of phen, the remaining Fe^{II} bound in the $[Fe(phen)_3]^{2+}$ complex would require a strongly acidic medium for oxidation. Such a medium would enhance undesired side reactions. Hence a suitable initial pH should be selected for the complete reduction of H_2O_2.

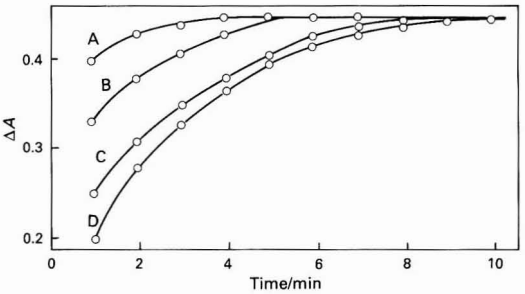

Fig. 5. Variation of H_2O_2 - Fe^{II} reaction period with pH. Sample cell contents, 10^{-4} M Fe^{II} and 4×10^{-4} M phen. Reference cell contents, same as sample cell plus 2×10^{-5} M H_2O_2; direct read-out of absorbance difference at 508 nm. Time scale represents the number of minutes elapsed between H_2O_2 and phen additions. pH: A, 1.1; B, 1.5; C, 2.5; and D, 3.5

The procedure for determining the optimum pH interval was followed (see under Experimental). The absorption differences were plotted as a function of the time period allowed for the reaction of H_2O_2 prior to the addition of phen (Fig. 5). The time required for the complete reaction of H_2O_2 is increased at higher pH.

Therefore, a pH of between 1 and 3 should be selected for the rapid reduction of H_2O_2 by Fe^{II}. At the same time, the effect of dissolved oxygen is minimised, and the precipitation of iron(III) hydroxide prevented. After allowing 10 min for the reaction of H_2O_2, the subsequent colour development with phen should be carried out in the pH range 2–6.

Effect of Interferents

The stabiliser chemicals that usually exist in commercial solutions of H_2O_2 were investigated with respect to their effects on the determination of H_2O_2. For 2.5×10^{-5} M H_2O_2, up to 8.3×10^{-3} M urea gave an absorption difference of 0.04–0.05 A less than the expected value, the magnitude of which was not dependent on the concentration of urea. Up to 2.4×10^{-3} M acetanilide gave a similar result, *i.e.*, 0.02–0.03 A less than expected. Nevertheless, H_2O_2 could be determined in the presence of both substances by the method of standard additions. Potassium bromide did not interfere, whereas $CoSO_4$ interfered seriously and the determination of H_2O_2 was not possible. The anions F^-, Cl^- and SO_4^{2-} did not interfere. Phosphate accelerated the Fe^{II} - H_2O_2 reaction, but a concentration of PO_4^{3-} of >100 p.p.m. required the use of more phen than usual.

The Zn^{II}, Cu^{II}, Cd^{II} and Fe^{III} cations that also formed complexes with phen did not interfere at concentrations of <10–12 p.p.m, whereas Hg^{II}, Ag^{I} and Sn^{II} did interfere As regards the possible use of the proposed method for the determination of H_2O_2 in biological materials, uric acid, adenine and guanine did not have any effect whereas cysteine interfered, possibly due to the presence of the thio group in its structure.

Clearly, oxidising agents having a higher standard potential than that of the Fe^{III} - Fe^{II} couple or reductants capable of reducing H_2O_2 should not be present in the determination of H_2O_2.

Application of the Method to the Analysis of an Organic Peroxide

It was found that 1 mol of EMKP yielded 1 mol of H_2O_2 in solution which could be determined by the proposed method, although EMKP actually contains 2 molecules of peroxide oxygen per molecule, *i.e.*, $C_2H_5C(OOH)(CH_3)OOC(OOH)(CH_3)C_2H_5$. Such determinations should be carried out with respect to the same type of organic peroxide as the standard of comparison. The peroxide content of commercial 1,4-dioxane could also be determined by this method.

Sensitivity and Precision

As the molar absorptivity of the method for the determination of H_2O_2 is 2.22×10^4 l mol^{-1} cm^{-1}, a minimum measurable absorbance difference of 0.01 in a 1-cm cell corresponds to a concentration of 4.50×10^{-7} M, or 15.3 p.p.b., of H_2O_2. The relative standard deviation of ten measurements at the 10^{-5} M level is about 4%.

Recommended Procedure for the Determination of H_2O_2 With Phen

Place 1 ml of a 1.0×10^{-2} M $FeSO_4$ solution prepared in 0.05 M H_2SO_4 in a 100-ml calibrated flask. Add a suitable aliquot of the H_2O_2 sample containing 1–4 μmol of H_2O_2 and adjust the pH to 1–3 if necessary. Stopper the flask and mix well at room temperature for 10 min. Add a 4-fold amount (compared with Fe^{II}) of phen, *i.e.*, 4 ml of the 1.0×10^{-2} M solution. (Adjust the pH to 2–6 prior to the addition of phen if necessary.) Dilute to the mark with water and transfer the mixture into the reference cuvette. With a reagent blank not containing H_2O_2 measure the absorbance difference at 508 nm and then calculate the molar concentration of H_2O_2 by dividing the absorbance difference by the molar absorptivity.

For a single-beam spectrophotometer, run four standards and one blank with three different aliquots of the sample and calculate the peroxide content from the calibration graph, plotted as ΔA *versus* concentration.

References

1. Stokes, H. N., and Cain, J. R., *J Am. Chem. Soc.*, 1907, **29**, 411.
2. Ragazzi, E., and Vanin, G. M., *Bull. Chim. Farm.*, 1961, **100**, 745.
3. Petruj, J., Zehnacker, S., Sedlar, J., and Marchal, J., *Analyst*, 1986, **111**, 671.
4. Isaacs, M. L., *J. Am. Chem. Soc.*, 1922, **44**, 1662.
5. Patrick, W. A., and Wagner, H. B., *Anal. Chem.*, 1949, **21**, 1279.
6. Ovenston, T. C. J., and Rees, W. T., *Analyst*, 1950, **75**, 204.
7. Graf, E., and Penniston, J T., *Clin. Chem.*, 1980, **26**, 658.
8. Eisenberg, G. M., *Ind. Eng. Chem. Anal. Ed.*, 1943, **15**, 327.
9. Allsopp, C. B., *Analyst*, 1941, **66**, 371.
10. Cohen, I. R., and Purcell, T. C., *Anal. Chem.*, 1967, **39**, 131.
11. Matsubara, C., and Takamura, K., *Microchem. J.*, 1977, **22**, 505.
12. Krause, A., and Slawek, J., *Monatsh. Chem.*, 1968, **99**, 1494.
13. Sychev, A. Y., Isak, V. G., and Nguyen, V. S., Deposited Document, 1980, SPSTL 56 Khp-D80; *Chem. Abstr.*, 1982, **96**, 144444c.
14. Aziz, F., and Mirza, G. A., *Talanta*, 1964, **11**, 889.
15. Das-Gupta, B. R., and Boroff, D. A., *Anal. Chem.*, 1968, **40**, 2060.
16. Celechovsky, J., Krejci, E., and Krejci, V., *Cesk. Farm.*, 1957, **6**, 103; *Chem. Zentralbl.*, 1958, **129**, 1660.
17. Meloan, C. E., Mauck, M., and Huffman, C., *Anal. Chem.*, 1961, **33**, 104.
18. Warburg, O., and Krippahi, G., *Z. Naturforsch.*, 1963, **18**, 340.
19. Schneider, J., and Csanyi, L. J., *Mikrochim. Acta*, 1976, **2**, 271.
20. Bubyreva, N. S., Bukhareva, V. I., Kirakosyon, A. K., Pantyukhova, T. A., and Rozenblyum, N. D, *Zavod. Lab.*, 1969, **35**, 1044.
21. Dukes, E. K., and Hyder, M. L., *Anal. Chem.*, 1964, **36**, 1689.
22. Margulova, T. K., Shavlova, T. S., Kuznetsov, V. S., Eshchenko, M. K., Poltarakova, L. P., and Chvatov, V. N., *Teploenergetika (Moscow)*, 1977, **4**, 91.
23. Filippova, K. I., and Stankevich, L P., *Sb. Tr. Mosk. Inzh-Stroit. Inst.*, 1971, **69**, 116.
24. Frew, J. E., Jones, P., and Scholes, G., *Anal. Chim. Acta*, 1983, **155**, 139.
25. Csanyi, L. J., *Microchem. J.*, 1981, **26**, 10.

26. Matsubara, C., and Takamura, K., *J. Pharmacobio-Dyn.*, 1980, **3**, S-3; *Chem. Abstr.*, 1980, **93**, 128202e.
27. Matsubara, C., and Takamura, K., *Bunseki Kagaku*, 1981, **30**, 682.
28. Umemoto, S., *Tokai-ku Suisan Kenkyusho Kenkyu Hokoku*, 1985, **116**, 57; *Chem. Abstr.*, 1986, **104**, 49938s.
29. Saito, Y., Mifune, M., and Nakashima, S., *Chem. Pharm. Bull.*, 1987, **35**, 869.
30. Johnson, K. S., Sakamoto-Arnold, C. M., Willason, S. W., and Beehler, C. L., *Anal. Chim. Acta*, 1987, **201**, 83.
31. Zepp, R. G., Skurlatov, Y. I., and Ritmiller, L. F., *Environ. Technol. Lett.*, 1988, **9**, 287.
32. Bailey, R., and Boltz, D. F., *Anal. Chem.*, 1959, **31**, 117.
33. Smith, G. F., and Richter, F. P., "Phenanthroline and Substituted Phenanthroline Indicators," G. Frederick Smith Chemical Company, Columbus, OH, 1944.
34. Macartney, D. H., *Can. J. Chem.*, 1986, **64**, 1936.
35. Pang, Y., and Xu, J., *Yaowu Fenxi Zazhi*, 1984, **4**, 350; *Chem. Abstr.*, 1985, **102**, 84504c.
36. Job, P., *Compt. Rend.*, 1925, **180**, 928.
37. Meyer, R. J., Pietsch, E. H. E., and Kotowski, A., *Editors*, "Gmelins Handbuch der Anorganischen Chemie, Part B," Springer-Verlag, Berlin, 1974, pp. 278–281, 802 and 822.
38. Meyer, R. J., Pietsch, E. H. E., and Kotowski, A., *Editors*, "Gmelins Handbuch der Anorganischen Chemie," Springer-Verlag, Berlin, 1974, pp. 158 and 677.
39. Dean, J. A., *Editor*, "Lange's Handbook of Chemistry," McGraw-Hill, New York, 1978.

Paper 9/00896I
Received March 1st, 1989
Accepted July 4th, 1989

SHORT PAPERS

Separation of the *ortho, meta* and *para* Isomers of Aminophenol by High-performance Liquid Chromatography

Chris J. Dowle and Andrew P. Malyan
ICI Wilton Materials Research Centre, P.O. Box 90, Wilton, Middlesbrough, Cleveland TS6 8JE, UK
Alasdair M. Matheson
Department of Pure and Applied Chemistry, University of Strathclyde, 295 Cathedral Street, Glasgow G1 1XL, UK

Reversed-phase high-performance liquid chromatography on a polystyrene - divinylbenzene column was applied to the qualitative and quantitative analysis of aminophenol positional isomers. The method is simple, rapid and more reproducible than the normal-phase system used previously.

Keywords: *Reversed-phase high-performance liquid chromatography; normal-phase high-performance liquid chromatography; aminophenol analysis*

The analysis of aminophenol isomers present in hair-dye using normal-phase ion-pair high-performance liquid chromatography (HPLC)[1] has overcome some of the difficulties associated with earlier techniques.[2,3] However, this requires a complex, six-component mobile phase. Reversed-phase systems have also been developed using less common, expensive stationary phases.[4,5] A normal-phase method was developed in our laboratories to monitor the purity of *meta*-aminophenol as a starting product in a polymerisation process. However, this was not very successful for studying aminophenol isomers and is discussed further here.

This paper describes an alternative, simple, routine method for the qualitative and quantitative analysis of aminophenol positional isomers, using a polystyrene - divinylbenzene column.

Experimental

Reagents

HPLC-grade solvents were obtained from Fisons.

All standard reagents and chemicals were obtained in the highest available purity from Aldrich, BDH and Eastman Kodak.

Apparatus

The HPLC system consisted of an Altex Model 110A pump, a Rheodyne 7125 injection valve with a 10-mm^3 loop, a Spectra-Physics SP8400XR UV - visible detector (λ = 295 nm) and a Knauer oven unit. A Polymer Laboratories PLRP-S HPLC column (250 × 4.7 mm i.d.) and Hichrom S5NH column (250 × 4.7 mm i.d.) were used for the reversed- and normal-phase methods, respectively.

Procedure

Normal-phase method

This was performed isocratically at a flow-rate of 2 cm^3 min^{-1} at ambient temperature. Stock solution A consisted of 1.0 g of tetraethylenepentamine dissolved in 100 cm^3 of methanol - dichloromethane (10 + 90). The mobile phase was prepared by adding 20 cm^3 of stock solution A, 180 cm^3 of dichloromethane and 100 cm^3 of methanol to a 1000-cm^3 calibrated flask and making up to the mark with hexane.

The column was conditioned before use with approximately 50 cm^3 of 10% v/v stock solution - dichloromethane. All samples were dissolved in dichloromethane - methanol (80 + 20).

Reversed-phase method

This was performed isocratically at a flow-rate of 1 cm^3 min^{-1}

Table 1. Resolution of adjacent aminophenol peaks at different concentrations of organic modifier

Concentration of modifier in mobile phase, % v/v	R_s (*para* - *meta*)	R_s (*meta* - *ortho*)
5	1.36	2.72
10	1.37	3.52
11	1.06	2.91
15	0.94	2.46

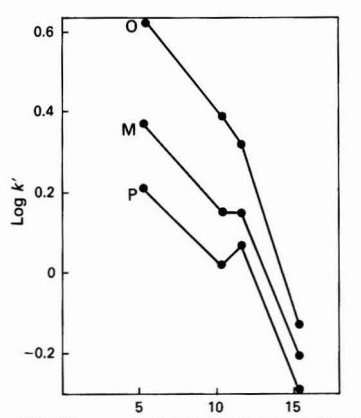

Fig. 1. Graph of logarithm of phase capacity ratio (k') *versus* modifier (CH_3CN) concentration at 80 °C, illustrating subsequent variation in solute retention. O, *ortho*-Aminophenol; M, *meta*-aminophenol; and P, *para*-aminophenol

over a range of temperatures with a water - acetonitrile eluent. Samples were dissolved in the appropriate eluent for the experiment being carried out.

A series of calibration standards covering the range 0–600 p.p.m. were prepared for both methods. Reproducibility was examined by repeated injections of 0.2% m/v *meta*-aminophenol in the eluent used in the optimised methods.

Results and Discussion

Two parameters were altered in the reversed-phase system: the modifier concentration and oven temperature.

Table 2. Resolution of adjacent aminophenol peaks at selected oven temperatures

Temperature/°C	R_s (*para* - *meta*)	R_s (*meta* - *ortho*)
24	0.98	3.01
40	1.23	3.01
60	1.06	2.71
80	1.37	3.52

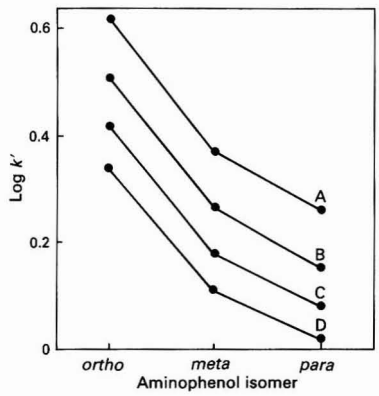

Fig. 2. Graph of logarithm of phase capacity ratio (k') against the different aminophenol isomers highlighting the effect of temperature on the system. Mobile phase: water - acetonitrile (90 + 10). Temperature: A, 24; B, 40; C, 60; and D, 80 °C

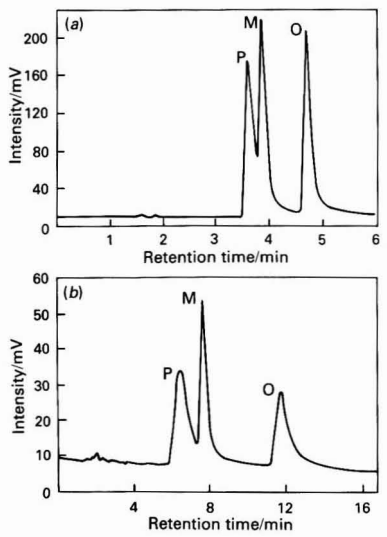

Fig. 3. Chromatograms obtained for (*a*) H_2O - CH_3CN (85 + 15) at 80 °C; and (*b*) H_2O - CH_3CN (90 + 10) at 24 °C. O, *ortho*-Aminophenol; M, *meta*-aminophenol; and P, *para*-aminophenol

The modifier concentration was adjusted from 95 + 5 to 85 + 15 v/v water - acetonitrile. The variation of the phase capacity ratio (k') with respect to the modifier content is shown in Fig. 1. This indicates that the polystyrene - divinylbenzene column interacts with the solute more strongly when the amount of modifier is decreased. The optimum resolution between pairs of adjacent isomers appeared to be obtained with water - acetonitrile (90 + 10). This was confirmed by calculation of the R_s values[6] (the relative resolution between pairs of solutes at 10% peak height) as given in Table 1.

Varying the oven temperature had a considerable impact on the chromatography as can be seen from Fig. 2. The results follow a predictable trend, namely, that at higher oven temperatures, the rate of mass transfer is more efficient, thus giving rise to peaks that elute more rapidly with greater sensitivity. Accordingly, from the values of R_s calculated from these results (Table 2), 80 °C was chosen as the optimum oven temperature. The R_s values of adjacent aminophenol peaks for the normal-phase method were: *ortho* - *para* 3.32 and *para* - *meta* 1.99.

Representative chromatograms for the two methods are shown in Figs. 3 and 4. The normal-phase method offers improved resolution, but has several serious drawbacks in comparison with the reversed-phase system, namely, severe drifting of peak position, a laborious conditioning step and long equilibration times. The relative standard deviations of the normal- and reversed-phase methods were 11.6 and 1.4%, respectively, for nine successive measurements of the retention time of the *meta* isomer. This highlights the superiority of

Table 3. Values of the correlation coefficient obtained from calibrations of each isomer for the normal- and reversed-phase methods

Analyte	Correlation coefficient: Normal-phase method	Correlation coefficient: Reversed-phase method
ortho-Aminophenol . .	0.9995	0.9996
meta-Aminophenol . .	0.9987	0.9980
para-Aminophenol . .	0.9997	0.9993

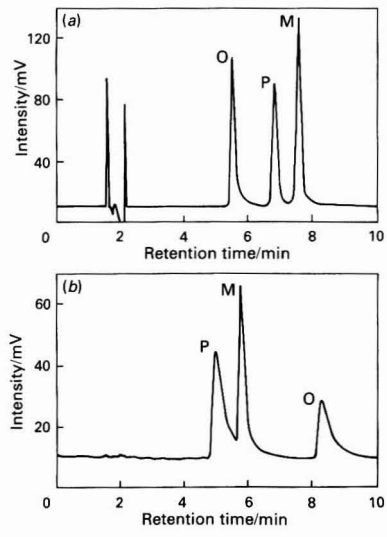

Fig. 4. Representative chromatograms of (*a*) normal-phase; and (*b*) optimised reversed-phase methods. O, *ortho*-Aminophenol; M, *meta*-aminophenol; and P, *para*-aminophenol

the polystyrene - divinylbenzene system in terms of reproducibility. Additionally, the system can be set up and running within 10 min as opposed to 45–60 min for the normal-phase method. A further disadvantage of the normal-phase system is that a residue forms in the mobile phase if it is left overnight.

Calibrations were very good for the *ortho-*, *meta-* and *para*-aminophenols for both the reversed- polystyrene - divinylbenzene and normal-phase methods, with similar values for the linear correlation coefficients, as can be seen from Table 3. Linear calibrations of peak area *versus* concentration were achieved for all isomers over the range 0–600 p.p.m.

Conclusions

A simple and rapid reversed-phase method suitable for the qualitative and quantitative analysis of *ortho-*, *meta-* and *para*-aminophenol has been developed. The system uses a polystyrene - divinylbenzene column to overcome the drawbacks associated with the previously preferred method. Although separation of the first pair of peaks is slightly poorer than in the previous normal-phase method, the reversed-phase system proved to be simpler, faster and more reproducible than the former method.

References

1. Hoogewijs, G., and Massart, D. L., *J. Pharm. Belg.*, 1983, **38**, 76.
2. Lien, D. H., "7th International Congress on Cosmetics, Quality and Safety," Blackwell Scientific, London, 1974, pp. 24–41.
3. Corbett, J. F., *in* Venkataraman, K., *Editor*, "The Analytical Chemistry of Synthetic Dyes," Wiley, New York, 1977, Chapter 18.
4. Goto, M., Koyanagi, Y., and Ishii, D., *J. Chromatogr.*, 1981, **208**, 261.
5. Allen Chang, C., Wu, Q., and Armstrong, D. W., *J. Chromatogr.*, 1986, **354**, 454.
6. Braithwaite, A., and Smith, F. J., "Chromatographic Methods," Chapman and Hall, London and New York, 1986.

Paper 9/03060C
Received July 19th, 1989
Accepted August 16th, 1989

Sensitive Benedict Test

Qing Chen, Nancy Klemm, Gregory Duncan and Ingming Jeng*
Department of Biochemistry, University of Missouri-Columbia, School of Medicine Neurochemistry Research Unit, Missouri Institute of Psychiatry, 5400 Arsenal, St. Louis, MO 63139, USA

The Benedict reaction is a versatile test for the detection of easily oxidised compounds. The use of 2,2′-bicinchoninic acid to detect the production of copper(I) in the Benedict test is described. This produced a test that is more sensitive than the classical Benedict test. A sensitive spot test for Benedict-positive compounds and a spray for compounds on thin-layer chromatographic plates is also described. Compounds are classified into three categories according to their sensitivity to the proposed Benedict test.

Keywords: *Benedict test; 2,2′-bicinchoninic acid; hydroxyketone; hydroxyaldehyde; ketoaldehyde*

The Benedict reaction is an extremely versatile test for the detection of numerous, easily oxidised compounds.[1] Included in the list of Benedict-positive compounds are reducing sugars, hydrazines, α-hydroxyketones, α-hydroxyaldehydes and α-ketoaldehydes. Under appropriate conditions these compounds selectively reduce copper(II) ion to copper(I) oxide, which appears as a yellow or red precipitate. This traditional method, although popular and useful, suffers from insensitivity, is not quantitative and is inapplicable to thin-layer chromatographic systems. We recently observed that the production of copper(I) ion in the classical Benedict test could be conveniently quantified by using 2,2′-bicinchoninic acid, which has also been employed to detect copper(I) formed in other reactions.[2,3] This paper describes the conditions required for utilising this principle in a sensitive spot test for Benedict-reactive compounds. Further, a method for detecting Benedict-positive compounds in thin-layer chromatographic plates is presented.

Results

For the spot test, we found the following method, adopted from a reported method for glucose and other reducing sugars,[2] appropriate. Briefly, 971 mg of disodium 2,2′-bicinchoninate is dissolved in an aqueous solution of 31.75 g of $Na_2HCO_3.H_2O$ and 12.1 g of NaH_2CO_3 to a total volume of 500 ml (solution A). For solution B, 624 mg of $CuSO_4.5H_2O$ and 631 mg of L-serine are dissolved in water to a total volume of 500 ml. Previously we had confirmed that L-serine is superior to tartrate as a selective complexing agent and tartrate is more specific for the determination of protein.[3] Both solutions A and B are kept refrigerated, stored in brown bottles. The test reagent is prepared just before use by mixing equal volumes of solutions A and B (we used one drop of test reagent and one drop of sample). The resulting solutions are heated on a heating block (set at 100 °C) or over a Bunsen burner in tubes covered with plastic caps containing small holes. At this stage the development of an intense purple colour constitutes a positive test. In general, the reaction is time and temperature dependent.

According to reactivity, compounds can be classified into the following categories.

Class A. Strongly positive compounds that develop significant colour within 10 min without heating. The colour intensifies upon heating. Examples are 2,4-dinitrophenylhydrazine, phenylhydrazine, L-ascorbic acid, 4-aminophenol, hydroxylamine, glucose and 4-hydroxyphenylglyoxal. A 0.02 mM solution is the lowest detection limit. In general, this group consists of the reducing sugars, hydrazines and easily oxidised α-ketoaldehydes, such as 4-hydroxyphenylglyoxal. It should be noted that non-activated α-ketoaldehydes belong to class B. 4-Hydroxphenylglyoxal is about five times more reactive than other non-activated α-ketoaldehydes, such as phenylglyoxal.

Class B. Moderately active compounds, the colour development of which requires 10 min or more of heating. Examples are butane-2,3-dione, pentane-2,3-dione, hexane-2,3-dione, hexane-3,4-dione, pyruvaldehyde, 1-phenylpropane-1,2-dione, phenylglyoxal hydrate, glyoxal and 4-methoxyphenylglyoxal. Heating for longer times up to 30 min, improves the sensitivity of the method. This group consists of most α-ketoaldehydes and aliphatic α-diketones. It should be noted that aromatic diketones are inactive and belong to class C. In general, a 0.1 mM solution is detectable.

Class C. Inactive compounds such as 2-hydroxyacetophenone, 3-hydroxyacetophenone, 4-hydroxyacetophenone, 2-methoxyacetophenone, 3-methoxyacetophenone, 4-methoxyacetophenone, 4-nitroacetophenone, 4,4′-dimethylbenzil, benzil and benzaldehyde belong to class C. Most of the non-substituted ketones or aldehydes are inactive as in the classical Benedict test. It should be noted that the 4-hydroxyphenyl group itself apparently does not impart reactivity, in contrast to the positive reaction in other similar reactions.[3]

We found that Benedict-positive compounds on thin-layer silica plates could be detected as follows. After the plate holding the samples was sprayed with the test reagent, it was heated in a microwave or conventional oven. Alternatively, the plate, covered with a clean glass plate, could be heated by steam over a beaker of boiling water. The purple spots appeared within 10 min. In general, a spot containing 10^{-9} nmol of class A or 10^{-8} nmol of class B compound is detectable.

Discussion

In the proposed method the time and temperature required for the formation of the colour are critical to distinguish between various classes of compounds. This method is several thousand times more sensitive than the well practised Benedict test, which involves visual inspection of the precipitates. It should also be noted that 10% ethanol or 10% sodium dodecyl sulphate was found to be tolerated in this assay. Organic compounds, less soluble in water, could be diluted initially in either ethanol or sodium dodecyl sulphate before further dilution in water prior to reaction.

* To whom correspondence should be addressed.

References

1. Shriner, R. L., Fuson, R. C., and Curtin, D. Y., "The Systematic Identification of Organic Compounds—A Laboratory Manual," John Wiley, New York, 1967, pp. 117–118.
2. Waffenschmidt, S., and Jaenicke, L., *Anal. Biochem.*, 1987, **165**, 337.
3. Smith, P. K., Krohn, R. I., Hermanson, G. T., Mallia, A. K., Gartner, F. H., Provenzano, M. D., Fujimoto, E. K., Goeke, N. M., Olson, B. J., and Klenk, D. C., *Anal. Biochem.*, 1985, **150**, 76.

Paper 9/03037I
Received July 18th, 1989
Accepted August 2nd, 1989

Letters

Letter by Dr. M. J. Cardone

I have read the recent paper by Bosch Reig and Campíns Falcó[1] and would like the opportunity to show that it actually represents an innovative extension of the corrigible error correction (CEC) technique.[2,3] They have shown that with their procedure an analyte concentration can be obtained free of bias error (both constant and proportional) both from a direct known interferent and from the true method blank under carefully stipulated conditions. Further, a determination of an interferent concentration can also be made simultaneously. It is this latter part of the procedure that I would also like to critique.

x,y-Co-ordinates Coincident Point

The extension of the CEC technique lies in the use of multipoint signal data (in this instance, a spectrum) such as is provided with spectrophotometry. By use of standard additions plots at each of two carefully chosen wavelengths (validated as described in reference 1) Bosch Reig and Campíns Falcó utilise the condition of remote extrapolation to the x,y-co-ordinates coincident point in the same manner as was carried out in a recent CEC paper.[4] This procedure yields an analyte concentration in the units of the abscissa (x-co-ordinate) free from both constant and proportional systematic errors. (For the significance of the y-co-ordinate see later.)

Why the analyte concentration would be bias free, a most remarkable fact, is not discussed in the literature as far as I am aware, was not fully explained in reference 4 nor was it explained in reference 1.

Proportional error is eliminated by virtue of the fact that the method of standard additions (MOSA) provides an *in situ* normalisation because the same procedural operation is performed on the unspiked and spiked samples, so that a constant percentage bias is introduced on the samples across the dynamic range.[2,3]

How the constant error is eliminated is to be found in the mathematical operation for the calculation of the coincident point, the intersection of the two standard additions plots. Solving two straight-line equations simultaneously reduces to a subtraction of the two y-response signals, thereby resulting in a cancellation of the constant error that is incorporated in each. Examples of this principle can be found in the classical Youden two-sample collaborative interlaboratory procedure that yields the well known Youden plot[5,6] and in the first quantitative calculation of the true method blank by Kimball and Tufts,[7] described more fully in reference 3.

The ability to obtain a bias-free analyte concentration is then not unique as it can be achieved via the CEC technique from two standard additions plots using two different sized samples for spiking.[4] However, the ability presented by Bosch Reig and Campíns Falcó[1] to separate constant error into its components whenever multipoint data permits is a significant development deserving of close examination.

y-Co-ordinate coincident point

Bosch Reig and Campíns Falcó state that the y-co-ordinate, A_H (Fig. 1 of reference 1) is the analytical signal due to the interferent. This statement is only partially correct. In fact, the A_H signal is due to the interferent plus the true method blank, or TYB (total Youden blank) as it is called in CEC terminology. It should be noted that both of these components are constant systematic errors with the former, the interferent, of the fixed systematic type, hence corrigible as against variable systematic errors that are incorrigible.[2,3] Bosch Reig and Campíns Falcó carefully and correctly ensure that the interferent is a constant corrigible error by their stipulation that it exhibits constant absorbance over the wavelength range of interest (Fig. 3 of reference 1) and that this stipulation is validated (Fig. 5 of reference 1).

In Fig. 1 of reference 1, the analytical signal, S, consists of that due to the analyte, the interferent and the true method blank, the TYB. The overlooking of the TYB component has been a consistent error of omission in the analytical literature and which has been discussed thoroughly in the CEC literature.[2,3] Failure to subtract the TYB component from the total signal is an incorrect standard additions model, as was shown recently,[4] and produces biased results. Notwithstanding, the procedure of Bosch Reig and Campíns Falcó results in a separation of the analyte concentration from the total constant error concentration and this fact is of considerable importance.

Why then do Bosch Reig and Campíns Falcó obtain such acceptable results for the interferent concentration in spite of the fact that it is the total constant error concentration and not just the interferent concentration? As I do not have the raw data, I cannot answer this question conclusively. However, I do have an explanation that they can examine. As the samples used were simple solution dye mixtures, essentially matrixless in the sense that they are indistinguishable from reference standard mixtures for a reference standard curve, and as in spectrophotometry, it is usual for Beer's law plots to pass through the origin, it is highly probable that the TYB component for these examples is statistically essentially zero. Any small acceptable analytical value would be contained within the normal variance of the method.

Recommended CEC Procedure

Bosch Reig and Campíns Falcó have presented their procedure as a free-standing MOSA technique, independent of a standard response curve. This is most certainly true when applicable under the stipulated conditions, for the bias-free determination of the analyte concentration. However, if the method were to be applied to more complex materials, such as pharmaceutical dosage forms or environmental samples where a significant TYB value were present, the determination of a known interferent would not be possible without bias from the TYB. In such a situation, correction of the analytical signal, S, for use in Fig. 1 of reference 1 would be required. An example of applying the TYB for total signal correction for use in a free-standing MOSA application was given recently by Ferrus and Torrades.[8]

Unless Bosch Reig and Campíns Falcó present some new information in a subsequent paper, the only way in which a true sample blank can be determined at present is by means of the Youden one-sample regression procedure[2,3,8] or its earlier equivalent alternatives.[7] In the examples of reference 1, this would simply involve selection of an appropriate dye mixture sample and varying the amount over the linear dynamic range across and including the maximum response values of the standard additions samples, all at one of the selected wavelengths. The resulting intercept value of the linear regression straight line is the TYB. It should be noted that in this procedure, the TYB value represents a separation from a total signal in which the analyte and interferent signal components remain superimposed. Under the conditions stipulated for the wavelengths, the probabilities are that the TYB determined in a similar manner at the second wavelength would be a statistically equivalent value. If they are not, a complex matrix interaction problem would be indicated, and a question of validity of the subsequent interferent determination would have to be examined.

In conclusion, Bosch Reig and Campíns Falcó have presented a valid and important addition to the free-standing

status of the method of standard additions for a bias-free analyte determination with their multipoint data technique, where applicable. However, the simultaneous determination of a corrigible interferent is only possible if a true method blank, TYB is absent. If present, a Youden one-sample regression determination of the TYB is required in order to correct the total analytical signals. It is for this reason, as this is the situation more often than not with complex samples, that I consider their technique to be an important and potentially useful extension of the CEC technique.

Mario J. Cardone
Chemistry Department
Rutgers University
Piscataway, NJ 08864, USA

Paper 9/00832B
Received February 23rd, 1989

Reply by Dr. F. Bosch Reig and Dr. P. Campíns Falcó

First, we thank Dr. M. J. Cardone for the interest he has taken in our paper.[1] We know his work and consider it to be a major contribution to the obtainment of unbiased analytical results.

His letter includes some remarks about the determination of the interferent by our method, which we will deal with here with the aim of extending and clarifying the fundamentals of the method.

We originally conceived and developed the H-point standard additions method (HPSAM) for application to multicomponent samples and samples with complex matrices. In reference 1 the method was applied to matrixless samples such as mixtures of dyes with the aim of showing how to calculate an analyte concentration ($C_X = -C_H$, abscissa of the H-point) free from constant and proportional systematic errors.

In dealing with binary mixtures, the HPSAM also allows the interferent concentration (C_Y) to be determined from A_H (the ordinate of the H-point) in the absence of a constant bias—only the proportional bias is eliminated by the HPSAM in quantifying interferents.

The occurrence of a constant bias due to the sample matrix (TYB, total Youden blank) was always considered in developing our method. The samples used in reference 1 were mixtures of dyes, and the statistically calculated TYB was virtually zero. This is also frequently the situation with more complex samples than those used in reference 1. Moreover, when the analyte signal is only modified by the matrix effect, the HPSAM allows both proportional and constant bias errors to be corrected, and the latter to be calculated. In this event, the two selected wavelengths can be chosen arbitrarily thanks to the very nature of the TYB, and an unbiased analyte concentration can be obtained by performing a single set of experiments and applying the multipoint data technique. Application of the corrigible error correction (CEC) technique,[2,3] on the other hand, entails carrying out two sets of experiments.

The above considerations are expressed theoretically below. Let us consider an unknown containing an analyte X and an interferent Y subject to a constant bias error, TYB. As previously,[1] we select two wavelengths (λ_1, λ_n) from the analyte and the interferent spectra and relate them with their corresponding absorbance values through the following expressions:

$$A_i = b_i + m_i\lambda_j \qquad (\lambda_1 \geqslant \lambda_j \geqslant \lambda_n) \quad .. \quad (1)$$

for the analyte (X) and

$$A' = b + m\lambda_j \qquad (m = 0) \quad .. \quad .. \quad (2)$$

for the interferent (Y), where b and m are the intercepts and slopes of the corresponding straight lines, respectively. The subscript i refers to the different solutions for m additions of the analyte concentration prepared in order to apply the standard additions method and the subscript j indicates a wavelength in the λ_1–λ_n range.

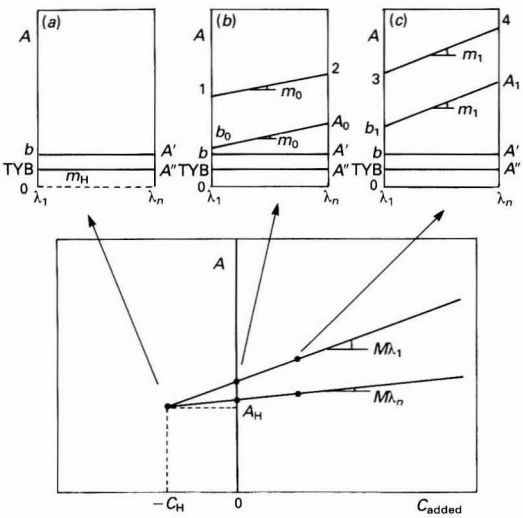

Fig. 1. H-point standard additions plots. For details see text

This condition is fulfilled because the interferent features a constant absorbance at the two selected wavelengths.

Let us also consider the TYB, which will normally be the same at the two selected wavelengths, *i.e.*,

$$A'' = \text{TYB} \quad .. \quad .. \quad .. \quad .. \quad (3)$$

Hence, the over-all equation corresponding to the first solution ($i = 0$) used to apply the method of standard additions (MOSA), which only contains the sample, with no added analyte, will be

$$A_0 + A' + A'' = b_0 + b + m_0\lambda_j + \text{TYB} \quad .. \quad (4)$$

The plot of A *versus* λ is shown in Fig. 1(*b*).

The MOSA starts by calculating the unknown concentration by extrapolation when the ordinate value is zero. Then, taking into account that, according to the HPSAM, $A_i = 0$ for $m_i = m = 0$ this is the H-point [Fig. 1(*a*)], at which the slope of the straight line of the $A = f(\lambda)$ plot for the analyte equals that of the interferent. The over-all equation will thus be reduced to

$$b + \text{TYB} = A' + A'' = A_H \quad .. \quad .. \quad (5)$$

Obviously, for TYB = 0, $b = A' = A_H$ and therefore, b can be related to the interferent concentration. Hence, in the absence of the interferent, TYB = $A'' = A_H$ and TYB can be determined readily.

Let us now consider the instance involving two constant systematic errors. The $A = f(\lambda)$ plot, corresponding to the first addition of the MOSA, is shown in Fig. 1(*c*) and the over-all equation is

$$A_1 + A' + A'' = b_1 + b + \text{TYB} + m_1\lambda_j \quad .. \quad (6)$$

These concepts can be clarified by plotting the absorbance as a function of the added analyte concentration (C_i) at the two selected wavelengths (Fig. 1). The MOSA equation will be

$$A\lambda_1 = b_i + b + M\lambda_1 C_i + \text{TYB} \quad .. \quad .. \quad (7)$$

for λ_1, and

$$A\lambda_n = A_i + A' + M\lambda_n C_i + \text{TYB} \quad .. \quad .. \quad (8)$$

for λ_n, where $M\lambda_1$ and $M\lambda_n$ are the slopes of the MOSA plots.

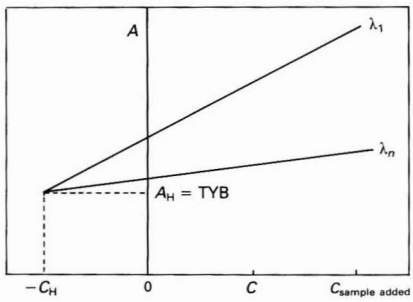

Fig. 2. Plot of the H-point standard additions method

The H-point is common to the two MOSA plots and is given by

$$b_i + b + M\lambda_1 C_i + \text{TYB} = A_i + A' + M\lambda_n C_i + \text{TYB} \quad (9)$$

or

$$C_i(M\lambda_1 - M\lambda_n) = A_i + A' - b_i - b \quad .. \quad (10)$$

As $A' = b$, then

$$C_i = (A_i - b_i)/(M\lambda_1 - M\lambda_n) = C_X(M\lambda_n - M\lambda_1)/(M\lambda_1 - M\lambda_n) = -C_X = -C_H \quad .. \quad .. \quad .. \quad .. \quad (11)$$

The analyte concentration can thus be obtained free from constant and proportional bias errors.

By substituting the C_i value obtained into equations (7) and (8) A_H can be determined through equation (12)

$$A_H = b_i + b + M\lambda_1(-C_H) + \text{TYB} \quad .. \quad (12)$$

As $b_i = M\lambda_1 C_H$, then

$$A_H = b + \text{TYB} \quad .. \quad .. \quad .. \quad (13)$$

Hence, it is possible to obtain an unbiased analyte concentration directly on application of the HPSAM if the constant bias is the same at the two selected wavelengths.

The interferent concentration will be free from proportional, but not from constant bias, which requires evaluation by Youden's method[9] or the CEC technique.[2,3] We agree with Dr. M. J. Cardone on this point; however, it is not essential that the TYB be the same at the two selected wavelengths as it can be evaluated at both and later used to construct the HPSAM graph by plotting $A\lambda_1 - \text{TYB}\lambda_1$ and $A\lambda_n - \text{TYB}\lambda_n$ as a function of the added concentration.

The HPSAM was applied to mixtures of dyes and metal ions, and to organic compounds in reference 1. All samples were found to have a TYB of zero. However, we are currently dealing with multi-component mixtures and samples with complex matrices, which therefore require correction of the constant bias by applying the Youden method or the CEC technique, or even the HPSAM by substituting the added analyte concentration by the added sample concentration (Fig. 2). The A_H value thus obtained is equivalent to the TYB if this is equivalent at the two selected wavelengths. In this way, the HPSAM, like the Youden method and the CEC technique, permits the occurrence of TYB to be detected; in addition, it allows one to determine whether it is constant at the two selected wavelengths.

Francisco Bosch Reig
Pilar Campíns Falcó
Department of Analytical Chemistry
Faculty of Chemistry
University of Valencia
Burjasot
Spain

Paper 9/00832B
Received June 19th, 1989

References

1. Bosch Reig, F., and Campíns Falcó, P., *Analyst*, 1988, **113**, 1011.
2. Cardone, M. J., *Anal. Chem.*, 1986, **58**, 438.
3. Cardone, M. J., *J. Assoc. Off. Anal. Chem.*, 1983, **66**, 1283.
4. Cardone, M. J., *Anal. Chem.*, 1987, **59**, 2818.
5. Youden, W. J., and Steiner, E. H., "Statistical Manual of the AOAC," Association of Official Analytical Chemists, Arlington, VA, 1975.
6. Cardone, M. J., *J. Assoc. Off. Anal. Chem.*, 1983, **66**, 1257.
7. Kimball, R. H., and Tufts, L. E., *Anal. Chem.*, 1947, **19**, 150.
8. Ferrus, R., and Torrades, F., *Anal. Chem.*, 1988, **60**, 1281.
9. Youden, W. J., *Anal. Chem.*, 1947, **19**, 946.

BOOK REVIEWS

Food. The Chemistry of its Components. Second Edition
T. P. Coultate. Pp. xi + 325. Royal Society of Chemistry. 1988. Price £9.95. ISBN 0 85186 433 3.

The first edition of this book was excellent and I am glad to say that this second edition is equally as good, if not better. It is intended to describe the basic chemistry of the more important food components and how their properties influence their role in both raw and processed foods. The book assumes at least a basic knowledge of organic chemistry but the non-scientist could probably still derive much useful information from its pages.

The material is divided into chapters on the basis of food components rather than commodities. Thus, Chapters 2–5 cover sugars, polysaccharides, lipids and proteins, which may be considered as the macroconstituents. Each chapter starts with structural information about the compounds in the group before moving on to discuss their chemistry and their relevance to particular foods. Some of the chapters have a section on analysis, whereas this is omitted from others. Sugar and amino acid analysis is discussed but methods for lipids are not, apart from triglyceride structures.

The classification of the material changes somewhat after these initial chapters, which are based on chemical components, to groupings based on their properties. Chapter 6 deals with colours, 7 with flavours, 8 with vitamins and 9 with preservatives. The chapter on colours covers the natural colour of foods, the use of natural colorants, the significance of the browning reaction to colour formation and also synthetic colours. These is a vast amount of material in only 30 pages and of necessity some of the aspects, *e.g.*, analysis, are not covered very fully. The controversy over the use of synthetic dyes is treated objectively, which is refreshing to see. Chapter 7 on flavours starts with a somewhat confusing description of aroma, taste and flavour. The definitions of these characteristics are very precise and it is a shame that they should be used so loosely. The characteristics of acetic acid are in no small part associated with its volatility. Covering all of the vitamins in less than 40 pages is also no mean achievement and a reasonable coverage has been obtained. Modern nomenclature has been used with the exception of thiamin, where a final "e" persists. The use of the negative notation for complex units, *e.g.*, $(100\ g)^{-1}$, seems cumbersome. Why not use per 100 g as in per sample? The chapter on preservatives deals with traditional methods of food preservation, pickling, smoking, etc., right through to the use of synthetic additives and even irradiation. The author, like the present reviewer, would seem not to be in total agreement with food irradiation.

Chapter 10 on "undesirables" is a new addition from the first edition and covers the chemistry of a wide range of endogenous components and contaminants. This is an excellent chapter with a distinct "green" appearance. It is interesting to note that many, if not most, of the instances of contaminated food arise from poor domestic practices. In Chapter 11 the title "minerals" is used to describe those metals in foods which are nutritionally desirable rather than the toxic metals covered in the previous chapter. The final chapter deals with the most important component of foods—water, and it is rather surprising to find this tucked away at the end. It should be Chapter 1.

Dr. Coultate must be congratulated on maintaining his momentum from the first edition through to this new edition. He writes in an excellent style, and apart from a few areas of ambiguity, the scientific content is first class. The book should be mandatory reading for all first-year food scientists, medical students (who seem to know very little about food) and anyone else who has an interest in the food we eat. I wish my name was on the cover.

Robert Macrae

The Scientific Examination of Documents. Methods and Techniques
David Ellen. *Ellis Horwood Series in Forensic Science.* Pp. 182. Ellis Horwood. 1989. Price £33.95. ISBN 0 7458 0551 5 (Ellis Horwood); 0 470 21347 7 (Halsted Press).

The introduction to this volume describes clearly and concisely the field of document examination in forensic science. The stated objectives are to outline the principles, methods and techniques employed and to enable lawyers, police officers and other investigators to understand the basis of the science. Chapters 2 and 3 give a fairly comprehensive description of handwriting in its various forms, the variation between normal writings and the accidental and deliberate modification of handwriting. These set the scene for Chapter 4, which deals with handwriting comparison and explains the various considerations that a document examiner must apply to his findings before he can assess their proper weight and form an opinion as to authorship. The author explains why, in certain instances, a document examiner cannot positively identify a writer and can only give a qualified opinion. The results of an examiner's analysis of poor or extremely limited material are frequently not up to the expectations of the investigator or lawyer. It may be that, having read the chapters on handwriting examination, and appreciated the complex considerations involved, future expectations may be somewhat more realistic.

Document examiners in the UK cover other aspects of documents and the author goes on to deal with each of these. The principles of typescript and typewriter examination are outlined and the increasing difficulties of identifying the output from new technology, such as dot-matrix and laser printers, are indicated. Further chapters deal in adequate detail with paper and ink examinations, especially non-destructive, instrumental techniques, with examination and identification of printed and photocopied documents and with the numerous other aspects of documents that an examiner must be prepared to handle. These include examination of indented impressions of writing, folds and creases, staples, damaged documents, opened and re-sealed envelopes, the sequencing of crossed-lines and document photography.

In the final chapter, "Document Examination in Court," the author has tended to depart from his declared target audience and has written it more from the witness point of view. However, lawyers would do well to heed his advice that a conference with the expert is often very helpful in order both to understand his testimony and introduce it in the most effective way.

This relatively small, well produced volume achieves most of its stated objectives, although perhaps a few more illustrations in the handwriting section would have been welcome. An index is provided and chapters conclude with an up-to-date reading list for those who wish to investigate the subject matter in more detail.

In these relatively few pages David Ellen has written a very readable, comprehensive account of the scientific examination of documents. The book is recommended to anyone who wishes to use the services of a document examiner and to other forensic scientists seeking a contemporary account of this particular discipline. It is unfortunate, however, that the price means that it is unlikely to reach a wider readership.

Paul A. M. Beard

Advances in Steroid Analysis '87. Proceedings of the 3rd Symposium on the Analysis of Steroids, Sopron, Hungary, October 20–22 1987
Edited by S. Görög. Pp. xiii + 583. Akadémiai Kiadó. 1988. Price £33. ISBN 963 05 5229 9.

This book is the proceedings of the 3rd Symposium on Analysis of Steroids held in Hungary in October 1987. Printed and published in Hungary, the text is in English and like all conference proceedings these days, is generated from author-prepared texts. However, unlike many such works, in this instance a length has obviously not been specified; texts range from 3 to 32 pages.

First impressions are poor. The book is produced on poor paper with a cheap binding. In the review copy several pages were overprinted with different pages. The quality of some manuscripts left a lot to be desired in terms of clarity of reproduction of gas chromatography traces. But these impressions are not confirmed on closer inspection. The scientific content is very good and covers the widest range of analytical techniques for steroids.

Basically, the book is divided into five sections, covering receptor binding studies, immunoassays (both radio- and enzyme), chromatography including mass spectrometry, clinical applications and miscellaneous topics which include papers on synthesis, biosynthesis, electrochemistry and dialysis. More than half of the texts are produced by Eastern European workers, giving an insight into the high level of research carried out in Hungary and Czechoslovakia especially. However, the bulk of the chromatography papers were provided by other workers, mainly from the USA or Western Europe.

Personally, I found the section on clinical applications of most interest. Although the development of specific and sensitive assays for steroids in biofluids show a high level of ingenuity, nonetheless the reasons for developing such assays are often lost. The section on clinical applications such as measuring androgen levels in ageing, stress or metabolites after treatment with cyproterone or medroxyprogesterone acetate show clearly why assays are needed.

In conclusion, this book is a good coverage of an important field of bioanalysis, despite its somewhat unprepossessing appearance. It should be read by most clinical biochemists working in the field of steroid analysis, and would be a useful tome for anyone working in biomedical research.

N. J. Haskins

X-Ray Fluorescence Spectrometry
Ron Jenkins. Pp. x + 175. Wiley Interscience. 1988. Price £40.60. ISBN 0 471 83675 3.

This book is well written, is presented in logical easy to read sections and represents a good introductory text to the subject of X-ray analysis applicable to the analytical chemist. The text takes the reader through from the basic production and interaction of X-rays with matter to current developments and applications of the technique. Each of the chapters is clearly illustrated with simple easy to understand diagrams. Perhaps the biggest criticism of the book is the title, as it takes some time to get specifically into X-ray fluorescence spectrometry (XRF), with the first three chapters tending to present a more general introduction to X-ray analysis. This is probably more a problem with the title than the text, as the material presented is both interesting and gives a good balance to the book in general. Whilst on the critical side, the price is, as always, too high for such relevant texts.

Following the first chapter on the production and properties of X-rays, the second chapter describes a wide range of X-ray techniques based on absorption, diffraction and fluorescence, with relevant applications in areas such as X-ray diagnostics, tomography, level and thickness gauging, security systems and non-destructive testing in general. The subject of X-ray diffraction, in particular powder methods, is covered in some detail in Chapter 3.

The main theme of the book, XRF, really starts at Chapter 4 with a very good basic introduction into the fundamental principles of the technique, and a clear description of wavelength and energy-dispersive methods. The relative merits of these two modes of operation form the basis of an individual chapter as do more novel versions of the technique, such as total reflection XRF (TRXRF) and the use of synchrotron (SSXRF) and proton excited (PIXE) sources. The final five chapters take the reader through the practical applications of XRF. These start with sample preparation for solid and liquid samples present in both large and small amounts, and the important area of sample pre-concentration techniques. Considerable time is devoted to qualitative and quantitative analysis, with particular reference to background, statistical counting errors and matrix effects. Calibration procedures are naturally covered at length for both single and multiple elemental determinations. The final chapter considers the place of XRF in elemental analysis by comparison to other instrumental methods and suggests future developments and applications of the technique.

The technique of X-ray fluorescence represents an important instrumental tool in elemental analysis, which currently finds applications in over 15 000 laboratories worldwide. This new book in the monograph series on analytical chemistry by Ron Jenkins is not only a good introductory text to the subject, but also emphasises the assimilation of recent technology into XRF instrumentation and stresses current techniques in sample methodology. The book represents a good text for any current or potential user of XRF and forms the basis of an excellent, but expensive volume, for students of analytical chemistry with an interest in elemental analysis.

S. J. Haswell

Analysis of Trace Organics in the Aquatic Environment
Edited by B. K. Afghan and Alfred S. Y. Chau. Pp. 346. CRC Press. 1989. Price £130.50. ISBN 0 8493 4626 6.

This book is the latest offering from the generally excellent series of monographs published by CRC Press and is the final volume in a four-volume set which reviews the analysis of trace organics in the aquatic environment. The final volume has nine chapters devoted to volatile organics, toxaphene, organometallics, humic acids, PAH, phenols, dioxins, phthalates and PCBs. It is intended to provide a reference source for university students and practicising environmental chemists with sufficient detail to enable readers to determine trace constituents in an accurate manner.

In general, the authors have achieved their objective with an excellent collection of comprehensive and informative reviews on the analysis of environmental chemicals of topical interest. Disappointingly, but almost inevitable in books of this type, the reviews only cover the literature up to, and including, 1986. This probably explains one of the notable omissions, namely references to the analysis of tributyltin compounds in environmental samples by capillary gas chromatography. There is also, surprisingly, no reference in any of the chapters to the numerous "Blue Book" methods produced by the UK Department of the Environment Standing Committee of Analysts, which provide developed methods for many of the organics covered in this book.

Despite these limitations and a few annoying typographical errors, I found the book a useful and timely reference work for practical information on the analysis of a range of organics. Undoubtedly it will be widely consulted in my laboratory and in other laboratories directly involved with the analysis of these compounds in aquatic samples. However, at £130.50 for some 346 pages it is expensive and this will unfortunately preclude its purchase by individual scientists involved or interested in this topic.

C. D. Watts

Metal Speciation. Theory, Analysis and Application
James R. Kramer and Herbert E. Allen. Pp. xiii + 357. Lewis. 1988. Price £43.60. ISBN 0 87371 140 8.

This book was written following a workshop on metal speciation, held at Jekyll Island, Georgia, in May 1987. It contains articles written by different authors on the topic of the title. I am glad to have had the opportunity to review the book, as I enjoyed reading it. The topic of metal speciation is covered in a broad and varied manner, and the articles are interesting to read. Generally, each article presents a review of a particular aspect of speciation, and usually also contains recent data. The book mainly covers freshwater aspects, although some marine applications are discussed as well. Of general interest are the applications to biological uptake including that by humans.

The following topics are covered: speciation of aluminium (Öhman and Sjöberg), adsorption of inorganic species (Leckie), adsorption of organic species (Stone), speciation in groundwater (Theis) and sulphide, iron and manganese speciation in lakes (Buffle *et al.*). Analytical aspects are treated in chapters on the following topics: comparison of voltammetric measurements with model calculations (Shuman), measurement of binding sites on humic substances (Perdue), chromatographic techniques (Marshall) and sediment partitioning (Tessier and Campbell). Speciation in the marine environment: platinum group metals and Periodic Table neighbours (Goldberg *et al.*). Speciation and its effects on uptake by plants, animals and human beings are covered in chapters on speciation in agriculture (Chaney), sediments and soils (Gunn *et al.*), bioaccumulation and toxicity (Wood) and bioavailability to humans (Sandstead). One chapter concerns waste water treatment (Patterson).

This book provides a good introduction to many aspects of the topic of speciation, and I am happy to recommend it to third-year students of environmental or aquatic chemistry. I think this book is also a useful addition to the library of scientists already familiar with the topic.

C. M. G. van den Berg

Luminescence Applications in Biological, Chemical, Environmental and Hydrological Sciences
Edited by Marvin C. Goldberg. *ACS Symposium Series 383.* Pp. xii + 251. American Chemical Society. 1989. Price $59.95 (USA and Canada); $71.95 (Export). ISBN 0 8412 1260 X.

This book is an extended version of the proceedings of a symposium sponsored by the ACS Division of Environmental Chemistry and held at Denver in April 1987. It contains 14 camera-ready chapters by authors from American companies and universities.

The breadth of applications of molecular luminescence is demonstrated by the titles in this book; from spectrofluorimetric analyses of cell responses to groundwater monitoring using remote laser-induced fluorescence, from element-specific epifluorescence microscopy to peroxyoxalate chemiluminescence. Clearly, this is not a general textbook but it should appeal to researchers from various backgrounds who are active in the field of molecular luminescence.

The technique has developed greatly in recent years, *e.g.*, for chromatographic detection, in the use of synchronous scanning, the use of tunable lasers as sources, solid-state luminescence, luminescent labels and chemical excitation and each of these areas is covered in one or more chapters. This book is therefore a useful addition to the library of research specialists in the field of molecular luminescence.

P. J. Worsfold

CUMULATIVE AUTHOR INDEX

JANUARY 1990

INSTRUCTIONS TO AUTHORS

The Analyst publishes papers on all aspects of the theory and practice of analytical chemistry, fundamental and applied, inorganic and organic, including chemical, physical, biochemical, clinical, pharmaceutical, biological, automatic and computer-based methods. Papers on new approaches to existing methods, new techniques and instrumentation, detectors and sensors, and new areas of application with due attention to overcoming limitations and to underlying principles are all equally welcome. Papers may be submitted for publication by members of The Royal Society of Chemistry or by non-members. There is no page charge for papers published in *The Analyst*.

The following types of papers will be considered.

Full papers, describing original work.

Short papers: the criteria regarding originality are the same as for full papers, but short papers generally report less extensive investigations or are of limited breadth of subject matter.

Communications, which must be on an urgent matter and be of obvious scientific importance. Rapidity of publication is enhanced if diagrams are omitted, but tables and formulae can be included. Communications receive priority and are usually published within 5–8 weeks of receipt. They are intended for brief descriptions of work that has progressed to a stage at which it is likely to be valuable to workers faced with similar problems. A fuller paper may be offered subsequently, if justified by later work. Communications will normally be examined by one referee.

Reviews, which must be a critical evaluation of the existing state of knowledge on a particular facet of analytical chemistry.

Every paper (except Communications) will be submitted to at least two referees, by whose advice the Editorial Board of *The Analyst* will be guided as to its acceptance or rejection. Papers that are accepted must not be published elsewhere except by permission. Submission of a manuscript will be regarded as an undertaking that the same material is not being considered for publication by another journal.

Regional Advisory Editors. For the benefit of potential contributors outside the United Kingdom, a Panel of Regional Advisory Editors exists. Requests for help or advice on any matter related to the preparation of papers and their submission for publication in *The Analyst* can be sent to the nearest member of the Panel. Currently serving Regional Advisory Editors are listed in each issue of *The Analyst*.

Manuscripts. Papers should be typewritten in double spacing on one side *only* of the paper. Three copies of text and illustrations should be sent to the **Editor, The Analyst, The Royal Society of Chemistry, Thomas Graham House, Science Park, Milton Road, Cambridge CB4 4WF,** and a further copy retained by the author.

Proofs. The address to which proofs are to be sent should accompany the paper. Proofs should be carefully checked and returned immediately (by Air Mail from outside Europe).

Reprints. Fifty reprints of each paper are supplied free on request. Additional reprints can be purchased if ordered at the time of publication. Details are sent to authors with the proofs.

Notes on the Writing of Papers for *The Analyst*

Manuscripts should be in accordance with the style and usage shown in recent copies of *The Analyst*. Conciseness of expression should be aimed at: clarity is increased by adopting a logical order of presentation, with suitable paragraph or section headings.

To facilitate abstracting and indexing by Chemical Abstracts Service, and other abstracting organisations, it would be helpful if at least one forename could be included with each author's family name.

Descriptions of new methods should be supported by experimental results showing accuracy, precision and selectivity.

The recommended order of presentation is as indicated below:

(*a*) *Title.* This should be as brief as is consistent with an adequate indication of the original features of the work. The analytical method used in the work should be mentioned in the title.

(*b*) *Synopsis.* A synopsis of about 100 words, giving the salient features and drawing attention to the novel aspects, should be provided for all papers.

(*c*) *Keywords.* Up to 5 keywords or key phrases, indicating the topics of importance in the work described, should be included after the synopsis.

(*d*) *Aim of investigation.* An introductory statement of the object of the investigation with any essential historical background, followed, if necessary, by a *brief* account of preliminary experimental work.

(*e*) *Description of the experimental procedures.* Working details must be given concisely. Analytical procedures should preferably be given in the form of instructions; well known operations should not be described in detail.

(*f*) *Results.* These are best presented in tabular form, followed by any statistical evaluation, which should be in accordance with accepted practice.

(*g*) *Discussion of results.* This section will comment on the scope of the method and its validity, followed by a statement of any conclusions drawn from the work.

Nomenclature. Current internationally recognised (IUPAC) chemical nomenclature should be used. Common trivial names may be used, but should first be defined in terms of IUPAC nomenclature.

SI units. The SI system of units should be used. These units are summarised in the Appendix. The effect on current style of papers for *The Analyst* includes the following:

(*a*) dimensions should preferably be given in metres (m) or in millimetres (mm);

(*b*) temperatures should be expressed in K or °C (not °F);

(*c*) wavelengths should be expressed in nanometres (nm) (not mμ);

(*d*) frequency should be expressed in Hz (or kHz, etc.), not in c/s or c.p.s.; rotational frequency can be denoted by use of s^{-1}; in mass spectrometry, signal intensity should be expressed in counts s^{-1} and not in Hz;

(*e*) radionuclide activity will be expressed in becquerels (Bq) or curies (Ci); 1 Ci = 3.7×10^{10} Bq;

(*f*) the micron (μ) will not be used; 10^{-6} m will be 1 μm.

Abbreviations. SI units should be used. Molarity is generally expressed as a decimal fraction (*e.g.*, 0.375 M). Abbreviational full stops are omitted after the common contractions of metric units (*e.g.*, ml, g, μg, mm) and other units represented by symbols. Abbreviations other than those of recognised units should be avoided in the text.

Percentage concentrations of solutions should be stated in internationally recognised terms. Thus the symbols "m" instead of "w" for mass and "v" for volume are to be used. The following show the manner of expressing these percentages together with an acceptable alternative given in parentheses: % m/m (g per 100 g); % m/v (g per 100 ml); % v/v. Further implications of the use of the term "mass" are that "relative atomic mass" of an element (A_r) replaces atomic weight, and "relative molecular mass" of a substance (M_r) replaces molecular weight.

Concentrations of solutions of the common acids are often conveniently given as dilutions of the concentrated acids, such as "dilute hydrochloric acid (1 + 4)," which signifies 1 volume of the concentrated acid mixed with 4 volumes of water. This avoids the ambiguity of 1 : 4, which might represent either 1 + 4 or 1 + 3. Dilutions of other solutions can be expressed in a similar manner.

Tables and diagrams. The number of tables should be kept to a minimum. Column headings should be brief. Tables consisting of only two columns can often be arranged horizontally. Tables must be supplied with titles and be so set out as to be understandable without reference to the text.

Either tables or graphs may be used but not both for the same set of results, unless important additional information is given by so doing. The information given by a straight-line calibration graph can usually be conveyed adequately as an equation or statement in the text.

The style used in headings to tables and in labels on the axes of graphs, where the numbers represent numerical values, is, for example: Volume/ml. The diagonal line (solidus) will not be used to represent "per". In accordance with the SI system, units such as grams per millilitre are already expressed in the form g ml^{-1}. For a table (or graph), this would appear as: Concentration of solution/g ml^{-1}. It should be noted that the "combined" unit, g ml^{-1}, must not have any "intrusive" numbers. To express concentration in grams per 100 millilitres, the word "per" will still be required: Concentration/g per 100 ml. It may be preferable for an author to express concentrations in grams per litre (g l^{-1}) rather than grams per 100 ml.

Most diagrams will be retraced and lettered in order to achieve uniform line thicknesses and lettering size and style, so it is not essential to prepare specially traced drawings. However, all diagrams should be carefully and clearly drawn on good quality paper and should be clearly lettered. If possible, complicated flow charts, circuit diagrams, etc., should be supplied as artwork for direct reproduction in order to avoid time-consuming and expensive redrawing.

Three sets of illustrations should be provided, two sets of which may be made by any convenient copying process for transmission to the referees.

All diagrams should be accompanied by a separately typed set of captions. Wherever possible, extensive identifying lettering should be placed in the caption rather than on lines on graphs, etc.

Photographs. Photographs should be submitted only if they convey essential information that cannot be shown in any other way. They should be submitted as glossy or matt prints made to give the maximum detail. Colour photographs will be accepted only when a black-and-white photograph fails to show some vital feature and can be supplied either as prints or transparencies.

References. References should be numbered serially in the text by means of superscript figures, *e.g.*, Foote and Delves,[1] Burns *et al.*[2] or Hirozawa,[3] and collected in numerical order under "References" at the end of the paper. They should be listed, with the authors' initials, in the following form (double-spaced typing):

1. Foote, J. W., and Delves, H. T., *Analyst,* 1983, **108**, 492.
2. Burns, D. T., Glockling, F., and Harriott, M., *J. Chromatogr.*, 1980, **200**, 305.
3. Hirozawa, S. T., *in* Kolthoff, I. M., and Elving, P. J., *Editors,* "Treatise on Analytical Chemistry, Part II," Volume 14, Wiley, New York, 1971, p. 23.

Journal titles should be abbreviated according to the *Chemical Abstracts Service Source Index* (*CASSI*).

For books, the edition (if not the first), the publisher and the place and date of publication should be given, followed by the page number.

Authors must, in their own interest, check their lists of references against the original papers; second-hand references are a frequent source of error. The number of references must be kept to a minimum.

Appendix

The SI System of Units

In the SI system there are seven base units—

Physical quantity	*Name of unit*	*Symbol for unit*
length	metre	m
mass	kilogram	kg
time	second	s
electric current	ampere	A
thermodynamic temperature	kelvin	K
amount of substance	mole	mol
luminous intensity	candela	cd

There are two supplementary dimensionless units for plane angle (radian, rad) and solid angle (steradian, sr). Some derived SI units that have special names are as follows—

Physical quantity	*Name of unit*	*Symbol for unit*	*Definition of unit*
energy	joule	J	$kg\ m^2\ s^{-2}$
force	newton	N	$kg\ m\ s^{-2} = J\ m^{-1}$
power	watt	W	$kg\ m^2\ s^{-3} = J\ s^{-1}$
electric charge	coulomb	C	A s
electric potential difference	volt	V	$kg\ m^2\ s^{-3}\ A^{-1} = J\ A^{-1}\ s^{-1}$
electric resistance	ohm	Ω	$kg\ m^2\ s^{-3}\ A^{-2} = V\ A^{-1}$
electric capacitance	farad	F	$A^2\ s^4\ kg^{-1}\ m^{-2} = A\ s\ V^{-1}$
frequency	hertz	Hz	s^{-1}
magnetic flux density (magnetic induction)	tesla	T	$kg\ s^{-2}\ A^{-1} = V\ s\ m^{-2}$
radionuclide activity	becquerel	Bq	s^{-1}

Examples of other derived SI units are—

Physical quantity	*SI unit*	*Symbol for unit*
area	square metre	m^2
volume	cubic metre	m^3
density	kilogram per cubic metre	$kg\ m^{-3}$
velocity	metre per second	$m\ s^{-1}$
angular velocity	radian per second	$rad\ s^{-1}$
acceleration	metre per second squared	$m\ s^{-2}$
magnetic field strength	ampere per metre	$A\ m^{-1}$

Certain units will be allowed in conjunction with the SI system, *e.g.*—

Physical quantity	*Name of unit*	*Symbol for unit*	*Definition of unit*
volume	litre	l	$10^{-3}\ m^3 = dm^3$
magnetic flux density (magnetic induction)	gauss	G	10^{-4} T
temperature, t	degree Celsius	°C	$t/°C = T/K - 273.16$
radionuclide activity	curie	Ci	3.7×10^{10} Bq
energy	electronvolt	eV	1.6021×10^{-19} J

The common units of time (*e.g.*, minute, hour, day) and the angular degree (°) will continue to be used in appropriate contexts.

Decimal multiples and submultiples have the following names and symbols (for use as prefixes)—

10^{-3}	milli	m	10^3	kilo	k
10^{-6}	micro	μ	10^6	mega	M
10^{-9}	nano	n	10^9	giga	G
10^{-12}	pico	p	10^{12}	tera	T
			10^{15}	peta	P
			10^{18}	exa	E

Compound prefixes (*e.g.*, mμm) should not be used; 10^{-9} m = 1 nm.

The Royal Society of Chemistry,
Thomas Graham House,
Science Park, Milton Road,
Cambridge CB4 4WF, UK

FIRST FOLD HERE

THE ANALYST READER ENQUIRY SERVICE
For further information about any of the products featured in the advertisements in this issue, write the appropriate number on the postcard, detach and post.

FOLD HERE

THE ANALYST READER ENQUIRY SERVICE JAN'90

For further information about any of the products featured in the advertisements in this issue, please write the appropriate number in one of the boxes below.
Postage paid if posted in the British Isles but overseas readers must affix a stamp.

PLEASE USE BLOCK CAPITALS LEAVING A SPACE BETWEEN WORDS *Valid 12 months*

1 NAME

2 COMPANY

PLEASE GIVE YOUR BUSINESS ADDRESS IF POSSIBLE. IF NOT, PLEASE TICK HERE ☐

3 STREET

4 TOWN

5 COUNTY
POST CODE

6 COUNTRY

7 DEPARTMENT/
DIVISION

8 YOUR JOB TITLE/
POSITION

9 TELEPHONE NO

OFFICE USE ONLY REC'D PROC'D

FOLD HERE

Postage will be paid by Licensee

Do not affix Postage Stamps if posted in Gt. Britain, Channel Islands, N. Ireland or the Isle of Man

BUSINESS REPLY SERVICE
Licence No. WD 106

Reader Enquiry Service
The Analyst
The Royal Society of Chemistry
Burlington House, Piccadilly
LONDON
W1E 6WF
England

ANALAO 115(1) 1–124 (1990) January 1990

The Analyst

The Analytical Journal of The Royal Society of Chemistry

CONTENTS

Typeset and printed by Black Bear Press Limited, Cambridge, England